

**NONLINEAR ANALYSIS OF
SMART COMPOSITE PLATE AND SHELL STRUCTURES**

A Dissertation

by

SEUNG JOON LEE

Submitted to the Office of Graduate Studies of
Texas A&M University
in partial fulfillment of the requirements for the degree of

DOCTOR OF PHILOSOPHY

May 2004

Major Subject: Civil Engineering

**NONLINEAR ANALYSIS OF
SMART COMPOSITE PLATE AND SHELL STRUCTURES**

A Dissertation

by

SEUNG JOON LEE

Submitted to Texas A&M University
in partial fulfillment of the requirements
for the degree of

DOCTOR OF PHILOSOPHY

Approved as to style and content by:

J. N. Reddy
(Chair of Committee)

Ravinder Chona
(Member)

Hayes E. Ross, Jr.
(Member)

Harry L. Jones
(Member)

Paul N. Roschke
(Head of Department)

May 2004

Major Subject: Civil Engineering

ABSTRACT

Nonlinear Analysis of

Smart Composite Plate and Shell Structures. (May 2004)

Seung Joon Lee, B.S., Yeungnam University;

M.S., Yeungnam University

Chair of Advisory Committee: Dr. J. N. Reddy

Theoretical formulations, analytical solutions, and finite element solutions for laminated composite plate and shell structures with smart material laminae are presented in the study. A unified third-order shear deformation theory is formulated and used to study vibration/deflection suppression characteristics of plate and shell structures. The *von Kármán* type geometric nonlinearity is included in the formulation. Third-order shear deformation theory based on Donnell and Sanders nonlinear shell theories is chosen for the shell formulation. The smart material used in this study to achieve damping of transverse deflection is the Terfenol-D magnetostrictive material. A negative velocity feedback control is used to control the structural system with the constant control gain.

The Navier solutions of laminated composite plates and shells of rectangular planeform are obtained for the simply supported boundary conditions using the linear theories. Displacement finite element models that account for the geometric nonlinearity and dynamic response are developed. The conforming element which has eight degrees of freedom per node is used to develop the finite element model. Newmark's time integration scheme is used to reduce the ordinary differential equations in time to algebraic equations. Newton-Raphson iteration scheme is used to solve the resulting nonlinear finite element equations.

A number of parametric studies are carried out to understand the damping characteristics of laminated composites with embedded smart material layers.

To my beloved family

ACKNOWLEDGMENTS

First of all, my utmost gratitude and thanks are extended to my advisor, Dr. J. N. Reddy, for his encouragement, counsel, confidence, patience and constructive criticism throughout the research. His vast knowledge and insight into the area of mechanics and materials have helped me get through some obstacles along the way.

I wish to thank Dr. Ravinder Chona and Dr. Harry L. Jones for serving on my committee and for their valuable remarks. I also wish to thank Dr. Harry Hogan from the Department of Mechanical Engineering for his technical advices.

I would like to express special thanks to Dr. Hayes E. Ross for his sincere friendship and support. Special thanks are also expressed to Dr. Roger P. Bligh at Texas Transportation Institute (TTI) for his guidance and support during my graduate study at Texas A&M University. I thank the fellow members in the Advanced Computational Mechanics Laboratory (ACML) for their freindship during my stay at ACML.

I am also grateful for the financial suport from the Army Research Office (ARO) through the Grant DAAD19-01-1-0483 during this work.

Last but not least, I would like to thank my wife, Young A Park, and my son, Yoon Dong Lee, for their unwavering support, patience, encouragement and love which provided me the strength to complete this study.

TABLE OF CONTENTS

	Page
ABSTRACT	iii
ACKNOWLEDGMENTS	v
TABLE OF CONTENTS	vi
LIST OF FIGURES	ix
LIST OF TABLES.....	xvi
 1. INTRODUCTION	 1
1.1. General.....	1
1.2. Smart Materials.....	2
1.3. Background Literature.....	4
1.4 Present Study	7
 2. THEORETICAL FORMULATIONS.....	 9
2.1. Methodology.....	9
2.2. Displacement Field and Strains	9
2.2.1. Displacement Field and Strains for Plates	9
2.2.2. Kinetics of Shells	12
2.2.3. Displacement Field and Strains for Shells	14
2.3. Equations of Motion	19
2.3.1. Equations of Motion for TSDT Plates	20
2.3.2. Equations of Motion for Special Cases.....	23
2.3.3. Equations of Motion for TSDT Donnell Shell Theory	27
2.3.4. Equations of Motion for TSDT Sanders Shell Theory	28
2.4. Constitutive Relations.....	30
2.5. Velocity Feedback Control.....	32
2.6. Laminated Constitutive Equations.....	34
 3. ANALYTICAL SOLUTIONS	 36
3.1. Analytical Solutions for Laminated Composite Plates.....	36
3.1.1. Introduction.....	36
3.1.2. Boundary Conditions	36
3.1.3. Navier Solution	37
3.2. Analytical Solutions for Laminated Composite Shells.....	40

	Page
3.2.1. Modified Sanders Shell Theory	40
3.2.2. Navier Solutions of Shell Theories	41
3.3. Vibration Control.....	47
3.4. Analytical Results for Laminated Composite Plates	48
3.4.1. Vibration Suppression of Different Modes	49
3.4.2. Effect of Lamina Material Properties.....	49
3.4.3. Effect of Plate Theories.....	50
3.4.4. Effect of Smart Material Position	56
3.4.5. Effect of Lamina Thickness	60
3.4.6. Effect of Feedback Coefficients.....	61
3.4.7. Variation of T_s and e_r for Different Laminates	64
3.5. Analytical Results for Laminated Composite Shells.....	66
3.5.1. The General.....	66
3.5.2. Effect of Shell Theories	71
3.5.3. Effect of R_2/a	74
3.5.4. Effect of Shell Types.....	78
3.5.5. Effect of Material Properties	78
4. FINITE ELEMENT FORMULATIONS	86
4.1. Virtual Work Statements	86
4.1.1. Virtual Work Statements for Laminated Composite Plates	86
4.1.2. Virtual Work Statements for Laminated Composite Shells.....	89
4.2. Finite Element Model	94
4.3. Transient Analysis	97
4.4. Nonlinear Analysis	99
4.5. Computer Implementation.....	100
4.6. Preliminary Linear Finite Element Results	100
4.6.1. Simply Supported Laminated Composite Plates.....	105
4.6.2. Deflection Suppression Time.....	108
4.6.3. Effect of Lamina Thickness	108
4.6.4. Effect of Feedback Coefficients.....	109
4.6.5. Other Effects on Deflection Control	111
5. RESULTS OF NONLINEAR ANALYSIS	118
5.1. Nonlinear Static Results	120
5.2. Nonlinear Transient Results for Laminated Composite Plates.....	127
5.2.1. Load and Time Increments	127
5.2.2. Effect of Plate Theories.....	127
5.2.3. Effect of Lamination Schemes	132

	Page
5.2.4. Effect of Loading Conditions.....	135
5.2.5. Effect of Boundary Conditions	139
5.3. Nonlinear Transient Results for Laminated Composite Shells	144
5.3.1. Effect of Shell Theories	144
5.3.2. Effect of R_2/a	149
5.3.3. Effect of Shell Types.....	149
5.3.4. Effect of Lamination Schemes	156
5.3.5. Effect of Boundary Conditions	157
5.3.6. Effect of Loading Conditions.....	157
5.4. Nonlinear Results under Thermomechanical Loads.....	157
5.4.1. Static Results under Themomechanical Loads	167
5.4.2. Laminated Composite Plates under Themomechanical Loads	171
5.4.3. Laminated Composite Shells under Themomechanical Loads	191
6. CONCLUSIONS	199
6.1. Concluding Remarks	199
6.2. Recommendations for Future Work	201
REFERENCES	203
APPENDIX A EULER-LAGRANGE EQUATIONS OF TSDT SANDERS SHELL THEORY IN TERMS OF DISPLACEMENTS	210
APPENDIX B FINITE ELEMENT COEFFICIENTS BY TSDT DONNELL (DMV) SHELL THEORY	216
APPENDIX C FINITE ELEMENT COEFFICIENTS BY TSDT SANDERS (SANDERS-KOITER) SHELL THEORY	226
VITA.....	238

LIST OF FIGURES

FIGURE	Page
2. 1 Geometry and coordinate system of laminated plate	10
2. 2 Geometry and coordinate system of laminated shell	12
2. 3 Force and moment resultants on a plate element	22
2. 4 Closed-loop feedback control system	33
3. 1 Simply supported boundary conditions (SS-1 and SS-2) for TSDT	36
3. 2 Suppression characteristics for different modes of vibration.....	51
3. 3 Effect of material properties on vibration suppression	52
3. 4 Effect of the different plate theories on vibration suppression	54
3. 5 Vibration suppression characteristics for different smart material location	57
3. 6 Vibration suppression times for CFRP laminated plate.....	59
3. 7 Effect of lamina thickness on vibration suppression	61
3. 8 Effect of feedback coefficient on the suppression time	63
3. 9 Variation of T_s and e_r with respect to Z_m	65
3. 10 Vibration suppression characteristics of CFRP spherical shells ($R_2/a = 10$) for the different mode; (a) Thin shell ($a/h = 100$), (b) Thick shell ($a/h = 10$)...	68
3. 11 Vibration suppression characteristics of CFRP spherical shells ($R_2/a = 3$) for the different lamination; (a) Thin shell ($a/h = 100$), (b) Thick shell ($a/h = 10$)	70
3. 12 Vibration suppression characteristics of CFRP cylindrical shells for different shell theories; (a) Thin shell ($R_2/a = 2$), (b) Thick shell ($R_2/a = 2$)..	73
3. 13 Effect of R_2/a on vibration suppression characteristics of CFRP spherical shells; (a) Thin shell ($a/h = 100$), (b) Thick shell ($a/h = 10$).....	75

FIGURE	Page
3. 14 Effect of R_2/a on vibration suppression characteristics of CFRP cylindrical shells; (a) Thin shell ($a/h = 100$), (b) Thick shell ($a/h = 10$).....	76
3. 15 Effect of R_2/a on vibration suppression characteristics of CFRP doubly curved shells; (a) Thin shell ($a/h = 100$), (b) Thick shell ($a/h = 10$).....	77
3. 16 Vibration suppression characteristics for different CFRP shells; (a) Thin shell ($a/h = 100$), (b) Thick shell ($a/h = 10$).....	79
3. 17 Effect of elastic material properties on vibration suppression characteristics for thin ($a/h = 100$) shells; (a) spherical shell, (b) cylindrical shell, (c) doubly curved shell.....	84
4. 1 Conforming rectangular element with eight degrees of freedom per node.....	95
4. 2 Flow chart of the nonlinear transient analysis of a problem	101
4. 3 Finite element meshes of laminated composite plates	102
4. 4 Effect of finite element modeling of CFRP composite plates; (a) Simply supported antisymmetric laminates, (b) Clamped antisymmetric laminates, (c) Simply supported symmetric laminates, (d) Clamped symmetric laminates	103
4. 5 Center deflection predicted by the analytical and finite element methods for the case of symmetric cross-ply CFRP laminated plate.....	105
4. 6 Center displacements by the different plate theories for simply supported cross-ply CFRP laminated plates; (a) (m,90,0,90,0) _s , (b) (0,90,0,90,m) _s	106
4. 7 Effect of the lamina material properties on the damping of deflection in symmetric cross-ply laminated plate (m,90,0,90,0) _s	107
4. 8 Effect of the smart material layer position on the deflection for the symmetric cross-ply CFRP laminated plate.....	107
4. 9 Effect of the thickness of smart material layers on the deflection damping characteristics of symmetric cross-ply laminated plate (m,90,0,90,0) _s	110
4. 10 Effect of the magnitude of the feedback coefficients on the suppression time for symmetric cross-ply CFRP laminated plate (m,90,0,90,0) _s	111

FIGURE	Page
4. 11 Center displacement for symmetric angle-ply CFRP laminated plate.....	113
4. 12 Effect of the smart layer position for symmetric general angle-ply CFRP laminated plate	114
4. 13 Effect of boundary conditions (a) Comparison of simply supported and clamped laminates, (b) smart layer positions.....	115
4. 14 Nondimensionalized center deflection under uniform load.....	116
4. 15 Nondimensionalized center deflection under suddenly applied uniform load...	116
4. 16 Nondimensionalized center displacement for simply supported laminated plates under sinusoidal and uniformly distributed loads.....	117
5. 1 Six boundary conditions used in this study.....	119
5. 2 Load-deflection curve for the different lamination schemes with SSSS boundary conditions under uniformly distributed loading: (a) $a/h=10$, (b) $a/h=100$	125
5. 3 Load-deflection curve for the cross-ply laminates with the different boundary conditions under uniformly distributed sinusoidal loading: (a) $a/h=10$, (b) $a/h=100$	126
5. 4 Effect of load intensity on the nonlinear transient responses for the symmetric cross-ply laminates with SSSS boundary conditions under uniformly distributed loading using TSDT: (a) $a/h=10$, (b) $a/h=100$	128
5. 5 Effect of time increments on the nonlinear transient analyses for the symmetric cross-ply laminates with SSSS boundary conditions under uniformly distributed loading using TSDT: (a) $a/h=10$, (b) $a/h=100$	129
5. 6 Effect of plate theories on the nonlinear transient responses for the symmetric cross-ply thick ($a/h=10$) laminates with SSSS boundary conditions under uniformly distributed loading, $q_0 = 5 \times 10^7$: (a)Details, (b)Nonlinear responses.....	130

FIGURE

Page

5. 7 Effect of lamination schemes on the transient responses with SSSS boundary conditions under uniformly distributed loading:
 (a) $a/h=10$ ($q_0 = 5 \times 10^7$), (b) $a/h=100$ ($q_0 = 5 \times 10^3$)..... 134
5. 8 Effect of loading conditions on the transient responses with SSSS boundary conditions: (a) cross-ply laminates ($a/h=10$) with $q_0 = 5 \times 10^7$, (b) cross-ply laminates ($a/h=100$) with $q_0 = 10^4$, (c) angle-ply laminates ($a/h=10$) with $q_0 = 5 \times 10^7$, (d) angle-ply laminates ($a/h=100$) with $q_0 = 10^4$, (e) general angle-ply laminates ($a/h=10$) with $q_0 = 5 \times 10^7$, (f) the asymmetric general angle-ply laminates ($a/h=100$) with $q_0 = 10^4$ 135
5. 9 Effect of boundary conditions on the transient responses under uniformly distributed loading: (a) cross-ply laminates ($a/h=10$) with $q_0 = 10^7$, (b) cross-ply laminates ($a/h=100$) $q_0 = 10^4$, (c) angle-ply laminates ($a/h=10$) with $q_0 = 10^7$, (d) angle-ply laminates ($a/h=100$) $q_0 = 10^4$, (e) general angle-ply laminates ($a/h=10$) with $q_0 = 10^7$, (f) the asymmetric general angle-ply laminates ($a/h=100$) $q_0 = 10^4$ 139
5. 10 Effect of shell theory on the nonlinear transient analysis for the symmetric cross-ply cylindrical shell: (a) thin shell ($a/h=100$), (b) thick shell ($a/h=10$).. 145
5. 11 Effect of time increments on the nonlinear transient analysis for the symmetric cross-ply cylindrical shell ($R_2/a=200$): (a) thin shell ($a/h=100$), (b) thick shell ($a/h=10$)..... 148
5. 12 Effect of R_2/a for cylindrical cross-ply shell under uniform load in SSSS boundary condition; (a) thin shell ($a/h=100$), (b) thick shell ($a/h=10$) 151
5. 13 Effect of shell type for the cross-ply thick ($a/h=10$) shell under uniform load in SSSS boundary condition; (a) $R_2/a=5$, (b) $R_2/a=50$ 152
5. 14 Effect of shell type for the cross-ply thin ($a/h=100$) shell under uniform load in SSSS boundary condition; (a) $R_2/a=5$, (b) $R_2/a=50$ 153

FIGURE

Page

5. 15	Effect of R_2/a for spherical cross-ply shell under uniform load in SSSS boundary condition; (a) thin shell ($a/h=100$), (b) thick shell ($a/h=10$)	154
5. 16	Effect of R_2/a for doubly-curved cross-ply shell under uniform load in SSSS boundary condition; (a) thin shell ($a/h=100$), (b) thick shell ($a/h=10$)	155
5. 17	Effect of lamination schemes for cylindrical shell under uniform load in SSSS boundary condition; (a) thin shell ($a/h=100$), (b) thick shell ($a/h=10$)	158
5. 18	Effect of lamination schemes for spherical shell under uniform load in SSSS boundary condition; (a) thin shell ($a/h=100$), (b) thick shell ($a/h=10$)	159
5. 19	Effect of lamination schemes for doubly-curved shell under uniform load in SSSS boundary condition; (a) thin shell ($a/h=100$), (b) thick shell ($a/h=10$)	160
5. 20	Effect of boundary conditions for cross-ply cylindrical shell under uniform load; (a) thin shell ($a/h=100$, $R_2/a=100$), (b) thick shell ($a/h=10$, $R_2/a=50$)	162
5. 21	Effect of boundary conditions for cross-ply spherical shell under uniform load; (a) thin shell ($a/h=100$, $R_2/a=20$), (b) thick shell ($a/h=10$, $R_2/a=10$)	163
5. 22	Effect of boundary conditions for cross-ply doubly-curved shell under uniform load; (a) thin shell ($a/h=100$, $R_2/a=10$), (b) thick shell ($a/h=10$, $R_2/a=20$).....	164
5. 23	Effect of loading conditions for cross-ply cylindrical shell in SSSS boundary condition; (a) thin shell ($a/h=100$, $R_2/a=5$), (b) thick shell ($a/h=10$, $R_2/a=5$).....	166
5. 24	Effect of the plate theories on static behaviors of simply supported thick cross-ply laminates under mechanical and thermal load; (a) CLPT, (b) FSDT, (c) TSDT	169
5. 25	Thermomechanical behavior of simply supported thin cross-ply laminates.....	170

FIGURE	Page
5. 26 Effect of the laminations on static behaviors of simply supported laminated plates under mechanical and thermal load; (a) Thick laminate, (b) Thin laminate	172
5. 27 Effect of R_2/a on static behavior of cross-ply cylindrical shell under thermomechanical load: (a) Thick shell ($a/h=10$, $\Delta T=100^\circ C$), (b) Thin shell ($a/h=100$, $\Delta T=10^\circ C$).....	173
5. 28 Temperature effect on static behavior of cross-ply cylindrical shell under thermomechanical load: (a) Thick shell ($a/h=10$, $R_2/a=2$), (b) Thin shell ($a/h=100$, $R_2/a=2$)	174
5. 29 Temperature effect on static behavior of cross-ply doubly-curved shell under thermomechanical load: (a) Thick shell ($a/h=10$, $R_2/a=10$), (b) Thin shell ($a/h=100$, $R_2/a=10$)	175
5. 30 Temperature effect on static behavior of cross-ply spherical shell under thermomechanical load: (a) Thick shell ($a/h=10$, $R_2/a=2$), (b) Thin shell ($a/h=100$, $R_2/a=2$)	176
5. 31 Transient behavior of the cross-ply laminates with simply supported boundary condition; (a) Thick laminate under impact load, (b) Thick laminate under uniform load, (c)Thin laminate under impact load, (d) Thin laminate under uniform load.....	178
5. 32 Transient behavior of the angle-ply laminates with simply supported boundary condition; (a) Thick laminate under impact load, (b) Thick laminate under uniform load, (c)Thin laminate under impact load, (d) Thin laminate under uniform load.....	180
5. 33 Transient behavior of the general laminates with simply supported boundary condition; (a) Thick laminate under impact load, (b) Thick laminate under uniform load, (c)Thin laminate under impact load, (d) Thin laminate under uniform load.....	182
5. 34 Effect of the elastic materials on the transient behavior of the thick cross-ply laminates with simply supported boundary condition; (a) Thick laminate under uniform load, (b) GrEp case, (c) GlEp case,(d) BrEp case.....	185

FIGURE	Page
5. 35 Effect of the elastic materials on the transient behavior of the thin cross-ply laminates with simply supported boundary condition; (a) Thin laminate under uniform load, (b) GrEp case, (c) GLEp case, (d) BrEp case.....	187
5. 36 Effect of the boundary conditions on the transient behavior of the cross-ply laminates; (a) Thick laminate under thermomechanical load, (b) Thin laminate under thermomechanical load	190
5. 37 Temperature effect on nonlinear transient behavior of cross-ply cylindrical shell ($R_2/a=2$) under thermomechanical load: (a) Thick shell ($a/h=10$), (b) Thin shell ($a/h=100$)	192
5. 38 Temperature effect on nonlinear transient behavior of cross-ply cylindrical shell ($R_2/a=200$) under thermomechanical load: (a) Thick shell ($a/h=10$), (b) Thin shell ($a/h=100$)	193
5. 39 Effect of R_2/a on nonlinear transient behavior of cross-ply shell under thermomechanical load: (a) Cylindrical shell ($a/h=100$, $\Delta T=10^\circ C$), (b) Spherical shell ($a/h=100$, $\Delta T=10^\circ C$)	195
5. 40 Effect of shell types on nonlinear transient behavior of cross-ply shell under thermomechanical load: (a) Thick shell ($a/h=10$, $\Delta T=100^\circ C$), (b) Thin shell ($a/h=100$, $\Delta T=10^\circ C$)	197
5. 41 Effect of boundary conditions on nonlinear transient behavior of cross-ply shell under thermomechanical load: (a) Thick shell ($a/h=10$, $\Delta T=150^\circ C$, $R_2/a=100$), (b) Thin shell ($a/h=100$, $\Delta T=10^\circ C$, $R_2/a=20$).....	198

LIST OF TABLES

TABLE		Page
3. 1	Material properties of magnetostrictive and elastic composite materials	49
3. 2	Inertial coefficients of symmetric cross-ply (m,90,0,90,0)s laminated plate	50
3. 3	Damping coefficients and frequencies for different materials	50
3. 4	Eigenvalue ($-\alpha_d \pm \omega_d$) obtained through the different plate theories	56
3. 5	Suppression times for different CFRP laminates	60
3. 6	Vibration suppression characteristics for the different lamina thickness	61
3. 7	Vibration suppression ratio for the different laminates	62
3. 8	Suppression time for two control gains for different laminates	63
3. 9	T_s and e_r parameter for different CFRP laminates	64
3. 10	Inertial coefficients of symmetric cross-ply (m,90,0,90,0)s laminated shell	67
3. 11	Effect of the mode on the Eigenvalues of the symmetric cross-ply (m,90,0,90,0)s CFRP spherical shells with $R_2/a = 10$	67
3. 12	Effect of the lamination scheme on the Eigenvalues of the symmetric cross-ply CFRP spherical shells with $R_2/a = 3$	69
3. 13	Eigenvalues of the symmetric cross-ply (m,90,0,90,0)s CFRP laminated shells by Donnell shell theory	71
3. 14	Eigenvalues of the symmetric cross-ply (m,90,0,90,0)s CFRP laminated shells by Sanders shell theory.	72
3. 15	Selected center displacement versus time of the symmetric cross-ply (m,90,0,90,0)s CFRP laminated shells with $R_2/a = 5$ by Sanders shell theory ..	80
3. 16	Maximum transverse deflection and vibration suppression time for the symmetric cross-ply (m,90,0,90,0)s CFRP laminated shells	81

TABLE	Page
3. 17 Vibration suppression characteristics for the thin symmetric cross-ply (m,90,0,90,0) _s laminated shells with the different composite materials.....	82
3. 18 Vibration suppression characteristics for the thick symmetric cross-ply (m,90,0,90,0) _s laminated shells with the different composite materials.....	83
4. 1 Deflection suppression time for the different smart layer positions on the symmetric cross-ply CFRP laminated plate (m,90,0,90,0) _s	108
4. 2 Suppression times for the different smart layer thicknesses in symmetric cross-ply laminated plate (m,90,0,90,0) _s	109
5. 1 Nondimensional center deflection (w/h) for symmetric cross-ply and angle-ply thick ($a/h = 10$) laminates under different load and boundary conditions..	121
5. 2 Nondimensional center deflection (w/h) for symmetric cross-ply and angle-ply thin ($a/h = 100$) laminates under different load and boundary conditions .	122
5. 3 Nondimensional center deflection (w/h) for symmetric and asymmetric general angle-ply thick ($a/h = 10$) laminates under different load and boundary conditions	123
5. 4 Nondimensional center deflection (w/h) for symmetric and asymmetric general angle-ply thin ($a/h = 100$) laminates under different load and boundary conditions	124
5. 5 Nondimensionalized transverse deflections versus time of the simply supported cross-ply laminates subjected to uniformly distributed load ($a/h = 10$; $\Delta t = 0.0001$; 4x4L mesh)	131
5. 6 Nondimensionalized transverse deflections versus time of the simply supported cross-ply laminates subjected to uniformly distributed load ($a/h = 100$; $\Delta t = 0.0005$; 4x4L mesh)	132
5. 7 Nondimensionalized maximum transverse deflections and deflection suppression time for different lamination schemes.....	133
5. 8 Nondimensionalized maximum transverse deflections and deflection suppression time by nonlinear TSDT.....	143

TABLE	Page
5. 9 Selected center displacement of the symmetric cross-ply thick ($a/h = 10$) shell with $R_2/a = 2$ by Donnell and Sanders shell theories.....	146
5. 10 Selected center displacement of the symmetric cross-ply thin ($a/h = 100$) shell with $R_2/a = 2$ by Donnell and Sanders shell theories.....	147
5. 11 Maximum transverse deflection and deflection suppression time for the symmetric cross-ply cylindrical shells	150
5. 12 Maximum transverse deflection and deflection suppression time for the symmetric cross-ply shells by Sanders shell theory	156
5. 13 Vibration suppression characteristics for the symmetric cross-ply laminated shells with the different lamination.....	161
5. 14 Nondimensionalized maximum transverse deflections and deflection suppression time by nonlinear TSDT.....	165
5. 15 Nondimensionalized center displacements of the simply supported thick cross-ply laminate under thermomechanical loading by CLPT, FSDT, and TSDT....	168
5. 16 Nonlinear nondimensionalized center displacements of the simply supported thin cross-ply laminate under thermomechanical loading by TSDT	168
5. 17 Nondimensionalized maximum center displacements and vibration suppression time of cross-ply laminates for different elastic materials	184
5. 18 Nondimensionalized maximum center displacements and vibration suppression time of CFRP cross-ply laminates under thermomechanical loading.....	189
5. 19 Maximum transverse deflection and vibration suppression time for the symmetric cross-ply cylindrical shells	194
5. 20 Nondimensionalized maximum center displacements and vibration suppression time of cross-ply laminates for different shell types	196

1. INTRODUCTION

1.1. General

Composite materials are widely used in a variety of structures, including army and aerospace vehicles, buildings and smart highways (i.e. civil infrastructure applications) as well in sports equipment and medical prosthetics. Laminated composite structures consist of several layers of different fiber-reinforced laminae bonded together to obtain desired structural properties (e.g. stiffness, strength, wear resistance, damping, and so on). The desired structural properties are achieved by varying the lamina thickness, lamina material properties, and stacking sequence (Reddy 2004 b).

The increased use of laminated composites in various types of structures led to considerable interests in their analysis. Composite materials exhibit high strength-to-weight and stiffness-to-weight ratios, which make them ideally suited for use in weight-sensitive structures. This weight reduction of structures leads to improvement of their structural performance, especially in space applications.

With the availability of functional materials and feasibility of embedding or bonding them to composite structures, new smart structural concepts are emerging to be attractive for potentially high-performance structural applications (Maugin 1988, Gandhi and Thompson 1992, and Srinivasan and McFarland 2001). A *smart structure* is the structure that has surface mounted or embedded sensors and actuators so that it has a capability to sense and take corrective action. Numerous conferences, workshops, and journals dedicated to smart materials and structures stand testimony to this growth. The technological implications of this class of materials and structures are immense: structures that monitor their own health, process monitoring, vibration isolation and control, medical applications, damage detection, noise control and shape control.

This dissertation follows the style and format of *Journal of Structural Engineering*.

As applications of active vibration/deflection controls in aerospace, automobile industries and building applications, the smart structures have received considerable attention (See Lowey 1997 for example). Vibration and shape control of structures is essential to achieve the desirable performance in modern structural systems. Advances made in design and manufacturing of smart structure systems improve the efficiency of the structural performance.

1.2. Smart Materials

Two of the basic elements of a smart structural system are actuators and sensors. These sensors and actuators may be either mounted on the flexible passive structure or embedded inside it. The sensing and control of flexible structures are primarily performed with the help of sensors and actuators which are made of smart materials. Smart materials can be divided into two main types: Passive smart materials are those that respond to external change without assistance. These materials are useful when there is only one correct response. Active smart materials utilize the feedback loop and recognize the change and response to the actuator circuit.

The commonly used smart materials are piezoelectric materials, magnetostrictive materials, electrostrictive materials, shape memory alloys, fiber optics, and electro-rheological fluids. Each smart material has a unique advantage of its own. Piezoelectric materials deform by mechanical loads, and deformation occurs due to the application of electric potential by a converse effect (Bailey and Hubbard 1985, Uchino 1986, Crawley and Luis 1987, and Yellin and Shen 1996). Examples of piezoelectric materials are Rochelle salt, quartz, and PZT ($\text{Pb}(\text{Zr,Ti})\text{O}_3$). Piezoelectric materials exhibit a linear relationship between the electric field and strains up to 100 V/mm. However, the relationship becomes nonlinear for large fields, and the material exhibits hysteresis (Uchino 1986). Furthermore, piezoelectric materials show dielectric aging and hence lack reproducibility of strains, i.e., a drift from zero state of strain is observed under cyclic electric field conditions (Cross and Jang 1988). Magnetostrictive materials produce

deformation (displacement) under magnetic field. Magnetostriction is the development of large mechanical deformations due to the rotations of small magnetic domains when subjected to an external magnetic field (Pratt and Flatau 1995). The shape memory alloys are suitable for static shape control and low frequency dynamic applications (Baz, Imam and McCoy 1990, and Anders, Rogers and Fuller 1991). The electro-rheologic fluids are a class of specially formulated suspensions which undergo a change in the resistance to flow (i.e. viscosity) due to an applied electric field (Choi, Sprecher and Conrad 1990). Among these materials, the piezoelectric and magnetostrictive materials have the capability to serve as sensing and actuation materials.

The magnetostrictive material selected for this study, Terfenol-D, has some dominant advantages as actuators and sensors over other materials. Terfenol-D is a commercially available magnetostrictive material in the form of particles deposited on thin sheets and it is an alloy of terbium, iron, and dysprosium. It can serve both as actuator and sensor and produce strains up to $2500 \mu\text{m}$, which is 10 times more than a piezoceramic material (Newnham 1993 and Kleinke and Unas 1994 a, b). It also has high energy density, negligible weight, and point excitation with a wide frequency bandwidth (Goodfriend and Shoop 1992, Dapino, Flatau, and Calkins 1997, Flatau, Dapino, and Calkins 1998, and Duenas and Carman 2000).

Mechanics of smart material systems involve coupling between electric, magnetic, thermal, and mechanical effects. In addition to this coupling, it may be necessary to account for geometric and material nonlinearities. Toupin (1956) was the first one to consider the material nonlinearity in electro-elastic formulations. Knops (1963) presented a two-dimensional theory of electrostriction and solved a simplified boundary value problem using complex potentials. Rotationally invariant nonlinear thermo-electro-elastic equations were derived by Tiersten (1971, 1993), Baumhauer and Tiersten (1973), and by Nelson (1978). Tiersten (1993) has stressed the importance of including nonlinear terms in the constitutive relations, particularly at large fields. Joshi (1991) presented nonlinear constitutive relations for piezoceramic materials.

Among the currently available sensors and actuators, the smallest ones are of the order of few millimeters. The reduction in size has tremendous technological benefits; however, clear understanding of reliability and system integrity is vital to the efficient and optimum use of these material systems. As dimensions get smaller, induced electro-thermo-mechanical fields get larger. Therefore, the material and geometric nonlinearities should be accounted for (Tzou, Bao, and Ye 1994, Carman and Mitrovic 1995, Kannan and Dasgupta 1997, Smith 1998, and Armstrong 2000).

1.3. Background Literature

The analysis of laminated composites is difficult due to the anisotropic structural behavior and complicated constituent interactions (Reddy 2004 b). Since the transverse shear modulus of composite material is usually very low compared to the in-plane modulus, the shear deformation effects are more pronounced in laminated composites subjected to transverse loads than in the isotropic plates under similar loading. A number of methodologies for the analysis of laminated composite plates and shells are available. The three-dimensional elasticity theory provides the most accurate solutions while the traditional plate and shell theories; namely, the classical theory and first-order and third-order shear deformation theories provide simpler and but adequate solutions for most applications.

The equivalent single-layer (ESL) theories are derived from the 3-D elasticity theory by making suitable assumptions concerning the kinematics of deformation through the thickness of the laminate. These assumptions allow the reduction of a 3-D problem to a 2-D problem. The simplest equivalent single-layer theories are the classical laminate plate theory (CLPT) (Whitney and Leissa 1969 and Whitney 1970), and the first-order shear deformation theory (FSDT) (Whitney and Pagano 1970, Reddy and Chao 1981, Reddy 1997, 2004 b). These theories adequately describe the kinematics of most laminated plates. However, for better inter-laminar stress distributions, higher-order theories need to be used. Reddy (1984a, b, 1997, 1999a, b) developed the equations of motion for the third-order

shear deformation theory for laminated composites using the principle of virtual displacements. The third-order shear deformation theory (TSDT) represents the plate kinematics better and yields better inter-laminar stress distributions. Quadratic variations of the transverse shear strains and stresses through the thickness of the laminate avoid the need for shear correction coefficients that are required in the first-order shear deformation theory.

Surveys of various shell theories can be found in the work of Naghdi (1956) and Bert (1980). Many of these theories were developed originally for thin shells, and are based on the Kirchhoff-Love kinematic hypothesis (classical shell theory) that straight lines normal to the undeformed midsurface remain straight and normal to the midsurface after deformation (i.e. the transverse shear strains are neglected). These theories often yield sufficiently accurate results when the material anisotropy is not severe. However, the classical theories are inadequate for a deformation description of shallow layered composite shells.

Dong and Tso (1972) and Dong, Pister, and Taylor (1962) presented the theory of laminated thin shells with orthotropic and anisotropic materials. Ambartsumyan (1964) analyzed the laminated orthotropic shell and considered the bending-stretching coupling effects. Gulati and Essenberg (1967) and Zukas and Vinson (1971) considered the effect of transverse shear deformation and transverse isotropy in the cylindrical shell. The first-order shear deformation theory of general shells can be found in Sanders (1959), Koiter (1960), and Kraus (1967). Reddy (1984c, 2004b) presented a shear deformation shell theory for laminated composite shells.

Higher-order shear deformation shell theories are also developed by Whitney and Sun 1974, Reddy and Liu (1985), Librescu, Khdeir, and Frederick (1989). They used the principle of virtual displacements to derive the equations of motion.

For nonlinear shell theory, Donnell (1935) presented a set of shell equations for cylindrical shells and his approximations were extended to shallow shells of general geometry which is known as Donnell-Mushtari-Vlasov (DMV) equations. Sanders (1959,

1963) and Koiter (1966) developed more refined nonlinear theory of shell, the Sanders-Koiter equations (also referred to as Sanders theory; Reddy 2004 b).

Bailey and Hubbard (1985) and Crawley and Luis (1987) demonstrated the feasibility of using piezoelectric actuators for free vibration reduction of cantilever beams. A self-sensing active constrained damping layer treatment for Euler-Bernoulli beam was studied by Yellin and Shen (1996). Baz, Iman and McCoy (1990) have investigated vibration control using shape memory alloy actuators and their characterization. Anders, Rogers and Fuller (1991) have analytically demonstrated their control of sound radiation from shape memory alloy hybrid composite panels. By changing the elastic properties of the host structure, Choi, Sprecher and Conrad (1990) demonstrated the vibration reduction effects of electrorheological fluid actuators in a composite beam.

Compared to other smart materials, the magnetostrictive material has significant advantages as actuators. A commercially available magnetostrictive material Terfenol-D is an alloy of terbium, iron, and dysprosium. The use of Terfenol-D particle sheets for vibration suppression has some advantages over other smart materials. In particular, it has easy embedability into host materials, such as the modern Carbon Fiber-Reinforced Polimeric (CFRP) composites, without significantly effecting the structural integrity.

Considerable effort is spent to understand the interaction between magnetostrictive layers and structural composite laminae, and the feasibility of using magnetostrictive materials for active vibration suppressions. Goodfriend and Shoop (1992), Hudson, Busbridge, and Piercy (1999, 2000), and Lim et al. (1999) reviewed the material properties of magnetostrictive material, Terfenol-D, with regard to its use in static and dynamic applications. Anjanaappa and Bi (1993, 1994 a, b) investigated the feasibility of using embedded magnetostrictive mini actuators for smart structural applications, such as vibration suppression of beams. Bryant, Fernandez and Wang (1993) presented results of an experiment in which a rod of magnetostrictive Terfenol-D was used in the dual capacity passive structural support element and an active vibration control actuator. A self-sensing magnetostrictive actuator design based on a linear model of magnetostrictive transduction

for Terfenol-D was developed and analyzed by Pratt and Flatau (1995) and Jones and Garcia (1996). Eda, et al. (1995), Anjanappa and Wu (1996), Krishna Murty, Anjanappa and Wu (1997) and Krishna Murty, et al. (1998) proposed magnetostrictive actuators that take advantage of easy embedability and remote excitation capability of magnetostrictive particle sheets as new actuators. Using a combination of magnetostrictive and ferromagnetic alloys, the combined passive and active damping strategy was proposed by Bhattacharya et al. (2000). Recently, Pulliam, McKnight, and Carman (2002) provided magnetostrictive particulate technology in damping applications.

Reddy (1999b, 2004 b) presented theoretical formulation and finite element formulation for general laminated composite plates. Ang, Reddy and Wang (2000) adopted Timoshenko beam theory to study the analytical solution for strain induced actuators. Reddy and Barbosa (2000) presented a general formulation and analytical solution for simply supported boundary conditions of laminated composite beams with embedded magnetostrictive layers. The Levy type analytical solutions for composite plate by third-order shear deformation theory was presented by Khdeir and Reddy (1999). Pradhan et al. (2001) employed first-order shear deformation theory to study the vibration control of laminated plates. They used a velocity feedback with constant gain distributed controller for vibration suppression.

1.4. Present Study

The main goal of this research is to develop efficient computational procedures for analyzing laminated composite plate and shell structures with embedded smart layers, while accounting for geometric nonlinearity (*von Kármán* sense) and thermo-mechanical effects. The temperature field is assumed to be uniformly distributed through the surface but vary through the thickness of the laminate, and the material properties are not dependent on temperature. Both nonlinear Donnell shell theory and Sanders nonlinear shell theory are used to derive the strains and the equations of motion by third-order shear deformation theory. Three different shell types, spherical, cylindrical, and doubly-curved shells, are

considered. A simple negative velocity feedback control in a closed loop is used to actively control the dynamic response of the structure. Newton-Raphson iteration method is used to solve the nonlinear algebraic equations resulting from the finite element approximation in space and Newmark's time integration scheme.

The present study is divided into three parts. First, the theoretical formulations for laminated composite plates and shells are developed. In the second part, the finite element formulations based on the previously developed theories are developed, and in the third part, various parametric studies are carried out to determine the response of laminated composite structures with smart material layers.

The development of theoretical formulations of composite plates and shells with smart material layers is based on a unified shear deformation theory that includes the CLPT, FSDT, and TSDT. The *von Kármán* strains, constitutive relations, equations of motions and negative velocity feedback are presented in Section 2. In Section 3, analytical solutions for simply supported laminated composite plate/shell structures are presented using the linear version of the plate and shell theories.

Development of the general finite element model for laminated composite plates and shells is discussed in Section 4; linear and nonlinear displacement finite element models for composite plate and shell structures are presented and computer implementation is discussed. The numerical results of linear analysis of laminated composite plates and shells are reported at the end of Section 4.

Section 5 is devoted to numerical results from the various parametric studies of laminated composite plate and shell structures, respectively. The parametric studies conducted include the effect of material properties, lamination schemes, smart layer position, boundary conditions, loading conditions, plate and shell theories, and so on.

Finally, the conclusions and recommendations for the future study of this study are presented in Section 6.

2. THEORETICAL FORMULATIONS

2.1. Methodology

The equivalent single-layer (ESL) models provide sufficiently accurate descriptions of global response for the thin to moderately thick laminates, e.g., gross deflection and fundamental vibration frequencies and associated mode shapes (Reddy 2004 b). The third-order shear deformation theory, which is based on the same assumptions as the classical and first-order plate theories, except for the assumptions on the straightness and normality of a transverse normal during deformation, is used mainly in this study. The reason for expanding the displacements up to the cubic term in the thickness coordinate is to have quadratic variation of the transverse shear stresses and strains through the thickness. This avoids the need for shear correction coefficients as required in the first-order shear deformation plate theory to account for the parabolic variation of the actual shear stress through the thickness of the laminate.

2.2. Displacement Field and Strains

2.2.1. Displacement Field and Strains for Plates

The plate under consideration is composed of a finite number of orthotropic layers of uniform thickness (see Figure 2.1). We begin with the following displacement field (Reddy, 2004):

$$u(x, y, z, t) = u_0 + z\phi_x + z^2\psi_1 + z^3\theta_1 \quad (2.1.a)$$

$$v(x, y, z, t) = v_0 + z\phi_y + z^2\psi_2 + z^3\theta_2 \quad (2.1.b)$$

$$w(x, y, z, t) = w_0 \quad (2.1.c)$$

where t is time, (u, v, w) are the displacements along the (x, y, z) coordinates, (u_0, v_0, w_0) are the displacements of a point on the middle surface and $\phi_x(x, y, 0, t) = \partial u / \partial z$ and

$\phi_y(x, y, 0, t) = \partial v / \partial z$ are the rotations at $z = 0$ of normals to the mid-surface about the y and x axes, respectively.

The particular choice of the displacement field in the equation is dictated by the desire to represent the transverse shear strains by quadratic functions of the thickness coordinate, z , and by the requirement that the transverse normal strain be zero. The function ψ_i and θ_i are determined using the condition that the transverse shear stresses, σ_{xz} and σ_{yz} vanish on the top and bottom surfaces of the plate.

The displacement field for the third-order shear deformation theory (TSDT) of plate now can be expressed in the form (Reddy 2004 b)

$$u(x, y, z, t) = u_0(x, y, t) + z\phi_x(x, y, t) - c_1 z^3 \left(\phi_x + \frac{\partial w_0}{\partial x} \right) \quad (2.2.a)$$

$$v(x, y, z, t) = v_0(x, y, t) + z\phi_y(x, y, t) - c_1 z^3 \left(\phi_y + \frac{\partial w_0}{\partial y} \right) \quad (2.2.b)$$

$$w(x, y, z, t) = w_0(x, y, t) \quad (2.2.c)$$

where the constant c_1 is given by $c_1 = 4/3h^2$, h being the total thickness of the laminate.

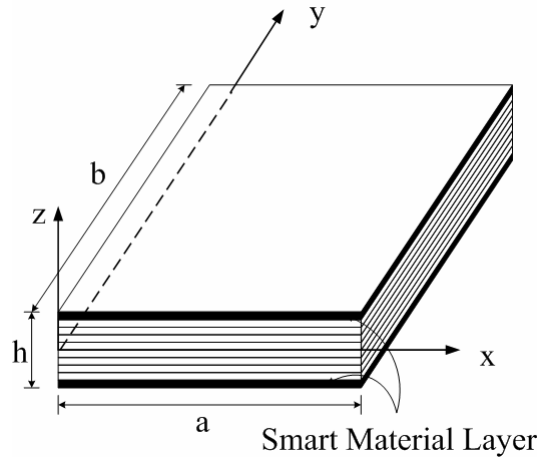


Figure 2.1 Geometry and coordinate system of laminated plate

The nonzero *von Kármán* nonlinear strains in the TSDT are

$$\begin{Bmatrix} \varepsilon_{xx} \\ \varepsilon_{yy} \\ \gamma_{xy} \end{Bmatrix} = \begin{Bmatrix} \varepsilon_{xx}^0 \\ \varepsilon_{yy}^0 \\ \gamma_{xy}^0 \end{Bmatrix} + z \begin{Bmatrix} \varepsilon_{xx}^1 \\ \varepsilon_{yy}^1 \\ \gamma_{xy}^1 \end{Bmatrix} + z^3 \begin{Bmatrix} \varepsilon_{xx}^3 \\ \varepsilon_{yy}^3 \\ \gamma_{xy}^3 \end{Bmatrix} \quad (2.3.a)$$

$$\begin{Bmatrix} \gamma_{yz} \\ \gamma_{xz} \end{Bmatrix} = \begin{Bmatrix} \gamma_{yz}^0 \\ \gamma_{xz}^0 \end{Bmatrix} + z^2 \begin{Bmatrix} \gamma_{yz}^2 \\ \gamma_{xz}^2 \end{Bmatrix} \quad (2.3.b)$$

where

$$\begin{Bmatrix} \varepsilon_{xx}^0 \\ \varepsilon_{yy}^0 \\ \gamma_{xy}^0 \end{Bmatrix} = \begin{Bmatrix} \frac{\partial u_0}{\partial x} + \frac{1}{2} \left(\frac{\partial w_0}{\partial x} \right)^2 \\ \frac{\partial v_0}{\partial y} + \frac{1}{2} \left(\frac{\partial w_0}{\partial y} \right)^2 \\ \frac{\partial u_0}{\partial y} + \frac{\partial v_0}{\partial x} + \frac{\partial w_0}{\partial x} \frac{\partial w_0}{\partial y} \end{Bmatrix} \quad (2.4.a)$$

$$\begin{Bmatrix} \varepsilon_{xx}^1 \\ \varepsilon_{yy}^1 \\ \gamma_{xy}^1 \end{Bmatrix} = \begin{Bmatrix} \frac{\partial \phi_x}{\partial x} \\ \frac{\partial \phi_y}{\partial y} \\ \frac{\partial \phi_x}{\partial y} + \frac{\partial \phi_y}{\partial x} \end{Bmatrix} \quad (2.4.b)$$

$$\begin{Bmatrix} \varepsilon_{xx}^3 \\ \varepsilon_{yy}^3 \\ \gamma_{xy}^3 \end{Bmatrix} = -c_1 \begin{Bmatrix} \frac{\partial \phi_x}{\partial x} + \frac{\partial^2 w_0}{\partial x^2} \\ \frac{\partial \phi_y}{\partial y} + \frac{\partial^2 w_0}{\partial y^2} \\ \frac{\partial \phi_x}{\partial y} + \frac{\partial \phi_y}{\partial x} + 2 \frac{\partial^2 w_0}{\partial x \partial y} \end{Bmatrix} \quad (2.4.c)$$

$$\begin{Bmatrix} \gamma_{yz}^0 \\ \gamma_{xz}^0 \end{Bmatrix} = \begin{Bmatrix} \phi_y + \frac{\partial w_0}{\partial y} \\ \phi_x + \frac{\partial w_0}{\partial x} \end{Bmatrix} \quad (2.4.d)$$

$$\begin{Bmatrix} \gamma_{yz}^2 \\ \gamma_{xz}^2 \end{Bmatrix} = -c_2 \begin{Bmatrix} \phi_y + \frac{\partial w_0}{\partial y} \\ \phi_x + \frac{\partial w_0}{\partial x} \end{Bmatrix} \quad (2.4.e)$$

and $c_2 = \frac{4}{h^2}$.

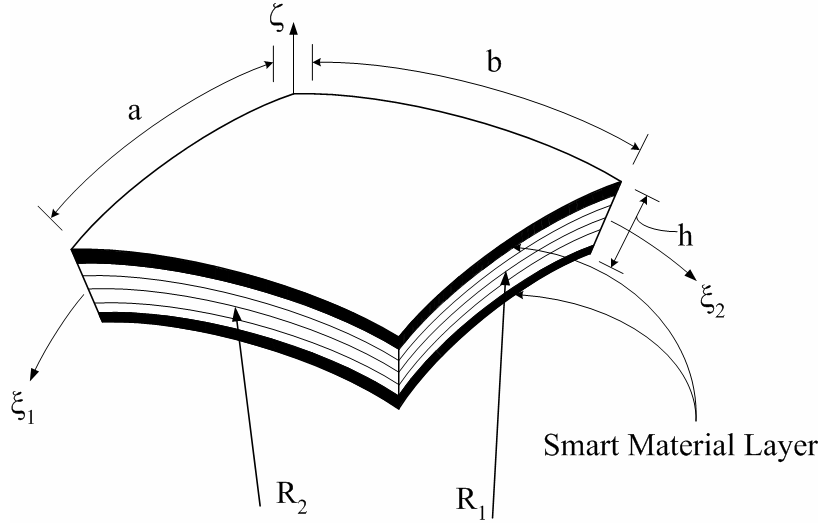


Figure 2.2 Geometry and coordinate system of laminated shell

2.2.2. Kinetics of Shells

Let (ξ_1, ξ_2, ζ) denote the orthogonal curvilinear coordinates such that the ξ_1 – and ξ_2 – curves are lines of curvature on the mid-surface $\zeta = 0$, and ζ – curves are straight lines perpendicular to the surface $\zeta = 0$ (see Figure 2.2). For cylindrical, spherical, and doubly-curved shells discussed in this study, the lines of principal curvature coincide with

the coordinate lines. The values of the principal radii of curvature of the middle surface are denoted by R_1 and R_2 . For additional details consult the textbook by Reddy (2004 b).

The total tensile force on the differential element in the ξ_1 direction is $N_1\alpha_2 d\xi_2$. This force can be computed by integrating $\sigma_1 dA_2$ over the thickness of the shell.

$$N_1\alpha_2 d\xi_2 = \int_{-h/2}^{h/2} \sigma_1 dA_2 = \alpha_2 \int_{-h/2}^{h/2} \sigma_1 \left(1 + \frac{\zeta}{R_2}\right) d\xi_2 d\zeta \quad (2.5)$$

where N_1 is the tensile force per unit length along a ξ_2 coordinate line, α_2 is the surface metric, and h is the thickness of the shell.

$$N_1 = \int_{-h/2}^{h/2} \sigma_1 \left(1 + \frac{\zeta}{R_2}\right) d\zeta \quad (2.6)$$

The remaining stress resultants per unit length can be derived in the similar way (Reddy 2004 b). The complete set of force and moment resultants is given by

$$\begin{Bmatrix} N_1 \\ N_2 \\ N_{12} \\ N_{21} \end{Bmatrix} = \int_{-h/2}^{h/2} \begin{Bmatrix} \sigma_1 \left(1 + \frac{\zeta}{R_2}\right) \\ \sigma_2 \left(1 + \frac{\zeta}{R_1}\right) \\ \sigma_6 \left(1 + \frac{\zeta}{R_2}\right) \\ \sigma_6 \left(1 + \frac{\zeta}{R_1}\right) \end{Bmatrix} d\zeta \quad (2.7.a)$$

$$\begin{Bmatrix} Q_1 \\ Q_2 \end{Bmatrix} = \int_{-h/2}^{h/2} \begin{Bmatrix} \sigma_5 \left(1 + \frac{\zeta}{R_2}\right) \\ \sigma_4 \left(1 + \frac{\zeta}{R_1}\right) \end{Bmatrix} d\zeta \quad (2.7.b)$$

$$\begin{Bmatrix} M_1 \\ M_2 \\ M_{12} \\ M_{21} \end{Bmatrix} = \int_{-h/2}^{h/2} \begin{Bmatrix} \zeta \sigma_1 \left(1 + \frac{\zeta}{R_2} \right) \\ \zeta \sigma_2 \left(1 + \frac{\zeta}{R_1} \right) \\ \zeta \sigma_6 \left(1 + \frac{\zeta}{R_2} \right) \\ \zeta \sigma_6 \left(1 + \frac{\zeta}{R_1} \right) \end{Bmatrix} d\zeta \quad (2.7.c)$$

The shear stress resultants N_{12} and N_{21} , and the twisting moments M_{12} and M_{21} are, in general, not equal. However, for shallow shell ($h/R_1, h/R_2$ less than $1/20$) ζ/R_1 and ζ/R_2 can be neglected in comparison with unity so that one has $N_{12}=N_{21} \equiv N_6$ and $M_{12}=M_{21} \equiv M_6$.

2.2.3. Displacement Field and Strains for Shells

The following form of the displacement field is assumed consistent with moderate thick shell assumptions (Reddy 2004 b):

$$u(\xi_1, \xi_2, \zeta, t) = u_0 + \zeta \phi_1 + \zeta^2 \psi_1 + \zeta^3 \theta_1 \quad (2.8.a)$$

$$v(\xi_1, \xi_2, \zeta, t) = v_0 + \zeta \phi_2 + \zeta^2 \psi_2 + \zeta^3 \theta_2 \quad (2.8.b)$$

$$w(\xi_1, \xi_2, \zeta, t) = w_0 \quad (2.8.c)$$

where (ϕ_1, ϕ_2) , (ψ_1, ψ_2) , and (θ_1, θ_2) are functions to be determined. The function ψ_i and θ_i can be determined by imposing traction free boundary conditions on the top and bottom surfaces of the laminated shell:

$$\sigma_5 \left(\xi_1, \xi_2, \pm \frac{h}{2}, t \right) = 0 \quad (2.9.a)$$

$$\sigma_4\left(\xi_1, \xi_2, \pm \frac{h}{2}, t\right) = 0 \quad (2.9.b)$$

The middle surface kinematic relations for Donnell shell theory are

$$\varepsilon_1 = \frac{\partial u}{\partial X_1} + \frac{w}{R_1} + \frac{1}{2} \left(\frac{\partial w}{\partial X_1} \right)^2 \quad (2.10.a)$$

$$\varepsilon_2 = \frac{\partial v}{\partial X_2} + \frac{w}{R_2} + \frac{1}{2} \left(\frac{\partial w}{\partial X_2} \right)^2 \quad (2.10.b)$$

$$\varepsilon_6 = \frac{\partial u}{\partial X_2} + \frac{\partial v}{\partial X_1} + \left(\frac{\partial w}{\partial X_1} \right) \left(\frac{\partial w}{\partial X_2} \right) \quad (2.10.c)$$

$$\varepsilon_5 = \frac{\partial w}{\partial X_1} + \frac{\partial u}{\partial z} \quad (2.10.d)$$

$$\varepsilon_4 = \frac{\partial w}{\partial X_2} + \frac{\partial v}{\partial z} \quad (2.10.e)$$

The Sanders kinematic relations can be written as

$$\varepsilon_1 = \frac{\partial u}{\partial X_1} + \frac{w}{R_1} + \frac{1}{2} \left(\frac{\partial w}{\partial X_1} - \frac{u}{R_1} \right)^2 \quad (2.11.a)$$

$$\varepsilon_2 = \frac{\partial v}{\partial X_2} + \frac{w}{R_2} + \frac{1}{2} \left(\frac{\partial w}{\partial X_2} - \frac{v}{R_2} \right)^2 \quad (2.11.b)$$

$$\varepsilon_6 = \frac{\partial u}{\partial X_2} + \frac{\partial v}{\partial X_1} + \left(\frac{\partial w}{\partial X_1} - \frac{u}{R_1} \right) \left(\frac{\partial w}{\partial X_2} - \frac{v}{R_2} \right) \quad (2.11.c)$$

$$\varepsilon_5 = \frac{\partial w}{\partial X_1} + \frac{\partial u}{\partial z} - \frac{u}{R_1} \quad (2.11.d)$$

$$\varepsilon_4 = \frac{\partial w}{\partial X_2} + \frac{\partial v}{\partial z} - \frac{v}{R_2} \quad (2.11.e)$$

According to the Donnell's shell kinematics, the displacement field for the third-order shear deformation theory (TSDT) that satisfies the traction free boundary conditions can be expressed such as

$$u_1 = u(\xi_1, \xi_2, \zeta, t) = u_0 + \zeta \phi_1 - c_1 \zeta^3 \left(\phi_1 + \frac{\partial w_0}{\partial X_1} \right) \quad (2.12.a)$$

$$u_2 = v(\xi_1, \xi_2, \zeta, t) = v_0 + \zeta \phi_2 - c_1 \zeta^3 \left(\phi_2 + \frac{\partial w_0}{\partial X_2} \right) \quad (2.12.b)$$

$$u_3 = w(\xi_1, \xi_2, \zeta, t) = w_0 \quad (2.12.c)$$

where (u, v, w) are the displacements along the orthogonal curvilinear coordinates, (u_0, v_0, w_0) are the displacements of a point on the middle surface and ϕ_1 and ϕ_2 are the rotations at $\zeta = 0$ of normals to the mid-surface with respect to the ξ_2 - and ξ_1 - axes, respectively. The constant c_1 is given by $c_1 = 4/3h^2$, h being the total thickness of the laminate.

The consistent Donnell's strains in the third-order shear deformation are

$$\begin{Bmatrix} \varepsilon_1 \\ \varepsilon_2 \\ \varepsilon_6 \end{Bmatrix} = \begin{Bmatrix} \varepsilon_1^0 \\ \varepsilon_2^0 \\ \varepsilon_6^0 \end{Bmatrix} + \zeta \begin{Bmatrix} \kappa_1^0 \\ \kappa_2^0 \\ \kappa_6^0 \end{Bmatrix} + \zeta^3 \begin{Bmatrix} \kappa_1^2 \\ \kappa_2^2 \\ \kappa_6^2 \end{Bmatrix} \quad (2.13.a)$$

$$\begin{Bmatrix} \varepsilon_4 \\ \varepsilon_5 \end{Bmatrix} = \begin{Bmatrix} \varepsilon_4^0 \\ \varepsilon_5^0 \end{Bmatrix} + \zeta^2 \begin{Bmatrix} \kappa_4^1 \\ \kappa_5^1 \end{Bmatrix} \quad (2.13.b)$$

where

$$\begin{Bmatrix} \varepsilon_1^0 \\ \varepsilon_2^0 \\ \varepsilon_6^0 \end{Bmatrix} = \begin{Bmatrix} \frac{\partial u_0}{\partial X_1} + \frac{w}{R_1} + \frac{1}{2} \left(\frac{\partial w_0}{\partial X_1} \right)^2 \\ \frac{\partial v_0}{\partial X_2} + \frac{w}{R_2} + \frac{1}{2} \left(\frac{\partial w_0}{\partial X_2} \right)^2 \\ \frac{\partial v_0}{\partial X_1} + \frac{\partial u_0}{\partial X_2} + \frac{\partial w_0}{\partial X_1} \frac{\partial w_0}{\partial X_2} \end{Bmatrix} \quad (2.14.a)$$

$$\begin{Bmatrix} \kappa_1^0 \\ \kappa_2^0 \\ \kappa_6^0 \end{Bmatrix} = \begin{Bmatrix} \frac{\partial \phi_1}{\partial X_1} \\ \frac{\partial \phi_2}{\partial X_2} \\ \frac{\partial \phi_2}{\partial X_1} + \frac{\partial \phi_1}{\partial X_2} \end{Bmatrix} \quad (2.14.b)$$

$$\begin{Bmatrix} \kappa_1^2 \\ \kappa_2^2 \\ \kappa_6^2 \end{Bmatrix} = -c_1 \begin{Bmatrix} \frac{\partial \phi_1}{\partial X_1} + \frac{\partial^2 w_0}{\partial X_1^2} \\ \frac{\partial \phi_2}{\partial X_2} + \frac{\partial^2 w_0}{\partial X_2^2} \\ \frac{\partial \phi_2}{\partial X_1} + \frac{\partial \phi_1}{\partial X_2} + 2 \frac{\partial^2 w_0}{\partial X_1 \partial X_2} \end{Bmatrix} \quad (2.14.c)$$

$$\begin{Bmatrix} \varepsilon_4^0 \\ \varepsilon_5^0 \end{Bmatrix} = \begin{Bmatrix} \phi_2 + \frac{\partial w_0}{\partial X_2} \\ \phi_1 + \frac{\partial w_0}{\partial X_1} \end{Bmatrix} \quad (2.14.d)$$

$$\begin{Bmatrix} \kappa_4^1 \\ \kappa_5^1 \end{Bmatrix} = -c_2 \begin{Bmatrix} \phi_2 + \frac{\partial w_0}{\partial X_2} \\ \phi_1 + \frac{\partial w_0}{\partial X_1} \end{Bmatrix} \quad (2.14.e)$$

where $c_2 = 3c_1$ and X_i denote the Cartesian coordinates ($dX_i = \alpha_i d\xi_i$, $i = 1, 2$)

The equivalent displacement field for the third-order shear deformation theory for Sanders kinematics is

$$u_1 = u(\xi_1, \xi_2, \zeta, t) = u_0 + \zeta \phi_1 - c_1 \zeta^3 \left(\phi_1 + \frac{\partial w_0}{\partial X_1} - \frac{u_0}{R_1} \right) \quad (2.15.a)$$

$$u_2 = v(\xi_1, \xi_2, \zeta, t) = v_0 + \zeta \phi_2 - c_1 \zeta^3 \left(\phi_2 + \frac{\partial w_0}{\partial X_2} - \frac{v_0}{R_2} \right) \quad (2.15.b)$$

$$u_3 = w(\xi_1, \xi_2, \zeta, t) = w_0 \quad (2.15.c)$$

and the strains are

$$\begin{Bmatrix} \varepsilon_1^0 \\ \varepsilon_2^0 \\ \varepsilon_6^0 \end{Bmatrix} = \begin{Bmatrix} \frac{\partial u_0}{\partial X_1} + \frac{w}{R_1} + \frac{1}{2} \left(\frac{\partial w_0}{\partial X_1} - \frac{u_0}{R_1} \right)^2 \\ \frac{\partial v_0}{\partial X_2} + \frac{w}{R_2} + \frac{1}{2} \left(\frac{\partial w_0}{\partial X_2} - \frac{v_0}{R_2} \right)^2 \\ \frac{\partial v_0}{\partial X_1} + \frac{\partial u_0}{\partial X_2} + \left(\frac{\partial w_0}{\partial X_1} - \frac{u_0}{R_1} \right) \left(\frac{\partial w_0}{\partial X_2} - \frac{v_0}{R_2} \right) \end{Bmatrix} \quad (2.16.a)$$

$$\begin{Bmatrix} \kappa_1^0 \\ \kappa_2^0 \\ \kappa_6^0 \end{Bmatrix} = \begin{Bmatrix} \frac{\partial \phi_1}{\partial X_1} \\ \frac{\partial \phi_2}{\partial X_2} \\ \frac{\partial \phi_2}{\partial X_1} + \frac{\partial \phi_1}{\partial X_2} \end{Bmatrix} \quad (2.16.b)$$

$$\begin{Bmatrix} \kappa_1^2 \\ \kappa_2^2 \\ \kappa_6^2 \end{Bmatrix} = -c_1 \begin{Bmatrix} \frac{\partial \phi_1}{\partial X_1} + \frac{\partial^2 w_0}{\partial X_1^2} - \frac{1}{R_1} \frac{\partial u}{\partial X_1} \\ \frac{\partial \phi_2}{\partial X_2} + \frac{\partial^2 w_0}{\partial X_2^2} - \frac{1}{R_2} \frac{\partial v}{\partial X_2} \\ \frac{\partial \phi_2}{\partial X_1} + \frac{\partial \phi_1}{\partial X_2} + 2 \frac{\partial^2 w_0}{\partial X_1 \partial X_2} - \frac{1}{R_2} \frac{\partial v}{\partial X_1} - \frac{1}{R_1} \frac{\partial u}{\partial X_2} \end{Bmatrix} \quad (2.16.c)$$

$$\begin{Bmatrix} \varepsilon_4^0 \\ \varepsilon_5^0 \end{Bmatrix} = \begin{Bmatrix} \phi_2 + \frac{\partial w_0}{\partial X_2} - \frac{v_0}{R_2} \\ \phi_1 + \frac{\partial w_0}{\partial X_1} - \frac{u_0}{R_1} \end{Bmatrix} \quad (2.16.d)$$

$$\begin{Bmatrix} \kappa_4^1 \\ \kappa_5^1 \end{Bmatrix} = -c_2 \begin{Bmatrix} \phi_2 + \frac{\partial w_0}{\partial X_2} - \frac{v_0}{R_2} \\ \phi_1 + \frac{\partial w_0}{\partial X_1} - \frac{u_0}{R_1} \end{Bmatrix} \quad (2.16.e)$$

where, $c_2 = 3c_1$

2.3. Equations of Motion

The governing equations of motion are derived using the dynamic version of the principle of virtual displacements (Hamilton's principle).

$$0 = \int_0^T (\delta U + \delta V - \delta K) dt \quad (2.17)$$

where δU , δV , and δK denote the virtual strain energy, virtual work done by external applied forces, and the virtual kinetic energy, respectively. For shell or plate structures, laminated or not, the integration over the domain is represented as the product of integration over the plane and integration over the thickness,

$$\int_{Vol} dV = \int_{-\frac{h}{2}}^{\frac{h}{2}} \int_{\Omega} d\Omega dz.$$

Thus, the above Equation (2.17) can be written to

$$\begin{aligned} 0 = & \int_0^t \left[\int_{-h/2}^{h/2} \left\{ \int_{\Omega}^{(k)} [\sigma_1 \delta \varepsilon_1^{(k)} + \sigma_2 \delta \varepsilon_2^{(k)} + \sigma_6 \delta \varepsilon_6^{(k)} + \sigma_4 \delta \varepsilon_4^{(k)} + \sigma_5 \delta \varepsilon_5^{(k)}] dx_1 dx_2 \right\} dz \right. \\ & \left. - \int_{\Omega} q \delta w dx_1 dx_2 - \int_{-h/2}^{h/2} \left\{ \int_{\Omega}^{(k)} \rho [\dot{u} \delta \dot{u} + \dot{v} \delta \dot{v} + \dot{w} \delta \dot{w}] dx_1 dx_2 \right\} dz \right] dt \end{aligned} \quad (2.18)$$

The governing equations of motion can be derived from Equation (2.18) by integrating the displacement gradients by parts to relieve the virtual displacements and setting the coefficients of δu , δv , δw , $\delta\phi_1$ and $\delta\phi_2$ to zero separately (i.e. use the Fundamental Lemma of calculus of variations; see Reddy 2002).

In the derivation, thermal and magnetostrictive effects are taken into consideration with the understanding that the material properties are independent of temperature and magnetic fields, and that the temperature T is a known function of position. Thus temperature and magnetic field enter the formulation only through constitutive equations.

2.3.1. Equations of Motion for TSDT Plates

The equations of motion of the third-order shear deformation theory (TSDT) are

$$\delta u: \quad \frac{\partial N_{xx}}{\partial x} + \frac{\partial N_{xy}}{\partial y} = I_0 \frac{\partial^2 u_0}{\partial t^2} + J_1 \frac{\partial^2 \phi_x}{\partial t^2} - c_1 I_3 \frac{\partial^2}{\partial t^2} \left(\frac{\partial w_0}{\partial x} \right) \quad (2.19.a)$$

$$\delta v: \quad \frac{\partial N_{xy}}{\partial x} + \frac{\partial N_{yy}}{\partial y} = I_0 \frac{\partial^2 v_0}{\partial t^2} + J_1 \frac{\partial^2 \phi_y}{\partial t^2} - c_1 I_3 \frac{\partial^2}{\partial t^2} \left(\frac{\partial w_0}{\partial y} \right) \quad (2.19.b)$$

$$\begin{aligned} \delta w: \quad & \frac{\partial \bar{Q}_x}{\partial x} + \frac{\partial \bar{Q}_y}{\partial y} + \frac{\partial}{\partial x} \left(N_{xx} \frac{\partial w_0}{\partial x} + N_{xy} \frac{\partial w_0}{\partial y} \right) + \frac{\partial}{\partial y} \left(N_{xy} \frac{\partial w_0}{\partial x} + N_{yy} \frac{\partial w_0}{\partial y} \right) \\ & + c_1 \left(\frac{\partial^2 P_{xx}}{\partial x^2} + 2 \frac{\partial^2 P_{xy}}{\partial x \partial y} + \frac{\partial^2 P_{yy}}{\partial y^2} \right) + q = I_0 \frac{\partial^2 w_0}{\partial t^2} - c_1^2 I_6 \frac{\partial^2}{\partial t^2} \left(\frac{\partial^2 w_0}{\partial x^2} + \right. \\ & \left. \frac{\partial^2 w_0}{\partial y^2} \right) + c_1 \left[I_3 \frac{\partial^2}{\partial t^2} \left(\frac{\partial u_0}{\partial x} + \frac{\partial v_0}{\partial y} \right) + J_4 \frac{\partial^2}{\partial t^2} \left(\frac{\partial \phi_x}{\partial x} + \frac{\partial \phi_y}{\partial y} \right) \right] \end{aligned} \quad (2.19.c)$$

$$\delta \phi_x: \quad \frac{\partial \bar{M}_{xx}}{\partial x} + \frac{\partial \bar{M}_{xy}}{\partial y} - \bar{Q}_x = \frac{\partial^2}{\partial t^2} \left(J_1 u_0 + K_2 \phi_x - c_1 J_4 \frac{\partial w_0}{\partial x} \right) \quad (2.19.d)$$

$$\delta \phi_y: \quad \frac{\partial \bar{M}_{xy}}{\partial x} + \frac{\partial \bar{M}_{yy}}{\partial y} - \bar{Q}_y = \frac{\partial^2}{\partial t^2} \left(J_1 v_0 + K_2 \phi_y - c_1 J_4 \frac{\partial w_0}{\partial y} \right) \quad (2.19.e)$$

where

$$\begin{aligned}
\overline{M}_{\alpha\beta} &= M_{\alpha\beta} - c_1 P_{\alpha\beta}, \quad \overline{Q}_\alpha = Q_\alpha - c_2 R_\alpha \quad (\alpha, \beta = x, y) \\
I_i &= \sum_{k=1}^N \int_k^{k+1} \rho^{(k)}(z)^i dz \quad (i = 0, 1, 2, \dots, 6), \\
J_i &= I_i - c_1 I_{i+2} \quad (i = 1, 4) \\
K_2 &= I_2 - 2c_1 I_4 + c_1^2 I_6
\end{aligned} \tag{2.20}$$

The primary and secondary variables of the third-order theory are

$$\text{Primary variables:} \quad u_n, u_s, w_0, \frac{\partial w_0}{\partial n}, \phi_n, \phi_s \tag{2.21}$$

$$\text{Secondary variables:} \quad N_{nn}, \quad N_{ns}, \quad \overline{V}_n, \quad P_{nn}, \quad \overline{M}_{nn}, \quad \overline{M}_{ns}$$

where \overline{V}_n and p are defined as

$$\begin{aligned}
\overline{V}_n &= c_1 \left[\left(\frac{\partial P_{xx}}{\partial x} + \frac{\partial P_{xy}}{\partial y} \right) n_x + \left(\frac{\partial P_{xy}}{\partial x} + \frac{\partial P_{yy}}{\partial y} \right) n_y \right] - c_1 \left[(I_3 \ddot{u}_0 + \right. \\
&\quad \left. J_4 \ddot{\phi}_x - c_1 I_6 \frac{\partial \ddot{w}_0}{\partial x} \right) n_x + \left(I_3 \ddot{v}_0 + J_4 \ddot{\phi}_y - c_1 I_6 \frac{\partial \ddot{w}_0}{\partial y} \right) n_y \right] \\
&\quad + (\overline{Q}_x n_x + \overline{Q}_y n_y) + P(w_0) + c_1 \frac{\partial P_{ns}}{\partial s}
\end{aligned} \tag{2.22.a}$$

$$P(w_0) = \left(N_{xx} \frac{\partial w_0}{\partial x} + N_{xy} \frac{\partial w_0}{\partial y} \right) n_x + \left(N_{xy} \frac{\partial w_0}{\partial x} + N_{yy} \frac{\partial w_0}{\partial y} \right) n_y \tag{2.22.b}$$

$$\begin{Bmatrix} N_{nn} \\ N_{ns} \end{Bmatrix} = \begin{bmatrix} n_x^2 & n_y^2 & 2n_x n_y \\ -n_x n_y & n_x n_y & n_x^2 - n_y^2 \end{bmatrix} \begin{Bmatrix} N_{xx} \\ N_{yy} \\ N_{xy} \end{Bmatrix} \tag{2.22.c}$$

$$\begin{Bmatrix} M_{nn} \\ M_{ns} \end{Bmatrix} = \begin{bmatrix} n_x^2 & n_y^2 & 2n_x n_y \\ -n_x n_y & n_x n_y & n_x^2 - n_y^2 \end{bmatrix} \begin{Bmatrix} M_{xx} \\ M_{yy} \\ M_{xy} \end{Bmatrix} \tag{2.22.d}$$

and (N_{xx}, N_{yy}, N_{xy}) denote the total in-plane forces, (M_{xx}, M_{yy}, M_{xy}) the moments, and (P_{xx}, P_{yy}, P_{xy}) and (R_x, R_y) denote the higher-order stress resultants (see Figure 2.3).

$$\begin{Bmatrix} N_{xx} \\ N_{yy} \\ N_{xy} \end{Bmatrix} = \int_{-\frac{h}{2}}^{\frac{h}{2}} \begin{Bmatrix} \sigma_{xx} \\ \sigma_{yy} \\ \sigma_{xy} \end{Bmatrix} dz \quad (2.23.a)$$

$$\begin{Bmatrix} M_{xx} \\ M_{yy} \\ M_{xy} \end{Bmatrix} = \int_{-\frac{h}{2}}^{\frac{h}{2}} \begin{Bmatrix} \sigma_{xx} \\ \sigma_{yy} \\ \sigma_{xy} \end{Bmatrix} z dz \quad (2.23.b)$$

$$\begin{Bmatrix} P_{xx} \\ P_{yy} \\ P_{xy} \end{Bmatrix} = \int_{-\frac{h}{2}}^{\frac{h}{2}} \begin{Bmatrix} \sigma_{xx} \\ \sigma_{yy} \\ \sigma_{xy} \end{Bmatrix} z^3 dz \quad (2.23.c)$$

$$\begin{Bmatrix} Q_y \\ Q_x \end{Bmatrix} = \int_{-\frac{h}{2}}^{\frac{h}{2}} \begin{Bmatrix} \sigma_{xz} \\ \sigma_{yz} \end{Bmatrix} dz \quad (2.23.d)$$

$$\begin{Bmatrix} R_y \\ R_x \end{Bmatrix} = \int_{-\frac{h}{2}}^{\frac{h}{2}} \begin{Bmatrix} \sigma_{xz} \\ \sigma_{yz} \end{Bmatrix} z^2 dz \quad (2.23.e)$$

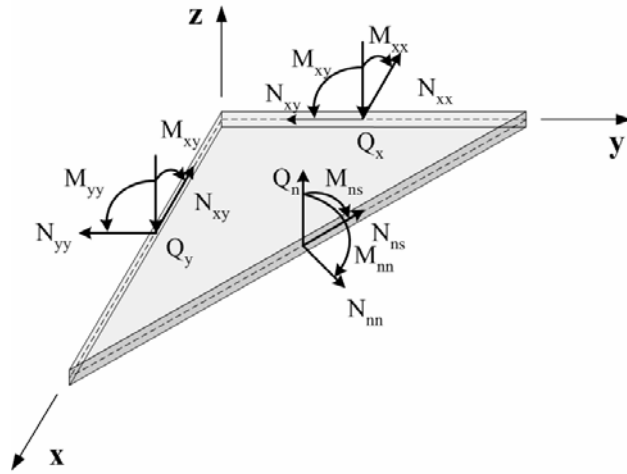


Figure 2.3 Force and moment resultants on a plate element

2.3.2. Equations of Motion for Special Cases

The current third-order shear deformation theory contains the classical and first-order shear deformation theories as special cases. By setting $c_1 = 0$ and the rotation become the slopes of the transverse deflection, one can obtain the classical laminated plate theory and by setting $c_1 = 0$, the first-order shear deformation theory can be obtained.

(1) The Classical Laminated Plate Theory

The displacement field for the classical laminated plate theory (CLPT) is of the form

$$u(x, y, z, t) = u_0(x, y, t) - z \frac{\partial w_0}{\partial x} \quad (2.24.a)$$

$$v(x, y, z, t) = v_0(x, y, t) - z \frac{\partial w_0}{\partial y} \quad (2.24.b)$$

$$w(x, y, z, t) = w_0(x, y, t) \quad (2.24.c)$$

where (u_0, v_0, w_0) denote the displacement of a material point at $(x, y, 0)$. Note that (u_0, v_0) are associated with extensional deformation of the plate while w_0 denotes the bending deflection.

The corresponding *von Kármán* strains of classical laminated plate theory are the following. The transverse strains $(\varepsilon_{xz}, \varepsilon_{yz}, \varepsilon_{zz})$ are identically zero in the classical laminated plate theory.

$$\begin{Bmatrix} \varepsilon_{xx} \\ \varepsilon_{yy} \\ \gamma_{xy} \end{Bmatrix} = \begin{Bmatrix} \varepsilon_{xx}^0 \\ \varepsilon_{yy}^0 \\ \gamma_{xy}^0 \end{Bmatrix} + z \begin{Bmatrix} \varepsilon_{xx}^1 \\ \varepsilon_{yy}^1 \\ \gamma_{xy}^1 \end{Bmatrix} \quad (2.25)$$

where

$$\begin{Bmatrix} \varepsilon_{xx}^0 \\ \varepsilon_{yy}^0 \\ \gamma_{xy}^0 \end{Bmatrix} = \begin{Bmatrix} \frac{\partial u_0}{\partial x} + \frac{1}{2} \left(\frac{\partial w_0}{\partial x} \right)^2 \\ \frac{\partial v_0}{\partial y} + \frac{1}{2} \left(\frac{\partial w_0}{\partial y} \right)^2 \\ \frac{\partial u_0}{\partial y} + \frac{\partial v_0}{\partial x} + \frac{\partial w_0}{\partial x} \frac{\partial w_0}{\partial y} \end{Bmatrix} \quad (2.26.a)$$

$$\begin{Bmatrix} \varepsilon_{xx}^1 \\ \varepsilon_{yy}^1 \\ \gamma_{xy}^1 \end{Bmatrix} = \begin{Bmatrix} -\frac{\partial^2 w_0}{\partial x^2} \\ -\frac{\partial^2 w_0}{\partial y^2} \\ -2 \frac{\partial^2 w_0}{\partial x \partial y} \end{Bmatrix} \quad (2.26.b)$$

where $(\varepsilon_{xx}^0, \varepsilon_{yy}^0, \gamma_{xy}^0)$ are the membrane stains, and $(\varepsilon_{xx}^1, \varepsilon_{yy}^1, \gamma_{xy}^1)$ are the flexural (bending) strains, known as the curvatures.

The equations of motion of the classical theory of laminated plates are given by

$$\delta u: \quad \frac{\partial N_{xx}}{\partial x} + \frac{\partial N_{xy}}{\partial y} = I_0 \frac{\partial^2 u_0}{\partial t^2} - I_1 \frac{\partial^2}{\partial t^2} \left(\frac{\partial w_0}{\partial x} \right) \quad (2.27.a)$$

$$\delta v: \quad \frac{\partial N_{xy}}{\partial x} + \frac{\partial N_{yy}}{\partial y} = I_0 \frac{\partial^2 v_0}{\partial t^2} - I_1 \frac{\partial^2}{\partial t^2} \left(\frac{\partial w_0}{\partial y} \right) \quad (2.27.b)$$

$$\begin{aligned} \delta w: \quad & \frac{\partial^2 M_{xx}}{\partial x^2} + 2 \frac{\partial^2 M_{xy}}{\partial x \partial y} + \frac{\partial^2 M_{yy}}{\partial y^2} + \frac{\partial}{\partial x} \left(N_{xx} \frac{\partial w_0}{\partial x} + N_{xy} \frac{\partial w_0}{\partial y} \right) \\ & + \frac{\partial}{\partial y} \left(N_{xy} \frac{\partial w_0}{\partial x} + N_{yy} \frac{\partial w_0}{\partial y} \right) + q = I_0 \frac{\partial^2 w_0}{\partial t^2} - \\ & I_2 \frac{\partial^2}{\partial t^2} \left(\frac{\partial^2 w_0}{\partial x^2} + \frac{\partial^2 w_0}{\partial y^2} \right) + I_1 \frac{\partial^2}{\partial t^2} \left(\frac{\partial u_0}{\partial x} + \frac{\partial v_0}{\partial y} \right) \end{aligned} \quad (2.27.c)$$

(2) *The First-order Shear Deformation Laminated Plate Theory*

The displacement field for the first-order shear deformation theory (FSDT) can be expressed in the form

$$u(x, y, z, t) = u_0(x, y, t) + z\phi_x(x, y, t) \quad (2.28.a)$$

$$v(x, y, z, t) = v_0(x, y, t) + z\phi_y(x, y, t) \quad (2.28.b)$$

$$w(x, y, z, t) = w_0(x, y, t) \quad (2.28.c)$$

where (u_0, v_0, w_0) denote the displacement of a point on the plane $z = 0$ and (ϕ_x, ϕ_y) are the rotations of a transverse normal about the y – and x – axis, respectively.

The *von Karmán Strains* associated with the displacement field are ($\varepsilon_{zz} = 0$)

$$\begin{Bmatrix} \varepsilon_{xx} \\ \varepsilon_{yy} \\ \gamma_{yz} \\ \gamma_{xz} \\ \gamma_{xy} \end{Bmatrix} = \begin{Bmatrix} \varepsilon_{xx}^0 \\ \varepsilon_{yy}^0 \\ \gamma_{yz}^0 \\ \gamma_{xz}^0 \\ \gamma_{xy}^0 \end{Bmatrix} + z \begin{Bmatrix} \varepsilon_{xx}^1 \\ \varepsilon_{yy}^1 \\ 0 \\ 0 \\ \gamma_{xy}^1 \end{Bmatrix} \quad (2.29)$$

where,

$$\begin{Bmatrix} \varepsilon_{xx}^0 \\ \varepsilon_{yy}^0 \\ \gamma_{yz}^0 \\ \gamma_{xz}^0 \\ \gamma_{xy}^0 \end{Bmatrix} = \begin{Bmatrix} \frac{\partial u_0}{\partial x} + \frac{1}{2} \left(\frac{\partial w_0}{\partial x} \right)^2 \\ \frac{\partial v_0}{\partial y} + \frac{1}{2} \left(\frac{\partial w_0}{\partial y} \right)^2 \\ \frac{\partial w_0}{\partial y} + \phi_y \\ \frac{\partial w_0}{\partial x} + \phi_x \\ \frac{\partial u_0}{\partial y} + \frac{\partial v_0}{\partial x} + \frac{\partial w_0}{\partial x} \frac{\partial w_0}{\partial y} \end{Bmatrix} \quad (2.30.a)$$

$$\begin{Bmatrix} \varepsilon_{xx}^I \\ \varepsilon_{yy}^I \\ 0 \\ 0 \\ \gamma_{xy}^I \end{Bmatrix} = \begin{Bmatrix} \frac{\partial \phi_x}{\partial x} \\ \frac{\partial \phi_y}{\partial y} \\ 0 \\ 0 \\ \frac{\partial \phi_x}{\partial y} + \frac{\partial \phi_y}{\partial x} \end{Bmatrix} \quad (2.30.b)$$

Note that $(\varepsilon_{xx}, \varepsilon_{yy}, \gamma_{xy})$ are linear through the plate thickness, while the transverse shear strains $(\gamma_{xz}, \gamma_{yz})$ are constant.

The equations of motions of FSDT are derived using the dynamic version of the principle of virtual displacements.

$$\delta u: \quad \frac{\partial N_{xx}}{\partial x} + \frac{\partial N_{xy}}{\partial y} = I_0 \frac{\partial^2 u_0}{\partial t^2} + I_1 \frac{\partial^2 \phi_x}{\partial t^2} \quad (2.31.a)$$

$$\delta v: \quad \frac{\partial N_{xy}}{\partial x} + \frac{\partial N_{yy}}{\partial y} = I_0 \frac{\partial^2 v_0}{\partial t^2} + I_1 \frac{\partial^2 \phi_y}{\partial t^2} \quad (2.31.b)$$

$$\begin{aligned} \delta w: \quad & \frac{\partial Q_x}{\partial x} + \frac{\partial Q_y}{\partial y} + \frac{\partial}{\partial x} \left(N_{xx} \frac{\partial w_0}{\partial x} + N_{xy} \frac{\partial w_0}{\partial y} \right) + \\ & \frac{\partial}{\partial y} \left(N_{xy} \frac{\partial w_0}{\partial x} + N_{yy} \frac{\partial w_0}{\partial y} \right) + q = I_0 \frac{\partial^2 w_0}{\partial t^2} \end{aligned} \quad (2.31.c)$$

$$\delta \phi_x: \quad \frac{\partial M_{xx}}{\partial x} + \frac{\partial M_{xy}}{\partial y} - Q_x = I_2 \frac{\partial^2 \phi_x}{\partial t^2} + I_1 \frac{\partial^2 u_0}{\partial t^2} \quad (2.31.d)$$

$$\delta \phi_y: \quad \frac{\partial M_{xy}}{\partial x} + \frac{\partial M_{yy}}{\partial y} - Q_y = I_2 \frac{\partial^2 \phi_y}{\partial t^2} + I_1 \frac{\partial^2 v_0}{\partial t^2} \quad (2.31.e)$$

2.3.3. Equations of Motion for TSDT Donnell Shell Theory

The Euler-Lagrange equations of nonlinear Donnell shell theory for TSDT are

$$\delta u: \quad \frac{\partial N_1}{\partial X_1} + \frac{\partial N_6}{\partial X_2} = I_0 \frac{\partial^2 u_0}{\partial t^2} + J_1 \frac{\partial^2 \phi_1}{\partial t^2} - c_1 I_3 \frac{\partial^2}{\partial t^2} \left(\frac{\partial w_0}{\partial X_1} \right) \quad (2.32.a)$$

$$\delta v: \quad \frac{\partial N_6}{\partial X_1} + \frac{\partial N_2}{\partial X_2} = I_0 \frac{\partial^2 v_0}{\partial t^2} + J_1 \frac{\partial^2 \phi_2}{\partial t^2} - c_1 I_3 \frac{\partial^2}{\partial t^2} \left(\frac{\partial w_0}{\partial X_2} \right) \quad (2.32.b)$$

$$\begin{aligned} \delta w: \quad & \frac{\partial \bar{Q}_1}{\partial X_1} + \frac{\partial \bar{Q}_2}{\partial X_2} + N(w_0) + c_1 \left(\frac{\partial^2 P_1}{\partial X_1^2} + 2 \frac{\partial^2 P_6}{\partial X_1 \partial X_2} + \frac{\partial^2 P_2}{\partial X_2^2} \right) \\ & + q - \frac{N_1}{R_1} - \frac{N_2}{R_2} = I_0 \frac{\partial^2 w_0}{\partial t^2} - c_1^2 I_6 \frac{\partial^2}{\partial t^2} \left(\frac{\partial^2 w_0}{\partial X_1^2} + \frac{\partial^2 w_0}{\partial X_2^2} \right) + \\ & c_1 \left[I_3 \frac{\partial^2}{\partial t^2} \left(\frac{\partial u_0}{\partial X_1} + \frac{\partial v_0}{\partial X_2} \right) + J_4 \frac{\partial^2}{\partial t^2} \left(\frac{\partial \phi_1}{\partial X_1} + \frac{\partial \phi_2}{\partial X_2} \right) \right] \end{aligned} \quad (2.32.c)$$

$$\delta \phi_1: \quad \frac{\partial \bar{M}_1}{\partial X_1} + \frac{\partial \bar{M}_6}{\partial X_2} - \bar{Q}_1 = J_1 \frac{\partial^2 u_0}{\partial t^2} + K_2 \frac{\partial^2 \phi_1}{\partial t^2} - c_1 J_4 \frac{\partial^2}{\partial t^2} \left(\frac{\partial w_0}{\partial X_1} \right) \quad (2.32.d)$$

$$\delta \phi_2: \quad \frac{\partial \bar{M}_6}{\partial X_1} + \frac{\partial \bar{M}_2}{\partial X_2} - \bar{Q}_2 = J_1 \frac{\partial^2 v_0}{\partial t^2} + K_2 \frac{\partial^2 \phi_2}{\partial t^2} - c_1 J_4 \frac{\partial^2}{\partial t^2} \left(\frac{\partial w_0}{\partial X_2} \right) \quad (2.32.e)$$

where

$$\begin{aligned} N(w_0) &= \frac{\partial}{\partial X_1} \left(N_1 \frac{\partial w_0}{\partial X_1} + N_6 \frac{\partial w_0}{\partial X_2} \right) + \frac{\partial}{\partial X_2} \left(N_6 \frac{\partial w_0}{\partial X_1} + N_2 \frac{\partial w_0}{\partial X_2} \right) \\ \bar{M}_\alpha &= M_\alpha - c_1 P_\alpha \quad (\alpha = 1, 2, 6), \quad \bar{Q}_\beta = Q_\beta - c_2 K_\beta \quad (\beta = 1, 2) \\ I_i &= \sum_{k=1}^N \int_k^{k+1} \rho^{(k)}(\zeta)^i d\zeta \quad (i = 0, 1, 2, \dots, 6), \\ J_i &= I_i - c_1 I_{i+2} \quad (i = 1, 4), \quad K_2 = I_2 - 2c_1 I_4 + c_1^2 I_6 \end{aligned} \quad (2.33)$$

2.3.4. Equations of Motion for TSDT Sanders Shell Theory

The equations of motion are

$$\begin{aligned} \delta u: \quad & \frac{\partial N_1}{\partial X_1} + \frac{\partial N_6}{\partial X_2} + \frac{\bar{Q}_1}{R_1} + N_1(u_0, v_0, w_0) + \frac{c_1}{R_1} \left(\frac{\partial P_1}{\partial X_1} + \frac{\partial P_6}{\partial X_2} \right) \\ & = \bar{I}_0 \frac{\partial^2 u_0}{\partial t^2} + \bar{J}_1 \frac{\partial^2 \phi_1}{\partial t^2} - c_1 \bar{I}_3 \frac{\partial^2}{\partial t^2} \left(\frac{\partial w_0}{\partial X_1} \right) \end{aligned} \quad (2.34.a)$$

$$\begin{aligned} \delta v: \quad & \frac{\partial N_6}{\partial X_1} + \frac{\partial N_2}{\partial X_2} + \frac{\bar{Q}_2}{R_2} + N_2(u_0, v_0, w_0) + \frac{c_1}{R_2} \left(\frac{\partial P_2}{\partial X_2} + \frac{\partial P_6}{\partial X_1} \right) \\ & = \bar{I}'_0 \frac{\partial^2 v_0}{\partial t^2} + \bar{J}'_1 \frac{\partial^2 \phi_2}{\partial t^2} - c_1 \bar{I}'_3 \frac{\partial^2}{\partial t^2} \left(\frac{\partial w_0}{\partial X_2} \right) \end{aligned} \quad (2.34.b)$$

$$\begin{aligned} \delta w: \quad & \frac{\partial \bar{Q}_1}{\partial X_1} + \frac{\partial \bar{Q}_2}{\partial X_2} + N_3(u_0, v_0, w_0) + c_1 \left(\frac{\partial^2 P_1}{\partial X_1^2} + 2 \frac{\partial^2 P_6}{\partial X_1 \partial X_2} + \frac{\partial^2 P_2}{\partial X_2^2} \right) \\ & + q - \frac{N_1}{R_1} - \frac{N_2}{R_2} = I_0 \frac{\partial^2 w_0}{\partial t^2} - c_1^2 I_6 \frac{\partial^2}{\partial t^2} \left(\frac{\partial^2 w_0}{\partial X_1^2} + \frac{\partial^2 w_0}{\partial X_2^2} \right) + \\ & c_1 \left[\bar{I}_3 \frac{\partial^2}{\partial t^2} \left(\frac{\partial u_0}{\partial X_1} \right) + \bar{I}'_3 \frac{\partial^2}{\partial t^2} \left(\frac{\partial v_0}{\partial X_2} \right) + J_4 \frac{\partial^2}{\partial t^2} \left(\frac{\partial \phi_1}{\partial X_1} + \frac{\partial \phi_2}{\partial X_2} \right) \right] \end{aligned} \quad (2.34.c)$$

$$\delta \phi_1: \quad \frac{\partial \bar{M}_1}{\partial X_1} + \frac{\partial \bar{M}_6}{\partial X_2} - \bar{Q}_1 = \bar{J}_1 \frac{\partial^2 u_0}{\partial t^2} + \bar{K}_2 \frac{\partial^2 \phi_1}{\partial t^2} - c_1 J_4 \frac{\partial^2}{\partial t^2} \left(\frac{\partial w_0}{\partial X_1} \right) \quad (2.34.d)$$

$$\delta \phi_2: \quad \frac{\partial \bar{M}_6}{\partial X_1} + \frac{\partial \bar{M}_2}{\partial X_2} - \bar{Q}_2 = \bar{J}'_1 \frac{\partial^2 v_0}{\partial t^2} + \bar{K}_2 \frac{\partial^2 \phi_2}{\partial t^2} - c_1 J_4 \frac{\partial^2}{\partial t^2} \left(\frac{\partial w_0}{\partial X_2} \right) \quad (2.34.e)$$

where

$$N_1(u_0, v_0, w_0) = -\frac{1}{R_1} \left[N_1 \left(\frac{\partial w_0}{\partial X_1} - \frac{u_0}{R_1} \right) + N_6 \left(\frac{\partial w_0}{\partial X_2} - \frac{v_0}{R_2} \right) \right] \quad (2.35.a)$$

$$N_2(u_0, v_0, w_0) = -\frac{1}{R_2} \left[N_6 \left(\frac{\partial w_0}{\partial X_1} - \frac{u_0}{R_1} \right) + N_2 \left(\frac{\partial w_0}{\partial X_2} - \frac{v_0}{R_2} \right) \right] \quad (2.35.b)$$

$$\begin{aligned}
N_3(u_0, v_0, w_0) = & \frac{\partial}{\partial X_1} \left[N_1 \left(\frac{\partial w_0}{\partial X_1} - \frac{u_0}{R_1} \right) + N_6 \left(\frac{\partial w_0}{\partial X_2} - \frac{v_0}{R_2} \right) \right] \\
& + \frac{\partial}{\partial X_2} \left[N_6 \left(\frac{\partial w_0}{\partial X_1} - \frac{u_0}{R_1} \right) + N_2 \left(\frac{\partial w_0}{\partial X_2} - \frac{v_0}{R_2} \right) \right]
\end{aligned} \tag{2.35.c}$$

$$\begin{aligned}
\bar{M}_\alpha &= M_\alpha - c_1 P_\alpha \quad (\alpha = 1, 2, 6), \quad \bar{Q}_\beta = Q_\beta - c_2 K_\beta \quad (\beta = 1, 2) \\
I_i &= \sum_{k=1}^N \int_k^{k+1} \rho^{(k)}(\zeta)^i d\zeta \quad (i = 0, 1, 2, \dots, 6), \\
J_i &= I_i - c_1 I_{i+2} \quad (i = 1, 4), \quad \bar{K}_2 = I_2 - 2c_1 I_4 + c_1^2 I_6, \\
c_1 &= \frac{4}{3h^2}, \quad c_2 = \frac{4}{h^2} \\
\bar{I}_0 &= I_0 + 2\frac{c_1}{R_1} I_3 + \left(\frac{c_1}{R_1} \right)^2 I_6, \quad \bar{I}'_0 = I_0 + 2\frac{c_1}{R_2} I_3 + \left(\frac{c_1}{R_2} \right)^2 I_6, \\
\bar{J}_1 &= J_1 + \frac{c_1}{R_1} J_4, \quad \bar{J}'_1 = J_1 + \frac{c_1}{R_2} J_4, \\
\bar{I}_3 &= I_3 + \frac{c_1}{R_1} I_6, \quad \bar{I}'_3 = I_3 + \frac{c_1}{R_2} I_6
\end{aligned} \tag{2.35.d}$$

(N_1, N_2, N_6) denote the total in-plane force resultants, (M_1, M_2, M_6) the moment resultants, and (P_1, P_2, P_6) and (K_1, K_2) denote the higher-order stress resultants.

$$\begin{Bmatrix} N_1 \\ N_2 \\ N_6 \end{Bmatrix} = \int_{-\frac{h}{2}}^{\frac{h}{2}} \begin{Bmatrix} \sigma_1 \\ \sigma_2 \\ \sigma_6 \end{Bmatrix} d\zeta \tag{2.36.a}$$

$$\begin{Bmatrix} M_1 \\ M_2 \\ M_6 \end{Bmatrix} = \int_{-\frac{h}{2}}^{\frac{h}{2}} \begin{Bmatrix} \sigma_1 \\ \sigma_2 \\ \sigma_6 \end{Bmatrix} \zeta d\zeta \tag{2.36.b}$$

$$\begin{Bmatrix} P_1 \\ P_2 \\ P_6 \end{Bmatrix} = \int_{-\frac{h}{2}}^{\frac{h}{2}} \begin{Bmatrix} \sigma_1 \\ \sigma_2 \\ \sigma_6 \end{Bmatrix} \zeta^3 d\zeta \tag{2.36.c}$$

$$\begin{Bmatrix} K_2 \\ K_1 \end{Bmatrix} = \int_{-\frac{h}{2}}^{\frac{h}{2}} \begin{Bmatrix} \sigma_5 \\ \sigma_4 \end{Bmatrix} \zeta^2 d\zeta \quad (2.36.d)$$

$$\begin{Bmatrix} Q_2 \\ Q_1 \end{Bmatrix} = \int_{-\frac{h}{2}}^{\frac{h}{2}} \begin{Bmatrix} \sigma_5 \\ \sigma_4 \end{Bmatrix} d\zeta \quad (2.36.e)$$

2.4. Constitutive Relations

In Sections 2.4 - 2.6, the equations are based on shell coordinate system. By setting (ξ_1, ξ_2, ζ) to (x, y, z) , the structural system returns to plate coordinates.

The plate and shell structure under consideration is composed of a finite number of orthotropic layers of uniform thickness. Each composite lamina of the shell is assumed to behave as an orthotropic material, with its material axes oriented arbitrarily with respect to the laminate coordinates. The smart material layer is assumed to be orthotropic in deriving the relations, but taken to be isotropic in actual calculations.

From the constitutive relations of the magnetostrictive layer (IEEE standard 319, 1976, 1990, Clark 1980), $\varepsilon = S\sigma + dH$, the constitutive relations for the k^{th} lamina (magnetostrictive layer) when referred to the shell laminate coordinates can be written

$$\begin{Bmatrix} \sigma_1 \\ \sigma_2 \\ \sigma_6 \end{Bmatrix}^{(k)} = \begin{bmatrix} \bar{Q}_{11} & \bar{Q}_{12} & \bar{Q}_{16} \\ \bar{Q}_{12} & \bar{Q}_{22} & \bar{Q}_{26} \\ \bar{Q}_{16} & \bar{Q}_{26} & \bar{Q}_{66} \end{bmatrix}^{(k)} \left(\begin{Bmatrix} \varepsilon_1 \\ \varepsilon_2 \\ \varepsilon_6 \end{Bmatrix} - \begin{Bmatrix} \bar{\alpha}_1 \\ \bar{\alpha}_2 \\ \bar{\alpha}_6 \end{Bmatrix}^{(k)} \Delta T \right) - \begin{bmatrix} 0 & 0 & \bar{e}_{31} \\ 0 & 0 & \bar{e}_{32} \\ 0 & 0 & \bar{e}_{36} \end{bmatrix}^{(k)} \begin{Bmatrix} 0 \\ 0 \\ H_\zeta \end{Bmatrix} \quad (2.37.a)$$

$$\begin{Bmatrix} \sigma_4 \\ \sigma_5 \end{Bmatrix}^{(k)} = \begin{bmatrix} \bar{Q}_{44} & \bar{Q}_{45} \\ \bar{Q}_{45} & \bar{Q}_{55} \end{bmatrix}^{(k)} \begin{Bmatrix} \varepsilon_4 \\ \varepsilon_5 \end{Bmatrix} - \begin{bmatrix} \bar{e}_{14} & \bar{e}_{24} & 0 \\ \bar{e}_{15} & \bar{e}_{25} & 0 \end{bmatrix}^{(k)} \begin{Bmatrix} 0 \\ 0 \\ H_\zeta \end{Bmatrix} \quad (2.37.b)$$

For the structural part of the composite structure, the part including the electric field intensity H_ζ should be excluded in the constitutive relations.

Equation (2.37) can also be written as

$$\{\sigma\}^{(k)} = [\bar{Q}]^{(k)} \{\varepsilon - \bar{\alpha} \Delta T\} - [\bar{e}]^{(k)} \{H_\zeta\} \quad (2.38)$$

where ΔT is temperature rise from a reference state, $\Delta T = T - T_0$, and $\bar{\alpha}_1$, $\bar{\alpha}_2$, and $\bar{\alpha}_6$ are the transformed thermal expansion coefficients.

$$\bar{\alpha}_1 = \alpha_1 \cos^2 \theta + \alpha_2 \sin^2 \theta \quad (2.39.a)$$

$$\bar{\alpha}_2 = \alpha_1 \sin^2 \theta + \alpha_2 \cos^2 \theta \quad (2.39.b)$$

$$\bar{\alpha}_6 = 2(\alpha_1 - \alpha_2) \sin \theta \cos \theta \quad (2.39.c)$$

The transformed stiffnesses \bar{Q}_{ij} are calculated from the plane stress-reduced stiffnesses Q_{ij} using the transformation relations,

$$\begin{aligned} \bar{Q}_{11} &= Q_{11} \cos^4 \theta + 2(Q_{12} + 2Q_{66}) \sin^2 \theta \cos^2 \theta + Q_{22} \sin^4 \theta \\ \bar{Q}_{12} &= (Q_{11} + Q_{22} - 4Q_{66}) \sin^2 \theta \cos^2 \theta + Q_{12} (\sin^4 \theta + \cos^4 \theta) \\ \bar{Q}_{22} &= Q_{11} \sin^4 \theta + 2(Q_{12} + 2Q_{66}) \sin^2 \theta \cos^2 \theta + Q_{22} \cos^4 \theta \\ \bar{Q}_{16} &= (Q_{11} - Q_{12} - 2Q_{66}) \sin \theta \cos^3 \theta + (Q_{12} - Q_{22} + 2Q_{66}) \sin^3 \theta \cos \theta \\ \bar{Q}_{26} &= (Q_{11} - Q_{12} - 2Q_{66}) \sin^3 \theta \cos \theta + (Q_{12} - Q_{22} + 2Q_{66}) \sin \theta \cos^3 \theta \\ \bar{Q}_{66} &= (Q_{11} + Q_{22} - 2Q_{12} - 2Q_{66}) \sin^2 \theta \cos^2 \theta + Q_{66} (\sin^4 \theta + \cos^4 \theta) \\ \bar{Q}_{44} &= Q_{44} \cos^2 \theta + Q_{55} \sin^2 \theta \\ \bar{Q}_{45} &= (Q_{55} - Q_{44}) \cos \theta \sin \theta \\ \bar{Q}_{55} &= Q_{55} \cos^2 \theta + Q_{44} \sin^2 \theta \end{aligned} \quad (2.40)$$

Here θ is the angle measured counter-clockwise from the shell x_1 coordinate to the material 1-coordinate. The coefficients $Q_{ij}^{(k)}$ are known in terms of engineering constants of the k th layer:

$$\begin{aligned} Q_{11} &= \frac{E_1}{1 - \nu_{12}\nu_{21}}, \quad Q_{12} = \frac{\nu_{12}E_2}{1 - \nu_{12}\nu_{21}} = \frac{\nu_{21}E_1}{1 - \nu_{12}\nu_{21}}, \quad Q_{22} = \frac{E_2}{1 - \nu_{12}\nu_{21}} \\ Q_{44} &= G_{23}, \quad Q_{55} = G_{13}, \quad Q_{66} = G_{12} \end{aligned} \quad (2.41)$$

and $\bar{e}_{ij}^{(k)}$ are the transformed magnetostrictive coupling moduli of the k^{th} lamina.

$$\begin{aligned} \bar{e}_{31} &= e_{31} \cos^2 \theta + e_{32} \sin^2 \theta \\ \bar{e}_{32} &= e_{31} \sin^2 \theta + e_{32} \cos^2 \theta \\ \bar{e}_{36} &= (e_{31} - e_{32}) \sin \theta \cos \theta \\ \bar{e}_{14} &= (e_{15} - e_{24}) \sin \theta \cos \theta \\ \bar{e}_{24} &= e_{24} \cos^2 \theta + e_{15} \sin^2 \theta \\ \bar{e}_{25} &= (e_{15} - e_{24}) \sin \theta \cos \theta \\ \bar{e}_{15} &= e_{15} \cos^2 \theta + e_{24} \sin^2 \theta \end{aligned} \quad (2.42)$$

2.5. Velocity Feedback Control

The smart layer produces an actuating force required to control vibration and deflection in a smart plate or shell structure, based on a control law. From a structural point of view, the two fundamental types for realizing control are the open-loop control and the closed-loop control known as the feedback control. A sensor to measure the output is not required for the open-loop control. The feedback strategy requires sensors for control system design and has the potential to give much better performance than the open-loop control (Franklin, Powell and Emani-Naeini 2000, Bishop and Dorf 2001). Because of the

simplicity, direct output measurement feedback control is a promising solution to the practical problems (Balas 1979, Chung, Liu and Chu 1993).

Magnetostrictive material is selected to actively control the structural system by the simple control algorithm, a negative velocity feedback control, where the feedback amplitude varies by the negative velocity. The constant control gain is assumed in this study.

Considering velocity proportional closed-loop feedback control shown in Figure 2.4, the magnetic field intensity H_ζ can be expressed in terms of coil constant k_c and coil current $I(\xi_1, \xi_2, t)$ which is related to the velocity as

$$H_\zeta(\xi_1, \xi_2, t) = k_c I(\xi_1, \xi_2, t) \quad (2.43)$$

$$k_c = \frac{n_c}{\sqrt{b_c^2 + 4r_c^2}} \quad (2.44)$$

$$I(\xi_1, \xi_2, t) = c(t) \frac{\partial w_0}{\partial t} \quad (2.45)$$

where b_c is the coil width, r_c is coil radius, n_c is number of turns in the coil, and $c(t)$ is the control gain (Krishna Murty, Anjanappa and Wu 1977)

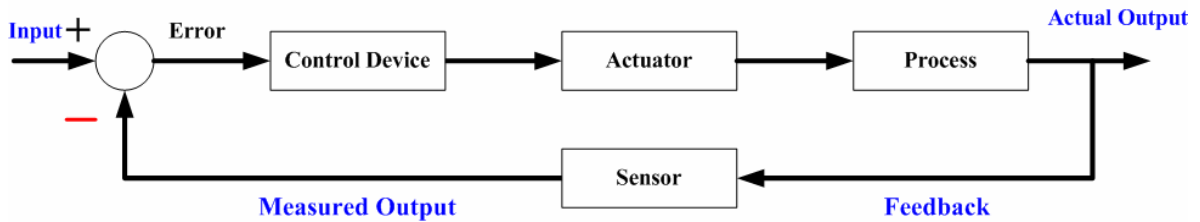


Figure 2.4 Closed-loop feedback control system

2.6. Laminated Constitutive Equations

The force resultants can be expressed in terms of the strain components as follows:

$$\begin{Bmatrix} \{N\} \\ \{M\} \\ \{P\} \end{Bmatrix} = \begin{bmatrix} [A] & [B] & [E] \\ [B] & [D] & [F] \\ [E] & [F] & [H] \end{bmatrix} \begin{Bmatrix} \{\varepsilon^0\} \\ \{\kappa^0\} \\ \{\kappa^2\} \end{Bmatrix} - \begin{Bmatrix} \{N^M\} \\ \{M^M\} \\ \{P^M\} \end{Bmatrix} - \begin{Bmatrix} \{N^T\} \\ \{M^T\} \\ \{P^T\} \end{Bmatrix} \quad (2.46.a)$$

$$\begin{Bmatrix} \{Q\} \\ \{R\} \end{Bmatrix} = \begin{bmatrix} [A] & [D] \\ [D] & [F] \end{bmatrix} \begin{Bmatrix} \{\varepsilon^0\} \\ \{\kappa^1\} \end{Bmatrix} \quad (2.46.b)$$

The stiffnesses A_{ij} , D_{ij} , and F_{ij} are defined for $i, j = 1, 2, 6$ as well as $i, j = 4, 5$. The stiffnesses B_{ij} , E_{ij} , and H_{ij} are defined only for $i, j = 1, 2, 6$. The coefficients of A_{ij} , B_{ij} , D_{ij} , E_{ij} , F_{ij} , and H_{ij} are given in terms of the layer coordinates ζ_{k+1} and ζ_k and lamina stiffnesses \bar{Q}_{ij} .

$$(A_{ij}, B_{ij}, D_{ij}, E_{ij}, F_{ij}, H_{ij}) = \sum_{k=1}^N \int_{\zeta_k}^{\zeta_{k+1}} \bar{Q}_{ij}^{(k)}(1, \zeta, \zeta^2, \zeta^3, \zeta^4, \zeta^6) d\zeta \quad (2.47)$$

The magnetostrictive stress resultants $\{N^M\}$, $\{M^M\}$, and $\{P^M\}$ are defined by

$$\begin{Bmatrix} N_1^M \\ N_2^M \\ N_6^M \end{Bmatrix} = \sum_{k=1}^{N_m} \int_{\zeta_k}^{\zeta_{k+1}} \begin{Bmatrix} e_{31} \\ e_{32} \\ e_{36} \end{Bmatrix}^{(k)} H_\zeta d\zeta \quad (2.48.a)$$

$$\begin{Bmatrix} M_1^M \\ M_2^M \\ M_6^M \end{Bmatrix} = \sum_{k=1}^{N_m} \int_{\zeta_k}^{\zeta_{k+1}} \begin{Bmatrix} e_{31} \\ e_{32} \\ e_{36} \end{Bmatrix}^{(k)} H_\zeta \zeta d\zeta \quad (2.48.b)$$

$$\begin{Bmatrix} P_1^M \\ P_2^M \\ P_6^M \end{Bmatrix} = \sum_{k=1}^{N_m} \int_{\zeta_k}^{\zeta_{k+1}} \begin{Bmatrix} e_{31} \\ e_{32} \\ e_{36} \end{Bmatrix}^{(k)} H_\zeta \zeta^3 d\zeta \quad (2.48.c)$$

again,

$$\begin{Bmatrix} \{N^M\} \\ \{M^M\} \\ \{P^M\} \end{Bmatrix} = \begin{Bmatrix} \{A_{3l}^M\} \\ \{B_{3l}^M\} \\ \{E_{3l}^M\} \end{Bmatrix} H_\varsigma = \begin{Bmatrix} \{\tilde{A}_{3l}^M\} \\ \{\tilde{B}_{3l}^M\} \\ \{\tilde{E}_{3l}^M\} \end{Bmatrix} \frac{\partial w}{\partial t} \quad (2.49)$$

The magnetostrictive stiffnesses $\{A_{3l}^M\}$, $\{B_{3l}^M\}$, and $\{E_{3l}^M\}$ are defined for $l = 1, 2, 6$.

$$(\tilde{A}_{3l}^M, \tilde{B}_{3l}^M, \tilde{E}_{3l}^M) = k_c c(t) (A_{3l}^M, B_{3l}^M, E_{3l}^M) = k_c c(t) \sum_{k=1}^{N_m} \int_{\varsigma_k}^{\varsigma_{k+1}} \bar{e}_{3l} (1, \varsigma, \varsigma^3) d\varsigma \quad (2.50)$$

where \bar{e}_{ij} is the transformed moduli of the actuating/sensing material, and H_ς is the electric field intensity, which should be excluded in the constitutive relations for the structural part of the composite structures.

The thermal stress resultants $\{N^T\}$, $\{M^T\}$, and $\{P^T\}$ are defined by

$$\begin{Bmatrix} N_1^T & M_1^T & P_1^T \\ N_2^T & M_2^T & P_2^T \\ N_6^T & M_6^T & P_6^T \end{Bmatrix} = \sum_{k=1}^N \int_{\varsigma_k}^{\varsigma_{k+1}} \begin{bmatrix} \bar{Q}_{11} & \bar{Q}_{12} & \bar{Q}_{16} \\ \bar{Q}_{12} & \bar{Q}_{22} & \bar{Q}_{26} \\ \bar{Q}_{16} & \bar{Q}_{26} & \bar{Q}_{66} \end{bmatrix}^{(k)} \begin{Bmatrix} \bar{\alpha}_1 \\ \bar{\alpha}_2 \\ \bar{\alpha}_6 \end{Bmatrix}^{(k)} (1 \ \varsigma \ \varsigma^3) \Delta T d\varsigma \quad (2.51)$$

where ΔT is temperature rise from the reference state and $\bar{\alpha}_1$, $\bar{\alpha}_2$, and $\bar{\alpha}_6$ are the transformed thermal expansion coefficients which are stated in Equation (2.39).

3. ANALYTICAL SOLUTIONS

3.1. Analytical Solutions for Laminated Composite Plates

3.1.1. Introduction

The exact solutions of partial differential equations on arbitrary domains and for general conditions are not always possible. However, for the simply supported boundary conditions, the linear version of Equation (2.19) can be solved exactly, provided the lamination scheme is cross-ply or anti-symmetric angle-ply laminates. Equations of motion for the third-order shear deformation theory describe five second-order, nonlinear, partial differential equations in terms of five generalized displacements $(u, v, w, \phi_x, \phi_y)$. For linear case, the in-plane displacements (u, v) are uncoupled from the bending deflections, (w, ϕ_x, ϕ_y) , and it is sufficient to consider only the bending equations, Equations (2.19.c), (2.19.d), and (2.19.e).

3.1.2. Boundary Conditions

For simply supported rectangular plates, it is possible to obtain the Navier solutions. There are two types of simply supported boundary conditions as shown in Figure 3.1. The geometry and coordinate system of the rectangular plate are shown in Figure 2.1.

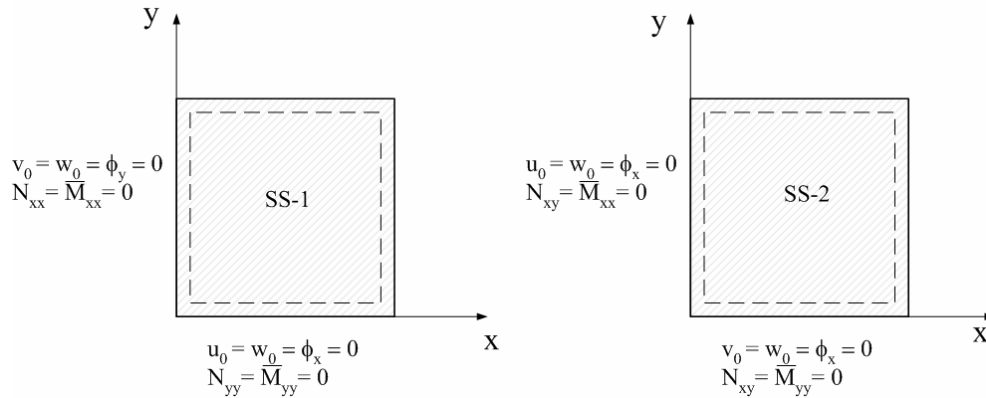


Figure 3.1 Simply supported boundary conditions (SS-1 and SS-2) for TSDT

The first type of simply supported boundary condition is denoted by SS-1 (used for cross-ply laminates), and they are

$$\begin{aligned}
u_0(x, 0, t) = 0, \quad u_0(x, b, t) = 0, \quad v_0(0, y, t) = 0, \quad v_0(a, y, t) = 0 \\
\phi_x(x, 0, t) = 0, \quad \phi_x(x, b, t) = 0, \quad \phi_y(0, y, t) = 0, \quad \phi_y(a, y, t) = 0 \\
w_0(x, 0, t) = 0, \quad w_0(x, b, t) = 0, \quad w_0(0, y, t) = 0, \quad w_0(a, y, t) = 0 \quad (3.1) \\
N_{xx}(0, y, t) = 0, \quad N_{xx}(a, y, t) = 0, \quad N_{yy}(x, 0, t) = 0, \quad N_{yy}(x, b, t) = 0 \\
\overline{M}_{xx}(0, y, t) = 0, \quad \overline{M}_{xx}(a, y, t) = 0, \quad \overline{M}_{yy}(x, 0, t) = 0, \quad \overline{M}_{yy}(x, b, t) = 0
\end{aligned}$$

The second type of simply supported boundary conditions are denoted by SS-2 (used for anti-symmetric angle-ply laminates), and they are

$$\begin{aligned}
u_0(0, y, t) = 0, \quad u_0(a, y, t) = 0, \quad v_0(x, 0, t) = 0, \quad v_0(x, b, t) = 0 \\
\phi_x(x, 0, t) = 0, \quad \phi_x(x, b, t) = 0, \quad \phi_y(0, y, t) = 0, \quad \phi_y(a, y, t) = 0 \\
w_0(x, 0, t) = 0, \quad w_0(x, b, t) = 0, \quad w_0(0, y, t) = 0, \quad w_0(a, y, t) = 0 \quad (3.2) \\
N_{xy}(0, y, t) = 0, \quad N_{xy}(a, y, t) = 0, \quad N_{xy}(x, 0, t) = 0, \quad N_{xy}(x, b, t) = 0 \\
\overline{M}_{xx}(0, y, t) = 0, \quad \overline{M}_{xx}(a, y, t) = 0, \quad \overline{M}_{yy}(x, 0, t) = 0, \quad \overline{M}_{yy}(x, b, t) = 0
\end{aligned}$$

For the case in which the in-plane displacements are uncoupled from the bending deflections, both the SS-1 and SS-2 boundary conditions reduce to the same, and they are given by

$$\begin{aligned}
w_0(x, 0, t) = 0, \quad w_0(x, b, t) = 0, \quad w_0(0, y, t) = 0, \quad w_0(a, y, t) = 0 \\
\phi_x(x, 0, t) = 0, \quad \phi_x(x, b, t) = 0, \quad \phi_y(0, y, t) = 0, \quad \phi_y(a, y, t) = 0 \quad (3.3) \\
\overline{M}_{xx}(0, y, t) = 0, \quad \overline{M}_{xx}(a, y, t) = 0, \quad \overline{M}_{yy}(x, 0, t) = 0, \quad \overline{M}_{yy}(x, b, t) = 0
\end{aligned}$$

3.1.3 Navier Solution

The above boundary conditions can be satisfied by the following expansions of the displacements for both anti-symmetric cross-ply and angle-ply laminates:

$$w_0(x, y, t) = \sum_{n=1}^{\infty} \sum_{m=1}^{\infty} W_{mn}(t) \sin \alpha x \sin \beta y \quad (3.4.a)$$

$$\phi_x(x, y, t) = \sum_{n=1}^{\infty} \sum_{m=1}^{\infty} X_{mn}(t) \cos \alpha x \sin \beta y \quad (3.4.b)$$

$$\phi_y(x, y, t) = \sum_{n=1}^{\infty} \sum_{m=1}^{\infty} Y_{mn}(t) \sin \alpha x \cos \beta y \quad (3.4.c)$$

where $\alpha = \frac{m\pi}{a}$ and $\beta = \frac{n\pi}{b}$, (W_{mn}, X_{mn}, Y_{mn}) are unknowns to be determined.

The loads are also expanded in double Fourier series

$$M_{xx}^M(x, y, t) = \sum_{m=1}^{\infty} \sum_{n=1}^{\infty} M_{mn}^1(t) \sin \alpha x \sin \beta y \quad (3.5.a)$$

$$M_{yy}^M(x, y, t) = \sum_{m=1}^{\infty} \sum_{n=1}^{\infty} M_{mn}^2(t) \sin \alpha x \sin \beta y \quad (3.5.b)$$

$$P_{xx}^M(x, y, t) = \sum_{m=1}^{\infty} \sum_{n=1}^{\infty} P_{mn}^1(t) \sin \alpha x \sin \beta y \quad (3.5.c)$$

$$P_{yy}^M(x, y, t) = \sum_{m=1}^{\infty} \sum_{n=1}^{\infty} P_{mn}^2(t) \sin \alpha x \sin \beta y \quad (3.5.d)$$

$$M_{mn}^1(t) = \frac{4}{ab} \int_0^a \int_0^b M_{xx}^M(x, y, t) \sin \alpha x \sin \beta y \, dx dy \quad (3.6.a)$$

$$M_{mn}^2(t) = \frac{4}{ab} \int_0^a \int_0^b M_{yy}^M(x, y, t) \sin \alpha x \sin \beta y \, dx dy \quad (3.6.b)$$

$$P_{mn}^1(t) = \frac{4}{ab} \int_0^a \int_0^b P_{xx}^M(x, y, t) \sin \alpha x \sin \beta y \, dx dy \quad (3.6.c)$$

$$P_{mn}^2(t) = \frac{4}{ab} \int_0^a \int_0^b P_{yy}^M(x, y, t) \sin \alpha x \sin \beta y \, dx dy \quad (3.6.d)$$

Substituting the above expansions into the governing equations expressed in terms of the generalized displacements, we obtain

$$\begin{aligned}
& \begin{bmatrix} S_{33} & S_{34} & S_{35} \\ S_{43} & S_{44} & S_{45} \\ S_{53} & S_{54} & S_{55} \end{bmatrix} \begin{Bmatrix} W_{mn} \\ X_{mn} \\ Y_{mn} \end{Bmatrix} + \begin{bmatrix} C_{33} & 0 & 0 \\ C_{43} & 0 & 0 \\ C_{53} & 0 & 0 \end{bmatrix} \begin{Bmatrix} \dot{W}_{mn} \\ \dot{X}_{mn} \\ \dot{Y}_{mn} \end{Bmatrix} \\
& + \begin{bmatrix} M_{33} & M_{34} & M_{35} \\ M_{43} & M_{44} & 0 \\ M_{53} & 0 & M_{55} \end{bmatrix} \begin{Bmatrix} \ddot{W}_{mn} \\ \ddot{X}_{mn} \\ \ddot{Y}_{mn} \end{Bmatrix} = \begin{Bmatrix} Q_{mn} \\ 0 \\ 0 \end{Bmatrix}
\end{aligned} \tag{3.7}$$

where

$$\begin{aligned}
S_{33} &= \bar{A}_{55}\alpha^2 + \bar{A}_{44}\beta^2 + c_1^2[H_{11}\alpha^4 + 2(H_{12} + 2H_{66})\alpha^2\beta^2 + H_{22}\beta^4] \\
S_{34} &= \bar{A}_{55}\alpha - c_1[\hat{F}_{11}\alpha^3 + (\hat{F}_{12} + 2\hat{F}_{66})\alpha\beta^2] = S_{43} \\
S_{35} &= \bar{A}_{44}\beta - c_1[\hat{F}_{22}\beta^3 + (\hat{F}_{12} + 2\hat{F}_{66})\alpha^2\beta] = S_{53} \\
S_{45} &= (\bar{D}_{12} + \bar{D}_{66})\alpha\beta = S_{54} \\
S_{44} &= \bar{A}_{55} + \bar{D}_{11}\alpha^2 + \bar{D}_{66}\beta^2, \quad S_{55} = \bar{A}_{44} + \bar{D}_{66}\alpha^2 + \bar{D}_{22}\beta^2 \\
M_{33} &= I_0 + c_1^2 I_6(\alpha^2 + \beta^2), \quad M_{34} = -c_1 J_4 \alpha = M_{43}, \quad M_{44} = K_2 = M_{55} \\
\begin{cases} M_{35} = -c_1 J_4 \beta = M_{53} \\ M_{35} = 0 = M_{53} \end{cases} & \begin{cases} \text{: for cross-ply laminates} \\ \text{: for Antisymmetric angle-ply laminates} \end{cases} \tag{3.8} \\
C_{34} &= C_{35} = C_{44} = C_{45} = C_{54} = C_{55} = 0 \\
C_{33} &= -c_1(\alpha^2 \tilde{E}_{31}^M + \beta^2 \tilde{E}_{32}^M), \quad C_{43} = \alpha(\tilde{B}_{31}^M - c_1 \tilde{E}_{31}^M) \\
C_{53} &= \beta(\tilde{B}_{32}^M - c_1 \tilde{E}_{32}^M), \quad I_i = \sum_{k=1}^N \int_k^{k+1} \rho^{(k)}(z)^i dz \quad (i = 0, 1, 2, \dots, 6) \\
J_i &= I_i - c_1 I_{i+2}, \quad K_2 = I_2 - 2c_1 I_4 + c_1^2 I_6 \\
\bar{A}_{ij} &= A_{ij} - 3c_1 D_{ij}, \quad \bar{D}_{ij} = D_{ij} - 3c_1 F_{ij}, \quad \hat{F}_{ij} = F_{ij} - c_1 H_{ij}
\end{aligned}$$

3.2. Analytical Solutions for Laminated Composite Shells

3.2.1. Modified Sanders Shell Theory

In this study, Donnell and Sanders nonlinear strain-displacement relations are utilized to derive the equation of motion. Sanders nonlinear shell theory is modified for shallow shells by omitting the following terms in the strain-displacement relations;

$$\begin{aligned} & \left(\frac{u_0}{R_1} \right)^2, \quad \left(\frac{v_0}{R_2} \right)^2, \quad \left(\frac{u_0}{R_1} \frac{v_0}{R_2} \right), \quad \left(\frac{u_0}{R_1} \right) \left(\frac{\partial w_0}{\partial X_1} \right), \quad \left(\frac{v_0}{R_2} \right) \left(\frac{\partial w_0}{\partial X_2} \right), \\ & \left(\frac{u_0}{R_1} \right) \left(\frac{\partial w_0}{\partial X_2} \right), \quad \left(\frac{v_0}{R_2} \right) \left(\frac{\partial w_0}{\partial X_1} \right) \end{aligned} \quad (3.9)$$

The equations of motions for modified Sanders shell theory are

$$\begin{aligned} & \frac{\partial N_1}{\partial X_1} + \frac{\partial N_6}{\partial X_2} + \frac{\bar{Q}_1}{R_1} + \frac{c_1}{R_1} \left(\frac{\partial P_1}{\partial X_1} + \frac{\partial P_6}{\partial X_2} \right) \\ & = \bar{I}_0 \frac{\partial^2 u_0}{\partial t^2} + \bar{J}_1 \frac{\partial^2 \phi_1}{\partial t^2} - c_1 \bar{I}_3 \frac{\partial^2}{\partial t^2} \left(\frac{\partial w_0}{\partial X_1} \right) \end{aligned} \quad (3.10.a)$$

$$\begin{aligned} & \frac{\partial N_6}{\partial X_1} + \frac{\partial N_2}{\partial X_2} + \frac{\bar{Q}_2}{R_2} + \frac{c_1}{R_2} \left(\frac{\partial P_2}{\partial X_2} + \frac{\partial P_6}{\partial X_1} \right) \\ & = \bar{I}'_0 \frac{\partial^2 v_0}{\partial t^2} + \bar{J}'_1 \frac{\partial^2 \phi_2}{\partial t^2} - c_1 \bar{I}'_3 \frac{\partial^2}{\partial t^2} \left(\frac{\partial w_0}{\partial X_2} \right) \end{aligned} \quad (3.10.b)$$

$$\begin{aligned} & \frac{\partial \bar{Q}_1}{\partial X_1} + \frac{\partial \bar{Q}_2}{\partial X_2} + N(w_0) + c_1 \left(\frac{\partial^2 P_1}{\partial X_1^2} + 2 \frac{\partial^2 P_6}{\partial X_1 \partial X_2} + \frac{\partial^2 P_2}{\partial X_2^2} \right) \\ & + q - \frac{N_1}{R_1} - \frac{N_2}{R_2} = I_0 \frac{\partial^2 w_0}{\partial t^2} - c_1^2 I_6 \frac{\partial^2}{\partial t^2} \left(\frac{\partial^2 w_0}{\partial X_1^2} + \frac{\partial^2 w_0}{\partial X_2^2} \right) \\ & + c_1 \left[\bar{I}_3 \frac{\partial^2}{\partial t^2} \left(\frac{\partial u_0}{\partial X_1} \right) + \bar{I}'_3 \frac{\partial^2}{\partial t^2} \left(\frac{\partial v_0}{\partial X_2} \right) + J_4 \frac{\partial^2}{\partial t^2} \left(\frac{\partial \phi_1}{\partial X_1} + \frac{\partial \phi_2}{\partial X_2} \right) \right] \end{aligned} \quad (3.10.c)$$

$$\frac{\partial \bar{M}_1}{\partial X_1} + \frac{\partial \bar{M}_6}{\partial X_2} - \bar{Q}_1 = \bar{J}_1 \frac{\partial^2 u_0}{\partial t^2} + \bar{K}_2 \frac{\partial^2 \phi_1}{\partial t^2} - c_1 J_4 \frac{\partial^2}{\partial t^2} \left(\frac{\partial w_0}{\partial X_1} \right) \quad (3.10.d)$$

$$\frac{\partial \bar{M}_6}{\partial X_1} + \frac{\partial \bar{M}_2}{\partial X_2} - \bar{Q}_2 = \bar{J}'_1 \frac{\partial^2 v_0}{\partial t^2} + \bar{K}_2 \frac{\partial^2 \phi_2}{\partial t^2} - c_1 J_4 \frac{\partial^2}{\partial t^2} \left(\frac{\partial w_0}{\partial X_2} \right) \quad (3.10.e)$$

where

$$\begin{aligned} N(w_0) &= \frac{\partial}{\partial X_1} \left(N_1 \frac{\partial w_0}{\partial X_1} + N_6 \frac{\partial w_0}{\partial X_2} \right) + \frac{\partial}{\partial X_2} \left(N_6 \frac{\partial w_0}{\partial X_1} + N_2 \frac{\partial w_0}{\partial X_2} \right) \\ \bar{M}_\alpha &= M_\alpha - c_1 P_\alpha \quad (\alpha = 1, 2, 6), \quad \bar{Q}_\beta = Q_\beta - c_2 K_\beta \quad (\beta = 1, 2) \\ I_i &= \sum_{k=1}^N \int_k^{k+1} \rho^{(k)}(\zeta)^i d\zeta \quad (i = 0, 1, 2, \dots, 6), \\ J_i &= I_i - c_1 I_{i+2} \quad (i = 1, 2, 4), \quad \bar{K}_2 = I_2 - 2c_1 I_4 + c_1^2 I_6, \\ \bar{I}_0 &= I_0 + 2 \frac{c_1}{R_1} I_3 + \left(\frac{c_1}{R_1} \right)^2 I_6, \quad \bar{I}'_0 = I_0 + 2 \frac{c_1}{R_2} I_3 + \left(\frac{c_1}{R_2} \right)^2 I_6, \\ \bar{J}_1 &= J_1 + \frac{c_1}{R_1} J_4, \quad \bar{J}'_1 = J_1 + \frac{c_1}{R_2} J_4, \\ \bar{I}_3 &= I_3 + \frac{c_1}{R_1} I_6, \quad \bar{I}'_3 = I_3 + \frac{c_1}{R_2} I_6 \end{aligned} \quad (3.11)$$

The Sanders nonlinear equations of motion with smart material layers for shallow shells which is expressed in terms of displacements by substituting for the force and moment resultants are summarized in the Appendix A.

3.2.2. Navier Solutions of Shell Theories

For simply-supported shells whose projection in the $x_1 x_2$ - plane is a rectangle, the linear version of Equation (2.32) for Donnell shell theory and Equation (2.34) for Sanders shell theory can be solved exactly, provided the lamination scheme is of antisymmetric cross-ply or symmetric cross-ply type. The Navier solution exists if the following stiffness coefficients are zero:

$$\begin{aligned} A_{i6} &= B_{i6} = D_{i6} = E_{i6} = F_{i6} = H_{i6} = 0, \quad (i = 1, 2) \\ A_{45} &= D_{45} = F_{45} = 0 \end{aligned} \quad (3.12)$$

The simply supported boundary condition (SS1) for the third-order shear deformation theory is assumed to be of the form

$$\begin{aligned}
u_0(x_1, 0, t) = 0, \quad u_0(x_1, b, t) = 0, \quad v_0(o, x_2, t) = 0, \quad v_0(a, x_2, t) = 0 \\
w_0(x_1, 0, t) = 0, \quad w_0(x_1, b, t) = 0, \quad w_0(0, x_2, t) = 0, \quad w_0(a, x_2, t) = 0 \\
\phi_1(x_1, 0, t) = 0, \quad \phi_1(x_1, b, t) = 0, \quad \phi_2(o, x_2, t) = 0, \quad \phi_2(a, x_2, t) = 0 \\
N_1(0, x_2, t) = 0, \quad N_1(a, x_2, t) = 0, \quad N_2(x_1, 0, t) = 0, \quad N_2(x_1, b, t) = 0 \\
\overline{M}_1(0, x_2, t) = 0, \quad \overline{M}_1(a, x_2, t) = 0, \quad \overline{M}_2(x_1, 0, t) = 0, \quad \overline{M}_2(x_1, b, t) = 0
\end{aligned} \tag{3.13}$$

where a and b denote the lengths along the x_1 – and x_2 – directions, respectively.

Following the Navier solution procedure, we assume the following solution form that satisfies the boundary conditions.

$$u_0(x_1, x_2, t) = \sum_{n=1}^{\infty} \sum_{m=1}^{\infty} U_{mn}(t) \cos \alpha x_1 \sin \beta x_2 \tag{3.14.a}$$

$$v_0(x_1, x_2, t) = \sum_{n=1}^{\infty} \sum_{m=1}^{\infty} V_{mn}(t) \sin \alpha x_1 \cos \beta x_2 \tag{3.14.b}$$

$$w_0(x_1, x_2, t) = \sum_{n=1}^{\infty} \sum_{m=1}^{\infty} W_{mn}(t) \sin \alpha x_1 \sin \beta x_2 \tag{3.14.c}$$

$$\phi_1(x_1, x_2, t) = \sum_{n=1}^{\infty} \sum_{m=1}^{\infty} X_{mn}(t) \cos \alpha x_1 \sin \beta x_2 \tag{3.14.d}$$

$$\phi_2(x_1, x_2, t) = \sum_{n=1}^{\infty} \sum_{m=1}^{\infty} Y_{mn}(t) \sin \alpha x_1 \cos \beta x_2 \tag{3.14.e}$$

where $\alpha = \frac{m\pi}{a}$ and $\beta = \frac{n\pi}{b}$. The transverse load q is also expanded in double Fourier sine series

$$q(x_1, x_2, t) = \sum_{n=1}^{\infty} \sum_{m=1}^{\infty} Q_{mn}(t) \sin \alpha x_1 \sin \beta x_2 \tag{3.15.a}$$

$$Q_{mn}(t) = \frac{4}{ab} \int_0^a \int_0^b q(x_1, x_2, t) \sin \alpha x_1 \sin \beta x_2 dx_1 dx_2 \tag{3.15.b}$$

Substituting Equations (3.14) and (3.15) into Equation (2.30) for Donnell shell theory and Equation (2.34) for Sanders' shell theory, we obtain

$$\begin{aligned}
 & \begin{bmatrix} S_{11} & S_{12} & S_{13} & S_{14} & S_{15} \\ S_{21} & S_{22} & S_{23} & S_{24} & S_{25} \\ S_{31} & S_{32} & S_{33} & S_{34} & S_{35} \\ S_{41} & S_{42} & S_{43} & S_{44} & S_{45} \\ S_{51} & S_{52} & S_{53} & S_{54} & S_{55} \end{bmatrix} \begin{Bmatrix} U_{mn} \\ V_{mn} \\ W_{mn} \\ X_{mn} \\ Y_{mn} \end{Bmatrix} + \begin{bmatrix} 0 & 0 & C_{13} & 0 & 0 \\ 0 & 0 & C_{23} & 0 & 0 \\ 0 & 0 & C_{33} & 0 & 0 \\ 0 & 0 & C_{43} & 0 & 0 \\ 0 & 0 & C_{53} & 0 & 0 \end{bmatrix} \begin{Bmatrix} \dot{U}_{mn} \\ \dot{V}_{mn} \\ \dot{W}_{mn} \\ \dot{X}_{mn} \\ \dot{Y}_{mn} \end{Bmatrix} \\
 & + \begin{bmatrix} M_{11} & 0 & M_{13} & M_{14} & 0 \\ 0 & M_{22} & M_{23} & 0 & M_{25} \\ M_{31} & M_{32} & M_{33} & M_{34} & M_{35} \\ M_{41} & 0 & M_{43} & M_{44} & 0 \\ 0 & M_{52} & M_{53} & 0 & M_{55} \end{bmatrix} \begin{Bmatrix} \ddot{U}_{mn} \\ \ddot{V}_{mn} \\ \ddot{W}_{mn} \\ \ddot{X}_{mn} \\ \ddot{Y}_{mn} \end{Bmatrix} = \begin{Bmatrix} 0 \\ 0 \\ Q_{mn} \\ 0 \\ 0 \end{Bmatrix} \quad (3.16)
 \end{aligned}$$

where coefficients S_{ij} , C_{ij} , and M_{ij} are defined below for the two theories.

(1) *Donnell shell theory*

$$S_{11} = -\alpha^2 A_{11} - \beta^2 A_{66}, \quad S_{12} = -\alpha\beta(A_{12} + A_{66})$$

$$S_{13} = \alpha \left(\frac{A_{11}}{R_1} + \frac{A_{12}}{R_2} \right) + c_1 \alpha (\alpha^2 E_{11} + \beta^2 E_{12} + 2\beta^2 E_{66})$$

$$S_{14} = -\alpha^2 \hat{B}_{11} - \beta^2 \hat{B}_{66}, \quad S_{15} = -\alpha\beta(\hat{B}_{12} + \hat{B}_{66})$$

$$S_{22} = -\alpha^2 A_{66} - \beta^2 A_{22}$$

$$S_{23} = \beta \left(\frac{A_{12}}{R_1} + \frac{A_{22}}{R_2} \right) + c_1 \beta (\alpha^2 E_{12} + \beta^2 E_{22} + 2\alpha^2 E_{66})$$

$$S_{24} = -\alpha\beta(\hat{B}_{12} + \hat{B}_{66}), \quad \hat{S}_{25} = -\alpha^2 \hat{B}_{66} - \beta^2 \hat{B}_{22}$$

$$\begin{aligned}
S_{33} &= -c_1^2 [H_{11}\alpha^4 + 2(H_{12} + 2H_{66})\alpha^2\beta^2 + H_{22}\beta^4] - \alpha^2 \hat{A}_{55} \\
&\quad - \beta^2 \hat{A}_{44} - 2\alpha^2 c_1 \left(\frac{E_{11}}{R_1} + \frac{E_{12}}{R_2} \right) - 2\beta^2 c_1 \left(\frac{E_{12}}{R_1} + \frac{E_{22}}{R_2} \right) \\
&\quad - \frac{1}{R_1} \left(\frac{A_{11}}{R_1} + \frac{A_{12}}{R_2} \right) - \frac{1}{R_2} \left(\frac{A_{12}}{R_1} + \frac{A_{22}}{R_2} \right), \\
S_{34} &= c_1 [\alpha^3 \hat{F}_{11} + \alpha\beta^2 (\hat{F}_{12} + 2\hat{F}_{66})] - \alpha \hat{A}_{55} + \alpha \left(\frac{\hat{B}_{11}}{R_1} + \frac{\hat{B}_{12}}{R_2} \right) \\
S_{35} &= c_1 [\beta^3 \hat{F}_{22} + \alpha^2 \beta (\hat{F}_{12} + 2\hat{F}_{66})] - \beta \hat{A}_{44} + \beta \left(\frac{\hat{B}_{12}}{R_1} + \frac{\hat{B}_{22}}{R_2} \right) \\
S_{44} &= -\alpha^2 \bar{D}_{11} - \beta^2 \bar{D}_{66} - \hat{A}_{55}, \quad S_{45} = -\alpha\beta (\bar{D}_{12} + \bar{D}_{66}) \\
S_{55} &= -\alpha^2 \bar{D}_{66} - \beta^2 \bar{D}_{22} - \hat{A}_{44} \\
\hat{B}_{ij} &= B_{ij} - c_1 E_{ij}, \quad \hat{D}_{ij} = D_{ij} - c_1 F_{ij}, \quad \hat{F}_{ij} = F_{ij} - c_1 H_{ij} \\
\bar{D}_{ij} &= \hat{D}_{ij} - c_1 \hat{F}_{ij} = D_{ij} - 2c_1 F_{ij} + c_1^2 H_{ij} \quad (i, j = 1, 2, 6) \\
\bar{A}_{ij} &= A_{ij} - 3c_1 D_{ij}, \quad \bar{D}_{ij} = D_{ij} - 3c_1 F_{ij} \\
\hat{A}_{ij} &= \bar{A}_{ij} - 3c_1 \bar{D}_{ij} = A_{ij} - 6c_1 D_{ij} + 9c_1^2 F_{ij} \quad (i, j = 4, 5) \\
M_{11} &= -I_0, \quad M_{13} = \alpha c_1 I_3, \quad M_{14} = -J_1, \quad M_{22} = -I_0 \\
M_{23} &= \beta c_1 I_3, \quad M_{25} = -J_1, \quad M_{33} = -I_0 - c_1^2 I_6 (\alpha^2 + \beta^2) \\
M_{34} &= c_1 J_4 \alpha, \quad M_{35} = c_1 J_4 \beta, \quad M_{44} = -K_2, \quad M_{55} = -K_2 \\
C_{31} &= \alpha \tilde{A}_{31}^M, \quad C_{32} = \beta \tilde{A}_{32}^M, \quad C_{33} = -c_1 (\alpha^2 \tilde{E}_{31}^M + \beta^2 \tilde{E}_{32}^M) + \frac{\tilde{A}_{31}^M}{R_1} + \frac{\tilde{A}_{32}^M}{R_2} \\
C_{43} &= \alpha (\tilde{B}_{31}^M - c_1 \tilde{E}_{31}^M), \quad C_{53} = \beta (\tilde{B}_{32}^M - c_1 \tilde{E}_{32}^M)
\end{aligned} \tag{3.17}$$

(2) *Sanders shell theory*

$$\begin{aligned}
S_{11} &= -\alpha^2 A_{11} - \beta^2 A_{66} \\
&\quad - \frac{1}{R_1} \left[\frac{1}{R_1} \hat{A}_{55} + 2c_1 (\alpha^2 E_{11} + \beta^2 E_{66}) - \frac{c_1^2}{R_1} (\alpha^2 H_{11} + \beta^2 H_{66}) \right] \\
S_{12} &= -\alpha\beta (A_{12} - A_{66}) \\
&\quad - \alpha\beta \left(\frac{c_1}{R_1} + \frac{c_1}{R_2} \right) (E_{12} + E_{66}) - \alpha\beta \frac{c_1}{R_1} \frac{c_1}{R_2} (H_{12} + H_{66}) \\
S_{13} &= \alpha \left(\frac{A_{11}}{R_1} + \frac{A_{12}}{R_2} \right) + c_1 \alpha (\alpha^2 E_{11} + \beta^2 E_{12} + 2\beta^2 E_{66}) \\
&\quad + \frac{\alpha}{R_1} \left[\hat{A}_{55} + c_1^2 (\alpha^2 H_{11} + \beta^2 H_{12} + 2\beta^2 H_{66}) + c_1 \left(\frac{E_{11}}{R_1} + \frac{E_{12}}{R_2} \right) \right] \\
S_{14} &= -\alpha^2 \hat{B}_{11} - \beta^2 \hat{B}_{66} + \frac{1}{R_1} \left[\hat{A}_{55} - c_1 (\alpha^2 \hat{F}_{11} + \beta^2 \hat{F}_{66}) \right] \tag{3.18} \\
S_{15} &= -\alpha\beta (\hat{B}_{12} + \hat{B}_{66}) - c_1 \frac{1}{R_1} \alpha\beta (\hat{F}_{12} + \hat{F}_{66}) \\
S_{22} &= -\alpha^2 A_{66} - \beta^2 A_{22} \\
&\quad - \frac{1}{R_2} \left[\frac{1}{R_2} \hat{A}_{44} + 2c_1 (\alpha^2 E_{66} + \beta^2 E_{22}) - \frac{c_1^2}{R_2} (\alpha^2 H_{66} + \beta^2 H_{22}) \right] \\
S_{23} &= \beta \left(\frac{A_{12}}{R_1} + \frac{A_{22}}{R_2} \right) + c_1 \beta (\alpha^2 E_{12} + \beta^2 E_{22} + 2\alpha^2 E_{66}) \\
&\quad + \frac{\beta}{R_2} \left[\hat{A}_{44} + c_1^2 (\alpha^2 H_{12} + \beta^2 H_{22} + 2\alpha^2 H_{66}) + c_1 \left(\frac{E_{12}}{R_1} + \frac{E_{22}}{R_2} \right) \right] \\
S_{24} &= -\alpha\beta (\hat{B}_{12} + \hat{B}_{66}) - c_1 \frac{1}{R_2} \alpha\beta (\hat{F}_{12} + \hat{F}_{66}) \\
S_{25} &= -\alpha^2 \hat{B}_{66} - \beta^2 \hat{B}_{22} + \frac{1}{R_2} \left[\hat{A}_{44} - c_1 (\alpha^2 \hat{F}_{66} + \beta^2 \hat{F}_{22}) \right]
\end{aligned}$$

$$\begin{aligned}
S_{33} = & -c_1^2[H_{11}\alpha^4 + 2(H_{12} + 2H_{66})\alpha^2\beta^2 + H_{22}\beta^4] - \alpha^2\hat{A}_{55} \\
& - \beta^2\hat{A}_{44} - 2\alpha^2c_1\left(\frac{E_{11}}{R_1} + \frac{E_{12}}{R_2}\right) - 2\beta^2c_1\left(\frac{E_{12}}{R_1} + \frac{E_{22}}{R_2}\right) \\
& - \frac{1}{R_1}\left(\frac{A_{11}}{R_1} + \frac{A_{12}}{R_2}\right) - \frac{1}{R_2}\left(\frac{A_{12}}{R_1} + \frac{A_{22}}{R_2}\right)
\end{aligned}$$

$$S_{34} = c_1[\alpha^3\hat{F}_{11} + \alpha\beta^2(\hat{F}_{12} + 2\hat{F}_{66})] - \alpha\hat{A}_{55} + \alpha\left(\frac{\hat{B}_{11}}{R_1} + \frac{\hat{B}_{12}}{R_2}\right)$$

$$S_{35} = c_1[\beta^3\hat{F}_{22} + \alpha^2\beta(\hat{F}_{12} + 2\hat{F}_{66})] - \beta\hat{A}_{44} + \beta\left(\frac{\hat{B}_{12}}{R_1} + \frac{\hat{B}_{22}}{R_2}\right)$$

$$S_{44} = -\alpha^2\bar{D}_{11} - \beta^2\bar{D}_{66} - \hat{A}_{55}, \quad S_{45} = -\alpha\beta(\bar{D}_{12} + \bar{D}_{66})$$

$$S_{55} = -\alpha^2\bar{D}_{66} - \beta^2\bar{D}_{22} - \hat{A}_{44}$$

$$\hat{B}_{ij} = B_{ij} - c_1E_{ij}, \quad \hat{D}_{ij} = D_{ij} - c_1F_{ij}, \quad \hat{F}_{ij} = F_{ij} - c_1H_{ij}$$

$$\bar{D}_{ij} = \hat{D}_{ij} - c_1\hat{F}_{ij} = D_{ij} - 2c_1F_{ij} + c_1^2H_{ij} \quad (i, j = 1, 2, 6)$$

$$\bar{A}_{ij} = A_{ij} - 3c_1D_{ij}, \quad \bar{D}_{ij} = D_{ij} - 3c_1F_{ij}$$

$$\hat{A}_{ij} = \bar{A}_{ij} - 3c_1\bar{D}_{ij} = A_{ij} - 6c_1D_{ij} + 9c_1^2F_{ij} \quad (i, j = 4, 5)$$

$$M_{11} = -\bar{I}_0, \quad M_{13} = \alpha c_1\bar{I}_3, \quad M_{14} = -\bar{J}_1$$

$$M_{22} = -\bar{I}'_0, \quad M_{23} = \beta c_1\bar{I}'_3, \quad M_{25} = -\bar{J}'_1$$

$$M_{33} = -I_0 - c_1^2I_6(\alpha^2 + \beta^2), \quad M_{34} = c_1J_4\alpha, \quad M_{35} = c_1J_4\beta$$

$$M_{44} = -\bar{K}_2, \quad M_{55} = -\bar{K}_2$$

$$C_{31} = \alpha\left(\tilde{A}_{31}^M + \frac{c_1}{R_1}\tilde{E}_{31}^M\right), \quad C_{32} = \beta\left(\tilde{A}_{32}^M + \frac{c_1}{R_2}\tilde{E}_{32}^M\right)$$

$$C_{33} = -c_1 (\alpha^2 \tilde{E}_{31}^M + \beta^2 \tilde{E}_{32}^M) + \frac{\tilde{A}_{31}^M}{R_1} + \frac{\tilde{A}_{32}^M}{R_2}$$

$$C_{43} = \alpha (\tilde{B}_{31}^M - c_1 \tilde{E}_{31}^M), \quad C_{53} = \beta (\tilde{B}_{32}^M - c_1 \tilde{E}_{32}^M)$$

3.3. Vibration Control

For vibration control, the solution of the governing equations are sought in the form

$$\begin{aligned} U_{mn}(t) &= U_0 e^{\lambda t}, \quad V_{mn}(t) = V_0 e^{\lambda t}, \quad W_{mn}(t) = W_0 e^{\lambda t} \\ X_{mn}(t) &= X_0 e^{\lambda t}, \quad Y_{mn}(t) = Y_0 e^{\lambda t} \end{aligned} \quad (3.19)$$

and obtain, for non-trivial solution, the result

$$\begin{vmatrix} \bar{S}_{11} & \bar{S}_{12} & \bar{S}_{13} & \bar{S}_{14} & \bar{S}_{15} \\ \bar{S}_{21} & \bar{S}_{22} & \bar{S}_{23} & \bar{S}_{24} & \bar{S}_{25} \\ \bar{S}_{31} & \bar{S}_{32} & \bar{S}_{33} & \bar{S}_{34} & \bar{S}_{35} \\ \bar{S}_{41} & \bar{S}_{42} & \bar{S}_{43} & \bar{S}_{44} & \bar{S}_{45} \\ \bar{S}_{51} & \bar{S}_{52} & \bar{S}_{53} & \bar{S}_{54} & \bar{S}_{55} \end{vmatrix} = 0 \quad (3.20)$$

where

$$\bar{S}_{ij} = S_{ij} + \lambda C_{ij} + \lambda^2 M_{ij} \quad (3.21)$$

For the plate case, the Equation (3.20) reduces to

$$\begin{vmatrix} \bar{S}_{33} & \bar{S}_{34} & \bar{S}_{35} \\ \bar{S}_{43} & \bar{S}_{44} & \bar{S}_{45} \\ \bar{S}_{53} & \bar{S}_{54} & \bar{S}_{55} \end{vmatrix} = 0 \quad (3.22)$$

Equations (3.20) and (3.22) give five sets of eigenvalues and three sets of eigenvalues, respectively. The lowest imaginary part corresponds to the transverse motion. The eigenvalue can be written as $\lambda = -\alpha_d + i\omega_d$, so that the damped motion is given by

$$w_0(x_1, x_2, t) = \frac{1}{\omega_d} e^{-\alpha_d t} \sin \omega_d t \sin \frac{m\pi x_1}{a} \sin \frac{n\pi x_2}{b} \quad (3.23)$$

In arriving at the last solution, the following initial conditions are used:

$$\begin{aligned} u_0(x_1, x_2, 0) &= 0, & \dot{u}_0(x_1, x_2, 0) &= 0 \\ v_0(x_1, x_2, 0) &= 0, & \dot{v}_0(x_1, x_2, 0) &= 0 \\ w_0(x_1, x_2, 0) &= 0, & \dot{w}_0(x_1, x_2, 0) &= 1 \\ \phi_1(x_1, x_2, 0) &= 0, & \dot{\phi}_1(x_1, x_2, 0) &= 0 \\ \phi_2(x_1, x_2, 0) &= 0, & \dot{\phi}_2(x_1, x_2, 0) &= 0 \end{aligned} \quad (3.24)$$

3.4. Analytical Results for Laminated Composite Plates

Using the analytical solutions developed in the previous sections, numerical studies are carried out. In particular, the effect of the position of the smart material layer, the thickness of the smart material layer and the elastic composite layer, and the material properties of the elastic layer, on the frequency and vibration suppression time of the laminated composite plate. Here, the vibration suppression time is defined as the time required to reducing the uncontrolled vibration amplitude to one-tenth of its initial amplitude. Various values of the vibration suppression time ratio T_s (suppression time divided by the maximum suppression time) are obtained as the distance between the magnetostrictive layers and the neutral axis is varied. The vibration suppression time ratio

can be shown to be $T_s = \frac{h_m}{2z_m}$, where h_m is the thickness of the magnetostrictive layer and

z_m is the distance between the mid plane of the magnetostrictive layer and the mid plane of the plate. Studies involving different lamination schemes, layer thickness, and control gain values have also been carried out.

Four different kinds of the elastic composite material are used. CFRP [composite fiber reinforced polymer], Gr-Ep (AS) [graphite-epoxy], Gl-Ep [glass epoxy], Br-Ep [boron

epoxy]. The material properties of magnetostrictive material, Terfenol-D, and typical composite materials are listed in Table 3.1.

Table 3.1 Material properties of magnetostrictive and elastic composite materials

Material	E_1 [GPa]	E_2 [GPa]	G_{13} [GPa]	G_{23} [GPa]	G_{12} [GPa]	ν_{12}	ρ [Kg m ⁻³]
Terfenol-D	26.5	26.5	13.25	13.25	13.25	0.00	9250
CFRP	138.6	8.27	4.96	4.12	4.96	0.26	1824
Gr-Ep(AS)	137.9	8.96	7.20	6.21	7.20	0.30	1450
Gl-Ep	53.78	17.93	8.96	3.45	8.96	0.25	1900
Br-Ep	206.9	20.69	6.9	4.14	6.9	0.30	1950

3.4.1. Vibration Suppression of Different Modes

The vibration suppression characteristics of the first five vibration modes of the composite plates are also studied. Displacement versus time is presented in Figures 3.2(a) and 3.2(b). From the figures, it can be seen that the vibration suppression time decreases very rapidly as mode number increases. This is because the amplitude of vibration that has to be suppressed decreases as the mode number increases. The results have been obtained for a CFRP ($m/90/0/90/0$)_S and Gr-Ep(AS) ($m/90/0/90/0$)_S laminated composites with $h_e = 1$ mm and $h_m = 1$ mm. Here m stands for the magnetostrictive material layer and the subscript “S” stands for symmetric.

3.4.2. Effect of Lamina Material Properties

The influence of lamina material properties on the amplitude of vibration and vibration suppression times has been studied and the results are tabulated. Table 3.2 lists the inertial coefficients of the different lamina materials used. The lamination scheme used in all the materials is ($m/90/0/90/0$)_S. This lamination scheme means that the laminated plate consists of 10 laminae, the fiber orientation being ($m/90/0/90/0/0/90/0/90/m$).

Table 3.2 Inertial coefficients of symmetric cross-ply (m,90,0,90,0)_s laminated plate

Material	Lamination Scheme	I_0 [kg m ⁻²]	$I_2 (\times 10^{-3})$ [kg]	$I_4 (\times 10^{-9})$ [kg m ²]	$I_6 (\times 10^{-14})$ [kg m ⁴]
CFRP	(m/90/0/90/0) _s	33.092	4.5399	8.5208	17.171
Gr-Ep(AS)	(m/90/0/90/0) _s	30.100	4.3803	8.3676	16.996
Gl-Ep	(m/90/0/90/0) _s	33.700	4.5723	8.5519	17.207
Br-Ep	(m/90/0/90/0) _s	34.100	4.5937	8.5724	17.230

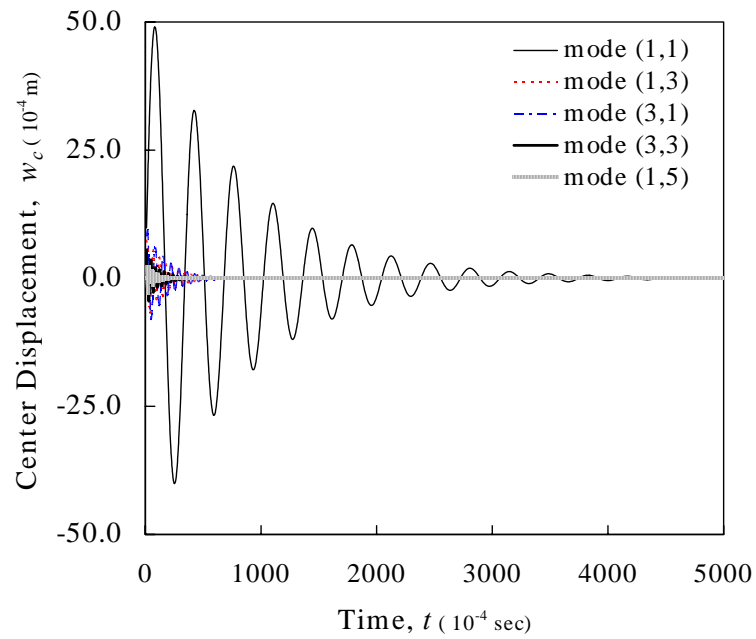
Table 3.3 contains the frequencies ω_d and damping coefficient α obtained using different composite materials. Figures 3.3(a) - 3.3(d) shows the vibration suppression characteristics of composite plates made up of different materials. Where the thickness of the lamina h_e is taken to be 1mm and the thickness of the smart material layer h_m is taken to be 1mm. It is observed that materials having almost same E_1/E_2 ratios have similar vibration suppression characteristics.

3.4.3. Effect of Plate Theories

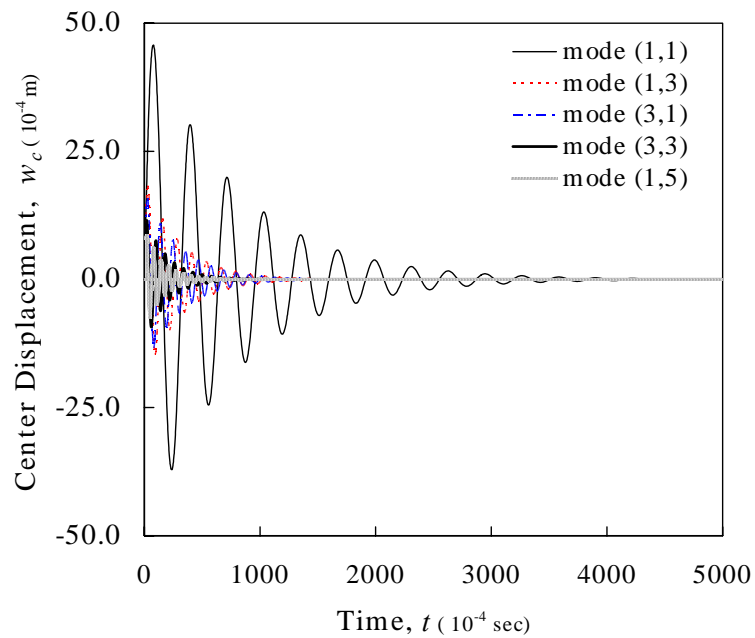
As mentioned in the introduction, the CLPT and FSDT theories are mere special cases of the TSDT. The comparison of the eigenvalues obtained by using all three theories is presented in Table 3.4. Figure 3.4 shows the vibration suppression behavior obtained from the each plate theory. It is observed that the CLPT theory gives higher frequencies of

Table 3.3 Damping coefficients and frequencies for different materials

Material	Lamination Scheme	$-\alpha_d \pm \omega_d$ [rad s ⁻¹]
CFRP	(m/90/0/90/0) _s	11.86 ± 184.508
Gr-Ep(AS)	(m/90/0/90/0) _s	13.043 ± 197.095
Gl-Ep	(m/90/0/90/0) _s	11.516 ± 162.968
Br-Ep	(m/90/0/90/0) _s	11.507 ± 212.05

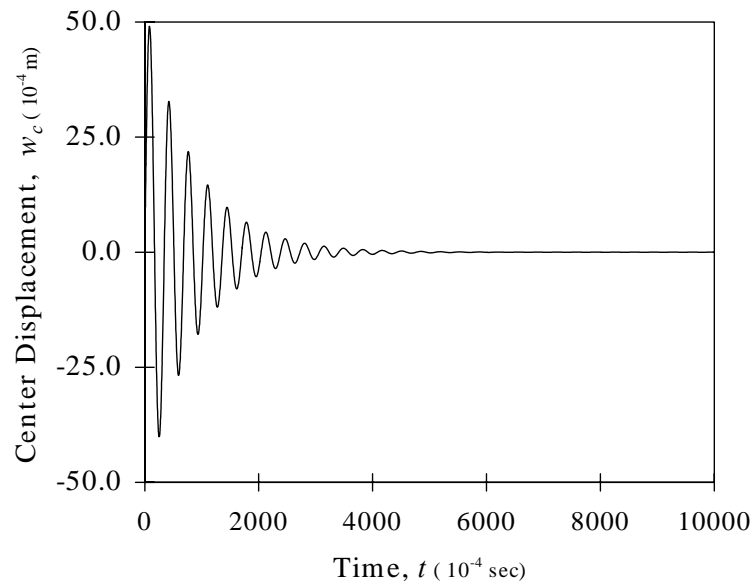


(a)CFRP (m/90/0/90/0)s

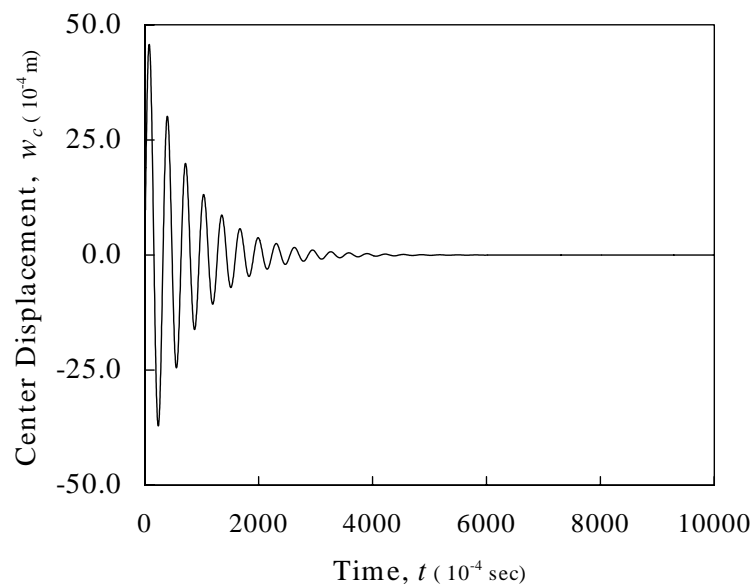


(b) Gr-Ep(AS) (m/90/0/90/0)s

Figure 3.2 Suppression characteristics for different modes of vibration

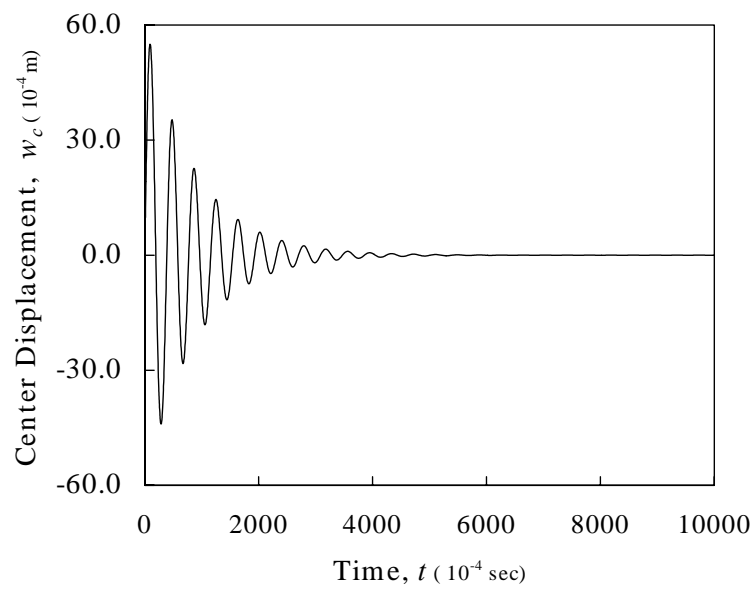


(a) CFRP (m/90/0/90/0)s

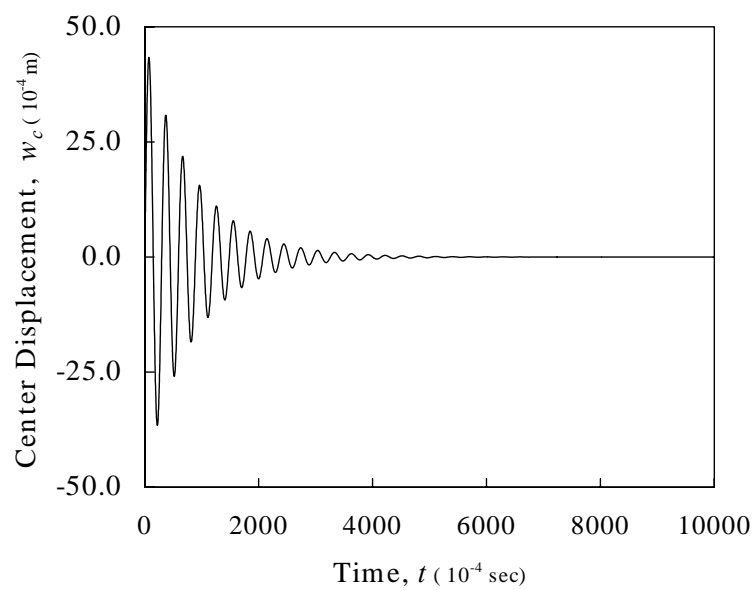


(b) GR-Ep(AS) (m/90/0/90/0)s

Figure 3.3 Effect of material properties on vibration suppression

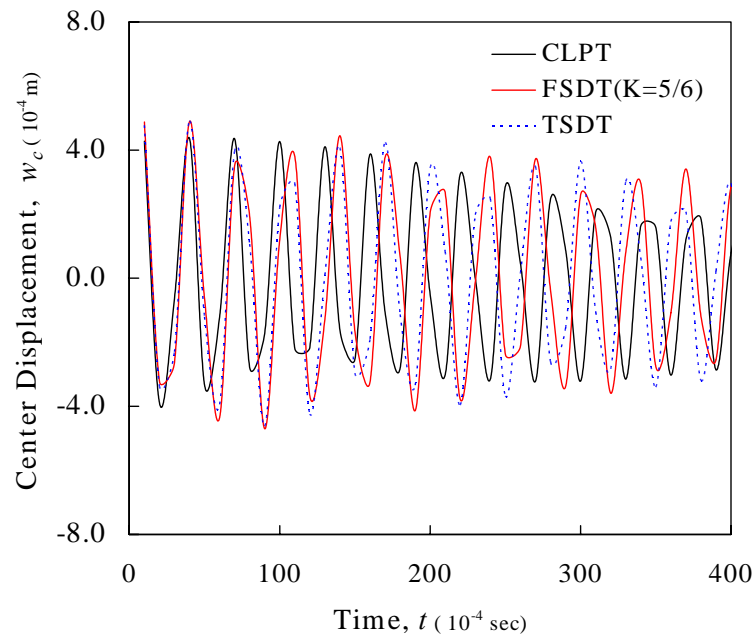


(c) Gl-Ep (m/90/0/90/0)s

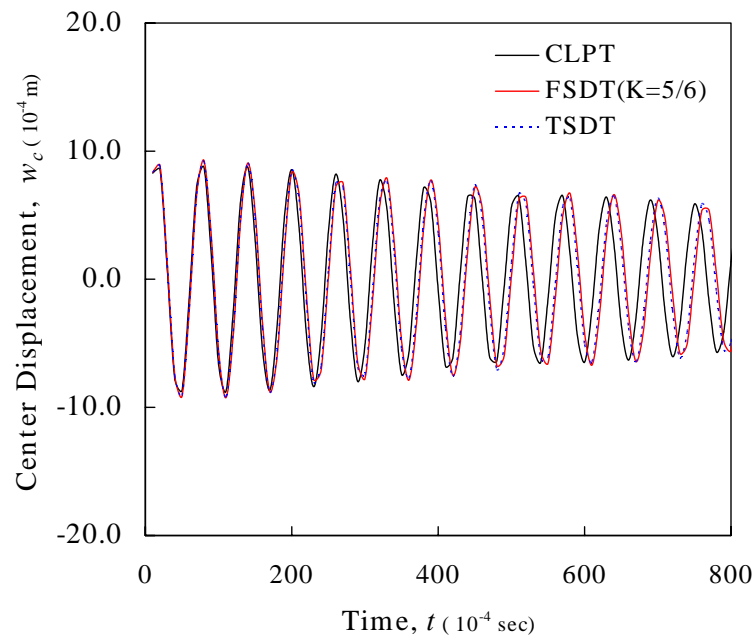


(d) Br-Ep (m/90/0/90/0)s

Figure 3.3 Continued

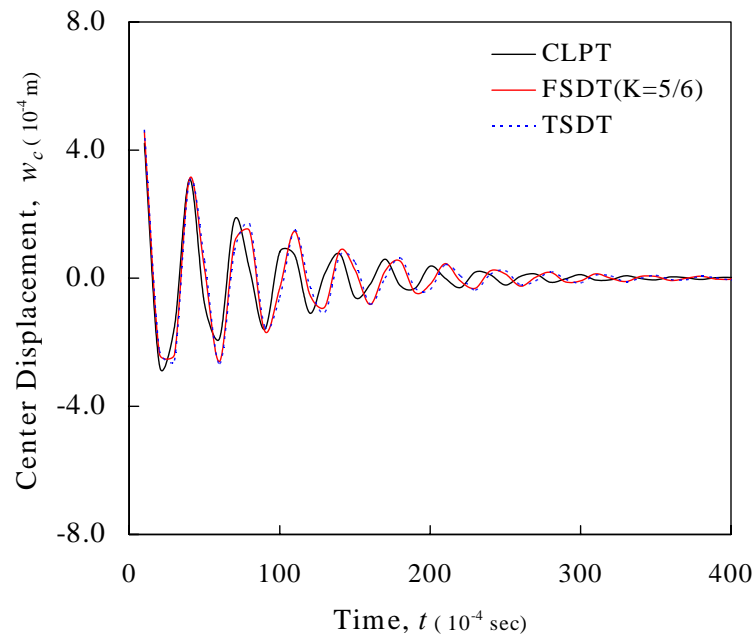


(a) CFRP $a/h=10$ (0/90/0/90/m)s

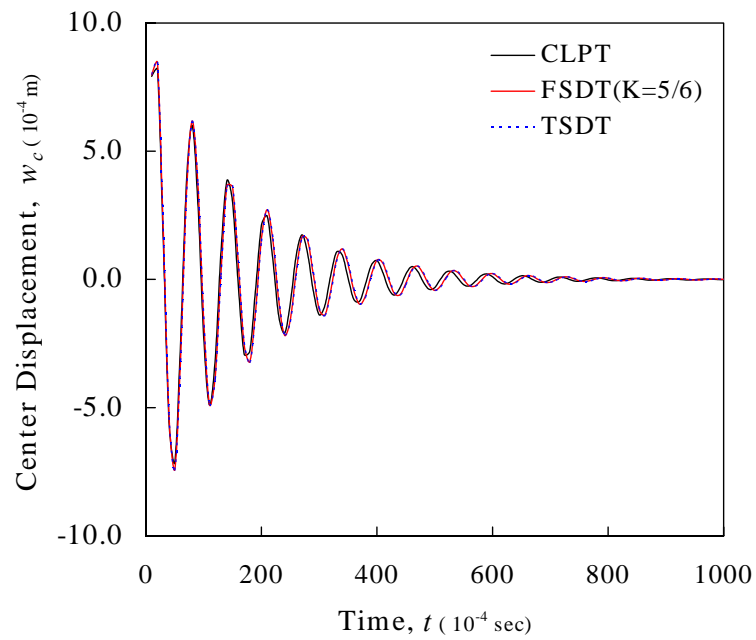


(b) CFRP $a/h=20$ (0/90/0/90/m)s

Figure 3.4 Effect of the different plate theories on vibration suppression



(c) Gr-Ep(AS) $a/h=10$ (m/90/0/90/0)s



(d) Gr-Ep(AS) $a/h=20$ (m/90/0/90/0)s

Figure 3.4 Continued

vibration. This is expected, since the CLPT theory renders the plate stiffer compared to the other two theories. Where the thickness of the lamina h_e is taken to be 1mm and the thickness of the smart material layer h_m is taken from 1 to 5 mm based on the ratio of a/h .

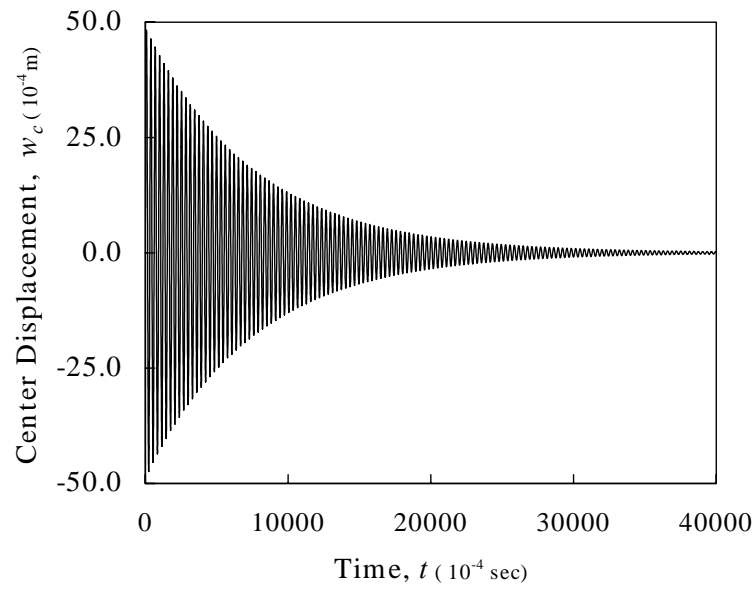
Table 3.4 Eigenvaluse ($-\alpha_d \pm \omega_d$) obtained through the different plate theories

Material	Lamination Scheme	a/h	CLPT	FSDT (k=5/6)	TSDT
CFRP	(0/90/0/90/m) _s	10	13.199 ± 2049	11.570 ± 1911	11.512 ± 1935
	(0/90/0/90/m) _s	20	6.599 ± 1024	6.372 ± 1006	6.368 ± 1009
Gr-Ep(AS)	(m/90/0/90/0) _s	10	126.95 ± 1945	117.32 ± 1866	116.592 ± 1848
	(m/90/0/90/0) _s	20	65.299 ± 986.2	63.449 ± 971.8	63.324 ± 969.2

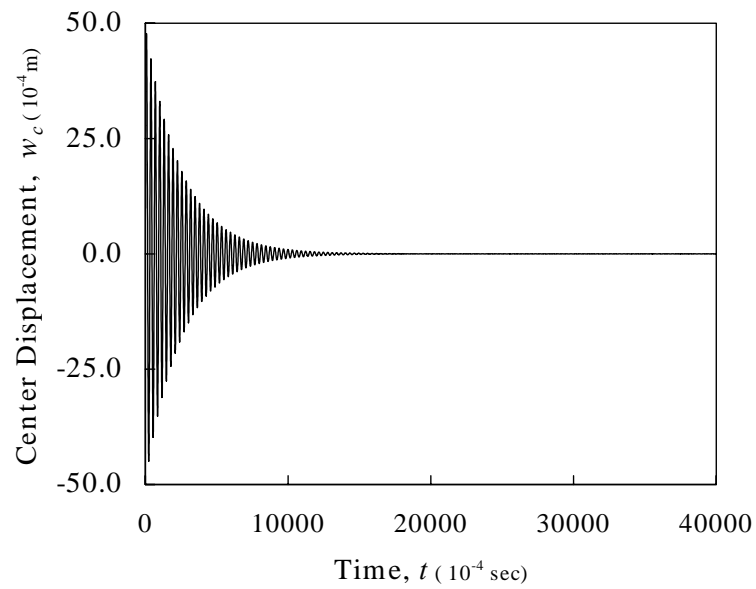
3.4.4. Effect of Smart Material Position

Next, suppression times for CFRP laminates are studied. The lamina thickness h_e is taken to be 1mm and the thickness of the smart material layer h_m is taken to be 1mm. The natural frequencies and the damping coefficients for different lamination schemes are obtained. The maximum deflection (W_{max}) of the composite plate and the suppression times have been calculated.

Figure 3.5 shows the displacement versus time for various laminates. It is observed that as the smart material layer is moved farther from the mid-plane the suppression time decreases. This is expected since the moment generated by the actuation of the smart material is more as the smart material is moved away from the mid-plane. Figure 3.6 shows the effect of the smart material layer location on the vibration suppression time. It is observed that the vibration suppression time does not show appreciable change when the distance of the smart material layer from the mid-plane is reduced from 0.045m to 0.015m, but then increases by almost an order of magnitude when the smart material layer is moved from 0.0015m to 0.0005m from the mid-plane. The eigenvalues and suppression time for each lamination schemes is tabulated in Table 3.5, where z_m denotes the positive distance from the center of the laminate to the center of the smart layer.

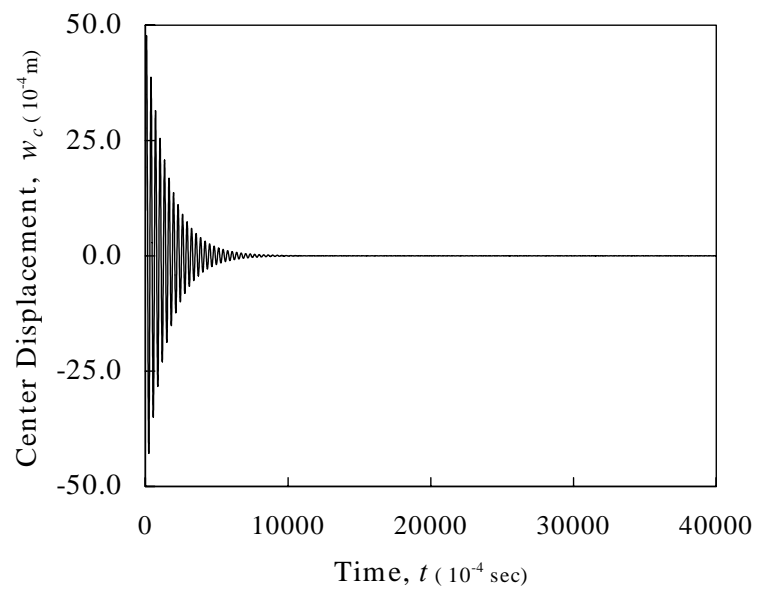


(a) CFRP (0/90/0/90/m)s

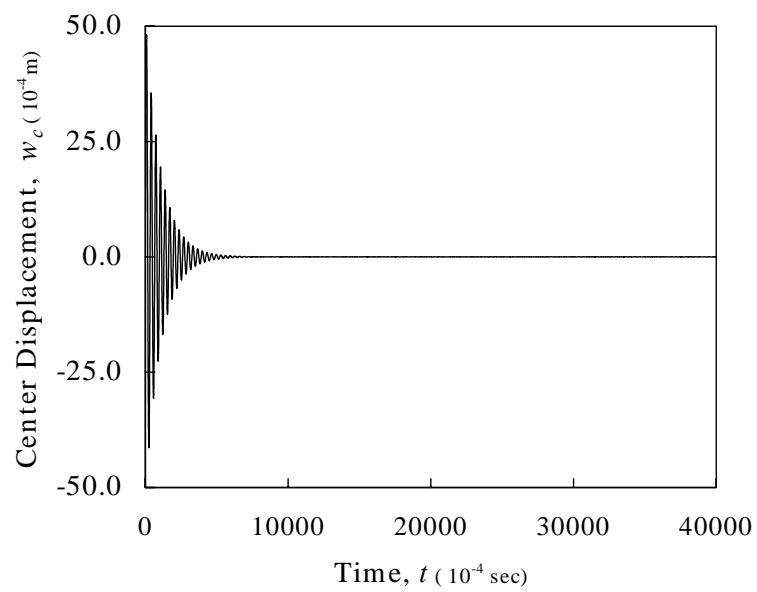


(b) CFRP (90/0/90/m/90)s

Figure 3.5 Vibration suppression characteristics for different smart material location

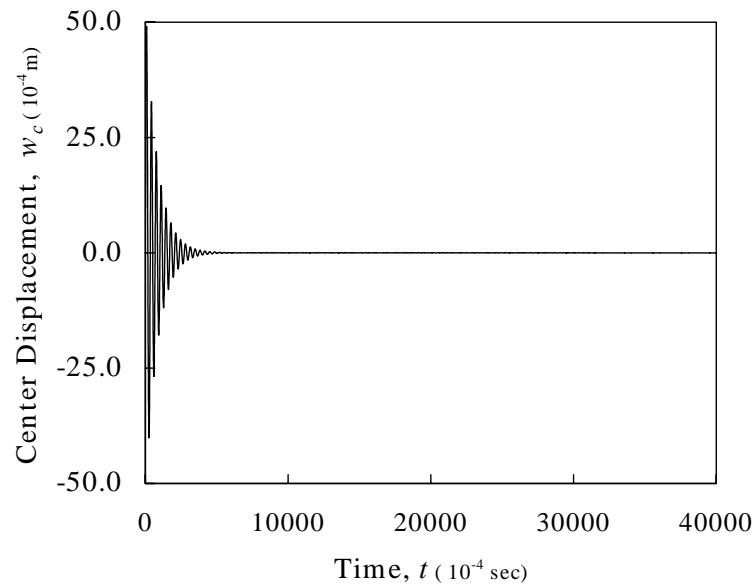


(c) CFRP (0/90/m/90/0)s



(d) CFRP (90/m/90/0/90)s

Figure 3.5 Continued



(e) CFRP (m/90/0/90/0)s

Figure 3.5 Continued

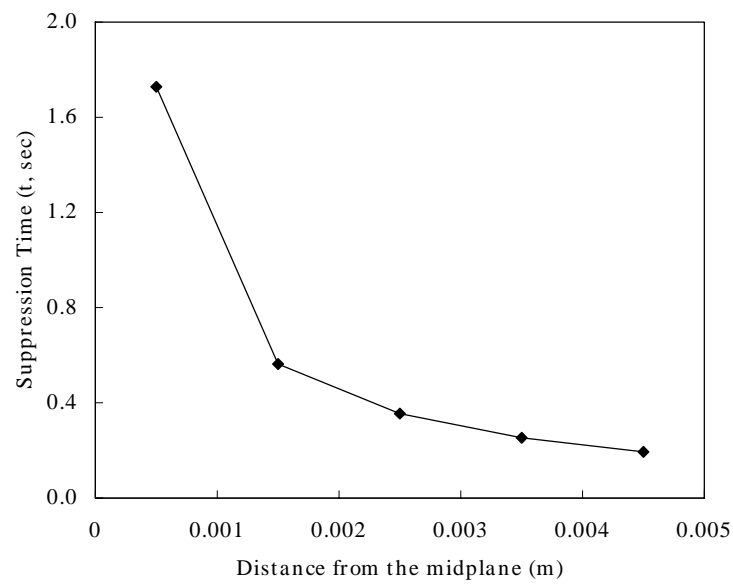


Figure 3.6 Vibration suppression times for CFRP laminated plate

Table 3.5 Suppression times for different CFRP laminates

Lamination Scheme	z_m (m)	$-\alpha_d$	$\pm \omega_d$	W_{\max} (10^{-3} m)	t at $W_{\max}/10$	T_s
(0/90/0/90/m) _s	0.0005	1.318	204.721	4.823	1.728	1.000
(90/0/90/m/90) _s	0.0015	3.954	202.800	4.771	0.563	0.333
(0/90/m/90/0) _s	0.0025	6.589	198.881	4.769	0.355	0.200
(90/m/90/0/90) _s	0.0035	9.224	192.823	4.815	0.253	0.143
(m/90/0/90/0) _s	0.0045	11.86	184.507	4.907	0.194	0.111

3.4.5. Effect of Lamina Thickness

The vibration characteristics are obtained for the CFRP laminate with the fiber orientation of (0/90/0/90/m)_s for different thicknesses of the lamina and smart material layers, keeping the control gain constant. The vibration frequencies, damping factors and suppression times are presented in Figure 3.7 and Table 3.6 for the different lamina thickness. Where h_e and h_m are the thicknesses of the elastic material layer and smart material layer, respectively.

Table 3.7 shows the effect of the position and thickness of the smart material layer and the thickness of the composite material laminae on the vibration suppression time ratio. It is observed that thinner smart material layers result in better attenuation of the vibration. This is due to a higher mass matrix that is caused by the large increase in the moment of inertia of the system when thickness of the smart material layer is increased. This increase is because the smart material layer has a density of almost five times to that of the composite material.

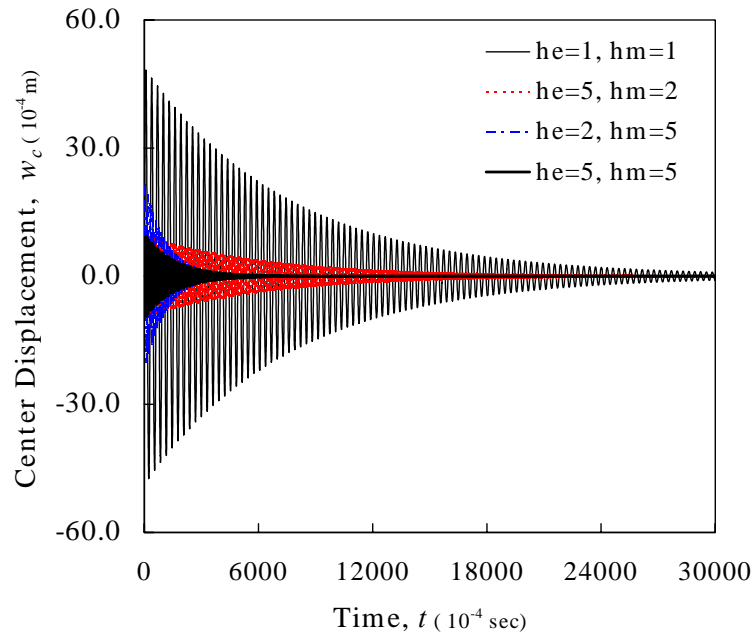


Figure 3.7 Effect of lamina thickness on vibration suppression

Table 3.6 Vibration suppression characteristics for the different lamina thickness

Thickness (mm)	$-\alpha_d$	$\pm \omega_d$	$W_{\max} (10^{-3} \text{ m})$	t at $W_{\max}/10$
$h_e = 1, h_m = 1$	1.318	204.721	4.823	1.728
$h_e = 5, h_m = 2$	1.533	1023.00	0.947	1.499
$h_e = 2, h_m = 5$	8.910	442.249	2.140	0.259
$h_e = 5, h_m = 5$	6.368	1009.00	0.920	0.368

3.4.6. Effect of Feedback Coefficients

The value of the feedback coefficient $c(t)k_c$ influences the vibration suppression characteristics. The study is performed on a CFRP laminate with thickness of the elastic layer to be 1mm and the thickness of the smart material to be 1 mm. Different lamination schemes are used and the position of the smart material layer is varied. Two different

values of the feedback coefficient are used: $c(t)k_c = 10^4$ and $c(t)k_c = 10^3$. The results obtained are presented in Table 3.8.

Table 3.7 Vibration suppression ratio for the different laminates

Lamination Scheme	Thickness (mm)	h_e/h_m	$z_m(m)$	T_s
(0/90/0/90/m) _s	$h_e = 1, h_m = 1$	1.0	0.0005	1.0000
	$h_e = 5, h_m = 2$	2.5	0.0010	1.0000
	$h_e = 2, h_m = 5$	0.4	0.0025	1.0000
	$h_e = 5, h_m = 5$	1.0	0.0025	1.0000
(90/0/90/m/90) _s	$h_e = 1, h_m = 1$	1.0	0.0015	0.3333
	$h_e = 5, h_m = 2$	2.5	0.0060	0.1667
	$h_e = 2, h_m = 5$	0.4	0.0045	0.5556
	$h_e = 5, h_m = 5$	1.0	0.0075	0.3333
(0/90/m/90/0) _s	$h_e = 1, h_m = 1$	1.0	0.0025	0.2000
	$h_e = 5, h_m = 2$	2.5	0.0110	0.0909
	$h_e = 2, h_m = 5$	0.4	0.0065	0.3846
	$h_e = 5, h_m = 5$	1.0	0.0125	0.2000
(90/m/90/0/90) _s	$h_e = 1, h_m = 1$	1.0	0.0035	0.1429
	$h_e = 5, h_m = 2$	2.5	0.0160	0.0476
	$h_e = 2, h_m = 5$	0.4	0.0085	0.2941
	$h_e = 5, h_m = 5$	1.0	0.0175	0.1429
(m/90/0/90/0) _s	$h_e = 1, h_m = 1$	1.0	0.0045	0.1111
	$h_e = 5, h_m = 2$	2.5	0.0210	0.0476
	$h_e = 2, h_m = 5$	0.4	0.0105	0.2381
	$h_e = 5, h_m = 5$	1.0	0.0225	0.1111

The variation of the vibration suppression time for different laminates and for two different values of the feedback control coefficient are presented in Figure 3.8. It can be seen that the suppression time increases when the value of the feedback coefficient decreases. This is because the damping coefficients decrease, thereby resulting in less damping. However, from Table 3.7, it can be noted that there is no appreciable change in

the natural frequency of vibration for different lamination schemes when the value of the feedback coefficient changes.

Table 3.8 Suppression time for two control gains for different laminates

Lamination Scheme	z_m (m)	$c(t)k_c = 10^3$				$c(t)k_c = 10^4$			
		$-\alpha_d$	$\pm \omega_d$	W_{\max} (10^{-3} m)	t at $W_{\max}/10$	$-\alpha_d$	$\pm \omega_d$	W_{\max} (10^{-3} m)	t at $W_{\max}/10$
(0/90/0/90/m) _s	0.0005	0.132	204.726	4.868	16.981	1.318	204.721	4.823	1.728
(90/0/90/m/90) _s	0.0015	0.395	202.838	4.908	5.612	3.954	202.800	4.771	0.563
(0/90/m/90/0) _s	0.0025	0.659	198.989	4.998	3.451	6.589	198.881	4.769	0.355
(90/m/90/0/90) _s	0.0035	0.922	193.041	5.140	2.387	9.224	192.823	4.815	0.253
(m/90/0/90/0) _s	0.0045	1.186	184.884	5.335	1.745	11.86	184.507	4.907	0.194

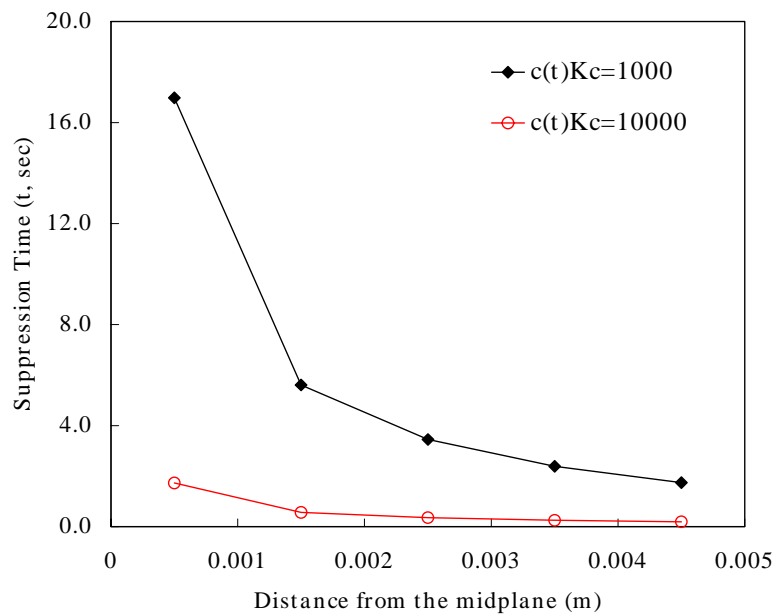


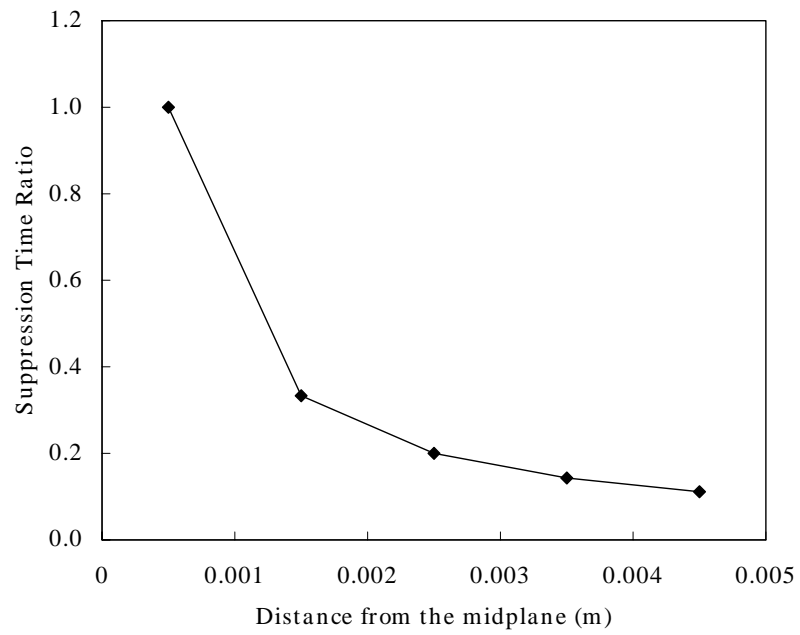
Figure 3.8 Effect of feedback coefficient on the suppression time

3.4.7. Variation of T_s and e_r for Different Laminates

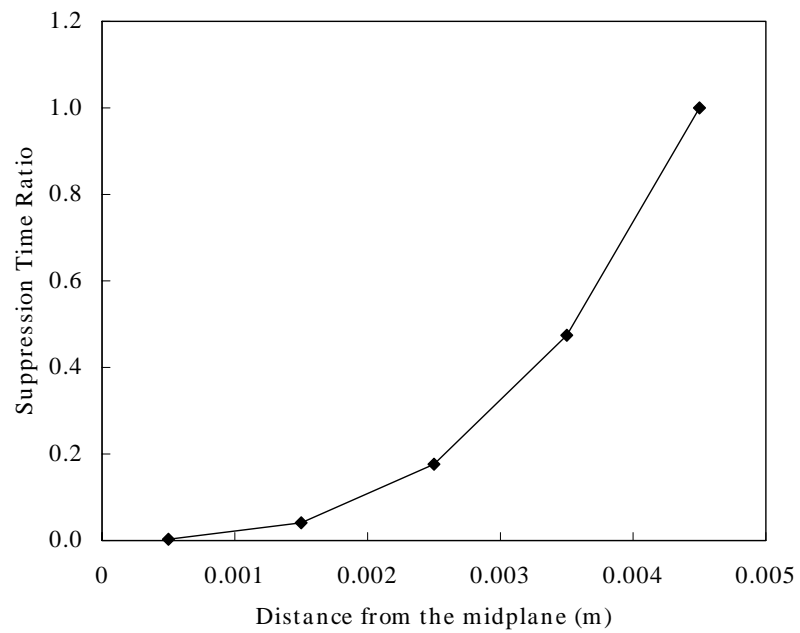
The variation of the vibration suppression ratio T_s and the normalized damping parameter $e_r = \varepsilon_{31} / \varepsilon_{\max}$ is studied for different positions of the smart material layer in the laminated composite plate. The results are tabulated in Table 3.9 and presented in Figure 3.9. From the earlier discussions, the vibration suppression ratio decreases when the smart material is moved away from the laminate. The normalized damping parameter increases as the smart material layer is moved away from the neutral axis. This is explained by the increased damping that is achieved when the smart material layer is moved away from the neutral axis. The variation is studied on a CFRP laminate with the thickness of the elastic composite layer and the thickness of the smart material layer being 1mm.

Table 3.9 T_s and e_r parameter for different CFRP laminates

Laminate Scheme	z_m (m)	T_s	ε_{31}	$e_r = \varepsilon_{31} / \varepsilon_{\max}$
(0/90/0/90/m) _s	0.0005	1.000	0.0295	0.0027
(90/0/90/m/90) _s	0.0015	0.333	0.4426	0.0407
(0/90/m/90/0) _s	0.0025	0.200	1.9177	0.1762
(90/m/90/0/90) _s	0.0035	0.143	5.1631	0.4743
(m/90/0/90/0) _s	0.0045	0.111	10.8867	1.0000



(a) Relations between T_s and z_m



(b) Relations between e_r and z_m

Figure 3.9 Variation of T_s and e_r with respect to z_m

3.5. Analytical Results for Laminated Composite Shells

Using the previously developed analytical solutions based on Donnell and Sanders shell theory, numerical parametric studies are carried out. Symmetric cross-ply laminated square shell ($a/b = 1$) with both the upper and lower surfaces embedded magnetostrictive material, Terfenol-D, is considered under the initial unit velocity in ζ direction for simply supported boundary condition. The laminated composite shells are composed of total 10 layers and all the layers are assumed to be of the same thickness. Three different shell types, spherical ($R_1 = R_2 = R$), cylindrical ($R_1 = \infty$), and doubly curved shell ($R_1 = 2R_2$ for this study), are considered with two side-to-thickness ratios $a/h = 10$ and 100 for the thick and thin shells. The elastic composite materials considered in here to study the effect of the elastic material are CFRP (composite fiber reinforced polymer), Gr-Ep(AS) (graphite-epoxy), Gl-Ep (glass-epoxy), and Br-Ep (boron-epoxy). The material properties of these materials are tabulated in Table 3.1.

The inertial coefficients with different elastic material are shown in Table 3.10 for thin and thick cross-ply (m,90,0,90,0)s laminated shells. Here m represents magnetostrictive layer, 90 and 0 for the angles of elastic material layer in degree and subscript s stands for symmetric.

3.5.1. The General

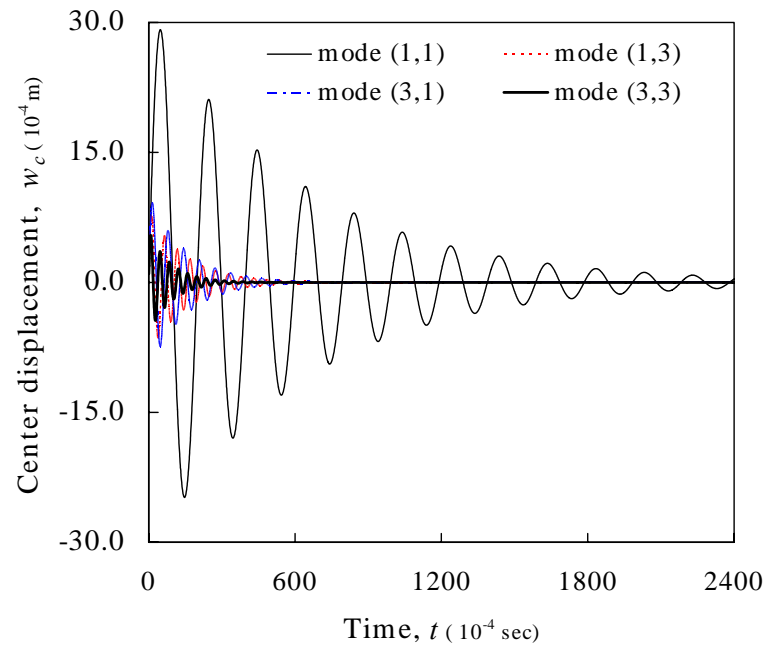
The symmetric cross-ply laminated CFRP spherical shells ($R_1 = R_2 = R$) are considered to study the effect of mode and smart layer position on the vibration suppression characteristics. Table 3.11 shows the frequency ϖ_d and damping coefficient $-\alpha_d$ of the symmetric cross-ply (m,90,0,90,0)s spherical shell with $R_2/a = 10$ for different modes in the case of thin and thick shells. It is observed that the maximum amplitude of vibration and vibration suppression can be found in the mode (1,1). This is because the amplitude of vibration that has to be suppressed decreases as the mode number increases. It can be seen clearly in Figure 3.10.

Table 3.10 Inertial coefficients of symmetric cross-ply (m,90,0,90,0)s laminated shell

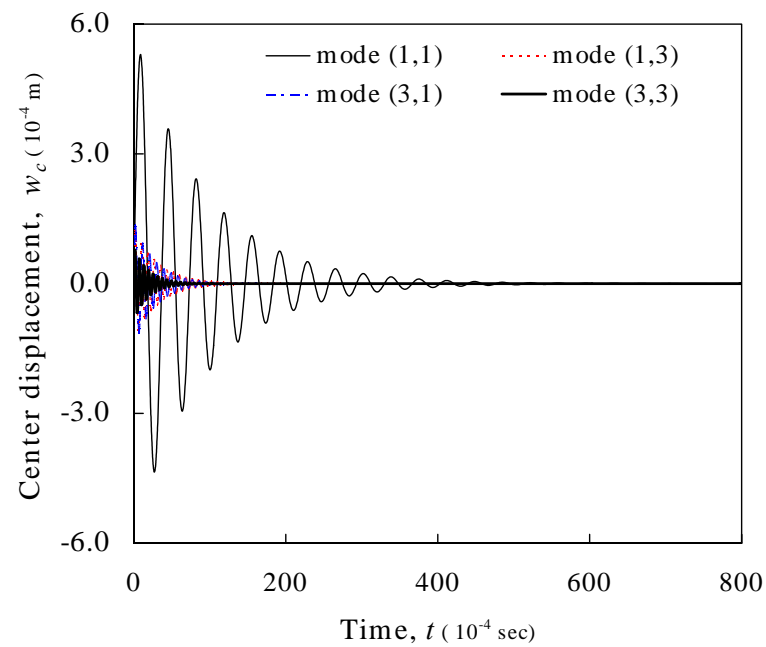
Thickness	Material	I_0 [kg m ⁻²]	I_2 [kg]	I_4 [kg m ²]	I_6 [kg m ⁴]
Thin Shell $a/h = 100$	CFRP	33.092	$0.45399(\times 10^{-3})$	$8.5208(\times 10^{-9})$	$17.171(\times 10^{-14})$
	Br-Ep	34.100	$0.45937(\times 10^{-3})$	$8.5724(\times 10^{-9})$	$17.230(\times 10^{-14})$
	Gr-Ep(AS)	30.100	$0.43803(\times 10^{-3})$	$8.3676(\times 10^{-9})$	$16.996(\times 10^{-14})$
	Gl-Ep	33.700	$0.45723(\times 10^{-3})$	$8.5519(\times 10^{-9})$	$17.207(\times 10^{-14})$
Thick Shell $a/h = 10$	CFRP	330.92	0.45399	$8.5208(\times 10^{-4})$	$17.171(\times 10^{-7})$
	Br-Ep	341.00	0.45937	$8.5724(\times 10^{-4})$	$17.230(\times 10^{-7})$
	Gr-Ep(AS)	301.00	0.43803	$8.3676(\times 10^{-4})$	$16.996(\times 10^{-7})$
	Gl-Ep	337.00	0.45723	$8.5519(\times 10^{-4})$	$17.207(\times 10^{-7})$

Table 3.11 Effect of the mode on the Eigenvalues of the symmetric cross-ply (m,90,0,90,0)s CFRP spherical shells with $R_2/a = 10$

Theory	Mode (m, n)	Thin Shell($a/h = 100$)		Thick Shell($a/h = 10$)	
		$-\alpha_d$	ω_d	$-\alpha_d$	ω_d
Donnell	mode (1, 1)	16.2933	316.8491	106.8430	1716.3063
	mode (1, 3)	66.3169	1200.4960	312.8574	7563.3768
	mode (3, 1)	66.5636	979.4863	364.1833	6733.5733
	mode (3, 3)	109.7777	1667.9786	521.5811	10462.7632
	mode (1, 5)	159.3204	3112.2032	513.8302	14610.7404
	mode (5, 1)	161.1095	2462.9380	643.1361	13498.9662
	mode (5, 5)	289.8144	4520.7199	928.7615	20614.5649
Sanders	mode (1, 1)	16.2814	316.7589	106.5941	1714.9065
	mode (1, 3)	66.2975	1200.3622	312.3166	7562.4308
	mode (3, 1)	66.5476	979.3728	363.7152	6732.6829
	mode (3, 3)	109.7507	1667.8271	520.8413	10461.8118
	mode (1, 5)	159.2856	3112.0733	513.1365	14610.0843
	mode (5, 1)	161.0844	2462.8316	642.5241	13498.3567
	mode (5, 5)	289.7587	4520.5710	927.7522	20613.9016



(a)



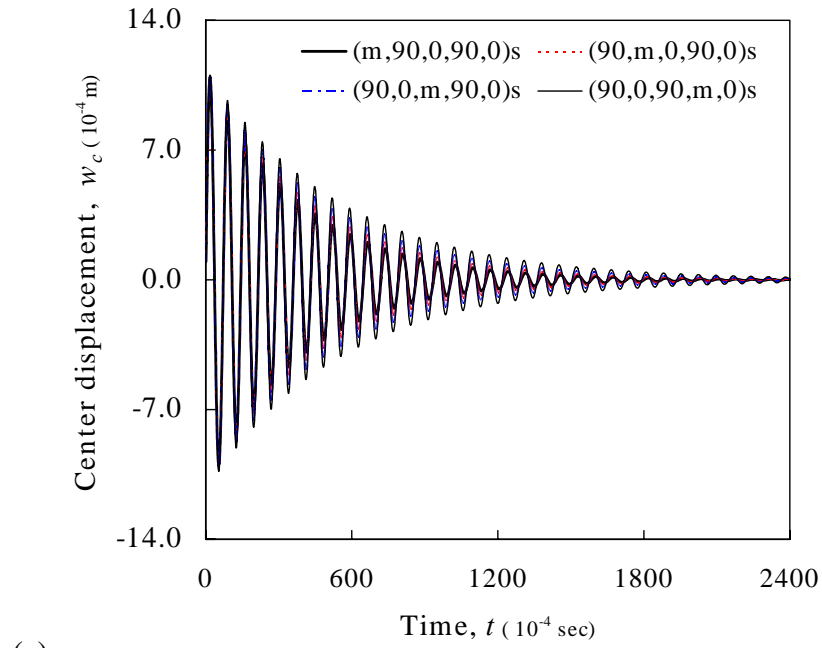
(b)

Figure 3.10 Vibration suppression characteristics of CFRP spherical shells ($R_2/a = 10$) for the different mode; (a) Thin shell ($a/h = 100$), (b) Thick shell ($a/h = 10$)

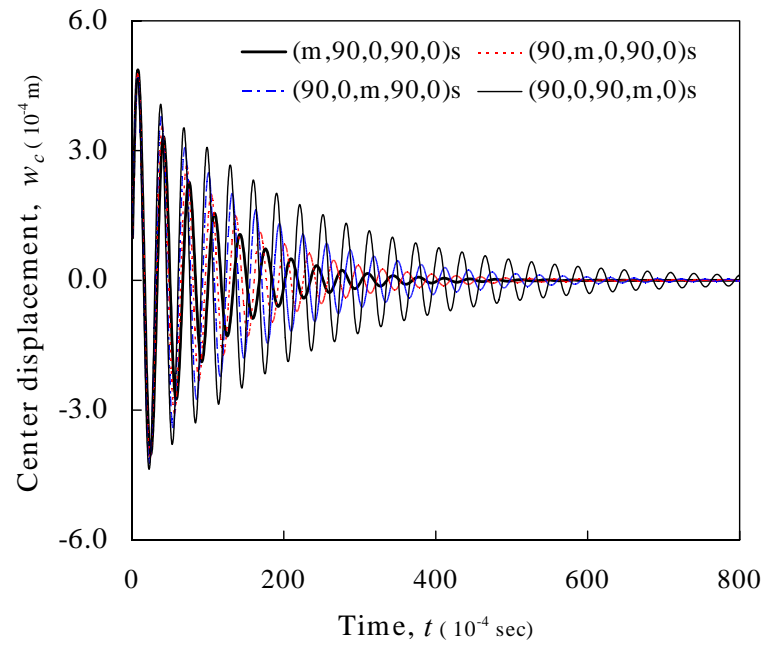
The effect of the position of smart material layer is studied with the symmetric cross-ply spherical shell with $R_2/a = 3$. Four different cross-ply laminates, (m,90,0,90,0)s, (90,m,0,90,0)s, (90,0,m,90,0)s, and (90,0,90,m,0)s are considered. It is observed that the damping coefficient $-\alpha_d$ increases with the distance between the smart layer and mid-plane of the shell. Thus, the vibration suppression time decreases as the smart material layers are moved from the mid-plane. The damping coefficients and frequencies for different smart layer positions are shown in Table 3.12. Figure 3.11 shows the vibration suppression characteristics of each lamination case. In case of thin shell, frequencies are close to each other so that the deviations are not obvious in the Figure. It is clear that (m,90,0,90,0)s lamination has the maximum vibration suppression and lowest frequency for thin and thick shells.

Table 3.12 Effect of the lamination scheme on the Eigenvalues of the symmetric cross-ply CFRP spherical shells with $R_2/a = 3$

Theory	Laminations	Thin Shell($a/h = 100$)		Thick Shell($a/h = 10$)	
		$-\alpha_d$	ω_d	$-\alpha_d$	ω_d
Donnell	(m,90,0,90,0)s	26.0966	872.7906	114.6203	1884.9296
	(90,m,0,90,0)s	23.5016	874.6319	91.7248	1964.5621
	(90,0,m,90,0)s	20.9074	876.0250	69.4512	2035.5273
	(90,0,90,m,0)s	18.3127	876.9696	47.0917	2076.0054
Sanders	(m,90,0,90,0)s	25.9807	872.4346	113.1522	1870.9359
	(90,m,0,90,0)s	23.4096	874.2427	90.4025	1949.5607
	(90,0,m,90,0)s	20.8393	875.6105	68.2815	2019.6510
	(90,0,90,m,0)s	18.2687	876.5381	46.1042	2059.6157



(a)



(b)

Figure 3.11 Vibration suppression characteristics of CFRP spherical shells ($R_2/a = 3$) for the different lamination; (a) Thin shell ($a/h = 100$), (b) Thick shell ($a/h = 10$)

3.5.2. Effect of Shell Theories

First, it should be mentioned that the difference between Donnell and Sanders third-order shear deformation shell theories is not significant in linear analysis. Tables 3.13 and 3.14 show the eigenvalues of symmetric cross-ply laminated shells by Donnell and Sanders shell theories. It is observed that Donnell shell theory gives higher frequency and damping coefficients than Sanders shell theory. As total thickness of shell structures is increasing and R_2/a value is decreasing, the numerical differences in eigenvalues become larger.

Table 3.13 Eigenvalues of the symmetric cross-ply (m,90,0,90,0)s CFRP laminated shells by Donnell shell theory

Thickness	R_2/a	Spherical Shell		Cylindrical Shell		Doubly Curved Shell	
		$-\alpha_d$	ω_d	$-\alpha_d$	ω_d	$-\alpha_d$	ω_d
Thin Shell $a/h = 100$	1	N/A*	N/A*	N/A*	N/A*	N/A*	N/A*
	2	32.2630	1280.8428	22.4376	663.7485	27.6324	973.8544
	3	26.0966	872.7906	19.0867	465.6132	22.6876	667.4403
	4	22.7193	667.9063	17.3330	370.4516	20.0711	516.1883
	5	20.6192	546.3928	16.2604	316.5267	18.4650	427.8527
	10	16.2933	316.8491	14.0782	224.9291	15.1902	267.1285
	20	14.0853	224.9884	12.9724	195.3690	13.5297	208.2258
	50	12.7514	191.5289	12.3055	186.2677	12.5286	188.4752
	100	12.3057	186.2710	12.0827	184.9354	12.1942	185.4901
	10^{99}	11.8596	184.5068	11.8596	184.5068	11.8596	184.5068
Thick Shell $a/h = 10$	1	N/A*	N/A*	N/A*	N/A*	N/A*	N/A*
	2	118.6162	2088.2579	110.7055	1795.2084	115.3906	1927.6191
	3	114.6203	1884.9296	108.6770	1742.5986	111.9508	1805.1097
	4	112.1085	1806.3593	107.4377	1723.5286	109.9357	1759.4761
	5	110.4533	1768.4574	106.6250	1714.5884	108.6401	1737.8266
	10	106.8430	1716.3063	104.8500	1702.5766	105.8701	1708.4458
	20	104.9037	1703.0031	103.8907	1699.5774	104.4029	1701.0371
	50	103.7019	1699.2899	103.2932	1698.7536	103.4984	1698.9809
	100	103.2953	1698.7708	103.0904	1698.6425	103.1931	1698.6966
	10^{99}	102.8859	1698.6124	102.8859	1698.6124	102.8859	1698.6124

* Since $R_2/h < 20$, the current formulation cannot be applied to this case

However, when one considers the vibration control behavior it is hard to see the differences (see Figure 3.12). Thus, the following numerical results and discussion regarding the vibration control characteristics in linear analysis are common in both Donnell and Sanders shell theories.

Table 3.14 Eigenvalues of the symmetric cross-ply (m,90,0,90,0)s CFRP laminated shells by Sanders shell theory

Thickness	R_2/a	Spherical Shell		Cylindrical Shell		Doubly Curved Shell	
		$-\alpha_d$	ω_d	$-\alpha_d$	ω_d	$-\alpha_d$	ω_d
Thin Shell $a/h = 100$	1	N/A*	N/A*	N/A*	N/A*	N/A*	N/A*
	2	32.0114	1280.3174	22.2974	663.0668	27.4689	973.3518
	3	25.9807	872.4346	19.0224	465.1745	22.6124	667.1056
	4	22.6525	667.6420	17.2959	370.1398	20.0276	515.9435
	5	20.5756	546.1846	16.2362	316.2927	18.4365	427.6626
	10	16.2814	316.7589	14.0715	224.8465	15.1822	267.0518
	20	14.0818	224.9568	12.9705	195.3450	13.5274	208.2015
	50	12.7506	191.5229	12.3050	186.2637	12.5280	188.4708
	100	12.3054	186.2695	12.0825	184.9344	12.1940	185.4890
	10^{99}	11.8596	184.5068	11.8596	184.5068	11.8596	184.5068
Thick Shell $a/h = 10$	1	N/A*	N/A*	N/A*	N/A*	N/A*	N/A*
	2	115.7878	2060.5069	109.1022	1774.0591	113.4495	1906.0331
	3	113.1522	1870.9359	107.8476	1732.7819	110.9302	1794.7113
	4	111.1736	1798.0837	106.9091	1717.9217	109.2775	1753.4483
	5	109.7873	1763.0312	106.2478	1710.9754	108.1661	1733.9142
	10	106.5941	1714.9065	104.7078	1701.6671	105.6867	1707.4516
	20	104.8007	1702.6525	103.8315	1699.3509	104.3248	1700.7892
	50	103.6659	1699.2348	103.2723	1698.7180	103.4705	1698.9421
	100	103.2782	1698.7575	103.0805	1698.6339	103.1797	1698.6873
	10^{99}	102.8859	1698.6124	102.8859	1698.6124	102.8859	1698.6124

* Since $R_2/h < 20$, the current formulation cannot be applied to this case.

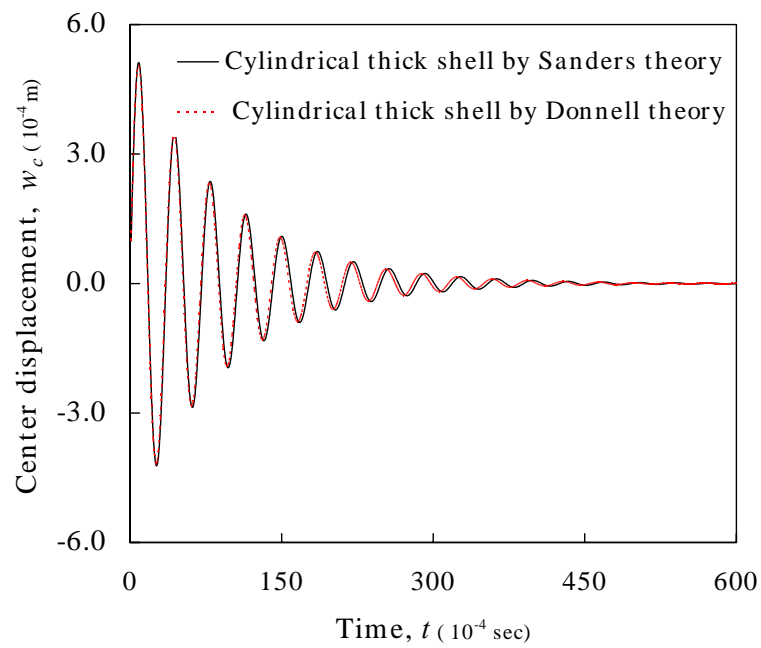
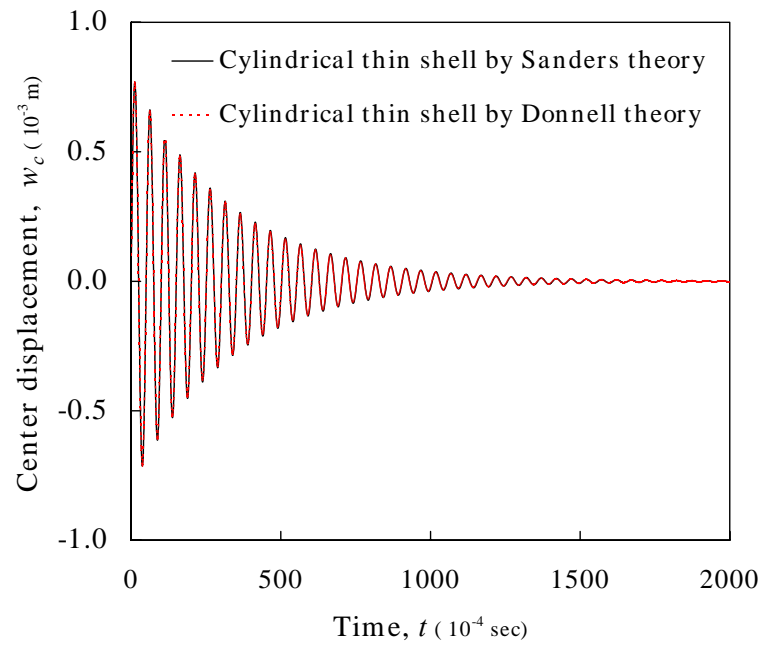


Figure 3.12 Vibration suppression characteristics of CFRP cylindrical shells for different shell theories; (a) Thin shell ($R_2/a = 2$), (b) Thick shell ($R_2/a = 2$)

3.5.3. Effect of R_2/a

Next, the effect of R_2/a on the vibration suppression characteristics is studied for spherical, cylindrical, and doubly curved CFRP shells. In this study doubly curved shell is chosen as $R_1 = 2R_2$ for specific example. Tables 3.13 for Donnell and 3.14 for Sanders shell theories show the frequency ϖ_d and damping coefficient $-\alpha_d$ of the thin and thick symmetric cross-ply (m,90,0,90,0)s shells with various R_2/a values. Here the cases of $R_2/a = 10^{99}$ pretends to a laminated composite plate. Note that the case of $R_2/a = 1$ is not available because the basic assumption of shallow shell ($h/R_1, h/R_2$ less than $1/20$) for current theory is not valid. The center displacements versus time for spherical, cylindrical, and doubly curved shells are shown in Figures 3.13 to 3.15, respectively. The Figures clearly show the vibration suppression characteristics for the selected R_2/a values for thin shell case.

It is observed that the damping coefficient $-\alpha_d$ and the frequency ϖ_d both increase with decreasing R_2/a value. Thus the shell with the smallest R_2/a shows the maximum vibration suppression. The same trend should hold for all shell types. It is also observed that the spherical shell has the largest damping coefficient and frequency and the cylindrical shell has the smallest damping coefficient and frequency. It is because of the fact that spherical shell has the smallest R_1 and doubly curved shell (in this study $R_1 = 2R_2$), and cylindrical shell has the largest R_1 ($R_1 = \infty$).

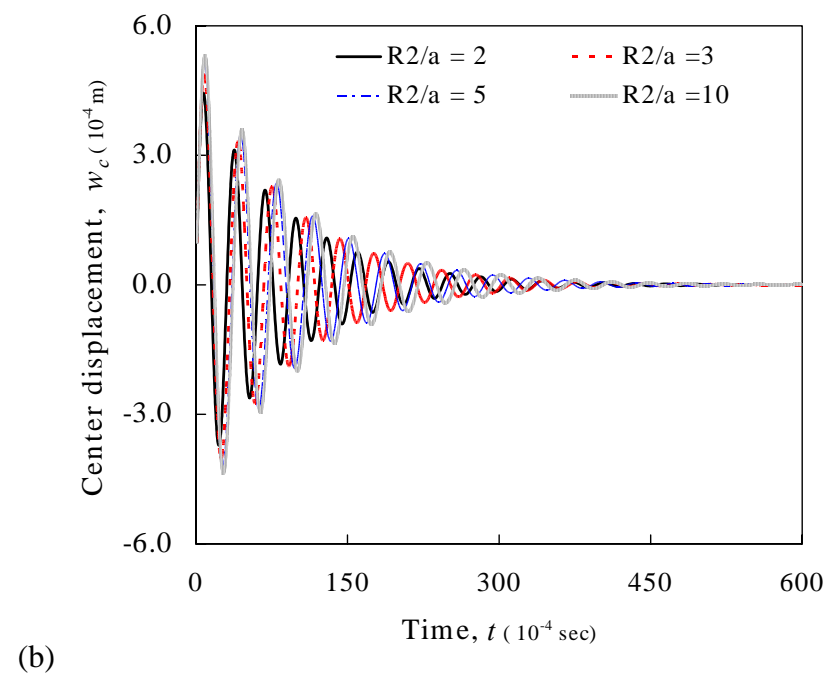
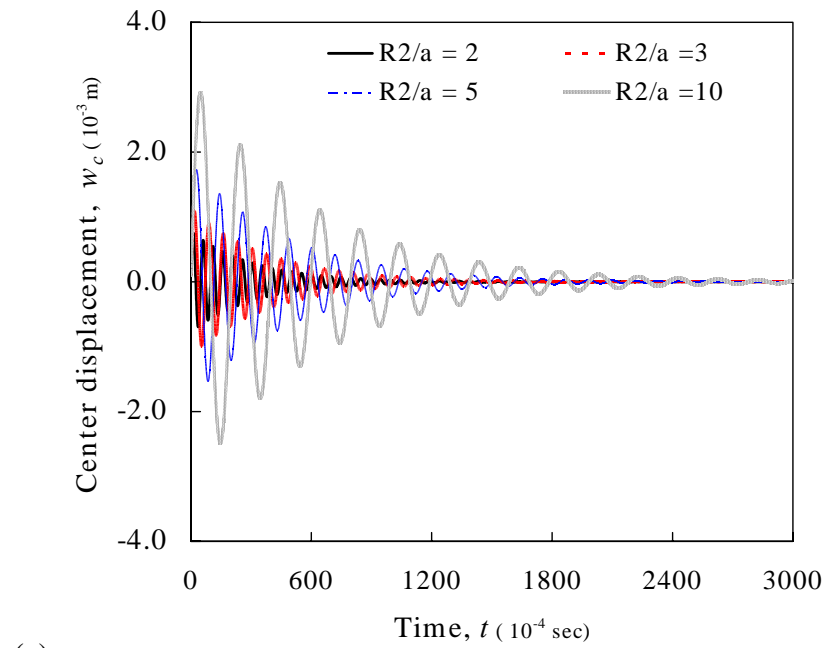


Figure 3.13 Effect of R_2/a on vibration suppression characteristics of CFRP spherical shells; (a) Thin shell ($a/h = 100$), (b) Thick shell ($a/h = 10$)

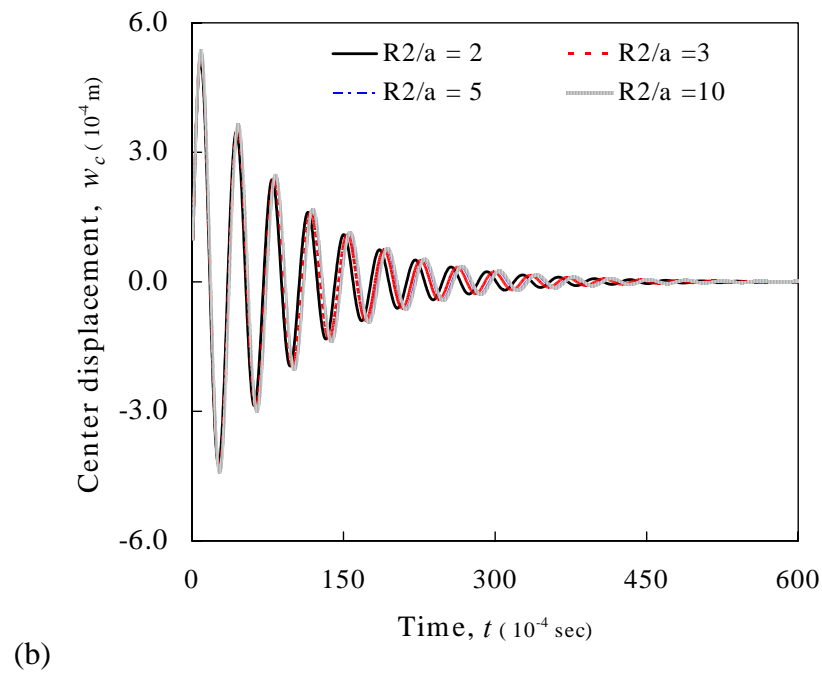
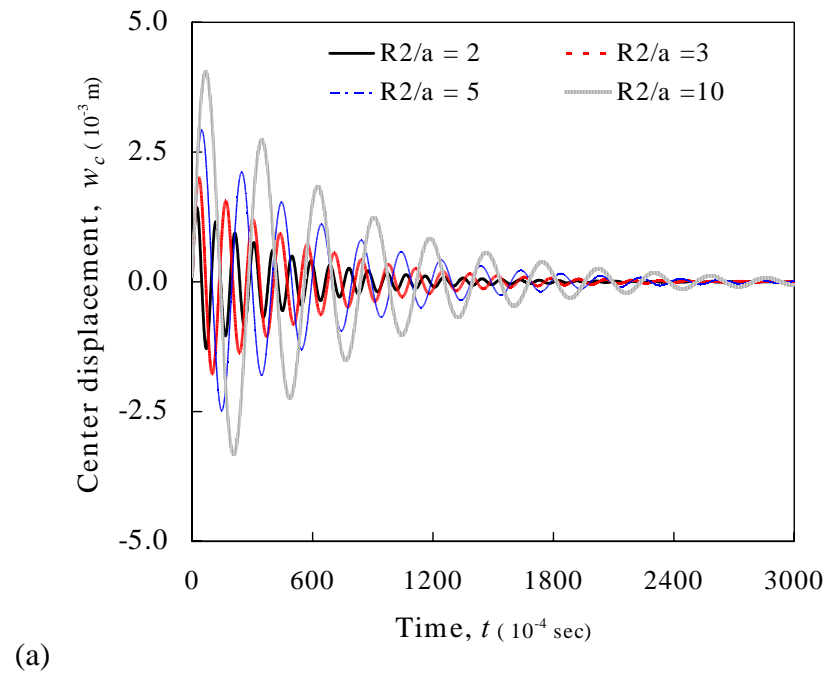
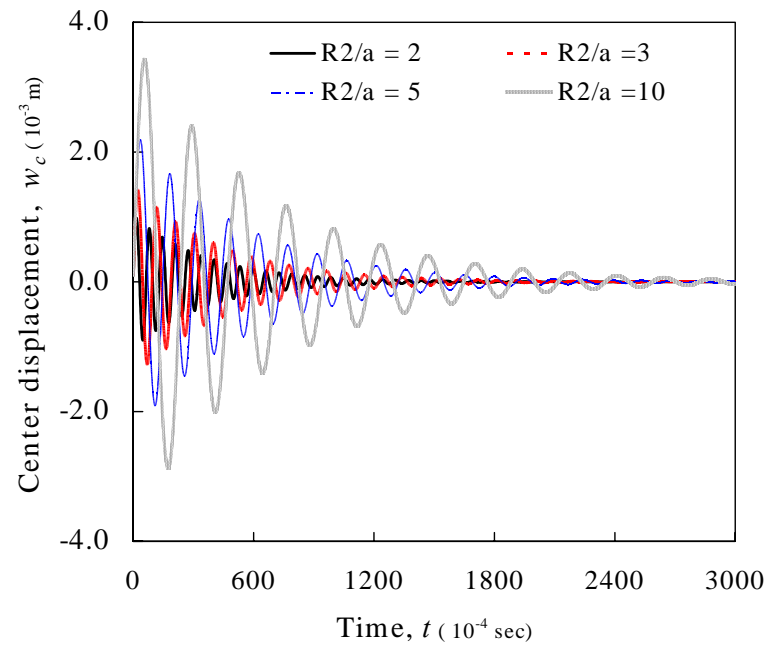
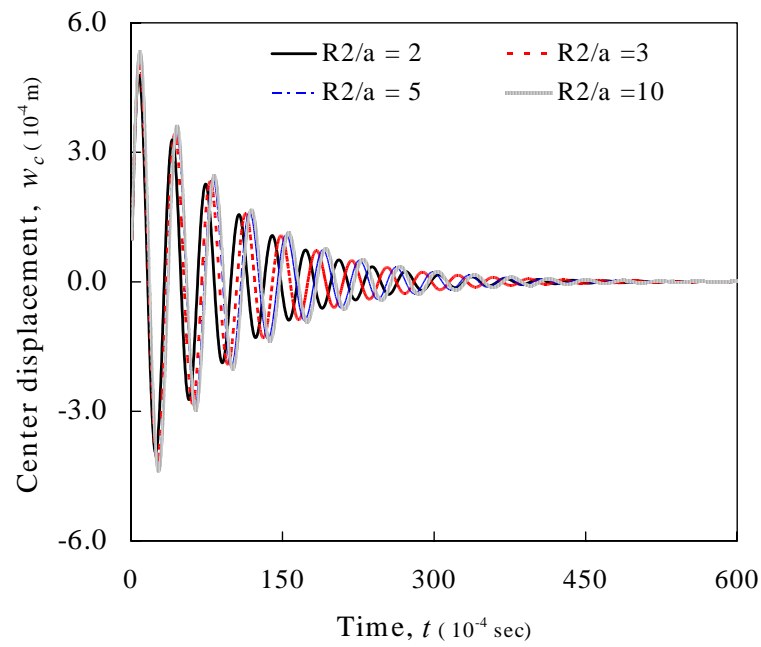


Figure 3.14 Effect of R_2/a on vibration suppression characteristics of CFRP cylindrical shells; (a) Thin shell ($a/h = 100$), (b) Thick shell ($a/h = 10$)



(a)



(b)

Figure 3.15 Effect of R_2/a on vibration suppression characteristics of CFRP doubly curved shells; (a) Thin shell ($a/h = 100$), (b) Thick shell ($a/h = 10$)

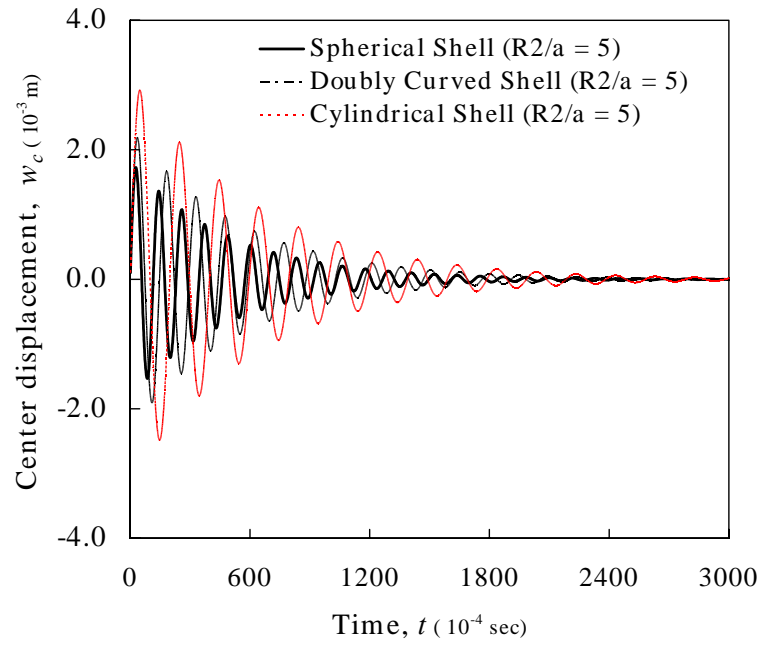
3.5.4. Effect of Shell Types

The comparison of vibration suppression characteristics between three different shell types could be found in Figure 3.16. Figure 3.16 shows the center displacements in case of $R_2/a = 5$ for thin shell, $R_2/a = 4$ for thick shell. It is clear that the spherical shell shows the maximum vibration suppression results from the Figure. Selected center displacement values versus time are tabulated in Table 3.15 for Sanders shell theory. The numerical results are for the thin and thick symmetric cross-ply (m,90,0,90,0)s shells with $R_2/a = 5$.

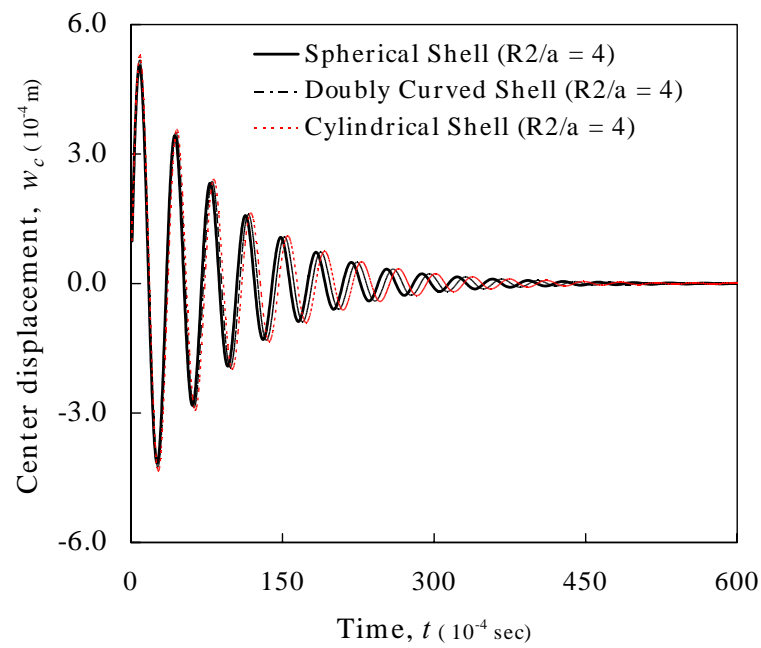
The maximum deflection and vibration suppression time have been tabulated in Table 3.16 for CFRP laminated shells. In this study, vibration suppression time is defined as the time required to reduce the center displacements to 10% of its uncontrolled magnitude. The maximum transverse deflection and vibration suppression time are occurred in cylindrical shell with the largest R_2/a . The spherical shell with the smallest R_2/a shows the minimum deflection and vibration suppression time.

3.5.5. Effect of Material Properties

Finally, the effect of elastic material property on the vibration suppression characteristics is studied for spherical, cylindrical, and doubly curved shells. Gr-Ep(AS), Gl-Ep, and Br-Ep are considered in addition to CFRP as elastic materials of laminated composite shells. The frequency ϖ_d , damping coefficient $-\alpha_d$, the maximum deflection w_{\max} , and vibration suppression time of the thin and thick shells with different elastic materials are tabulated in Tables 3.17 and 3.18. Figure 3.17 shows the vibration suppression of different elastic materials for the thin shells. The same trend of vibration suppression characteristics of CFRP shells could be found in the shells with different elastic materials. It is observed from the tables that Gl-Ep shows the largest damping coefficients, maximum deflections and the minimum vibration suppression time regardless of shell type and thickness.



(a)



(b)

Figure 3.16 Vibration suppression characteristics for different CFRP shells; (a) Thin shell ($a/h = 100$), (b) Thick shell ($a/h = 10$)

Table 3.15 Selected center displacement versus time of the symmetric cross-ply (m,90,0,90,0)s CFRP laminated shells with $R_2/a = 5$ by Sanders shell theory

t ($\times 10^4$ sec)	Center Displacement ($\times 10^4 m$)					
	Thin Shell ($a/h = 100$)			Thick Shell ($a/h = 10$)		
	Spherical shell	Cylindrical shell	Doubly curved shell	Spherical shell	Cylindrical shell	Doubly curved shell
1	0.9974	0.9982	0.9979	0.9840	0.9846	0.9843
2	1.9880	1.9920	1.9900	1.9160	1.9200	1.9180
3	2.9680	2.9810	2.9750	2.7690	2.7800	2.7750
4	3.9360	3.9640	3.9510	3.5190	3.5410	3.5310
5	4.8880	4.9390	4.9160	4.1430	4.1840	4.1650
7	6.7330	6.8640	6.8070	4.9580	5.0520	5.0100
10	9.3160	9.6760	9.5210	4.9890	5.2040	5.1070
15	12.9700	14.1000	13.6100	2.2940	2.7110	2.5240
20	15.6000	18.1000	17.0100	-1.7080	-1.3080	-1.4890
30	17.1700	24.4700	21.2100	-3.4200	-3.8790	-3.6800
40	13.7800	28.2600	21.5100	2.5420	2.0320	2.2720
50	6.5950	29.1500	17.9800	1.8760	2.6260	2.3020
70	-9.9890	22.5800	3.0300	-0.5872	-1.5450	-1.1250
90	-14.9000	7.9410	-12.8700	-0.3350	0.6835	0.2234
110	-3.9670	-8.7600	-19.0900	0.8771	-0.0524	0.3889
130	10.2200	-21.1200	-12.1800	-1.0900	-0.3655	-0.7385
150	12.6800	-24.7700	2.3300	1.0570	0.6022	0.8746
200	-12.1000	0.9747	12.3800	-0.4081	0.2315	-0.0799
250	9.6960	21.0400	-14.0700	0.0340	-0.3837	-0.2288
300	-6.1910	-1.2420	3.5030	0.1039	0.2109	0.2211
400	1.1520	1.4080	-11.0200	0.0693	-0.0522	0.0182
500	5.3800	-1.4950	5.3130	0.0044	-0.0191	-0.0247
700	2.2070	-1.5100	-6.4060	-0.0020	0.0013	0.0027
900	-2.5720	-1.3990	3.1620	0.0003	0.0000	-0.0003
1000	-2.1900	1.3200	-3.4700	0.0000	0.0001	-0.0001

Table 3.16 Maximum transverse deflection and vibration suppression time for the symmetric cross-ply (m,90,0,90,0)s CFRP laminated shells

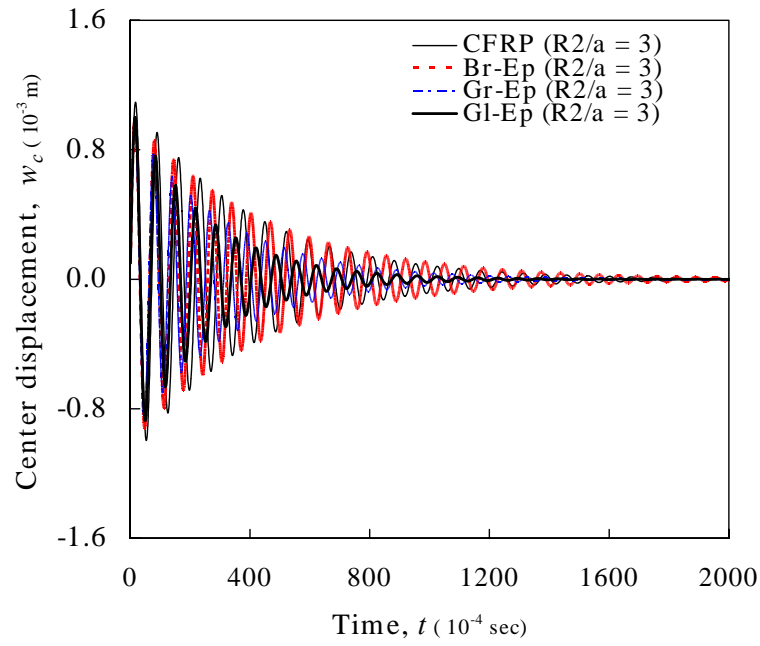
R_2/a	Shell Type	Thin Shell ($a/h = 100$)		Thick Shell ($a/h = 10$)	
		w_{\max}	$t(\text{sec})$ at $w_{\max}/10$	w_{\max}	$t(\text{sec})$ at $w_{\max}/10$
3	Spherical Shell	0.001094	0.0887	0.000487	0.0209
	Cylindrical Shell	0.002018	0.1247	0.000524	0.0225
	Doubly Curved Shell	0.001422	0.1059	0.000505	0.0217
5	Spherical Shell	0.001727	0.1125	0.000514	0.0222
	Cylindrical Shell	0.002920	0.1451	0.000531	0.0229
	Doubly Curved Shell	0.002187	0.1223	0.000523	0.0226
10	Spherical Shell	0.002916	0.1444	0.000530	0.0229
	Cylindrical Shell	0.004039	0.1756	0.000534	0.0230
	Doubly Curved Shell	0.003430	0.1591	0.000532	0.0230
50	Spherical Shell	0.004713	0.1895	0.000536	0.0231
	Cylindrical Shell	0.004850	0.1943	0.000536	0.0231
	Doubly Curved Shell	0.004790	0.1914	0.000536	0.0231
100	Spherical Shell	0.004850	0.1943	0.000536	0.0231
	Cylindrical Shell	0.004890	0.1975	0.000536	0.0231
	Doubly Curved Shell	0.004873	0.1956	0.000536	0.0231

Table 3.17 Vibration suppression characteristics for the thin symmetric cross-ply (m,90,0,90,0)s laminated shells with the different composite materials

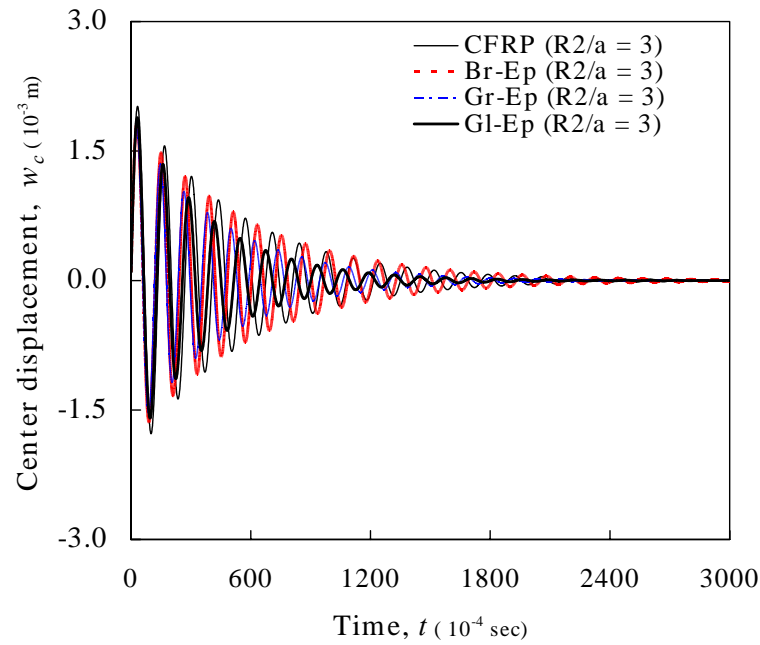
Thickness	Material	R_2/a	Shell Type	$-\alpha_d$	ω_d	w_{\max}	$t(\text{sec})$ at $w_{\max}/10$
Thin Shell $a/h = 100$	Br-Ep	3	Spherical	22.7268	972.4400	0.000992	0.0987
			Cylindrical	17.2074	520.6025	0.001824	0.1237
			Doubly Curved	20.0674	744.5307	0.001288	0.1123
		10	Spherical	15.0417	356.6537	0.002626	0.1553
			Cylindrical	13.2753	255.8587	0.003607	0.1778
			Doubly Curved	14.1640	302.0174	0.003079	0.1623
	Gr-Ep (AS)	3	Spherical	31.9361	1006.8317	0.000945	0.0702
			Cylindrical	22.6085	532.1451	0.001759	0.1031
			Doubly Curved	27.4022	767.8548	0.001232	0.0838
		10	Spherical	18.9261	357.2369	0.002579	0.1273
			Cylindrical	15.9857	246.9154	0.003666	0.1588
			Doubly Curved	17.4624	297.9251	0.003066	0.1316
	Gl-Ep	3	Spherical	40.5446	933.7043	0.001001	0.0560
			Cylindrical	26.1841	487.8336	0.001887	0.0876
			Doubly Curved	33.4922	709.4313	0.001309	0.0733
		10	Spherical	20.5195	321.6349	0.002818	0.1219
			Cylindrical	16.0851	214.3368	0.004158	0.1532
			Doubly Curved	18.3081	264.4086	0.003400	0.1261

Table 3.18 Vibration suppression characteristics for the thick symmetric cross-ply (m,90,0,90,0)s laminated shells with the different composite materials

Thickness	Material	R_2/a	Shell Type	$-\alpha_d$	ω_d	w_{\max}	$t(\text{sec})$ at $w_{\max}/10$
Thick Shell $a/h = 10$	Br-Ep	3	Spherical	105.8611	2115.7754	0.000437	0.0213
			Cylindrical	101.9342	1965.9601	0.000469	0.0230
			Doubly Curved	104.3097	2033.2345	0.000452	0.0222
		10	Spherical	101.1661	1947.3458	0.000474	0.0233
			Cylindrical	99.6938	1932.9803	0.000478	0.0235
			Doubly Curved	100.4647	1939.2729	0.000476	0.0235
	Gr-Ep (AS)	3	Spherical	131.2207	2063.4504	0.000438	0.0189
			Cylindrical	123.6701	1892.5972	0.000478	0.0191
			Doubly Curved	127.9278	1968.9198	0.000458	0.0189
		10	Spherical	121.6644	1868.2618	0.000484	0.0209
			Cylindrical	119.0876	1851.7913	0.000489	0.0195
			Doubly Curved	120.4154	1858.9472	0.000487	0.0195
	Gl-Ep	3	Spherical	131.0681	1782.7453	0.000500	0.0185
			Cylindrical	118.0475	1604.9161	0.000556	0.0205
			Doubly Curved	124.9809	1684.1377	0.000530	0.0195
		10	Spherical	113.8741	1575.5661	0.000566	0.0209
			Cylindrical	109.7757	1558.2955	0.000575	0.0212
			Doubly Curved	111.8580	1565.7502	0.000571	0.0210



(a)



(b)

Figure 3.17 Effect of elastic material properties on vibration suppression characteristics for thin ($a/h = 100$) shells; (a) spherical shell, (b) cylindrical shell, (c) doubly curved shell

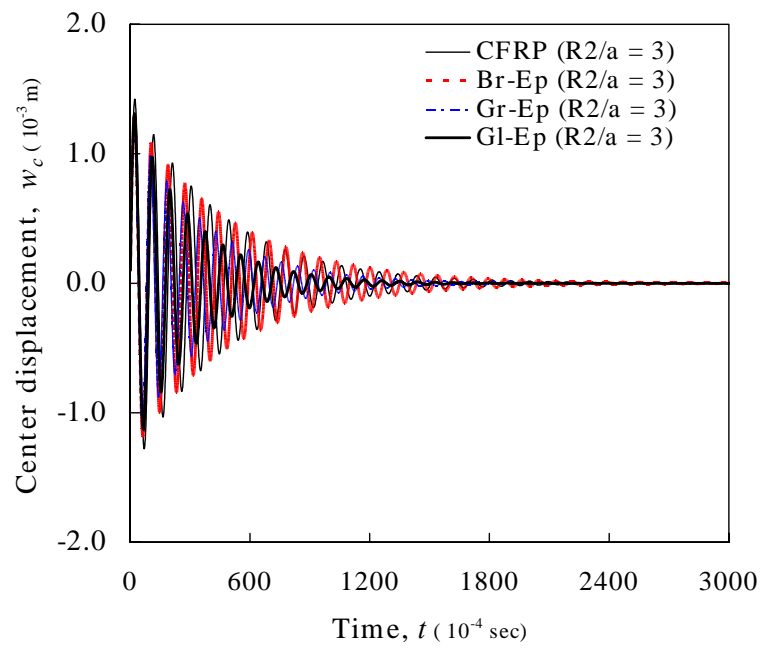


Figure 3.17 Continued

4. FINITE ELEMENT FORMULATIONS*

4.1. Virtual Work Statements

In this Section, the linear and nonlinear finite element formulations and numerical results of the linear analysis of laminated composite plate and shell structures are presented. Finite element models are developed using the weak forms of governing differential equations (see Reddy 2004 b).

4.1.1. Virtual Work Statements for Laminated Composite Plates

The virtual work statements of the TSDT over a typical finite element domain Ω^e are given by

$$0 = \int_{\Omega^e} \left\{ \frac{\partial \delta u_0}{\partial x} N_{xx} + \frac{\partial \delta u_0}{\partial y} N_{xy} + \delta u_0 \left[I_0 \frac{\partial^2 u_0}{\partial t^2} + J_1 \frac{\partial^2 \phi_x}{\partial t^2} - c_1 I_3 \frac{\partial^2}{\partial t^2} \left(\frac{\partial w_0}{\partial x} \right) \right] \right\} dxdy - \oint \{ \delta u_0 (N_{xx} n_x + N_{xy} n_y) \} ds \quad (4.1.a)$$

$$0 = \int_{\Omega^e} \left\{ \frac{\partial \delta v_0}{\partial x} N_{xy} + \frac{\partial \delta v_0}{\partial y} N_{yy} + \delta v_0 \left[I_0 \frac{\partial^2 v_0}{\partial t^2} + J_1 \frac{\partial^2 \phi_y}{\partial t^2} - c_1 I_3 \frac{\partial^2}{\partial t^2} \left(\frac{\partial w_0}{\partial y} \right) \right] \right\} dxdy - \oint_{\Gamma} \{ \delta v_0 (N_{xy} n_x + N_{yy} n_y) \} ds \quad (4.1.b)$$

$$0 = \int_{\Omega^e} \left\{ \frac{\partial \delta w_0}{\partial x} \bar{Q}_x + \frac{\partial \delta w_0}{\partial y} \bar{Q}_y - c_1 \left(\frac{\partial^2 \delta w_0}{\partial x^2} P_{xx} + 2 \frac{\partial^2 \delta w_0}{\partial x \partial y} P_{xy} + \frac{\partial^2 \delta w_0}{\partial y^2} P_{yy} \right) - \delta w_0 q + \frac{\partial \delta w_0}{\partial x} \left(N_{xx} \frac{\partial w_0}{\partial x} + N_{xy} \frac{\partial w_0}{\partial y} \right) + \frac{\partial \delta w_0}{\partial y} \right\} dxdy \quad (4.1.c)$$

*Part of the data reported in this section is reprinted with permission from “Transient analysis of laminated composite plates with embedded smart-material layers” by Lee, S.J., Reddy, J.N., and Romstan-Abadi, F. (2004), *Finite Elements in Analysis and Design*, 40, 463-483, Copyright 2004 by Elsevier Science B.V.

$$\begin{aligned}
& \left(N_{xy} \frac{\partial w_0}{\partial x} + N_{yy} \frac{\partial w_0}{\partial y} \right) + \delta w_0 I_0 \frac{\partial^2 w_0}{\partial t^2} + c_1^2 I_6 \left(\frac{\partial \delta w_0}{\partial x} \frac{\partial^3 w_0}{\partial x \partial t^2} + \right. \\
& \left. \frac{\partial \delta w_0}{\partial y} \frac{\partial^3 w_0}{\partial y \partial t^2} \right) - c_1 \left[I_3 \left(\frac{\partial \delta w_0}{\partial x} \frac{\partial^2 u_0}{\partial t^2} + \frac{\partial \delta w_0}{\partial y} \frac{\partial^2 v_0}{\partial t^2} \right) + J_4 \left(\frac{\partial \delta w_0}{\partial x} \right. \right. \\
& \left. \left. \frac{\partial^2 \phi_x}{\partial t^2} + \frac{\partial \delta w_0}{\partial y} \frac{\partial^2 \phi_y}{\partial t^2} \right) \right] \Bigg\} dx dy - \oint_{\Gamma} \delta w_0 \bar{V}_n ds - \oint_{\Gamma} \frac{\partial \delta w_0}{\partial n} p_{nn} ds \\
0 = & \int_{\Omega^e} \left\{ \frac{\partial \delta \phi_x}{\partial x} \bar{M}_{xx} + \frac{\partial \delta \phi_x}{\partial y} \bar{M}_{xy} + \delta \phi_x \bar{Q}_x + \delta \phi_x \left[\frac{\partial^2}{\partial t^2} (J_1 u_0 + K_2 \phi_x - \right. \right. \\
& \left. \left. c_1 J_4 \frac{\partial w_0}{\partial x}) \right] \right\} dx dy - \oint_{\Gamma} \{ \delta \phi_x (\bar{M}_{xx} n_x + \bar{M}_{xy} n_y) \} ds \tag{4.1.d} \\
0 = & \int_{\Omega^e} \left\{ \frac{\partial \delta \phi_y}{\partial x} \bar{M}_{xy} + \frac{\partial \delta \phi_y}{\partial y} \bar{M}_{yy} + \delta \phi_y \bar{Q}_y + \delta \phi_y \left[\frac{\partial^2}{\partial t^2} (J_1 v_0 + K_2 \phi_y - \right. \right. \\
& \left. \left. c_1 J_4 \frac{\partial w_0}{\partial y}) \right] \right\} dx dy - \oint_{\Gamma} \{ \delta \phi_y (\bar{M}_{xy} n_x + \bar{M}_{yy} n_y) \} ds \tag{4.1.e}
\end{aligned}$$

As a special case of TSDT, the virtual statements for classical laminated plate theory are

$$\begin{aligned}
0 = & \int_{\Omega^e} \left\{ \frac{\partial \delta u_0}{\partial x} N_{xx} + \frac{\partial \delta u_0}{\partial y} N_{xy} + \delta u_0 \left[I_0 \frac{\partial^2 u_0}{\partial t^2} - I_1 \frac{\partial^2}{\partial t^2} \left(\frac{\partial w_0}{\partial x} \right) \right] \right\} dx dy \\
& - \oint_{\Gamma} \left\{ \delta u_0 (N_{xx} n_x + N_{xy} n_y) \right\} ds \tag{4.2.a} \\
0 = & \int_{\Omega^e} \left\{ \frac{\partial \delta v_0}{\partial x} N_{xy} + \frac{\partial \delta v_0}{\partial y} N_{yy} + \delta v_0 \left[I_0 \frac{\partial^2 v_0}{\partial t^2} - I_1 \frac{\partial^2}{\partial t^2} \left(\frac{\partial w_0}{\partial y} \right) \right] \right\} dx dy \\
& - \oint_{\Gamma} \left\{ \delta v_0 (N_{xy} n_x + N_{yy} n_y) \right\} ds \tag{4.2.b}
\end{aligned}$$

$$\begin{aligned}
0 = \int_{\Omega^e} & \left\{ \left[-\frac{\partial^2 \delta w_0}{\partial x^2} M_{xx} - 2 \frac{\partial^2 \delta w_0}{\partial x \partial y} M_{xy} - \frac{\partial^2 \delta w_0}{\partial y^2} M_{yy} - \delta w_0 q + \frac{\partial \delta w_0}{\partial x} \right. \right. \\
& \left(N_{xx} \frac{\partial w_0}{\partial x} + N_{xy} \frac{\partial w_0}{\partial y} \right) + \frac{\partial \delta w_0}{\partial y} \left(N_{xy} \frac{\partial w_0}{\partial x} + N_{yy} \frac{\partial w_0}{\partial y} \right) + \delta w_0 I_0 \\
& \frac{\partial^2 w_0}{\partial t^2} + I_2 \frac{\partial^2}{\partial t^2} \left(\frac{\partial \delta w_0}{\partial x} \frac{\partial w_0}{\partial x} + \frac{\partial \delta w_0}{\partial y} \frac{\partial w_0}{\partial y} \right) - I_1 \frac{\partial^2}{\partial t^2} \left(\frac{\partial \delta w_0}{\partial x} u_0 \right. \\
& \left. \left. + \frac{\partial \delta w_0}{\partial y} v_0 \right) \right] \Bigg\} dx dy - \oint_{\Gamma} (\delta w_0 V_n + P_n) ds
\end{aligned} \tag{4.2.c}$$

where

$$\begin{aligned}
V_n = & \left[\left(\frac{\partial M_{xx}}{\partial x} + \frac{\partial M_{yy}}{\partial y} + N_{xx} \frac{\partial w_0}{\partial x} + N_{xy} \frac{\partial w_0}{\partial y} \right) n_x + \right. \\
& \left. \left(\frac{\partial M_{xy}}{\partial x} + \frac{\partial M_{yy}}{\partial y} + N_{xy} \frac{\partial w_0}{\partial x} + N_{yy} \frac{\partial w_0}{\partial y} \right) n_y \right] + \\
& \left[\left(I_1 \ddot{u}_0 - I_2 \frac{\partial \ddot{w}_0}{\partial x} \right) n_x + \left(I_1 \ddot{v}_0 - I_2 \frac{\partial \ddot{w}_0}{\partial y} \right) n_y \right]
\end{aligned} \tag{4.3.a}$$

$$P_n = \left(M_{xx} n_x + M_{xy} n_y \right) \frac{\partial \delta w_0}{\partial x} + \left(M_{xy} n_x + M_{yy} n_y \right) \frac{\partial \delta w_0}{\partial y} \tag{4.3.b}$$

For the first-order shear deformation theory, the virtual work statements are

$$\begin{aligned}
0 = \int_{\Omega^e} & \left\{ \frac{\partial \delta u_0}{\partial x} N_{xx} + \frac{\partial \delta u_0}{\partial y} N_{xy} + \delta u_0 \left[I_0 \frac{\partial^2 u_0}{\partial t^2} + I_1 \frac{\partial^2 \phi_x}{\partial t^2} \right] \right\} dx dy \\
& - \oint_{\Gamma} \left\{ \delta u_0 (N_{xx} n_x + N_{xy} n_y) \right\} ds
\end{aligned} \tag{4.4.a}$$

$$\begin{aligned}
0 = \int_{\Omega^e} & \left\{ \frac{\partial \delta v_0}{\partial x} N_{xy} + \frac{\partial \delta v_0}{\partial y} N_{yy} + \delta v_0 \left[I_0 \frac{\partial^2 v_0}{\partial t^2} + I_1 \frac{\partial^2 \phi_y}{\partial t^2} \right] \right\} dx dy \\
& - \oint_{\Gamma} \left\{ \delta v_0 (N_{xy} n_x + N_{yy} n_y) \right\} ds
\end{aligned} \tag{4.4.b}$$

$$0 = \int_{\Omega^e} \left\{ \frac{\partial \delta w_0}{\partial x} Q_x + \frac{\partial \delta w_0}{\partial y} Q_y - \delta w_0 q + \frac{\partial \delta w_0}{\partial x} \left(N_{xx} \frac{\partial w_0}{\partial x} + N_{xy} \frac{\partial w_0}{\partial y} \right) \right. \\ \left. + \frac{\partial \delta w_0}{\partial y} \left(N_{xy} \frac{\partial w_0}{\partial x} + N_{yy} \frac{\partial w_0}{\partial y} \right) + \delta w_0 I_0 \frac{\partial^2 w_0}{\partial t^2} \right\} dx dy - \oint_{\Gamma} \delta w_0 V_n ds \quad (4.4.c)$$

$$0 = \int_{\Omega^e} \left\{ \frac{\partial \delta \phi_x}{\partial x} M_{xx} + \frac{\partial \delta \phi_x}{\partial y} M_{xy} + \delta \phi_x Q_x + \delta \phi_x \left[I_2 \frac{\partial^2 \phi_x}{\partial t^2} + I_1 \frac{\partial^2 u_0}{\partial t^2} \right] \right\} dx dy \\ - \oint_{\Gamma} \left\{ \delta \phi_x (M_{xx} \eta_x + M_{xy} \eta_y) \right\} ds \quad (4.4.d)$$

$$0 = \int_{\Omega^e} \left\{ \frac{\partial \delta \phi_y}{\partial x} M_{xy} + \frac{\partial \delta \phi_y}{\partial y} M_{yy} + \delta \phi_y Q_y + \delta \phi_y \left[I_2 \frac{\partial^2 \phi_y}{\partial t^2} + I_1 \frac{\partial^2 v_0}{\partial t^2} \right] \right\} dx dy \\ - \oint_{\Gamma} \left\{ \delta \phi_y (M_{xy} \eta_x + M_{yy} \eta_y) \right\} ds \quad (4.4.e)$$

where

$$V_n = \left[\left(Q_x + N_{xx} \frac{\partial w_0}{\partial x} + N_{xy} \frac{\partial w_0}{\partial y} \right) n_x + \left(Q_y + N_{xy} \frac{\partial w_0}{\partial x} + N_{yy} \frac{\partial w_0}{\partial y} \right) n_y \right] \quad (4.5)$$

4.1.2. Virtual Work Statements for Laminated Composite Shells

(1) Donnell nonlinear shell theory

$$0 = \int_{\Omega^e} \left\{ \frac{\partial \delta u_0}{\partial X_1} N_1 + \frac{\partial \delta u_0}{\partial X_2} N_6 + \delta u_0 \left[I_0 \frac{\partial^2 u_0}{\partial t^2} + J_1 \frac{\partial^2 \phi_1}{\partial t^2} - \right. \right. \\ \left. \left. c_1 I_3 \frac{\partial^2}{\partial t^2} \left(\frac{\partial w_0}{\partial X_1} \right) \right] \right\} dX_1 dX_2 - \oint_{\Gamma^e} \{ \delta u_0 (N_1 n_1 + N_6 n_2) \} ds \quad (4.6.a)$$

$$0 = \int_{\Omega^e} \left\{ \frac{\partial \delta v_0}{\partial X_1} N_6 + \frac{\partial \delta v_0}{\partial X_2} N_2 + \delta v_0 \left[I_0 \frac{\partial^2 v_0}{\partial t^2} + J_1 \frac{\partial^2 \phi_2}{\partial t^2} - \right. \right. \\ \left. \left. c_1 I_3 \frac{\partial^2}{\partial t^2} \left(\frac{\partial w_0}{\partial X_2} \right) \right] \right\} dX_1 dX_2 - \oint_{\Gamma^e} \{ \delta v_0 (N_6 n_1 + N_2 n_2) \} ds \quad (4.6.b)$$

$$\begin{aligned}
0 = \int_{\Omega^e} & \left\{ \frac{\partial \delta w_0}{\partial X_1} \bar{Q}_1 + \frac{\partial \delta w_0}{\partial X_2} \bar{Q}_2 - c_1 \left(\frac{\partial^2 \delta w_0}{\partial X_1^2} P_1 + 2 \frac{\partial^2 \delta w_0}{\partial X_1 \partial X_2} P_6 + \frac{\partial^2 \delta w_0}{\partial X_2^2} P_2 \right) \right. \\
& - \delta w_0 q + \delta w_0 \left(\frac{N_1}{R_1} + \frac{N_2}{R_2} \right) + \delta w_0 I_0 \frac{\partial^2 w_0}{\partial t^2} + c_1^2 I_6 \left(\frac{\partial \delta w_0}{\partial X_1} \frac{\partial^3 w_0}{\partial X_1 \partial t^2} + \right. \\
& \left. \frac{\partial \delta w_0}{\partial X_2} \frac{\partial^3 w_0}{\partial X_2 \partial t^2} \right) - c_1 \left[I_3 \left(\frac{\partial \delta w_0}{\partial X_1} \frac{\partial^2 u_0}{\partial t^2} + \frac{\partial \delta w_0}{\partial X_2} \frac{\partial^2 v_0}{\partial t^2} \right) + J_4 \left(\frac{\partial \delta w_0}{\partial X_1} \frac{\partial^2 \phi_1}{\partial t^2} \right. \right. \\
& \left. \left. + \frac{\partial \delta w_0}{\partial X_2} \frac{\partial^2 \phi_2}{\partial t^2} \right) \right] + \frac{\partial \delta w_0}{\partial X_1} \left(N_1 \frac{\partial w_0}{\partial X_1} + N_6 \frac{\partial w_0}{\partial X_2} \right) + \frac{\partial \delta w_0}{\partial X_2} \left(N_6 \frac{\partial w_0}{\partial X_1} + N_2 \right. \\
& \left. \left. \frac{\partial w_0}{\partial X_2} \right) \right\} dX_1 dX_2 - \oint_{\Gamma^e} \delta w_0 \bar{V}_n ds - \oint_{\Gamma^e} \frac{\partial \delta w_0}{\partial n} p_{nn} ds
\end{aligned} \tag{4.6.c}$$

$$\begin{aligned}
0 = \int_{\Omega^e} & \left\{ \frac{\partial \delta \phi_1}{\partial X_1} \bar{M}_1 + \frac{\partial \delta \phi_1}{\partial X_2} \bar{M}_6 + \delta \phi_1 \bar{Q}_1 + \delta \phi_1 \left[J_1 \frac{\partial^2 u_0}{\partial t^2} + K_2 \frac{\partial^2 \phi_1}{\partial t^2} - \right. \right. \\
& \left. \left. c_1 J_4 \frac{\partial^2}{\partial t^2} \left(\frac{\partial w_0}{\partial X_1} \right) \right] \right\} dX_1 dX_2 - \oint_{\Gamma^e} \{ \delta \phi_1 (\bar{M}_1 n_1 + \bar{M}_6 n_2) \} ds
\end{aligned} \tag{4.6.d}$$

$$\begin{aligned}
0 = \int_{\Omega^e} & \left\{ \frac{\partial \delta \phi_2}{\partial X_1} \bar{M}_6 + \frac{\partial \delta \phi_2}{\partial X_2} \bar{M}_2 + \delta \phi_2 \bar{Q}_2 + \delta \phi_2 \left[J_1 \frac{\partial^2 v_0}{\partial t^2} + K_2 \frac{\partial^2 \phi_2}{\partial t^2} - \right. \right. \\
& \left. \left. c_1 J_4 \frac{\partial^2}{\partial t^2} \left(\frac{\partial w_0}{\partial X_2} \right) \right] \right\} dX_1 dX_2 - \oint_{\Gamma^e} \{ \delta \phi_2 (\bar{M}_6 n_1 + \bar{M}_2 n_2) \} ds
\end{aligned} \tag{4.6.e}$$

where

$$\begin{aligned}
\bar{V}_n = c_1 & \left[\left(\frac{\partial P_1}{\partial X_1} + \frac{\partial P_6}{\partial X_2} \right) n_1 + \left(\frac{\partial P_6}{\partial X_1} + \frac{\partial P_2}{\partial X_2} \right) n_2 \right] \\
& - c_1 \left[\left(\bar{I}_3 \ddot{u}_0 + J_4 \ddot{\phi}_1 - c_1 I_6 \frac{\partial \ddot{w}_0}{\partial X_1} \right) n_1 + \left(\bar{I}_3 \ddot{v}_0 + J_4 \ddot{\phi}_2 - c_1 I_6 \frac{\partial \ddot{w}_0}{\partial X_2} \right) n_2 \right] \\
& + \left(\bar{Q}_1 n_1 + \bar{Q}_2 n_2 \right) + N(w_0) + c_1 \frac{\partial P_{ns}}{\partial s}
\end{aligned} \tag{4.7.a}$$

$$N(w_0) = \left(N_1 \frac{\partial w_0}{\partial X_1} + N_6 \frac{\partial w_0}{\partial X_2} \right) n_1 + \left(N_6 \frac{\partial w_0}{\partial X_1} + N_2 \frac{\partial w_0}{\partial X_2} \right) n_2 \tag{4.7.b}$$

(2) Sanders nonlinear shell theory

$$\begin{aligned}
0 = \int_{\Omega^e} & \left\{ \frac{\partial \delta u_0}{\partial X_1} N_1 + \frac{\partial \delta u_0}{\partial X_2} N_6 - \delta u_0 \frac{\bar{Q}_1}{R_1} + \frac{c_1}{R_1} \left(\frac{\partial \delta u_0}{\partial X_1} P_1 + \frac{\partial \delta u_0}{\partial X_2} P_6 \right) + \delta u_0 \right. \\
& \left[\bar{I}_0 \frac{\partial^2 u_0}{\partial t^2} + \bar{J}_1 \frac{\partial^2 \phi_1}{\partial t^2} - c_1 \bar{I}_3 \frac{\partial^2}{\partial t^2} \left(\frac{\partial w_0}{\partial X_1} \right) \right] + \frac{\delta u_0}{R_1} \left[N_1 \left(\frac{\partial w_0}{\partial X_1} - \frac{u_0}{R_1} \right) + N_6 \right. \\
& \left. \left(\frac{\partial w_0}{\partial X_2} - \frac{v_0}{R_2} \right) \right] \Bigg\} dX_1 dX_2 - \oint_{\Gamma^e} \delta u_0 \left[\left(N_1 + \frac{c_1}{R_1} P_1 \right) n_1 + \left(N_6 + \frac{c_1}{R_1} P_6 \right) n_2 \right] ds
\end{aligned} \tag{4.8.a}$$

$$\begin{aligned}
0 = \int_{\Omega^e} & \left\{ \frac{\partial \delta v_0}{\partial X_1} N_6 + \frac{\partial \delta v_0}{\partial X_2} N_2 - \delta v_0 \frac{\bar{Q}_2}{R_2} + \frac{c_1}{R_2} \left(\frac{\partial \delta v_0}{\partial X_2} P_2 + \frac{\partial \delta v_0}{\partial X_1} P_6 \right) + \delta v_0 \right. \\
& \left[\bar{I}_0' \frac{\partial^2 v_0}{\partial t^2} + \bar{J}_1' \frac{\partial^2 \phi_2}{\partial t^2} - c_1 \bar{I}_3' \frac{\partial^2}{\partial t^2} \left(\frac{\partial w_0}{\partial X_2} \right) \right] + \frac{\delta v_0}{R_2} \left[N_6 \left(\frac{\partial w_0}{\partial X_1} - \frac{u_0}{R_1} \right) + N_2 \right. \\
& \left. \left(\frac{\partial w_0}{\partial X_2} - \frac{v_0}{R_2} \right) \right] \Bigg\} dX_1 dX_2 - \oint_{\Gamma^e} \delta v_0 \left[\left(N_6 + \frac{c_1}{R_2} P_6 \right) n_1 + \left(N_2 + \frac{c_1}{R_2} P_2 \right) n_2 \right] ds
\end{aligned} \tag{4.8.b}$$

$$\begin{aligned}
0 = \int_{\Omega^e} & \left\{ \frac{\partial \delta w_0}{\partial X_1} \bar{Q}_1 + \frac{\partial \delta w_0}{\partial X_2} \bar{Q}_2 - c_1 \left(\frac{\partial^2 \delta w_0}{\partial X_1^2} P_1 + 2 \frac{\partial^2 \delta w_0}{\partial X_1 \partial X_2} P_6 + \frac{\partial^2 \delta w_0}{\partial X_2^2} P_2 \right) \right. \\
& - \delta w_0 q + \delta w_0 \left(\frac{N_1}{R_1} + \frac{N_2}{R_2} \right) + \delta w_0 I_0 \frac{\partial^2 w_0}{\partial t^2} + c_1^2 I_6 \left(\frac{\partial \delta w_0}{\partial X_1} \frac{\partial^3 w_0}{\partial X_1 \partial t^2} + \right. \\
& \left. \frac{\partial \delta w_0}{\partial X_2} \frac{\partial^3 w_0}{\partial X_2 \partial t^2} \right) - c_1 \left[\left(\bar{I}_3 \frac{\partial \delta w_0}{\partial X_1} \frac{\partial^2 u_0}{\partial t^2} + \bar{I}_3' \frac{\partial \delta w_0}{\partial X_2} \frac{\partial^2 v_0}{\partial t^2} \right) + J_4 \left(\frac{\partial \delta w_0}{\partial X_1} \right. \right. \\
& \left. \left. \frac{\partial^2 \phi_1}{\partial t^2} + \frac{\partial \delta w_0}{\partial X_2} \frac{\partial^2 \phi_2}{\partial t^2} \right) \right] + \frac{\partial \delta w_0}{\partial X_1} \left[N_1 \left(\frac{\partial w_0}{\partial X_1} - \frac{u_0}{R_1} \right) + N_6 \left(\frac{\partial w_0}{\partial X_2} - \frac{v_0}{R_2} \right) \right] \\
& + \frac{\partial \delta w_0}{\partial X_2} \left[N_6 \left(\frac{\partial w_0}{\partial X_1} - \frac{u_0}{R_1} \right) + N_2 \left(\frac{\partial w_0}{\partial X_2} - \frac{v_0}{R_2} \right) \right] \Bigg\} dX_1 dX_2 - \oint_{\Gamma^e} \delta w_0 \bar{V}_n ds \\
& - \oint_{\Gamma^e} \frac{\partial \delta w_0}{\partial n} p_{nn} ds
\end{aligned} \tag{4.8.c}$$

$$0 = \int_{\Omega^e} \left\{ \frac{\partial \delta \phi_1}{\partial X_1} \bar{M}_1 + \frac{\partial \delta \phi_1}{\partial X_2} \bar{M}_6 + \delta \phi_1 \bar{Q}_1 + \delta \phi_1 \left[\bar{J}_1 \frac{\partial^2 u_0}{\partial t^2} + \bar{K}_2 \frac{\partial^2 \phi_1}{\partial t^2} - c_1 J_4 \frac{\partial^2}{\partial t^2} \left(\frac{\partial w_0}{\partial X_1} \right) \right] \right\} dX_1 dX_2 - \oint_{\Gamma^e} \{ \delta \phi_1 (\bar{M}_1 n_1 + \bar{M}_6 n_2) \} ds \quad (4.8.d)$$

$$0 = \int_{\Omega^e} \left\{ \frac{\partial \delta \phi_2}{\partial X_1} \bar{M}_6 + \frac{\partial \delta \phi_2}{\partial X_2} \bar{M}_2 + \delta \phi_2 \bar{Q}_2 + \delta \phi_2 \left[\bar{J}_1' \frac{\partial^2 v_0}{\partial t^2} + \bar{K}_2 \frac{\partial^2 \phi_2}{\partial t^2} - c_1 J_4 \frac{\partial^2}{\partial t^2} \left(\frac{\partial w_0}{\partial X_2} \right) \right] \right\} dX_1 dX_2 - \oint_{\Gamma^e} \{ \delta \phi_2 (\bar{M}_6 n_1 + \bar{M}_2 n_2) \} ds \quad (4.8.e)$$

where

$$\begin{aligned} \bar{V}_n = & c_1 \left[\left(\frac{\partial P_1}{\partial X_1} + \frac{\partial P_6}{\partial X_2} \right) n_1 + \left(\frac{\partial P_6}{\partial X_1} + \frac{\partial P_2}{\partial X_2} \right) n_2 \right] \\ & - c_1 \left[\left(\bar{I}_3 \ddot{u}_0 + J_4 \ddot{\phi}_1 - c_1 I_6 \frac{\partial \ddot{w}_0}{\partial X_1} \right) n_1 + \left(\bar{I}_3' \ddot{v}_0 + J_4 \ddot{\phi}_2 - c_1 I_6 \frac{\partial \ddot{w}_0}{\partial X_2} \right) n_2 \right] \\ & + \left(\bar{Q}_1 n_1 + \bar{Q}_2 n_2 \right) + c_1 \frac{\partial P_{ns}}{\partial s} + N_n(u_0, v_0, w_0) \end{aligned} \quad (4.9.a)$$

$$\begin{aligned} N_n(u_0, v_0, w_0) = & \left[N_1 \left(\frac{\partial w_0}{\partial X_1} - \frac{u_0}{R_1} \right) + N_6 \left(\frac{\partial w_0}{\partial X_2} - \frac{v_0}{R_2} \right) \right] n_1 \\ & + \left[N_6 \left(\frac{\partial w_0}{\partial X_1} - \frac{u_0}{R_1} \right) + N_2 \left(\frac{\partial w_0}{\partial X_2} - \frac{v_0}{R_2} \right) \right] n_2 \end{aligned} \quad (4.9.b)$$

For the modified Sanders shell theory for shallow shell, the virtual work statements are

$$\begin{aligned}
0 = \int_{\Omega^e} & \left\{ \frac{\partial \delta u_0}{\partial X_1} N_1 + \frac{\partial \delta u_0}{\partial X_2} N_6 - \delta u_0 \frac{\bar{Q}_1}{R_1} + \frac{c_1}{R_1} \left(\frac{\partial \delta u_0}{\partial X_1} P_1 + \frac{\partial \delta u_0}{\partial X_2} P_6 \right) + \right. \\
& \left. \delta u_0 \left[\bar{I}_0 \frac{\partial^2 u_0}{\partial t^2} + \bar{J}_1 \frac{\partial^2 \phi_1}{\partial t^2} - c_1 \bar{I}_3 \frac{\partial^2}{\partial t^2} \left(\frac{\partial w_0}{\partial X_1} \right) \right] \right\} dX_1 dX_2 \\
& - \oint_{\Gamma^e} \delta u_0 \left[\left(N_1 + \frac{c_1}{R_1} P_1 \right) n_1 + \left(N_6 + \frac{c_1}{R_1} P_6 \right) n_2 \right] ds
\end{aligned} \tag{4.10.a}$$

$$\begin{aligned}
0 = \int_{\Omega^e} & \left\{ \frac{\partial \delta v_0}{\partial X_1} N_6 + \frac{\partial \delta v_0}{\partial X_2} N_2 - \delta v_0 \frac{\bar{Q}_2}{R_2} + \frac{c_1}{R_2} \left(\frac{\partial \delta v_0}{\partial X_2} P_2 + \frac{\partial \delta v_0}{\partial X_1} P_6 \right) + \right. \\
& \left. \delta v_0 \left[\bar{I}_0' \frac{\partial^2 v_0}{\partial t^2} + \bar{J}_1' \frac{\partial^2 \phi_2}{\partial t^2} - c_1 \bar{I}_3' \frac{\partial^2}{\partial t^2} \left(\frac{\partial w_0}{\partial X_2} \right) \right] \right\} dX_1 dX_2 \\
& - \oint_{\Gamma^e} \delta v_0 \left[\left(N_6 + \frac{c_1}{R_2} P_6 \right) n_1 + \left(N_2 + \frac{c_1}{R_2} P_2 \right) n_2 \right] ds
\end{aligned} \tag{4.10.b}$$

$$\begin{aligned}
0 = \int_{\Omega^e} & \left\{ \frac{\partial \delta w_0}{\partial X_1} \bar{Q}_1 + \frac{\partial \delta w_0}{\partial X_2} \bar{Q}_2 - c_1 \left(\frac{\partial^2 \delta w_0}{\partial X_1^2} P_1 + 2 \frac{\partial^2 \delta w_0}{\partial X_1 \partial X_2} P_6 + \frac{\partial^2 \delta w_0}{\partial X_2^2} P_2 \right) \right. \\
& - \delta w_0 q + \delta w_0 \left(\frac{N_1}{R_1} + \frac{N_2}{R_2} \right) + \delta w_0 I_0 \frac{\partial^2 w_0}{\partial t^2} + c_1^2 I_6 \left(\frac{\partial \delta w_0}{\partial X_1} \frac{\partial^3 w_0}{\partial X_1 \partial t^2} + \right. \\
& \left. \frac{\partial \delta w_0}{\partial X_2} \frac{\partial^3 w_0}{\partial X_2 \partial t^2} \right) - c_1 \left[I_3 \left(\frac{\partial \delta w_0}{\partial X_1} \frac{\partial^2 u_0}{\partial t^2} + \frac{\partial \delta w_0}{\partial X_2} \frac{\partial^2 v_0}{\partial t^2} \right) + J_4 \left(\frac{\partial \delta w_0}{\partial X_1} \frac{\partial^2 \phi_1}{\partial t^2} \right. \right. \\
& \left. \left. + \frac{\partial \delta w_0}{\partial X_2} \frac{\partial^2 \phi_2}{\partial t^2} \right) \right] + \frac{\partial \delta w_0}{\partial X_1} \left(N_1 \frac{\partial w_0}{\partial X_1} + N_6 \frac{\partial w_0}{\partial X_2} \right) + \frac{\partial \delta w_0}{\partial X_2} \left(N_6 \frac{\partial w_0}{\partial X_1} + N_2 \right. \\
& \left. \frac{\partial w_0}{\partial X_2} \right) \left. \right\} dX_1 dX_2 - \oint_{\Gamma^e} \delta w_0 \bar{V}_n ds - \oint_{\Gamma^e} \frac{\partial \delta w_0}{\partial n} p_{nn} ds
\end{aligned} \tag{4.10.c}$$

$$\begin{aligned}
0 = \int_{\Omega^e} & \left\{ \frac{\partial \delta \phi_1}{\partial X_1} \bar{M}_1 + \frac{\partial \delta \phi_1}{\partial X_2} \bar{M}_6 + \delta \phi_1 \bar{Q}_1 + \delta \phi_1 \left[\bar{J}_1 \frac{\partial^2 u_0}{\partial t^2} + \bar{K}_2 \frac{\partial^2 \phi_1}{\partial t^2} - \right. \right. \\
& \left. \left. c_1 J_4 \frac{\partial^2}{\partial t^2} \left(\frac{\partial w_0}{\partial X_1} \right) \right] \right\} dX_1 dX_2 - \oint_{\Gamma^e} \{ \delta \phi_1 (\bar{M}_1 n_1 + \bar{M}_6 n_2) \} ds
\end{aligned} \tag{4.10.d}$$

$$\begin{aligned}
0 = \int_{\Omega^e} & \left\{ \frac{\partial \delta \phi_2}{\partial X_1} \bar{M}_6 + \frac{\partial \delta \phi_2}{\partial X_2} \bar{M}_2 + \delta \phi_2 \bar{Q}_2 + \delta \phi_2 \left[\bar{J}_1' \frac{\partial^2 v_0}{\partial t^2} + \bar{K}_2 \frac{\partial^2 \phi_2}{\partial t^2} - \right. \right. \\
& \left. \left. c_1 J_4 \frac{\partial^2}{\partial t^2} \left(\frac{\partial w_0}{\partial X_2} \right) \right] \right\} dX_1 dX_2 - \oint_{\Gamma^e} \{ \delta \phi_2 (\bar{M}_6 n_1 + \bar{M}_2 n_2) \} ds
\end{aligned} \tag{4.10.e}$$

where

$$\begin{aligned}
\bar{V}_n = c_1 & \left[\left(\frac{\partial P_1}{\partial X_1} + \frac{\partial P_6}{\partial X_2} \right) n_1 + \left(\frac{\partial P_6}{\partial X_1} + \frac{\partial P_2}{\partial X_2} \right) n_2 \right] \\
& - c_1 \left[\left(\bar{I}_3 \ddot{u}_0 + J_4 \ddot{\phi}_1 - c_1 I_6 \frac{\partial \ddot{w}_0}{\partial X_1} \right) n_1 + \left(\bar{I}_3 \ddot{v}_0 + J_4 \ddot{\phi}_2 - c_1 I_6 \frac{\partial \ddot{w}_0}{\partial X_2} \right) n_2 \right] \\
& + \left(\bar{Q}_1 n_1 + \bar{Q}_2 n_2 \right) + N(w_0) + c_1 \frac{\partial P_{ns}}{\partial s}
\end{aligned} \tag{4.11.a}$$

$$N(w_0) = \left(N_1 \frac{\partial w_0}{\partial X_1} + N_6 \frac{\partial w_0}{\partial X_2} \right) n_1 + \left(N_6 \frac{\partial w_0}{\partial X_1} + N_2 \frac{\partial w_0}{\partial X_2} \right) n_2 \tag{4.11.b}$$

4.2. Finite Element Model

The generalized displacements are approximated over the domain Ω by the expressions

$$u_0(x, y, t) = \sum_{i=1}^m u_i^e(t) \psi_i^e(x, y) \tag{4.12.a}$$

$$v_0(x, y, t) = \sum_{i=1}^m v_i^e(t) \psi_i^e(x, y) \tag{4.12.b}$$

$$w_0(x, y, t) = \sum_{i=1}^m \bar{\Delta}_i^e(t) \varphi_i^e(x, y) \tag{4.12.c}$$

$$\phi_x(x, y, t) = \sum_{i=1}^m X_i^e(t) \psi_i^e(x, y) \tag{4.12.d}$$

$$\phi_y(x, y, t) = \sum_{i=1}^m Y_i^e(t) \psi_i^e(x, y) \tag{4.12.e}$$

where ψ_i^e denotes the Lagrange interpolation functions and φ_i^e denotes the Hermite interpolation functions. The same Lagrange linear rectangular element for in-plane displacements (u_0, v_0) and rotations (ϕ_x, ϕ_y) and the conforming rectangular elements for bending deflections are used in this study. The conforming element is one of C^1 plate bending elements in which the interelement continuity of $w_0, w_{0,x}, w_{0,y}$ are satisfied (see Reddy 1997, 2004 b). The combined conforming rectangular element, which has eight degrees of freedom $u_0, v_0, w_0, w_{0,x}, w_{0,y}, w_{0,xy}, \phi_x, \phi_y$ per node, is shown in Figure 4.1. The four nodal values associated with w_0 are $\bar{\Delta}_1 = w_0$, $\bar{\Delta}_2 = \frac{\partial w_0}{\partial x}$, $\bar{\Delta}_3 = \frac{\partial w_0}{\partial y}$, $\bar{\Delta}_4 = \frac{\partial^2 w_0}{\partial x \partial y}$.

Substitution of the approximation, Equation (4.12) for $u_0, v_0, w_0, \phi_x, \phi_y$, into the weak forms yields the semidiscrete finite element model of the third-order shear deformation theory

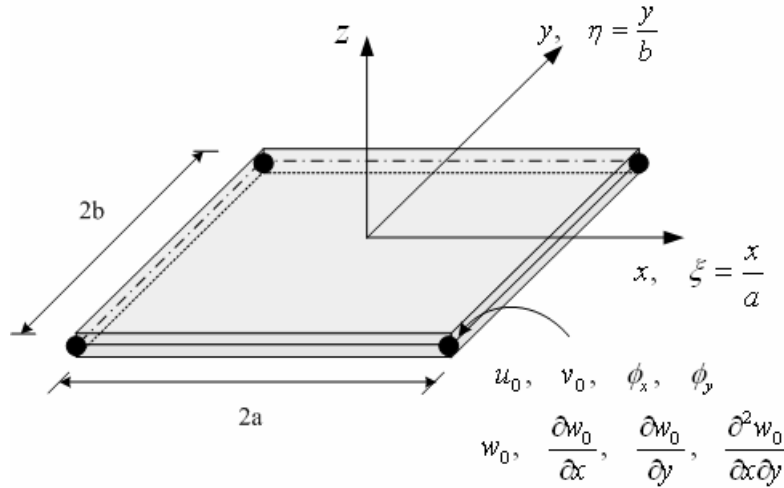


Figure 4.1 Conforming rectangular element with eight degrees of freedom per node

$$\begin{aligned}
& \begin{bmatrix} [K^{11}] & [K^{12}] & [K^{13}] & [K^{14}] & [K^{15}] \\ [K^{21}] & [K^{22}] & [K^{23}] & [K^{24}] & [K^{25}] \\ [K^{31}] & [K^{32}] & [K^{33}] & [K^{34}] & [K^{35}] \\ [K^{41}] & [K^{42}] & [K^{43}] & [K^{44}] & [K^{45}] \\ [K^{51}] & [K^{52}] & [K^{53}] & [K^{54}] & [K^{55}] \end{bmatrix} \begin{Bmatrix} \{u^e\} \\ \{v^e\} \\ \{\bar{\Delta}^e\} \\ \{X^e\} \\ \{Y^e\} \end{Bmatrix} + \\
& \begin{bmatrix} [C^{11}] & [C^{12}] & [C^{13}] & [C^{14}] & [C^{15}] \\ [C^{21}] & [C^{22}] & [C^{23}] & [C^{24}] & [C^{25}] \\ [C^{31}] & [C^{32}] & [C^{33}] & [C^{34}] & [C^{35}] \\ [C^{41}] & [C^{42}] & [C^{43}] & [C^{44}] & [C^{45}] \\ [C^{51}] & [C^{52}] & [C^{53}] & [C^{54}] & [C^{55}] \end{bmatrix} \begin{Bmatrix} \{\dot{u}^e\} \\ \{\dot{v}^e\} \\ \{\dot{\bar{\Delta}}^e\} \\ \{\dot{X}^e\} \\ \{\dot{Y}^e\} \end{Bmatrix} + \\
& \begin{bmatrix} [M^{11}] & [0] & [M^{13}] & [M^{14}] & [0] \\ [0] & [M^{22}] & [M^{23}] & [0] & [M^{25}] \\ [M^{13}]^T & [M^{23}]^T & [M^{33}] & [M^{34}] & [M^{35}] \\ [M^{14}]^T & [0] & [M^{34}]^T & [M^{44}] & [0] \\ [0] & [M^{25}]^T & [M^{53}]^T & [0] & [M^{55}] \end{bmatrix} \begin{Bmatrix} \{\ddot{u}^e\} \\ \{\ddot{v}^e\} \\ \{\ddot{\bar{\Delta}}^e\} \\ \{\ddot{X}^e\} \\ \{\ddot{Y}^e\} \end{Bmatrix} = \begin{Bmatrix} \{F^1\} \\ \{F^2\} \\ \{F^3\} \\ \{F^4\} \\ \{F^5\} \end{Bmatrix} \quad (4.13.a)
\end{aligned}$$

or

$$\sum_{\beta=1}^5 \sum_{j=1}^{n_\beta} \left(K_{ij}^{\alpha\beta} \Delta_j^\beta + C_{ij}^{\alpha\beta} \dot{\Delta}_j^\beta + M_{ij}^{\alpha\beta} \ddot{\Delta}_j^\beta \right) - F_i^\alpha = 0, \quad i = 1, 2, \dots, n \quad (4.13.b)$$

where $\alpha = 1, 2, 3, 4, 5$; $n_1 = n_2 = n_4 = n_5 = 4$ and $n_3 = 16$ for the conforming element, and the nodal values Δ_j^β are $\Delta_j^1 = u_j$, $\Delta_j^2 = v_j$, $\Delta_j^3 = \bar{\Delta}_j$, $\Delta_j^4 = X_j$, $\Delta_j^5 = Y_j$.

Since the equations of motion are expressed in terms of the displacements and the generalized displacements are the primary modal degrees of freedom, this finite element models are called displacement finite element models (Reddy 1997, 2004 b). The shear and membrane locking problem (Reddy 2004 a) in this displacement finite element model can be overcome by using the reduced integration for evaluating the shear stiffness coefficients.

The thermal source term corresponding to the deflection is nonlinear and this nonlinearity becomes significant at high temperature. In this study, the nodal values of deflection are treated as unknowns and the resulting force term is transferred to the left hand side of the Equation (4.13). Thus the term is included into the direct stiffness matrix and this avoids re-calculation of tangent stiffness matrix in Newton-Raphson iteration method.

The stiffness coefficients $K_{ij}^{\alpha\beta} = (K_{ij}^{\alpha\beta})_L + (K_{ij}^{\alpha\beta})_{NL} + (K_{ij}^{\alpha\beta})_{NL}^T$, mass coefficients $M_{ij}^{\alpha\beta}$, and active damping coefficients $C_{ij}^{\alpha\beta} = (C_{ij}^{\alpha\beta})_L + (C_{ij}^{\alpha\beta})_{NL}$ for Donnell and Sanders nonlinear shell theory are well defined in the Appendice B and C. where $(K_{ij}^{\alpha\beta})_L$ is the linear stiffness coefficients, $(K_{ij}^{\alpha\beta})_{NL}$ is the geometric and $(K_{ij}^{\alpha\beta})_{NL}^T$ is the thermal nonlinear stiffness coefficients, $(C_{ij}^{\alpha\beta})_L$ is the linear and $(C_{ij}^{\alpha\beta})_{NL}$ is the nonlinear damping coefficients. Note by setting $R_1 = R_2 = \infty$ from the finite element coefficients of Donnell nonlinear theory, the coefficients of laminated composite plates by Third-order shear deformation theory can be obtained. In the case of the first-order shear deformation theory, the resulting finite element model requires only C^0 continuity for generalized displacements.

4.3. Transient Analysis

The linear equations of motion can be solved using analytical methods, but those are algebraically complicated and require the determination of eigenvalues and eigenfunctions, as in the state-space approach. Newmark's numerical integration method (Reddy 1983, 1993) that takes advantage of the static solution form for spatial variation and uses a numerical method to solve the resulting differential equations in time is used to determine the transient response of laminated composites in this study. The constant-average-acceleration scheme is used for linear transient problem.

Using the Newmark's scheme, a second-order differential equation of the form,

$$[M] \{\ddot{\Delta}\} + [C] \{\dot{\Delta}\} + [K] \{\Delta\} = \{F\} \quad (4.14)$$

can be reduced to the fully discretized form:

$$[\hat{K}(\{\Delta\}_{s+1})] \{\Delta\}_{s+1} = \{\hat{F}\}_{s;s+1} \quad (4.15)$$

where the subscript $s + 1$ refers to the time t_{s+1} at which the solution is sought, and

$$[\hat{K}(\{\Delta\}_{s+1})] = [K(\{\Delta\}_{s+1})] + a_3[M]_{s+1} + a_6[C]_{s+1} \quad (4.16.a)$$

$$\{\hat{F}\}_{s;s+1} = \{F\}_{s+1} + [M]_{s+1} \{\tilde{A}\}_s + [C]_{s+1} \{\tilde{B}\}_s \quad (4.16.b)$$

$$\{\tilde{A}\}_s = a_3\{\Delta\}_s + a_4\{\dot{\Delta}\}_s + a_5\{\ddot{\Delta}\}_s \quad (4.16.c)$$

$$\{\tilde{B}\}_s = a_6\{\Delta\}_s + a_7\{\dot{\Delta}\}_s + a_8\{\ddot{\Delta}\}_s \quad (4.16.d)$$

where a_i are the parameters

$$\begin{aligned} a_1 &= (1-\alpha)\Delta t, \quad a_2 = \alpha\Delta t, \quad a_3 = \frac{2}{\gamma(\Delta t)^2}, \quad a_4 = a_3\Delta t \\ a_5 &= \frac{(1-\gamma)}{\gamma}, \quad a_6 = \frac{2\alpha}{\gamma\Delta t}, \quad a_7 = \frac{2\alpha}{\gamma} - 1, \quad a_8 = \Delta t \left(\frac{\alpha}{\gamma} - 1 \right) \end{aligned} \quad (4.17)$$

At the end of each time step, the new velocity vector $\{\dot{\Delta}\}_{s+1}$ and acceleration vector $\{\ddot{\Delta}\}_{s+1}$ are computed using

$$\{\ddot{\Delta}\}_{s+1} = a_3(\{\Delta\}_{s+1} - \{\Delta\}_s) - a_4\{\dot{\Delta}\}_s - a_5\{\ddot{\Delta}\}_s \quad (4.18.a)$$

$$\{\dot{\Delta}\}_{s+1} = \{\dot{\Delta}\}_s + a_1\{\ddot{\Delta}\}_s + a_2\{\ddot{\Delta}\}_{s+1} \quad (4.18.b)$$

4.3. Nonlinear Analysis

The resulting nonlinear algebraic equations must be solved by an iterative method. In iterative methods, the nonlinear equations are linearized by evaluating the nonlinear terms with the known solution from preceding iteration. The Newton-Raphson iteration method, which is based on the Taylor series expansion and uses the tangent stiffness matrix, is selected in this study. This Newton-Raphson iteration method yields a symmetric tangent stiffness matrix for all structural problems.

Solution of Equation (4.15) by the Newton-Raphson iteration method results in the following linearized equations for the incremental solution at the $(r+1)st$ iteration (see Reddy, 2004a).

$$\{\delta\Delta\} = -[\hat{K}^T(\{\Delta\}_{s+1}^r)]^{-1}\{R\}_{s+1}^r \quad (4.19)$$

where the tangent stiffness matrix is defined by

$$[\hat{K}^T(\{\Delta\}_{s+1}^r)] \equiv \left[\frac{\partial\{R\}}{\partial\{\Delta\}} \right]_{s+1}^r \quad (4.20)$$

$$\{R\}_{s+1}^r = [\hat{K}(\{\Delta\}_{s+1}^r)]\{\Delta\}_{s+1}^r - \{\hat{F}\}_{s,s+1} \quad (4.21)$$

The total solution is obtained from

$$\{\Delta\}_{s+1}^{r+1} = \{\Delta\}_{s+1}^r + \{\delta\Delta\} \quad (4.22)$$

Note that the tangent stiffness matrix is evaluated using the latest known solution, while the residual vector contains contributions from the latest known solution in computing $[K(\{\Delta\}_{s+1}^r)]\{\Delta\}_{s+1}^r$ and previous time step solution in computing $\{\hat{F}\}_{s,s+1}$.

The iteration process is continued until the difference between $\{\Delta\}_{s+1}^r$ and $\{\Delta\}_{s+1}^{r+1}$ is reduced to a preselected error tolerance. The error criterion used in this study is of the form

$$\sqrt{\frac{\sum_{k=1}^n |\Delta_k^{r+1} - \Delta_k^r|^2}{\sum_{k=1}^n |\Delta_k^{r+1}|^2}} < \varepsilon \quad (4.23)$$

where n is the total number of nodal generalized displacements in the finite element mesh, and ε is the error tolerance. The velocity and acceleration vectors are updated using Equation (4.18) only after convergence is reached for a given time step. The details of the tangent stiffness coefficients could be found in the Appendices B and C.

4.5. Computer Implementation

Computer implementation of nonlinear time-dependent problems is complicated by the fact that one must keep track of the solution vectors at different loads, times, and iteration. Thus, there are three levels of calculations (see Reddy 2004 a). Often, for a fixed value of load, one wishes to obtain the transient solution. Thus the outermost loop is on the number of load steps, followed by a loop on the number of time steps, and the inner most loop being on nonlinear equilibrium iterations. A flow chart of the general scheme is shown in Figure 4.2. In the present study the load loop is suppressed as we are dealing with a single load.

4.6. Preliminary Linear Finite Element Results

Linear finite element analysis is carried out to analyze the deflection suppression characteristics. The baseline of the simulations is the simply supported square laminate ($a/b = 1$, $a/h = 10$) under sinusoidal distributions of the initial velocity field

$$\frac{\partial w}{\partial t}(x, y, t = 0) = \sin \frac{\pi x}{a} \sin \frac{\pi y}{b} \quad (4.24)$$

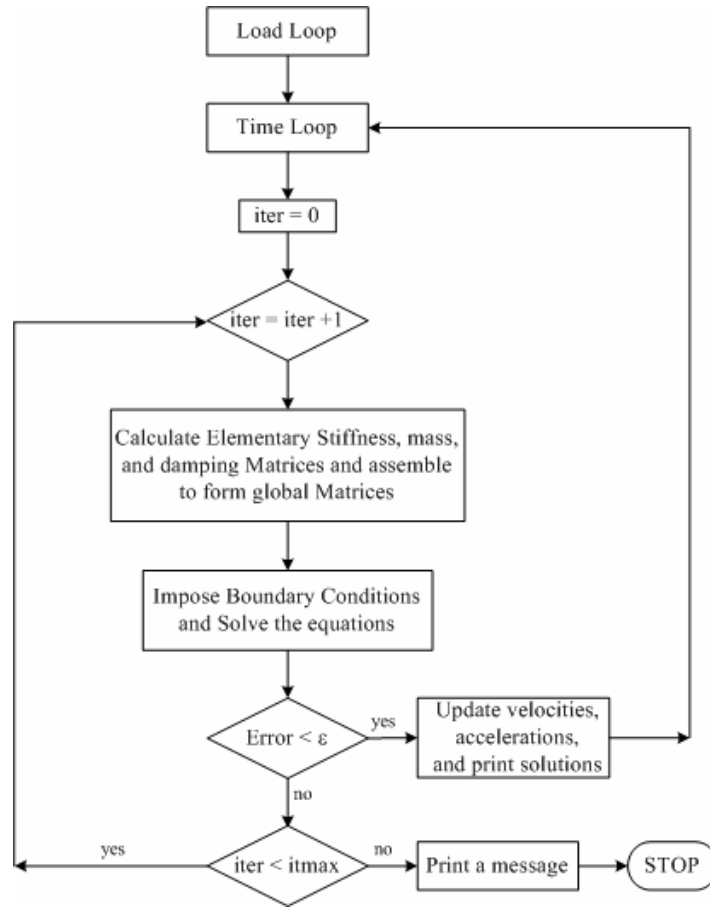


Figure 4.2 Flow chart of the nonlinear transient analysis of a problem

The time step selected in the linear transient study is $t = 0.0005\text{sec}$. The notation for lamination scheme $(\theta_1, \theta_2, \theta_3, \theta_4, m)_s$ means that there are 10 layers symmetrically placed about the midplane with the fiber orientations being $(\theta_1, \theta_2, \theta_3, \theta_4, m, m, \theta_4, \theta_3, \theta_2, \theta_1)$, where m stands for the magnetostrictive layer and subscript s stands for symmetric and *anti-s* stands for anti-symmetric lamination. The lamination schemes which are used in this study are symmetric cross-ply $(m, 90, 0, 90, 0)_s$, angle-ply $(m, 30, -30, 30, -30)_s$, general angle-ply $(m, 45, -45, 90, 0)_s$ laminates, anti-symmetric cross-ply $(m, 90, 0, 90, 0)_{\text{anti-s}}$, angle-ply $(m, 30, -30, 30, -30)_{\text{anti-s}}$, and general angle-ply $(m, 45, -45, 90, 0)_{\text{anti-s}}$ laminates. Simply supported and

clamped boundary conditions are selected to study the effect of boundary condition on the deflection control. The material properties of smart material, Terfenol-D, and the elastic composite materials which is used in this numerical example are listed in Table 3.1.

In finite element analysis, solution symmetries should be taken advantage of by identifying the computational domain to reduce computational effort. For a laminated composite plate with all edges simply-supported or clamped, a quadrant of the plate may be used as the computational domain as shown in Figure 4.3. Figures 4.4(a)-(d) shows the effects of the finite element results for the different laminations and boundary conditions. Quarter plate models with proper boundary conditions can be used in the antisymmetric laminates with simply supported boundary condition, but not for laminated plates with the clamped edges. For symmetric laminates, the simply supported cross-ply laminates can be modeled as a quarter plate. The boundary conditions along a line of symmetry should be correctly identified and imposed in the finite element model. When one is not sure of the solution symmetry, it is advised that the whole plate be modeled.

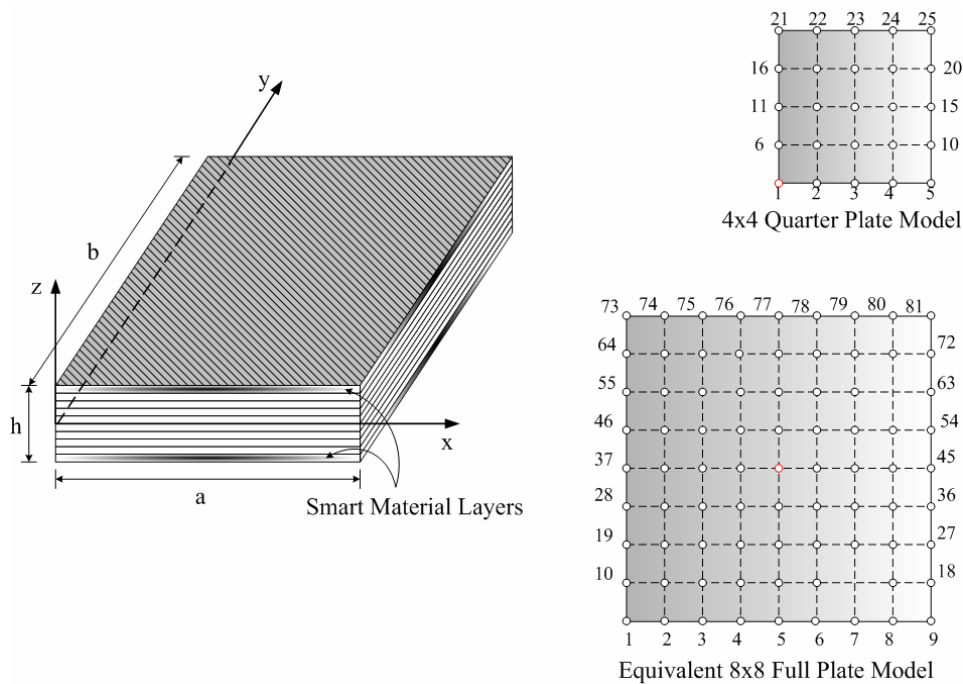
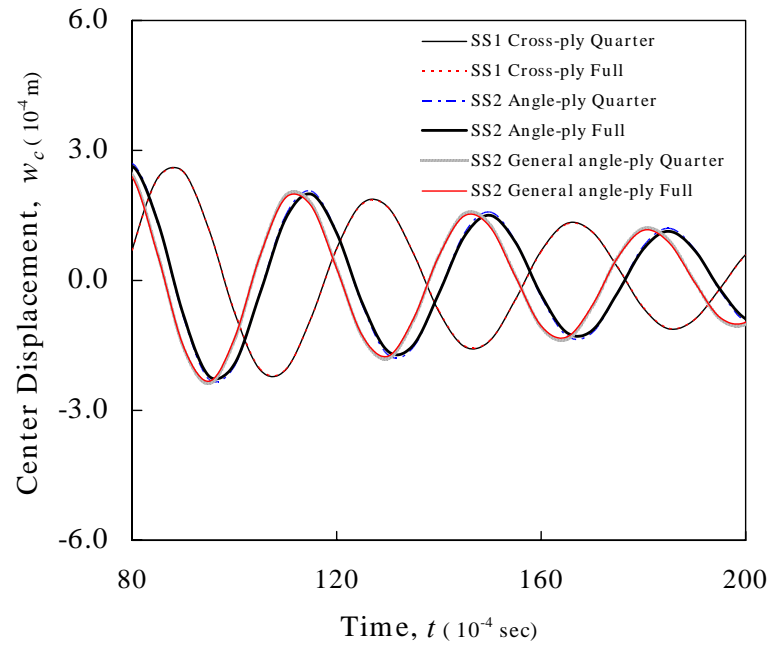
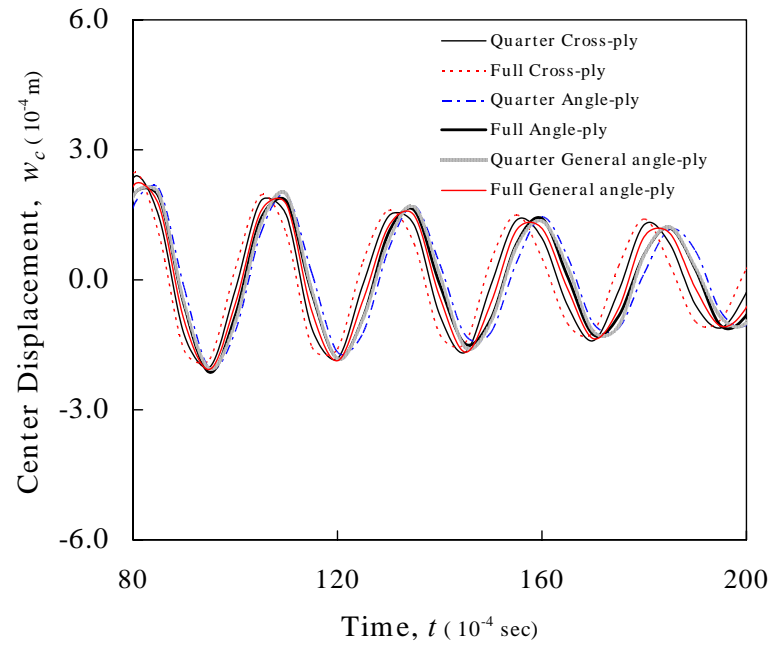


Figure 4.3 Finite element meshes of laminated composite plates



(a)



(b)

Figure 4.4 Effect of finite element modeling of CFRP composite plates; (a) Simply supported antisymmetric laminates, (b) Clamped antisymmetric laminates, (c) Simply supported symmetric laminates, (d) Clamped symmetric laminates

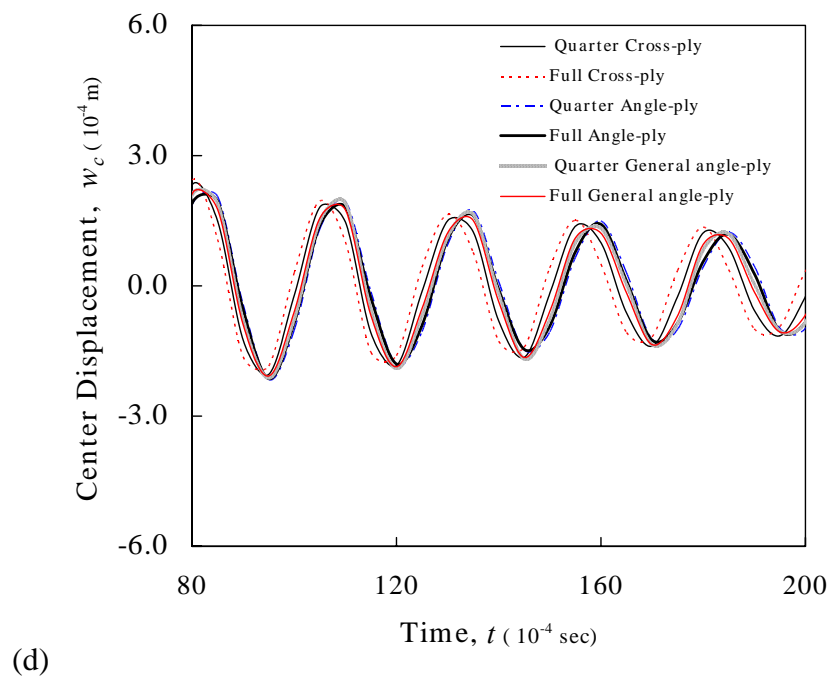
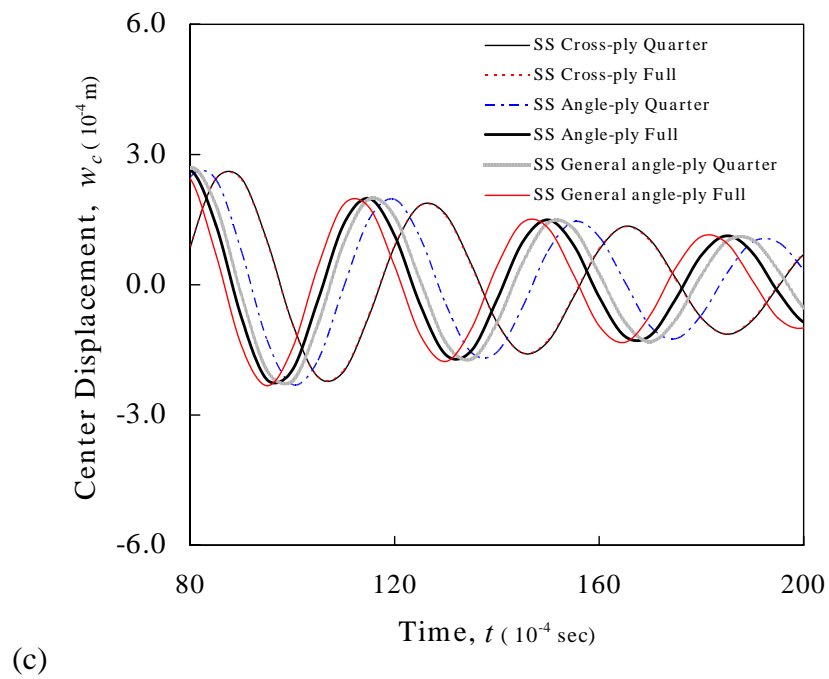


Figure 4.4 Continued

4.6.1. Simply Supported Laminated Composite Plates

To compare with the analytical results, the SS-1 boundary conditions and quarter plate model have been used for symmetric cross-ply laminates. The deflections predicted from the analytical (eigenvalue) analysis and transient finite element analysis are within the reasonable agreement, as shown in Figure 4.5 for cross-ply $(m,90,0,90,0)_s$ laminated plates. Figure 4.6 shows the central displacements using the different plate theories (CLPT, FSDT, and TSDT) for two different lamination schemes. It is observed that CLPT shows higher deflection suppression capacity in both cases. This is expected because the CLPT renders plate stiffer compared to the other theories. After studying the influence of lamina material properties on the amplitude of deflection and deflection suppression times, it is observed that materials having the almost same E_1/E_2 ratio have similar deflection suppression characteristics under the same lamination, loading and boundary conditions. Figure 4.7 shows the deflection damping characteristics for the different laminate materials

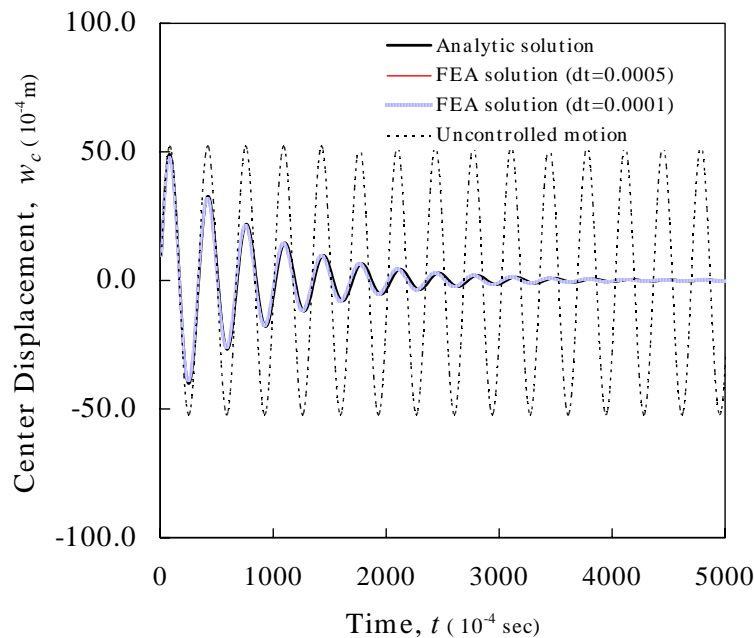
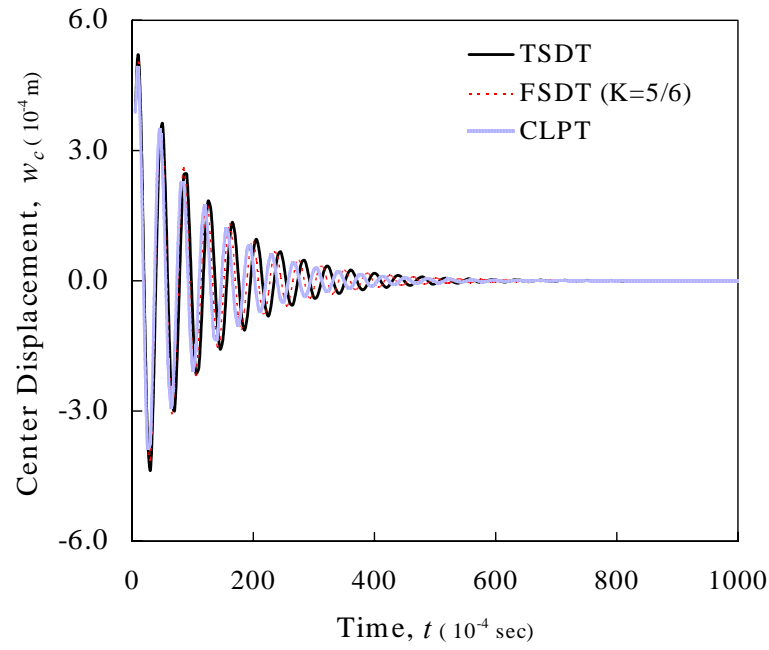
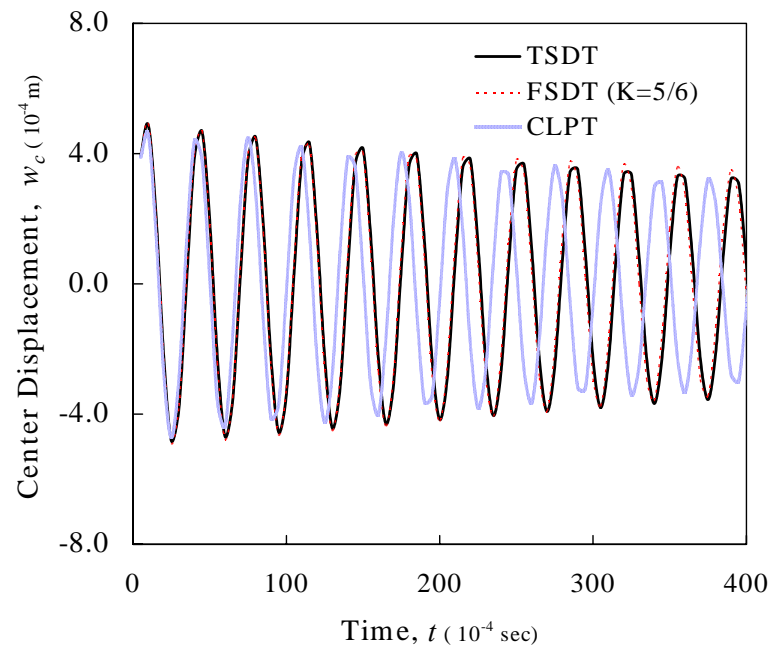


Figure 4.5 Center deflection predicted by the analytical and finite element methods for the case of symmetric cross-ply CFRP laminated plate



(a)



(b)

Figure 4.6 Center displacements by the different plate theories for simply supported cross-ply CFRP laminated plates; (a) $(m,90,0,90,0)_s$, (b) $(0,90,0,90,m)_s$

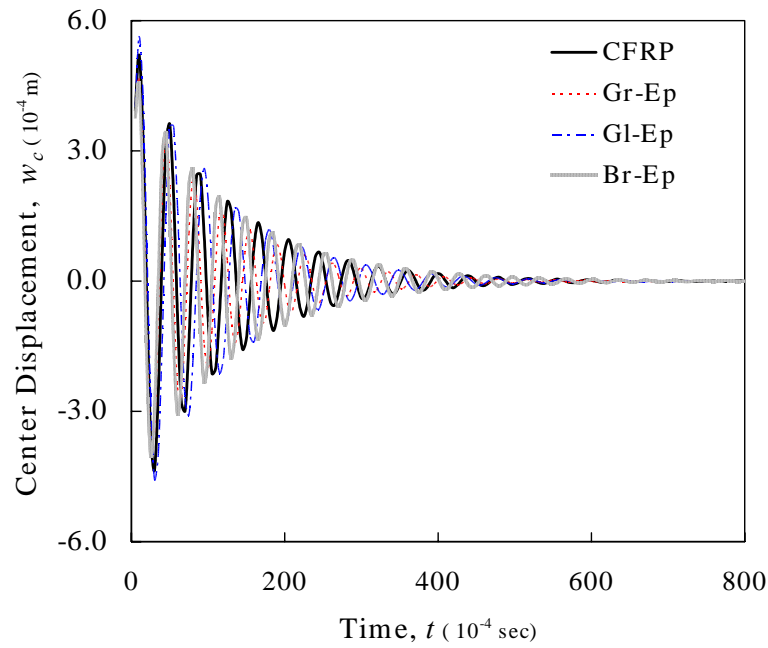


Figure 4.7 Effect of the lamina material properties on the damping of deflection in symmetric cross-ply laminated plate $(m,90,0,90,0)_s$

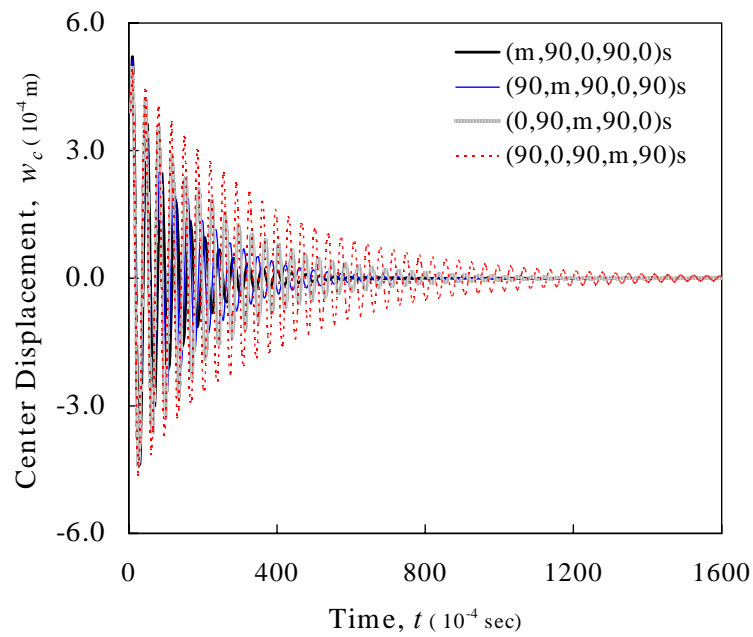


Figure 4.8 Effect of the smart material layer position on the deflection for the symmetric cross-ply CFRP laminated plate

4.6.2. Deflection Suppression Time

As stated earlier, the deflection suppression time is the time required to reduce the uncontrolled center deflection to one-tenth of its magnitude. The deflection suppression time ratio (suppression time divided by the maximum suppression time) can be shown to be $T_s = h_m / 2z_m$, where h_m is the thickness of the magnetostrictive layer and z_m is the positive distance between the mid plane of the magnetostrictive layer and the mid plane of the plate.

The effect of the smart layer positions on the deflection suppression can be shown in the Figure 4.8. It is observed that as the smart material layer is moved farther from the mid-plane the suppression time decreases, as may be expected because of the moment effect by smart layer actuations. The maximum deflections (W_{\max}) of the composite plate and the suppression times for the different position of smart layers are presented in Table 4.1.

Table 4.1 Deflection suppression time for the different smart layer positions on the symmetric cross-ply CFRP laminated plate (m,90,0,90,0)_s

Lamination Scheme	z_m (m)	T_s	W_{\max} (10^{-4} m)	t at $W_{\max}/10$
(m,90,0,90,0) _s	0.045	0.111	5.21	0.0285
(90,m,90,0,90) _s	0.035	0.143	5.09	0.0350
(0,90,m,90,0) _s	0.025	0.200	4.90	0.0480
(90,0,90,m,90) _s	0.015	0.333	4.85	0.0850
(0,90,0,90,m) _s	0.005	1.000	4.87	0.2560

4.6.3. Effect of Lamina Thickness

The effect of the thickness of smart-material layer on deflection damping characteristics is studied next. It is observed that thicker smart material layers result in better attenuation of the deflection. This is due to a larger mass inertia that is caused by the large increase in the moment of inertia of the system when thickness of the smart material

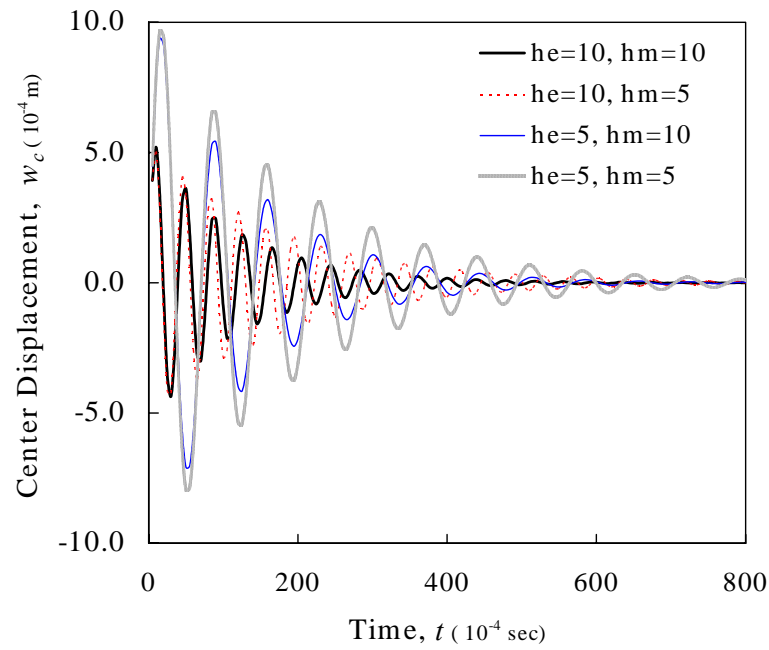
layer is increased. We note that the smart material layer has a density of five times that of the composite material. The suppression times and characteristics for different smart layer thicknesses are shown in Table 4.2 and Figure 4. 9.

Table 4.2 Suppression times for the different smart layer thicknesses in symmetric cross-ply laminated plate (m,90,0,90,0)_s

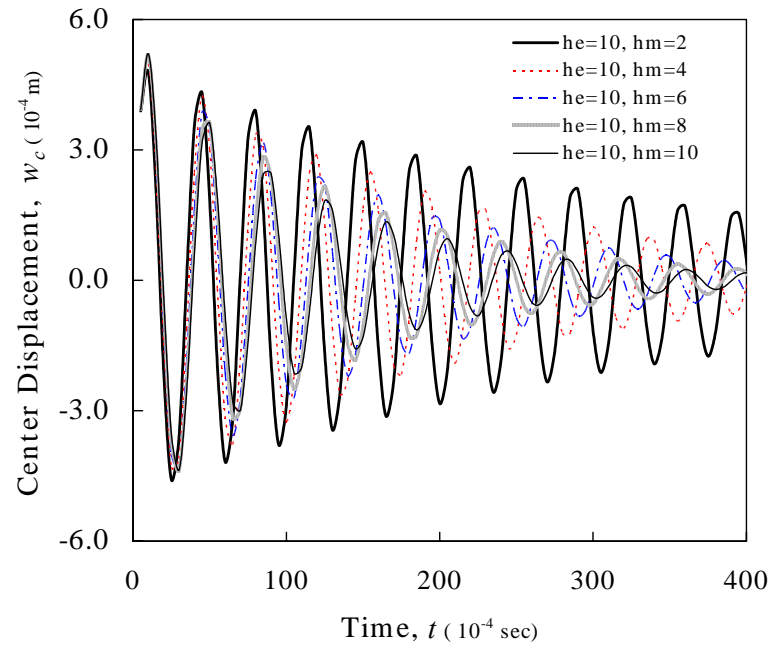
Lamina Thickness (mm)	z_m (m)	T_s	W_{\max} (10^{-4} m)	t at $W_{\max}/10$
$h_e = 10, h_m = 2$	0.0410	0.0244	4.77	0.0780
$h_e = 10, h_m = 4$	0.0420	0.0476	4.98	0.0485
$h_e = 10, h_m = 5$	0.0425	0.0588	5.05	0.0420
$h_e = 10, h_m = 6$	0.0430	0.0698	5.10	0.0350
$h_e = 10, h_m = 8$	0.0440	0.0909	5.17	0.0320
$h_e = 10, h_m = 10$	0.0450	0.1111	5.21	0.0285
$h_e = 5, h_m = 5$	0.0225	0.1111	9.12	0.0310
$h_e = 5, h_m = 10$	0.0250	0.2	9.45	0.0400

4.6.4. Effect of Feedback Coefficients

Figure 4.10 shows the effect of the feedback coefficient $c(t)k_c$ on the deflection suppression characteristics. Two different values of the feedback coefficient are used; 10^4 and 10^3 . It can be seen that the suppression time increases when the value of the feedback coefficient decrease. This is because the coefficients of the damping matrix decrease, thereby resulting in less damping.



(a)



(b)

Figure 4.9 Effect of the thickness of smart material layers on the deflection damping characteristics of symmetric cross-ply laminated plate $(m,90,0,90,0)_s$

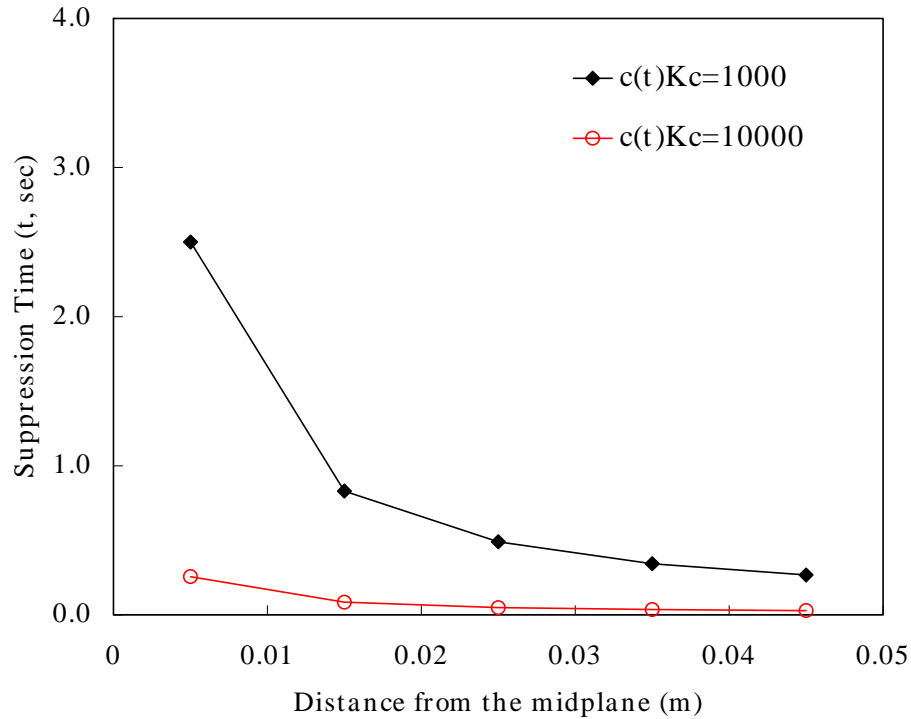


Figure 4.10 Effect of the magnitude of the feedback coefficients on the suppression time for symmetric cross-ply CFRP laminated plate $(m,90,0,90,0)_s$

4.6.5. Other Effects on Deflection Control

The deflection damping characteristics of symmetric angle-ply and general angle-ply laminated composites are studied using full plate F.E. models. Observations made earlier on various characteristics such as the effects of smart layer position, its thickness, and magnitude of the feedback coefficient are also valid for these laminates, as shown in Figures 4.11 and 4.12.

Next, fully clamped laminated plates are analyzed using 8×8 mesh in a full plate. The effect of the boundary conditions on the deflection is shown in the Figure 4.13. In Figure 4.13, 'S' represents all edges simply supported and 'C' represents all edges clamped boundary conditions. The maximum displacements of the simply supported plate are

greater than those of the clamped case, which is expected. Simply supported laminates, which have larger displacements, take less suppression time compared to the clamped laminates.

Since laminated composite structures are subjected to a variety of loading conditions during their service life, understanding of the response of these structures for various loading conditions is necessary. Numerical studies are also carried out to analyze smart laminated composites under uniformly distributed load q_0 instead of specified initial velocity field. Figure 4.14 shows the center deflection for selected simply supported and clamped laminates under continuously applied uniformly distributed loading, while Figure 4.15 shows the case under suddenly applied step loading. The effect of sinusoidal loading, $q(x, y) = q_0 \sin\left(\frac{\pi x}{a}\right) \sin\left(\frac{\pi y}{b}\right)$, on the central displacement has been studied. The results of symmetric cross-ply laminates with simply supported boundary conditions and subjected to sinusoidal and uniformly distributed loads are shown in Figure 4.16. Figures under the mechanical loading cases, the following nondimensionalized form is used for the transverse center displacements as $w_0(100) \frac{E_2 h^3}{b^4 q_0}$.

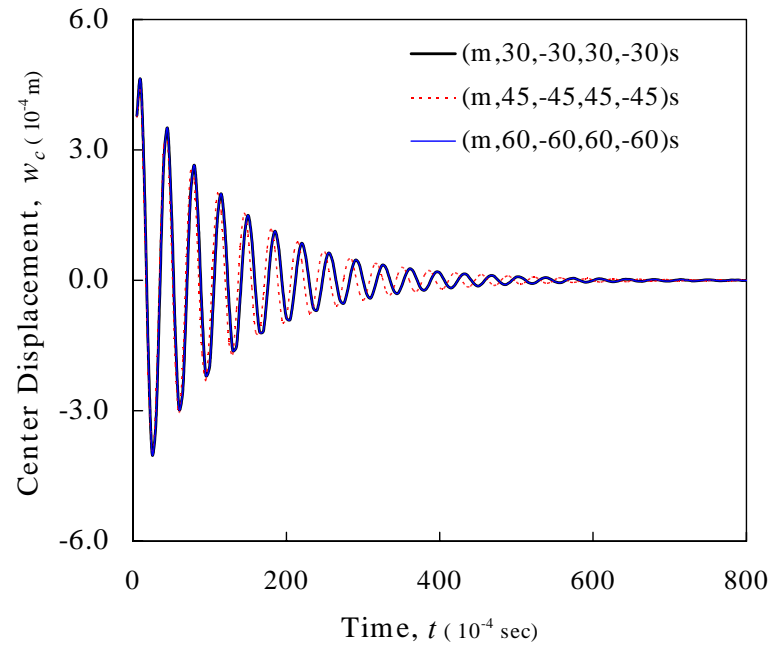
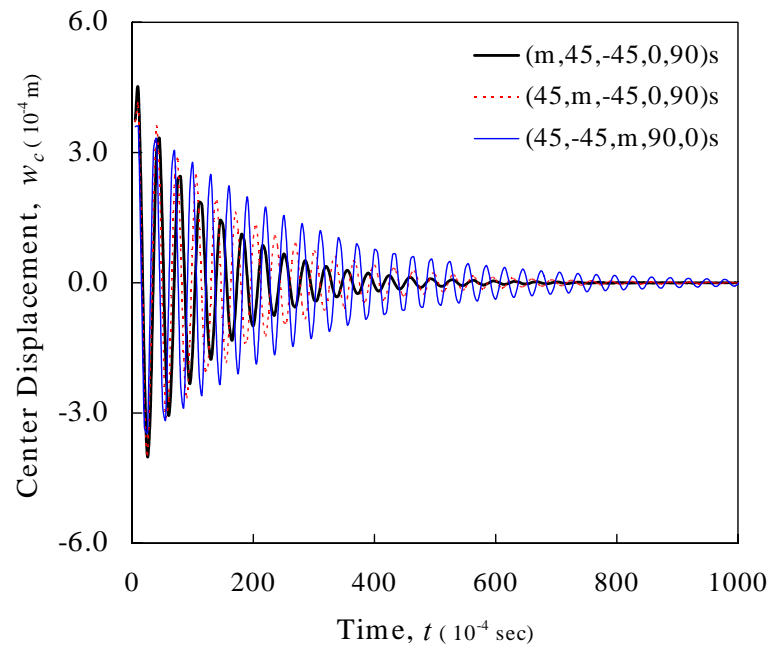
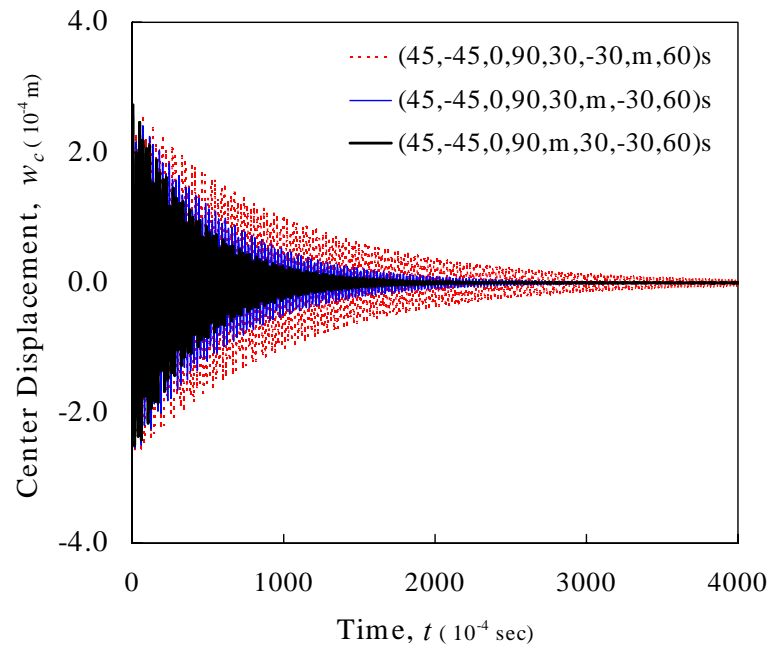
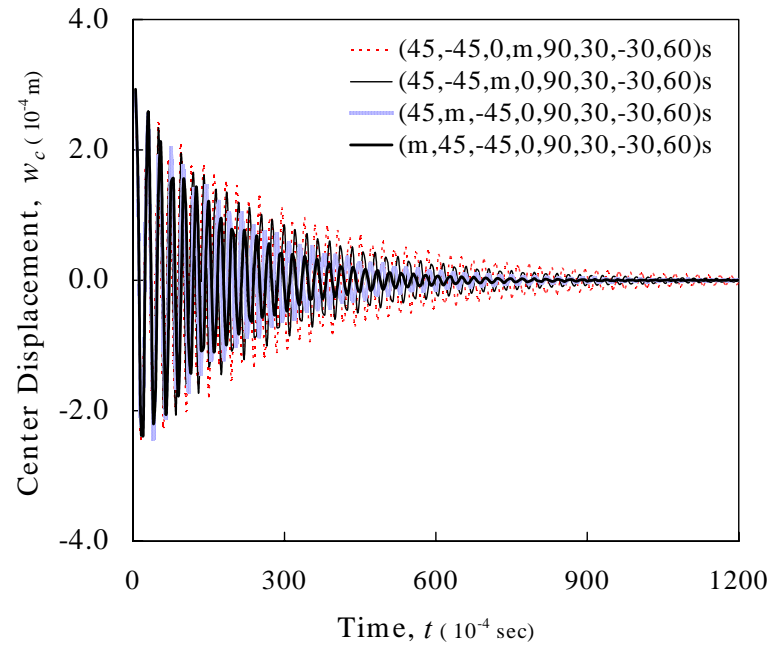


Figure 4.11 Center displacement for symmetric angle-ply CFRP laminated plate

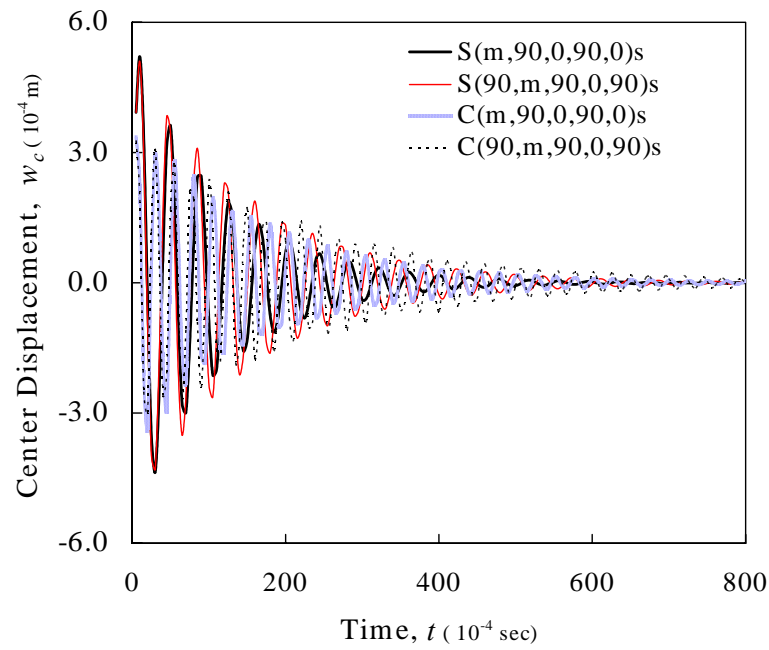


(a)

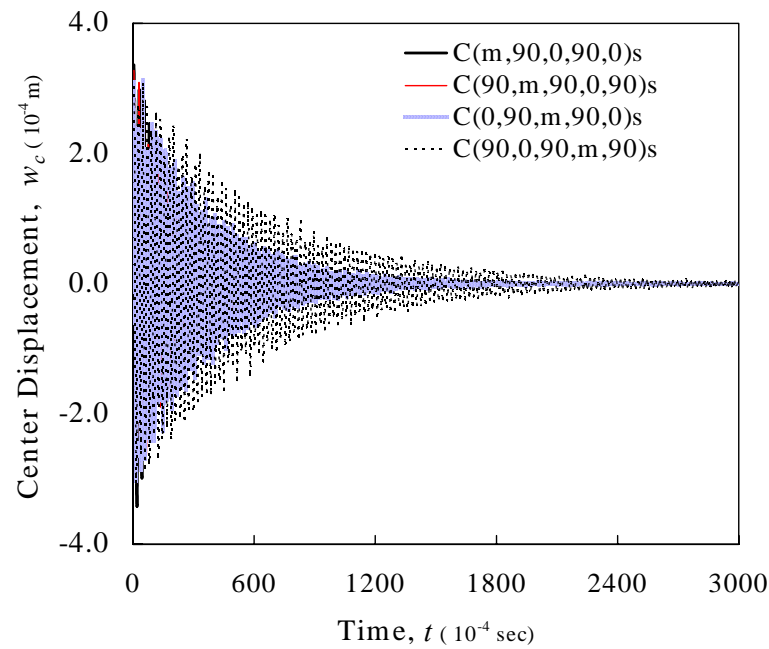


(b)

Figure 4.12 Effect of the smart layer position for symmetric general angle-ply CFRP laminated plate



(a)



(b)

Figure 4.13 Effect of boundary conditions (a) Comparison of simply supported and clamped laminates, (b) smart layer positions

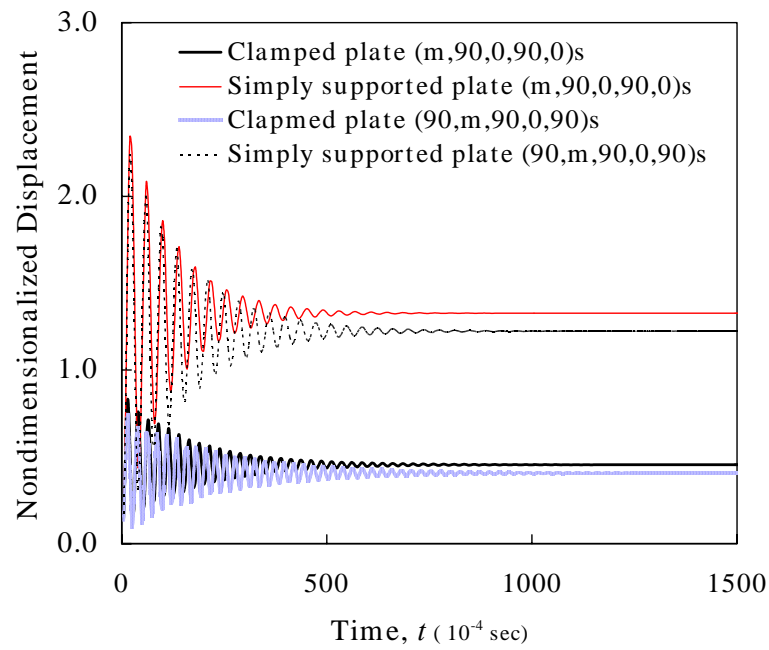


Figure 4.14 Nondimensionalized center deflection under uniform load

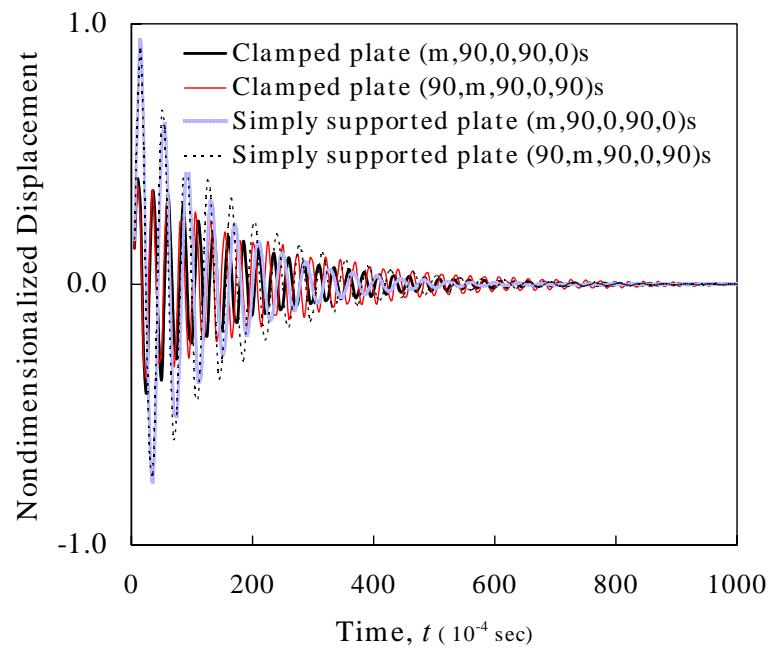
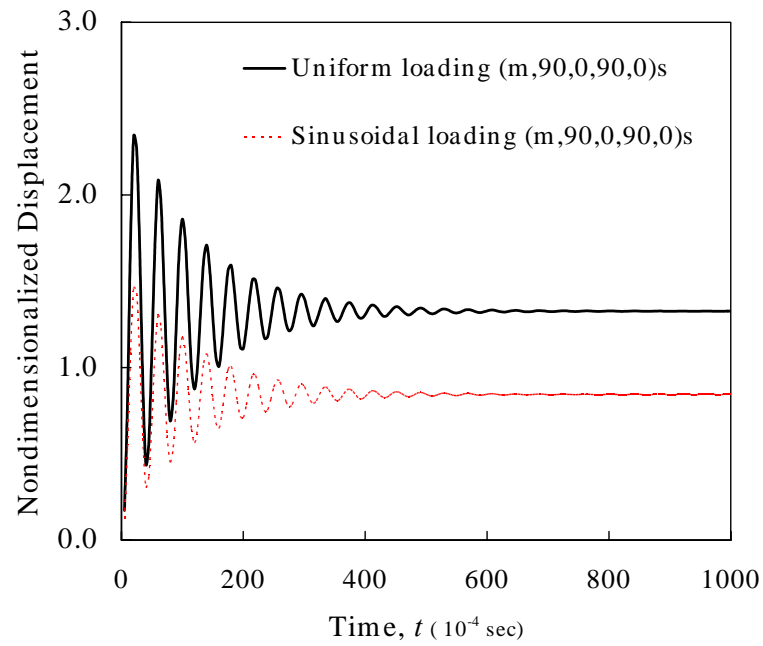
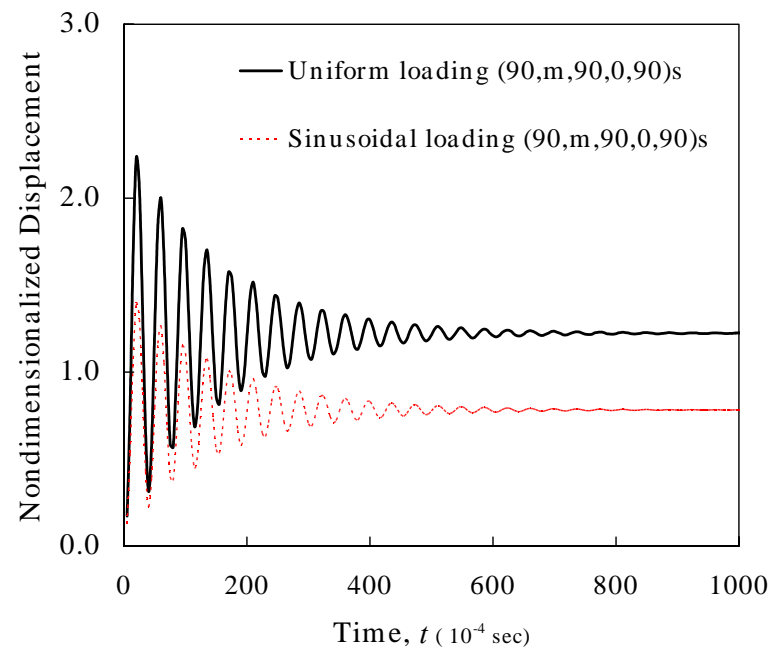


Figure 4.15 Nondimensionalized center deflection under suddenly applied uniform load



(a)



(b)

Figure 4.16 Nondimensionalized center displacement for simply supported laminated plates under sinusoidal and uniformly distributed loads

5. RESULTS OF NONLINEAR ANALYSIS*

In this Section, the numerical studies using the nonlinear finite element models developed in Section 4 for laminated composite plate and shell structures under mechanical loading are carried out. Recall that the nonlinearity accounted for is that of the *von Kármán* type.

Laminated composite square plate and shell ($a/b = 1$) with both the upper and lower surfaces embedded magnetostrictive materials is considered. The plate and shell structures considered here are made of composite fiber reinforced polymer (CFRP) and for magnetostrictive material, Terfenol-D. The material properties are presented in Table 3.1. The adhesive used to bond the structural layers or smart-material layers are neglected in the analysis. The laminated composite structures are composed of total 10 layers and all the layers are assumed to be of the same thickness. Two side-to-thickness ratios $a/h = 10$ and $a/h = 100$ are considered to represent the thick and thin laminated composites. Four different lamination schemes, symmetric cross-ply (m,90,0,90,0)s, symmetric angle-ply (m,45,-45,45,-45)s, symmetric general angle-ply (m,45,-45,0,90)s and asymmetric general angle-ply (m,45,-45,15,-15,0,90,30,-30,m) are considered to study the effect of lamination schemes on the deflection control. Six boundary conditions are considered to study the effects on deflection control. They are SSSS (SS), CCCC (CC), CCSS (CS), CCFE (CF), SSFE (SF) and CFSS (CFS) which are well shown in Figure 5.1. As a baseline of computer simulation, unless otherwise specified, symmetric cross-ply laminates with simply supported boundary condition are mainly used.

*Part of the data reported in this section is reprinted with permission from “Nonlinear deflection control of laminated plates using third-order shear deformation theory” by Lee, S.J., and Reddy, J.N. (2004), *Mechanics and Materials in Design*, 1, 1-29, Copyright 2004 by Kluwer Academic Publishers.

Three different plate theories, CLPT, FSDT, TSDT, are used to analyze plate structures. The shear correction factor used in FSDT is $5/6$. For laminated composite shells, Donnell and Sanders nonlinear shell theories are used. Three shell types, spherical ($R_1 = R_2$), cylindrical ($R_1 = \infty$), and doubly curved shell ($R_1 = 2R_2$), are considered with various R_2/a values.

As shown in the previous section, the biaxial symmetry may not be assumed even if the geometry and loading are symmetric but laminates are not symmetric (due to the bending-stretching coupling). In this study solution symmetries are considered only for the simply supported cross-ply laminated composite plate and shell to reduce the computational efforts and 4×4 meshes in a quadrant are used. For all other cases 8×8 meshes of the full models are used for the computational domains. Since locating smart material layers farthest from the mid-plane has the best effect on deflection suppression as shown in Sections 3 and 4, the smart layer position in this study is limited to both top and bottom layers. Feedback coefficient $k_c c(t)$ is assumed to be a constant, 10^4 , in this nonlinear analysis. The feedback coefficient effect could be found in section 4.6.4.

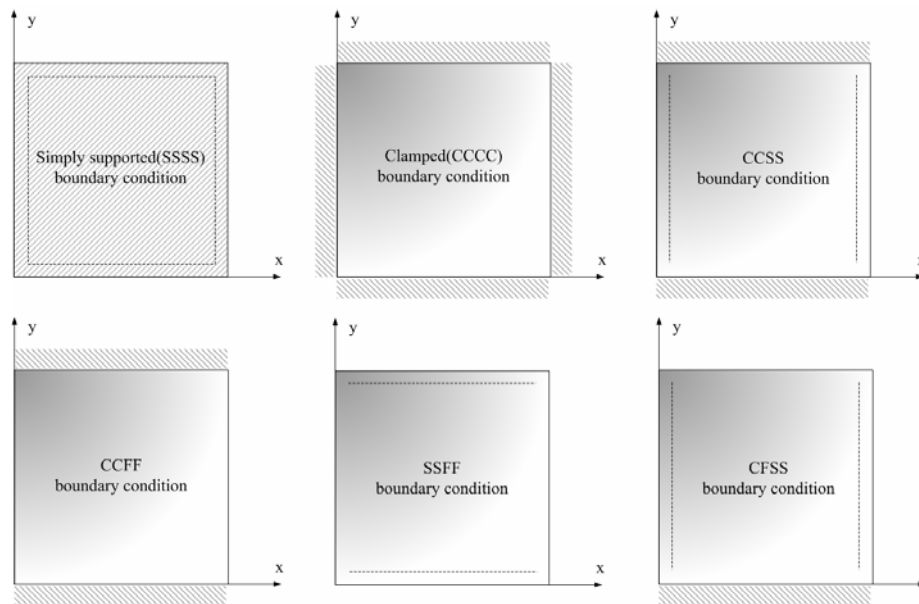


Figure 5.1 Six boundary conditions used in this study

Throughout numerical examples in this study, the center displacements are nondimensionalized as $\bar{w}_c = 100 \times w_0 E_2 h^3 / a^4 q_0$ for transient results. In static analysis center deflections are nondimensionalized as w/h and load parameter $\bar{p} = q_0 a^4 / E_2 h^4$ has been used. A tolerance of $\varepsilon = 10^{-2}$ is selected for convergence in the Newton-Raphson iteration scheme to check for convergence of the nodal displacements.

5.1. Nonlinear Static Results

Four different laminations schemes and six different boundary conditions are considered. The effect of plate thickness is also investigated. Results are presented tabular and/or graphical form.

In Figure 5.2, nondimensionalized deflections from the linear and nonlinear analyses have been plotted for different lamination schemes under uniformly distributed load. It is observed that symmetric angle-ply and asymmetric angle-ply laminates show very similar behavior in nonlinear analysis. The effect of the nonlinearity is apparent with increasing load intensity from the results presented in Figures.

The effect of different boundary conditions on nonlinear deflections is shown in Figure 5.3 and Tables 5.1 - 5.4. Nondimensionalized deflections have been plotted for the six different boundary conditions under uniformly distributed sinusoidal load. The magnitude of deflections in nonlinear analysis is in order of SSFF, CFSS, SSSS, CCFF, CCSS, and CCCC from the large value, which could be expected, for the thick and thin plates. Numerical values of nondimensional center deflection as function of the load parameter and loading condition for the three boundary conditions and two plate thicknesses are tabulated in Tables 5.1 and 5.2 for symmetric cross-ply and angle-ply laminates and Tables 5.3 and 5.4 for symmetric and asymmetric general angle-ply laminates.

Table 5.1 Nondimensional center deflection (w/h) for symmetric cross-ply and angle-ply thick ($a/h = 10$) laminates under different load and boundary conditions

Loading condition	Load parameter	Symmetric cross-ply			Symmetric angle-ply		
		SSSS	CCSS	CCCC	SSSS	CCSS	CCCC
Uniformly distributed load	1	0.01360	0.00615	0.00482	0.01059	0.00684	0.00521
	3	0.04078	0.01844	0.01445	0.03174	0.02052	0.01563
	5	0.06791	0.03073	0.02407	0.05285	0.03419	0.02604
	10	0.13519	0.06137	0.04810	0.10522	0.06826	0.05203
	15	0.20128	0.09187	0.07203	0.15666	0.10213	0.07792
	30	0.38866	0.18183	0.14292	0.30270	0.20165	0.15461
	45	0.55658	0.26838	0.21170	0.43415	0.29664	0.22905
	60	0.70614	0.35070	0.27777	0.55219	0.38629	0.30058
	80	0.88245	0.45357	0.36120	0.69315	0.49758	0.39100
	100	1.03880	0.54900	0.43938	0.81943	0.60038	0.47584
Sinusoidal load	1	0.00869	0.00422	0.00348	0.00684	0.00467	0.00376
	3	0.02606	0.01265	0.01044	0.02053	0.01402	0.01129
	5	0.04341	0.02107	0.01740	0.03420	0.02336	0.01881
	10	0.08666	0.04213	0.03478	0.06827	0.04669	0.03761
	15	0.12958	0.06313	0.05213	0.10208	0.06996	0.05636
	30	0.25519	0.12567	0.10386	0.20102	0.13908	0.11228
	45	0.37402	0.18707	0.15477	0.29469	0.20662	0.16731
	60	0.48504	0.24690	0.20458	0.38232	0.27205	0.22113
	80	0.62070	0.32378	0.26887	0.49002	0.35553	0.29060
	100	0.74426	0.39713	0.33055	0.58856	0.43461	0.35724

Table 5.2 Nondimensional center deflection (w/h) for symmetric cross-ply and angle-ply thin ($a/h = 100$) laminates under different load and boundary conditions

Loading condition	Load parameter	Symmetric cross-ply			Symmetric angle-ply		
		SSSS	CCSS	CCCC	SSSS	CCSS	CCCC
Uniformly distributed load	10	0.11888	0.03977	0.03136	0.08856	0.04832	0.03504
	20	0.23513	0.07946	0.06268	0.17548	0.09644	0.07002
	30	0.34668	0.11899	0.09390	0.25947	0.14420	0.10487
	40	0.45242	0.15827	0.12499	0.33978	0.19142	0.13954
	50	0.55200	0.19725	0.15591	0.41611	0.23799	0.17398
	60	0.64560	0.23585	0.18663	0.48852	0.28378	0.20813
	70	0.73368	0.27403	0.21710	0.55724	0.32873	0.24197
	80	0.81676	0.31174	0.24730	0.62259	0.37280	0.27544
	90	0.89541	0.34896	0.27722	0.68490	0.41594	0.30854
	100	0.97013	0.38566	0.30682	0.74449	0.45817	0.34123
Sinusoidal load	10	0.07518	0.02750	0.02290	0.05660	0.03307	0.02558
	20	0.14969	0.05497	0.04579	0.11278	0.06608	0.05113
	30	0.22294	0.08239	0.06864	0.16816	0.09898	0.07664
	40	0.29445	0.10973	0.09144	0.22243	0.13172	0.10208
	50	0.36386	0.13698	0.11418	0.27537	0.16424	0.12743
	60	0.43098	0.16411	0.13684	0.32683	0.19651	0.15267
	70	0.49572	0.19109	0.15940	0.37674	0.22849	0.17779
	80	0.55807	0.21792	0.18186	0.42508	0.26014	0.17974
	90	0.61811	0.24457	0.20420	0.47188	0.29143	0.22757
	100	0.67592	0.27103	0.22641	0.51719	0.32235	0.25221

Table 5.3 Nondimensional center deflection (w/h) for symmetric and asymmetric general angle-ply thick ($a/h = 10$) laminates under different load and boundary conditions

Loading condition	Load parameter	Symmetric general angle-ply			Asymmetric general angle-ply		
		SSSS	CCSS	CCCC	SSSS	CCSS	CCCC
Uniformly distributed load	1	0.01079	0.00677	0.00514	0.01094	0.00695	0.00509
	3	0.03236	0.02031	0.01542	0.03275	0.02086	0.01528
	5	0.05390	0.03385	0.02569	0.05448	0.03475	0.02546
	10	0.10737	0.06759	0.05132	0.10822	0.06940	0.05090
	15	0.16006	0.10113	0.07686	0.16091	0.10385	0.07626
	30	0.31071	0.19974	0.15244	0.31070	0.20539	0.15147
	45	0.44778	0.29398	0.22570	0.44668	0.30295	0.22457
	60	0.57170	0.38302	0.29599	0.56989	0.39570	0.29489
	80	0.72004	0.49362	0.38465	0.71804	0.51169	0.38379
	100	0.85376	0.59593	0.46767	0.85227	0.61950	0.46719
Sinusoidal load	1	0.00697	0.00463	0.00371	0.00706	0.00474	0.00368
	3	0.02090	0.01389	0.01114	0.02115	0.01422	0.01104
	5	0.03482	0.02314	0.01856	0.03521	0.02370	0.01840
	10	0.06952	0.04626	0.03711	0.07018	0.04736	0.03679
	15	0.10401	0.06931	0.05561	0.10480	0.07096	0.05515
	30	0.20531	0.13782	0.11077	0.20594	0.14117	0.10995
	45	0.30186	0.20480	0.16502	0.30188	0.20997	0.16396
	60	0.39279	0.26977	0.21804	0.39204	0.27692	0.21684
	80	0.50523	0.35275	0.28640	0.50360	0.36281	0.28516
	100	0.60858	0.43147	0.35190	0.60638	0.44467	0.35075

Table 5.4 Nondimensional center deflection (w/h) for symmetric and asymmetric general angle-ply thin ($a/h = 100$) laminates under different load and boundary conditions

Loading condition	Load parameter	Symmetric general angle-ply			Asymmetric general angle-ply		
		SSSS	CCSS	CCCC	SSSS	CCSS	CCCC
Uniformly distributed load	10	0.09090	0.04826	0.03450	0.09203	0.05012	0.03411
	20	0.18035	0.09633	0.06894	0.18178	0.10000	0.06817
	30	0.26716	0.14405	0.10326	0.26831	0.14950	0.10214
	40	0.35056	0.19127	0.13742	0.35110	0.19847	0.13595
	50	0.43019	0.23786	0.17135	0.43000	0.24679	0.16958
	60	0.50602	0.28372	0.20502	0.50509	0.29438	0.20296
	70	0.57819	0.32877	0.23839	0.57661	0.34117	0.23607
	80	0.64696	0.37296	0.27142	0.64484	0.38710	0.26887
	90	0.71261	0.41628	0.30410	0.71009	0.43215	0.30134
	100	0.77546	0.45871	0.33639	0.77263	0.47632	0.33345
Sinusoidal load	10	0.05799	0.03302	0.02518	0.05880	0.03418	0.02490
	20	0.11560	0.06598	0.05035	0.11687	0.06829	0.04979
	30	0.17252	0.09883	0.07547	0.17395	0.10227	0.07465
	40	0.22843	0.13154	0.10053	0.22978	0.13607	0.09945
	50	0.28313	0.16403	0.12550	0.28423	0.16967	0.12418
	60	0.33646	0.19629	0.15037	0.33719	0.20301	0.14882
	70	0.38834	0.22827	0.17513	0.38863	0.23607	0.17335
	80	0.43871	0.23446	0.19975	0.43854	0.26881	0.19776
	90	0.48759	0.29126	0.22422	0.48696	0.30122	0.22204
	100	0.53501	0.32224	0.24853	0.53394	0.33327	0.24617

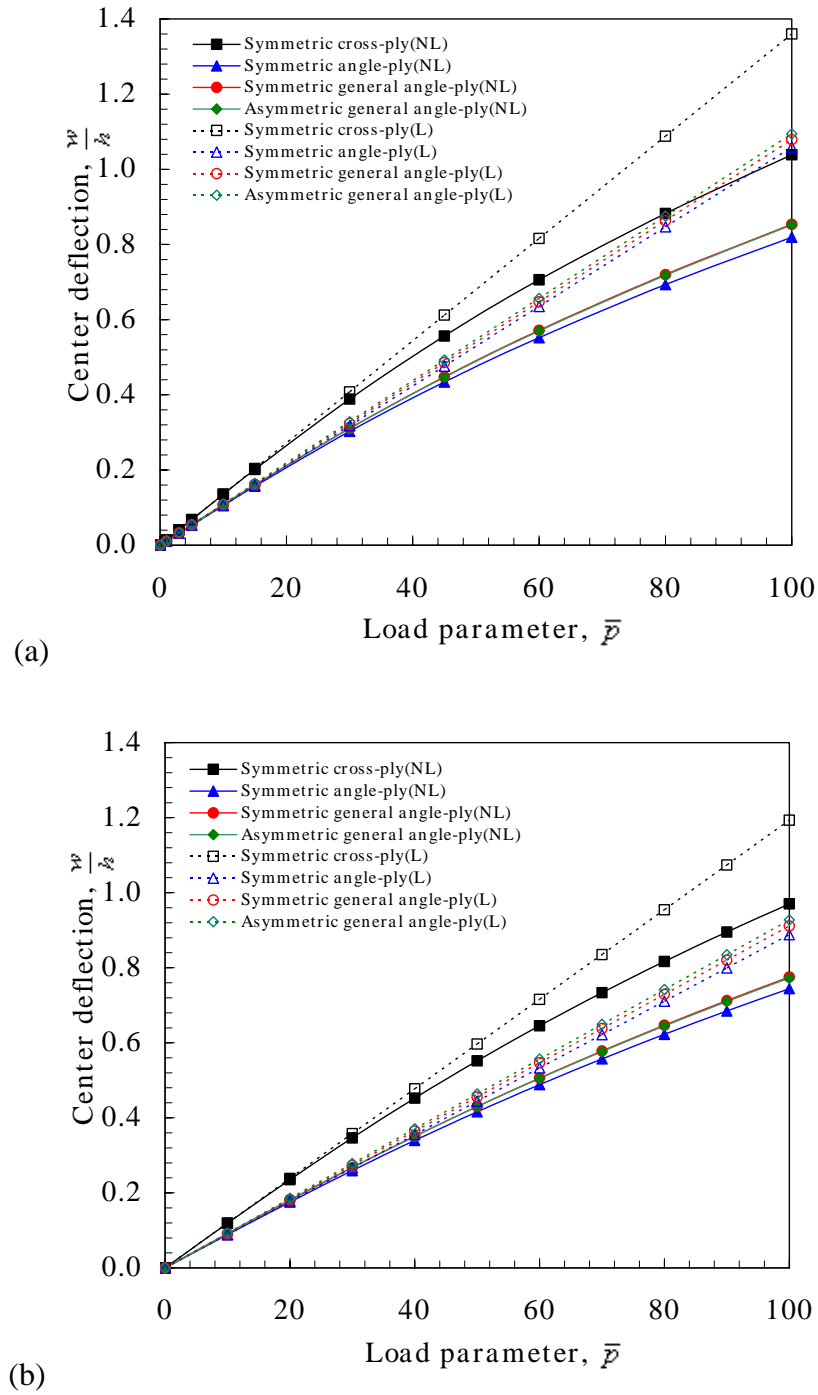


Figure 5.2 Load-deflection curve for the different lamination schemes with SSSS boundary conditions under uniformly distributed loading: (a) $a/h=10$, (b) $a/h=100$

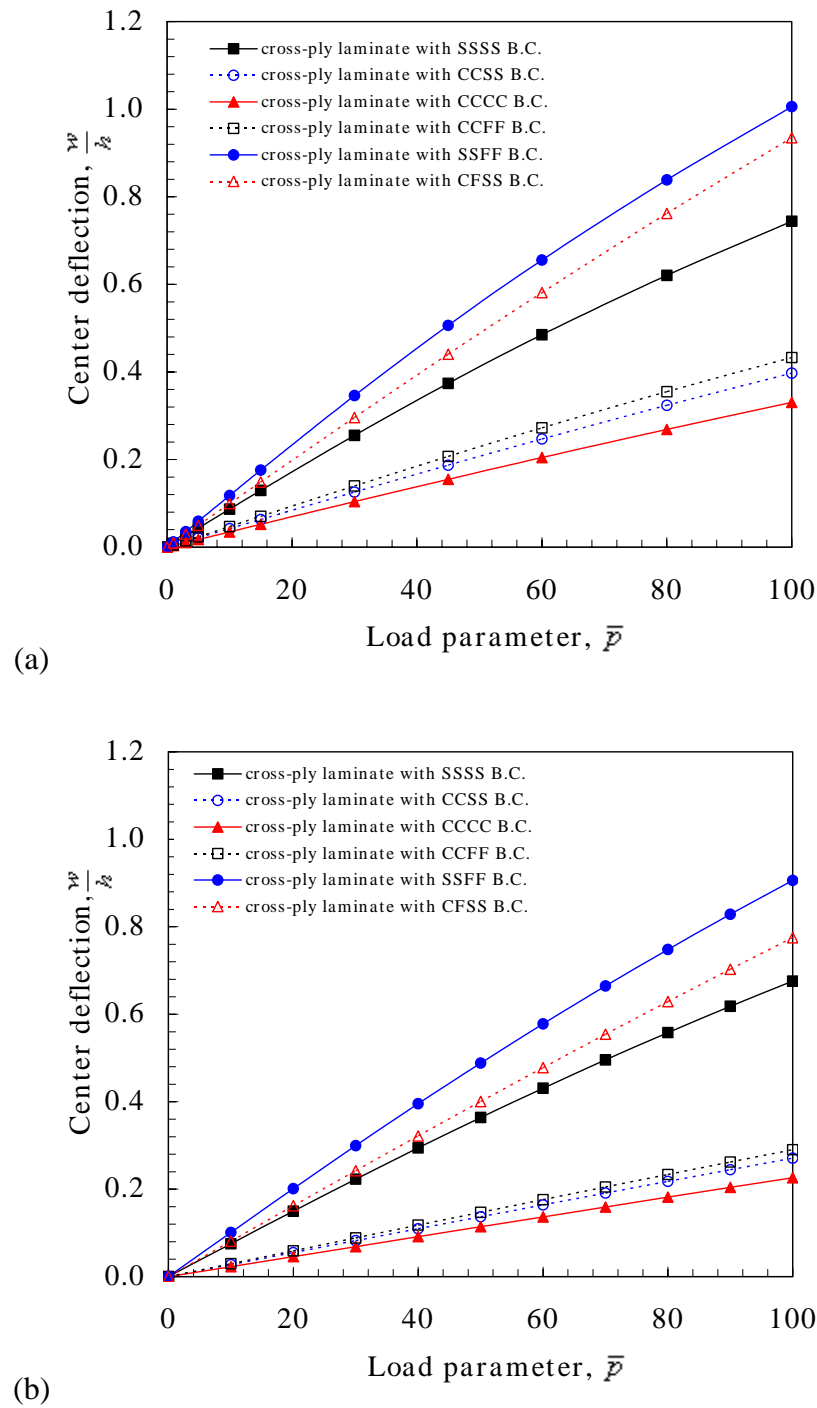


Figure 5.3 Load-deflection curve for the cross-ply laminates with the different boundary conditions under uniformly distributed sinusoidal loading: (a) $a/h=10$, (b) $a/h=100$

5.2. Nonlinear Transient Results for Laminated Composite Plates

5.2.1. Load and Time Increments

First, suitable load intensity and time increments are selected to achieve desired the accuracy and convergence of the solutions. The magnitude of the applied load is selected such that the problem can be solved without considering the load loop in nonlinear analysis. Numerical results are presented for simply supported cross-ply laminated plates. Note that the amplitude and period of the nondimensionalized center displacements decrease with increasing value of the load as shown in Figures 5.4(a) and 5.4(b). Load values of $q = 5.0 \times 10^7 q_0$ for the thick plates ($a/h = 10$) and $q = 1.0 \times 10^4 q_0$ for the thin plates ($a/h = 100$) are selected for the simply supported boundary conditions.

Newmark's time scheme with $\alpha = 0.5$ and $\gamma = 0.5$ (the constant-average acceleration method) is unconditionally stable for the linear analysis; however such stability is not available for nonlinear problems. Convergence studies were conducted to select a time increment that yielded a stable and accurate solution while keeping the computational time to a minimum. As shown in Figures 5.5(a) and 5.5(b), $\Delta t = 0.0001$ sec for the thick composite plates ($a/h = 10$) and $\Delta t = 0.0005$ sec for the thin composite plates ($a/h = 100$) is usable for the time step to satisfy the above conditions.

5.2.2. Effect of Plate Theories

Next, the effects of the different plate theories on the transient responses are considered. Linear and nonlinear responses obtained by the three different theories are presented in Figure 5.6(a). Figure 5.6(b) shows the controlled and uncontrolled motions for each theory. It is observed that the effect of nonlinearity on the transient responses is to decrease the amplitude and increase the frequency. Note that due to the large geometric nonlinearity effects the nonlinear transient behaviors between TSDT and other two theories are apparent. It is also observed that the CLPT theory gives higher frequencies and lower amplitudes. It is because CLPT theory renders the plate stiffer compared to the other two theories.

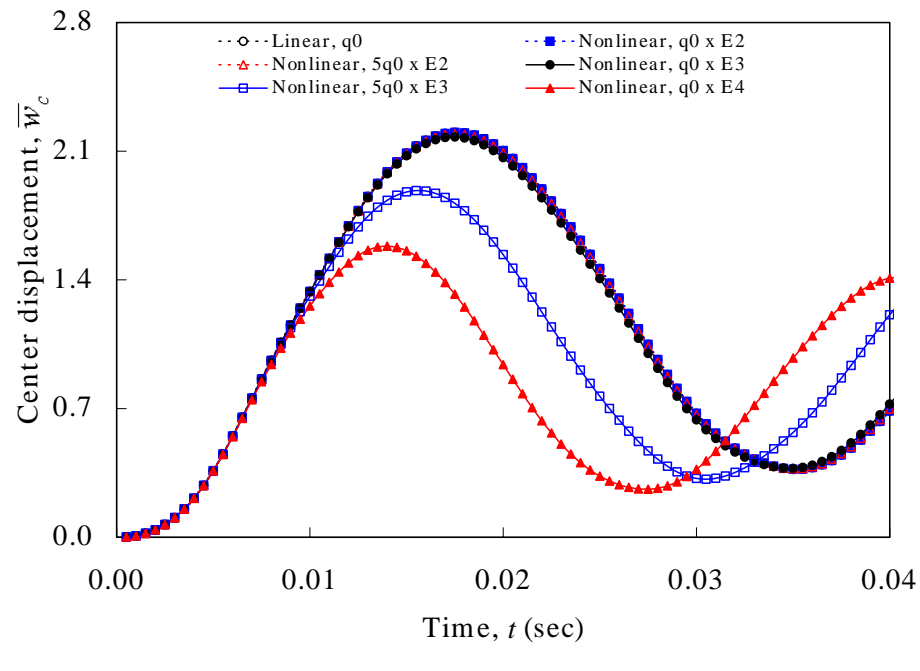
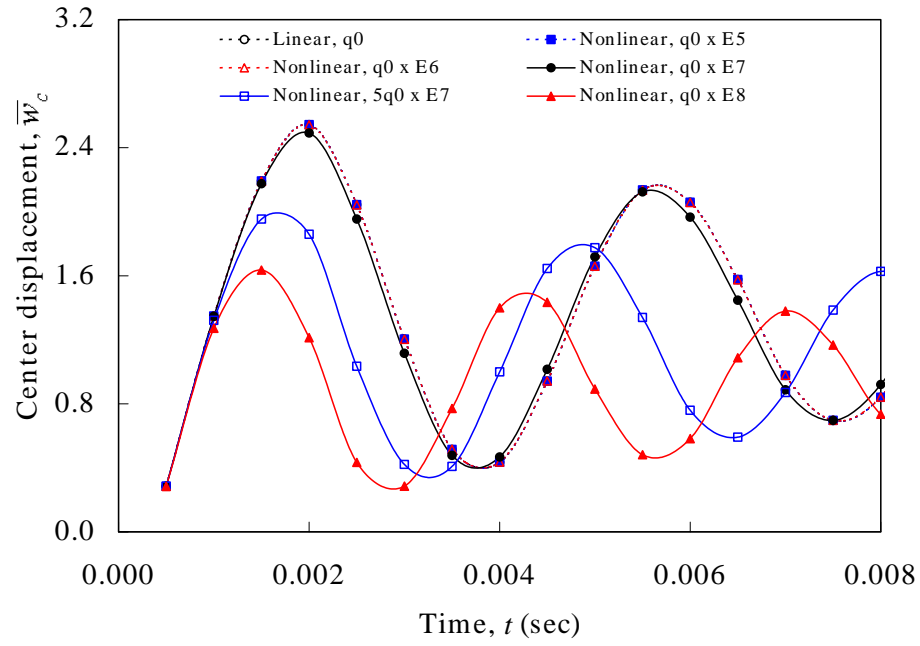


Figure 5.4 Effect of load intensity on the nonlinear transient responses for the symmetric cross-ply laminates with SSSS boundary conditions under uniformly distributed loading using TSĐT: (a) $a/h=10$, (b) $a/h=100$

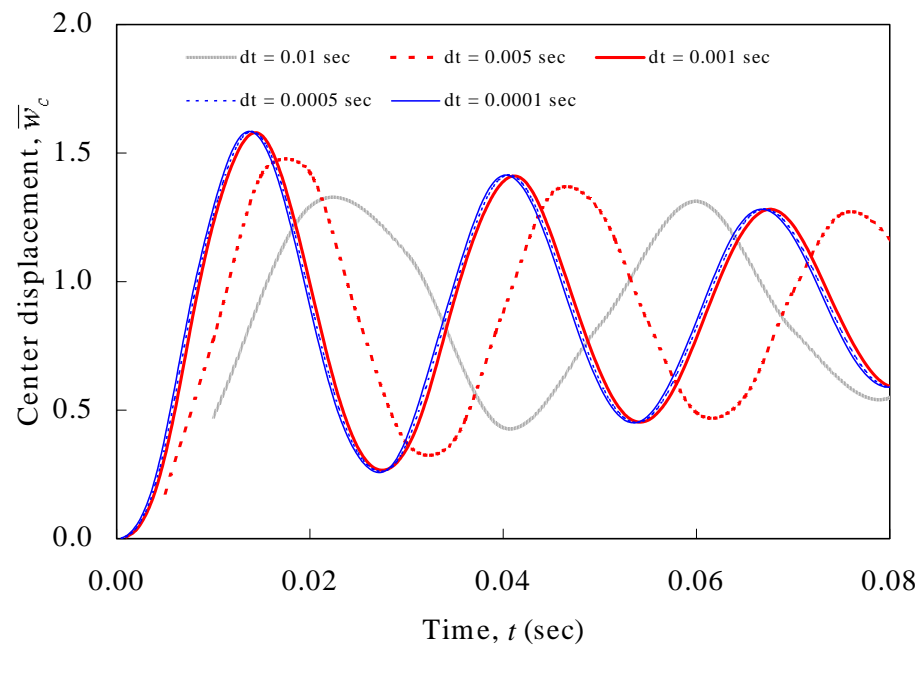
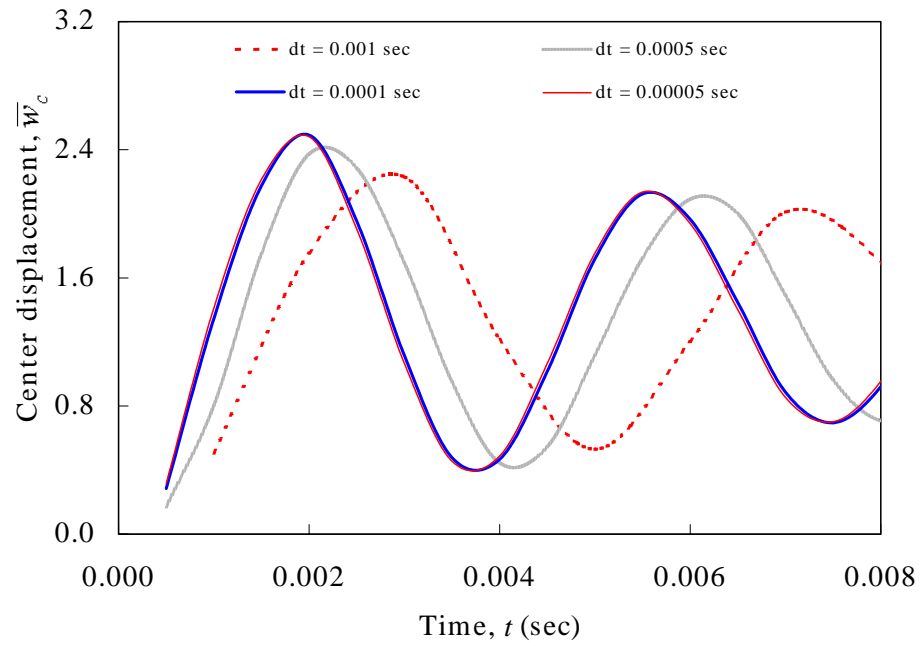


Figure 5.5 Effect of time increments on the nonlinear transient analyses for the symmetric cross-ply laminates with SSSS boundary conditions under uniformly distributed loading using TSDT: (a) $a/h=10$, (b) $a/h=100$

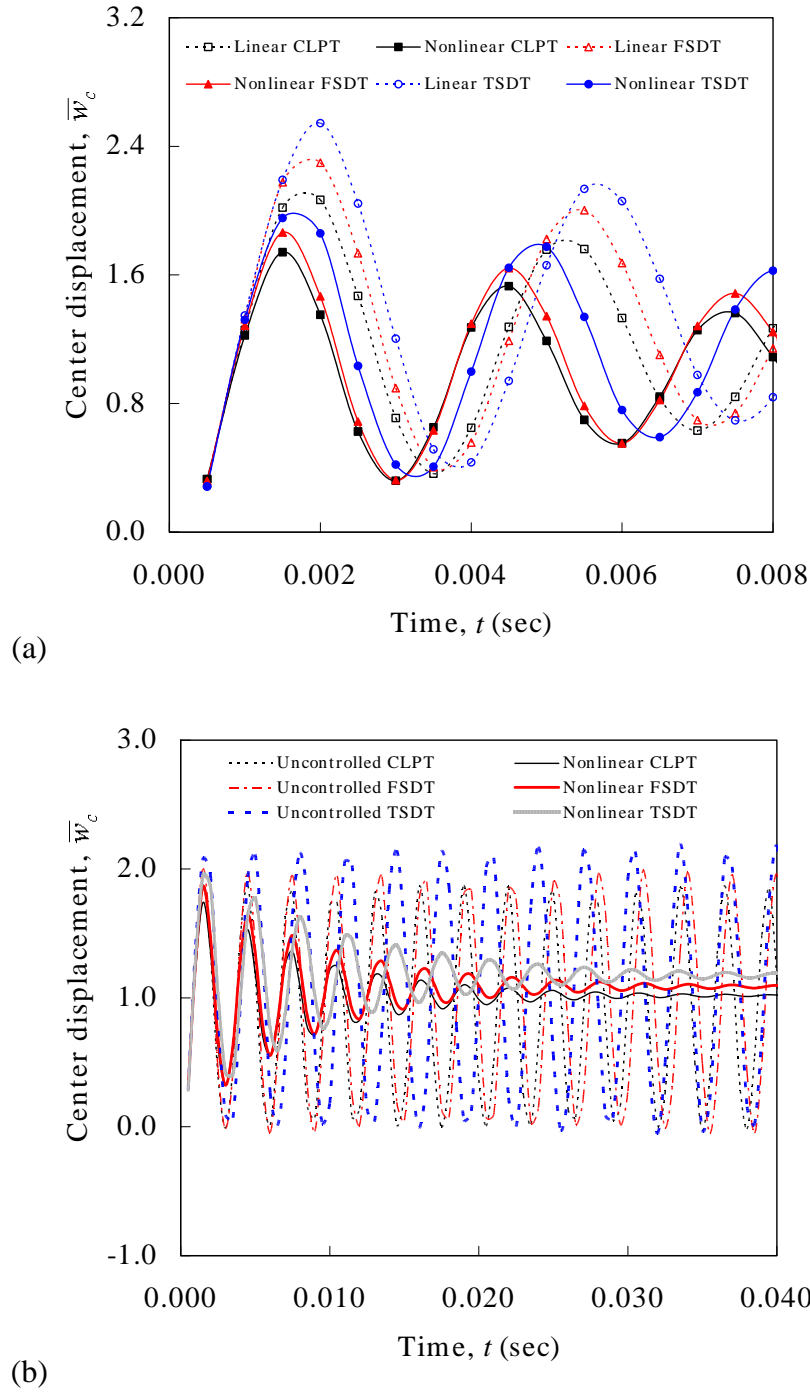


Figure 5.6 Effect of plate theories on the nonlinear transient responses for the symmetric cross-ply thick ($a/h=10$) laminates with SSSS boundary conditions under uniformly distributed loading, $q_0 = 5 \times 10^7$: (a)Details, (b)Nonlinear responses

Selected linear and nonlinear numerical results in transient responses are presented in Tables 5.5 and 5.6 for the composite plates under the uniformly distributed transverse load of intensity $q_0 = 5.0 \times 10^7$ and $q_0 = 1.0 \times 10^4$, respectively. The 4×4 meshes of the quadrant plate are used for all three different plate theories.

Table 5.5 Nondimensionalized transverse deflections versus time of the simply supported cross-ply laminates subjected to uniformly distributed load ($a/h = 10$; $\Delta t = 0.0001$; 4×4 L mesh)

t ($\times 10^3$ sec)	Nondimensionalized Center Displacement (\bar{w}_c) of the thick laminated plate					
	Linear Analysis			Nonlinear Analysis		
	CLPT	FSDT	TSDT	CLPT	FSDT	TSDT
0.5	0.3300	0.3179	0.2842	0.3297	0.3179	0.2841
1.0	1.2578	1.3249	1.3480	1.2233	1.2848	1.3210
1.5	2.0185	2.1768	2.1916	1.7416	1.8638	1.9535
2.0	2.0672	2.2983	2.5440	1.3522	1.4674	1.8584
3.0	0.7099	0.8962	1.2037	0.3200	0.3235	0.4205
4.0	0.6494	0.5573	0.4342	1.2732	1.2969	0.9988
6.0	1.3321	1.6739	2.0589	0.5533	0.5528	0.7597
8.0	1.2684	1.1432	0.8399	1.0895	1.2449	1.6265
10.0	0.9250	1.2147	1.7084	1.2176	1.2592	0.8573
15.0	1.2394	1.1407	1.0403	0.9007	0.9161	1.2591
20.0	1.1732	1.4209	1.4162	0.9885	1.0943	1.1821
30.0	1.1962	1.3103	1.2874	1.0165	1.0664	1.2147
40.0	1.1817	1.2636	1.3822	1.0219	1.0970	1.1899
60.0	1.1695	1.2750	1.3566	1.0189	1.0882	1.1735
80.0	1.1691	1.2772	1.3602	1.0185	1.0895	1.1747
100.0	1.1692	1.2849	1.3603	1.0185	1.0960	1.1749

Table 5.6 Nondimensionalized transverse deflections versus time of the simply supported cross-ply laminates subjected to uniformly distributed load ($a/h = 100$; $\Delta t = 0.0005$; 4×4 L mesh)

t ($\times 10^3$ sec)	Nondimensionalized Center Displacement (\bar{w}_c) of the thin laminated plate					
	Linear Analysis			Nonlinear Analysis		
	CLPT	FSDT	TSDT	CLPT	FSDT	TSDT
0.5	0.0016	0.0015	0.0016	0.0016	0.0015	0.0016
1.0	0.0077	0.0072	0.0079	0.0077	0.0072	0.0079
1.5	0.0200	0.0186	0.0207	0.0200	0.0186	0.0207
2.0	0.0386	0.0385	0.0408	0.0386	0.0385	0.0408
6.0	0.5738	0.5865	0.5499	0.5694	0.5813	0.5464
10.0	1.3316	1.3558	1.3376	1.2035	1.2308	1.2582
15.0	2.0564	2.0410	2.0894	1.2320	1.2271	1.5580
30.0	0.6271	0.5591	0.6741	0.6576	0.6966	0.3694
50.0	1.7982	1.7905	1.8194	0.4658	0.4843	0.6128
70.0	0.6552	0.7000	0.6324	0.5942	0.5808	1.1899
100.0	0.8561	0.8036	0.9235	0.7418	0.7754	0.9260
150.0	1.3147	1.3429	1.2786	0.8565	0.8826	1.0078
200.0	1.1082	1.0487	1.1903	0.8729	0.8840	0.9938
300.0	1.1651	1.1218	1.2202	0.8424	0.8439	0.9344
400.0	1.1727	1.1434	1.2074	0.8350	0.8404	0.9187
500.0	1.1700	1.1483	1.2084	0.8352	0.8414	0.9194

5.2.3. Effect of Lamination Schemes

The deflection suppression characteristics are studied for the different lamination schemes. The differences between the lamination schemes can be seen in Figure 5.7 for thick and thin plate cases. The maximum deflections and deflection suppression times of the linear and nonlinear analyses for the different lamination schemes with simply supported boundary condition under uniformly distributed loading by TSDT ($q = 10^7 q_0$ for $a/h=10$, $q = 10^4 q_0$ for $a/h=100$) have been tabulated in Table 5.7. Since the converged

transient solutions for each lamination scheme under the uniformly distributed loads are different the maximum deflection \tilde{w}_{\max} are defined as $\tilde{w}_{\max} = \bar{w}_{\max} - \bar{w}_{\text{converged}}$. Deflection suppression time is defined as the time required to reduce the center displacements to 10% of its uncontrolled magnitude. It is observed that it takes less deflection suppression time with increasing plate thickness and the effect of nonlinear analysis reduces the deflection suppression time. It is also reported that symmetric cross-ply lamination shows the bigger amplitude and period under the same boundary and loading conditions.

Table 5.7 Nondimensionalized maximum transverse deflections and deflection suppression time for different lamination schemes

Plate Thickness	Lamination Schemes	Linear Analysis		Nonlinear Analysis	
		\tilde{w}_{\max}	$t(\text{sec})$ at $\tilde{w}_{\max}/10$	\tilde{w}_{\max}	$t(\text{sec})$ at $\tilde{w}_{\max}/10$
$\frac{a}{h} = 10$	Symmetric cross-ply	1.1837	0.0245	0.8907	0.0225
	Symmetric angle-ply	0.8536	0.0285	0.6648	0.0230
	Symmetric general angle-ply	0.8825	0.0290	0.7153	0.0280
	Asymmetric general angle-ply	0.8385	0.0275	0.6907	0.0235
$\frac{a}{h} = 100$	Symmetric cross-ply	1.1984	0.1770	0.9204	0.1750
	Symmetric angle-ply	0.8804	0.2120	0.7094	0.1710
	Symmetric general angle-ply	0.9034	0.2150	0.7444	0.1750
	Asymmetric general angle-ply	0.9224	0.2170	0.7404	0.1740

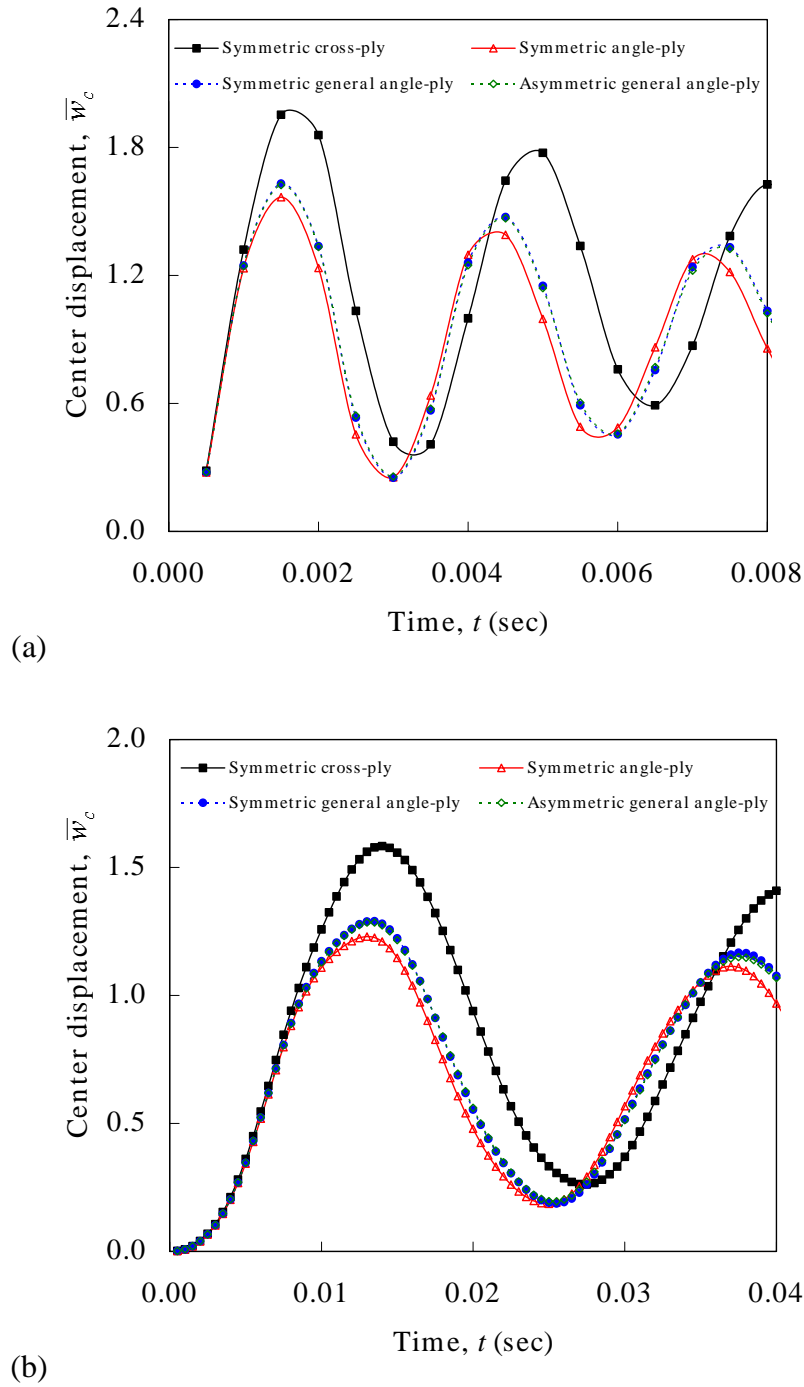


Figure 5.7 Effect of lamination schemes on the transient responses with SSSS boundary conditions under uniformly distributed loading: (a) $a/h=10$ ($q_0 = 5 \times 10^7$), (b) $a/h=100$ ($q_0 = 5 \times 10^3$)

5.2.4. Effect of Loading Conditions

The effect of applied loading conditions on the deflection suppression can be seen from Figures 5.8(a)-(f). The four different loading conditions are considered to study their effect on the response. They are uniformly distributed load (UMD), uniformly distributed sinusoidal load (SUMD), uniformly distributed impact load (IMD) and uniformly distributed sinusoidal impact load (SIMD). Since the first two loadings are continuously applied over the computational domain during the analysis the converged transient solution is different for each case. The figures show the differences between the loading conditions on transient response effects for the different lamination schemes.

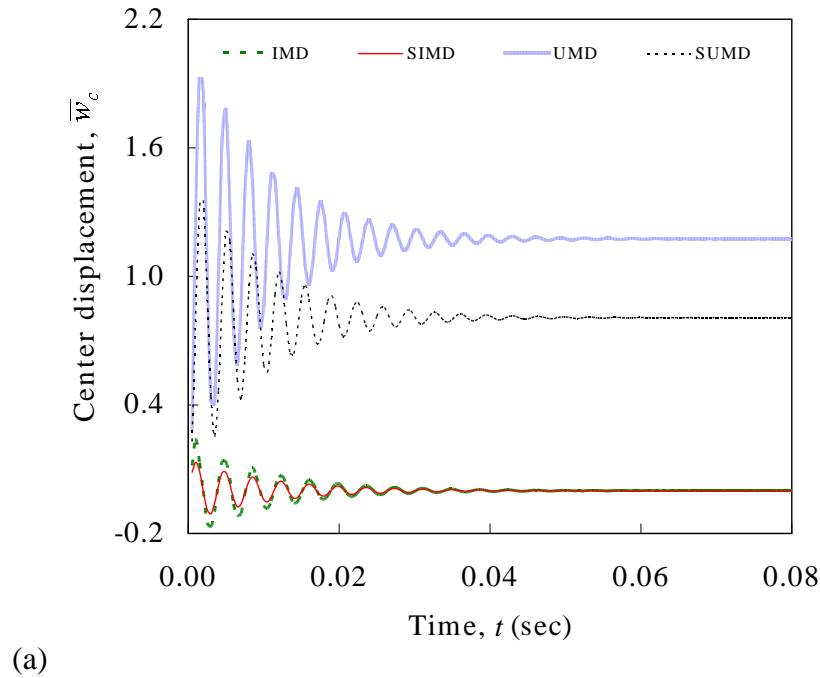
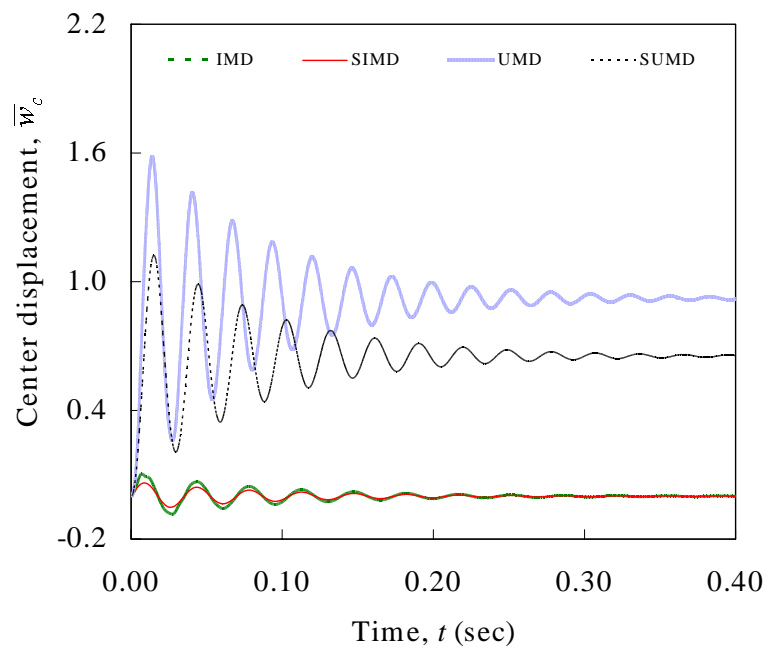
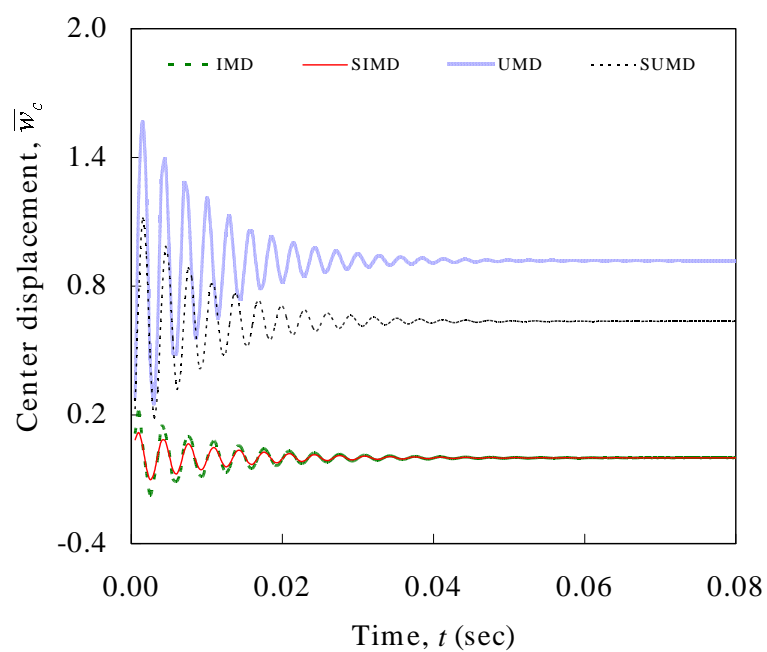


Figure 5.8 Effect of loading conditions on the transient responses with SSSS boundary conditions: (a) cross-ply laminates ($a/h=10$) with $q_0 = 5 \times 10^7$, (b) cross-ply laminates ($a/h=100$) with $q_0 = 10^4$, (c) angle-ply laminates ($a/h=10$) with $q_0 = 5 \times 10^7$, (d) angle-ply laminates ($a/h=100$) with $q_0 = 10^4$, (e) general angle-ply laminates ($a/h=10$) with $q_0 = 5 \times 10^7$, (f) the asymmetric general angle-ply laminates ($a/h=100$) with $q_0 = 10^4$

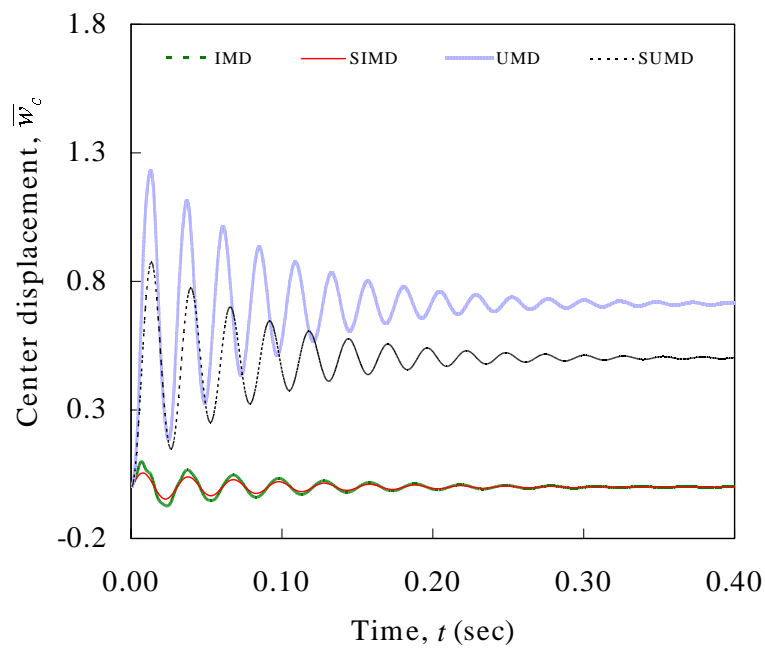


(b)

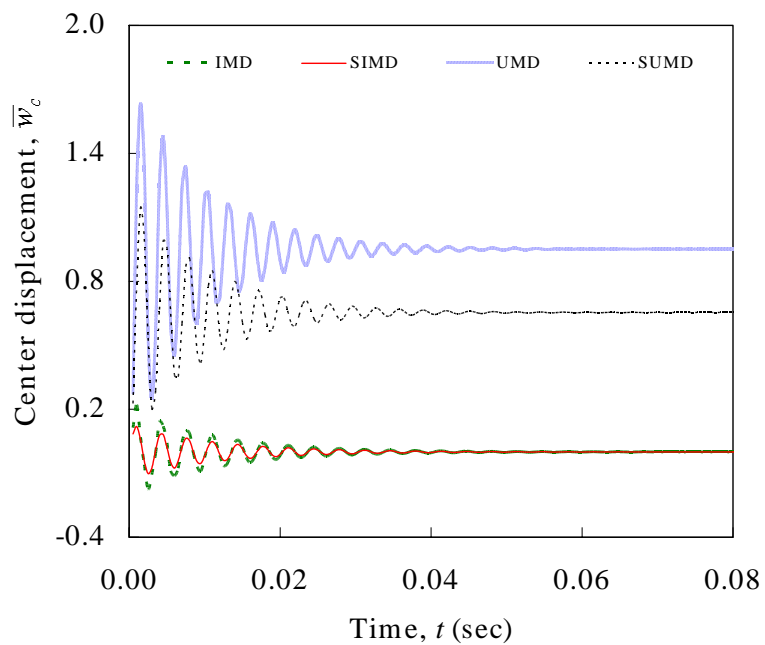


(c)

Figure 5.8 Continued

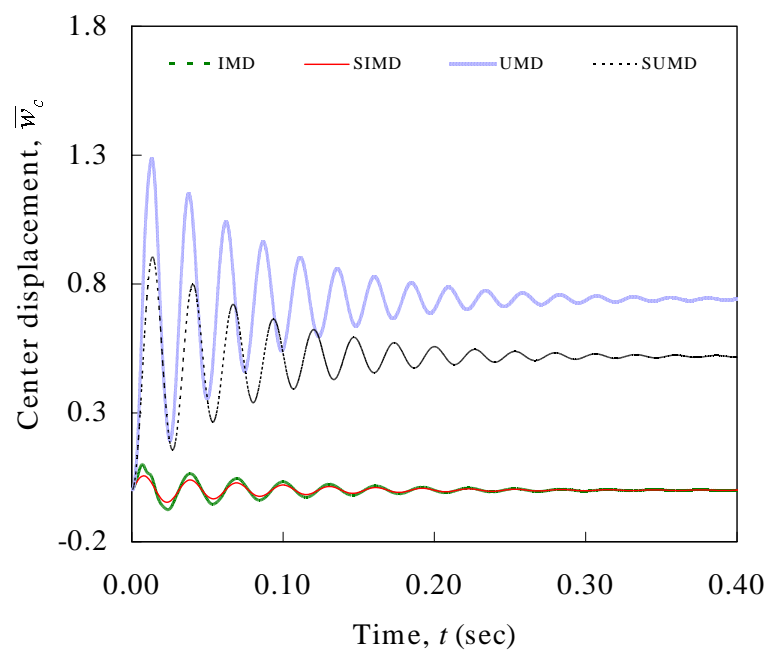


(d)



(e)

Figure 5.8 Continued



(f)

Figure 5.8 Continued

5.2.5. Effect of Boundary Conditions

The effect of boundary conditions on the deflection suppression is studied using the six different boundary conditions: SSSS (SS), CCCC (CC), CCSS (CS), CCFF (CF), SSFF (SF) and CFSS (CFS). Figure 5.9 contains the center displacements for various boundary conditions under different loading. The effect of the boundary conditions on amplitude and frequency is apparent from this Figure. Regardless of plate thickness and loading condition, SSFF boundary conditions show the largest amplitude values. The maximum deflections and deflection suppression times for each boundary condition have been tabulated in Table 5.8.

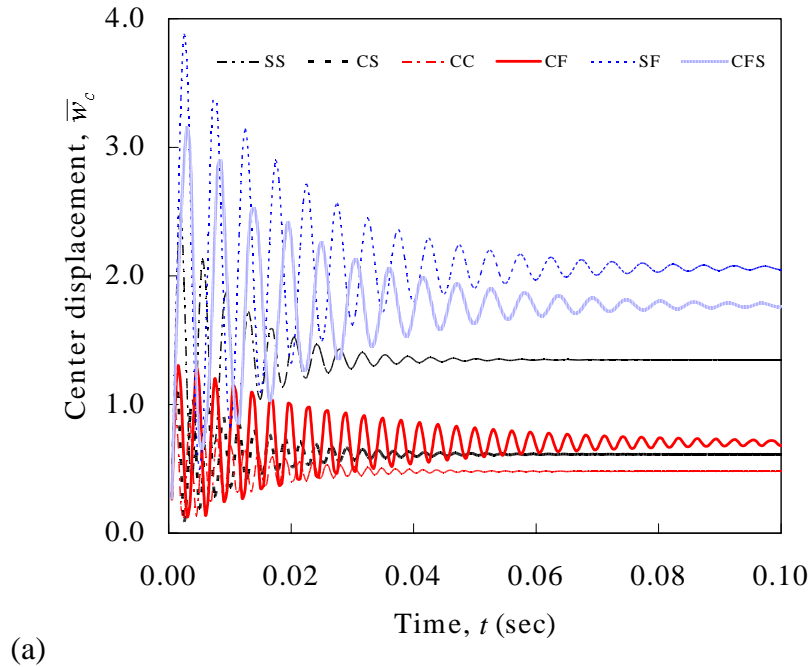
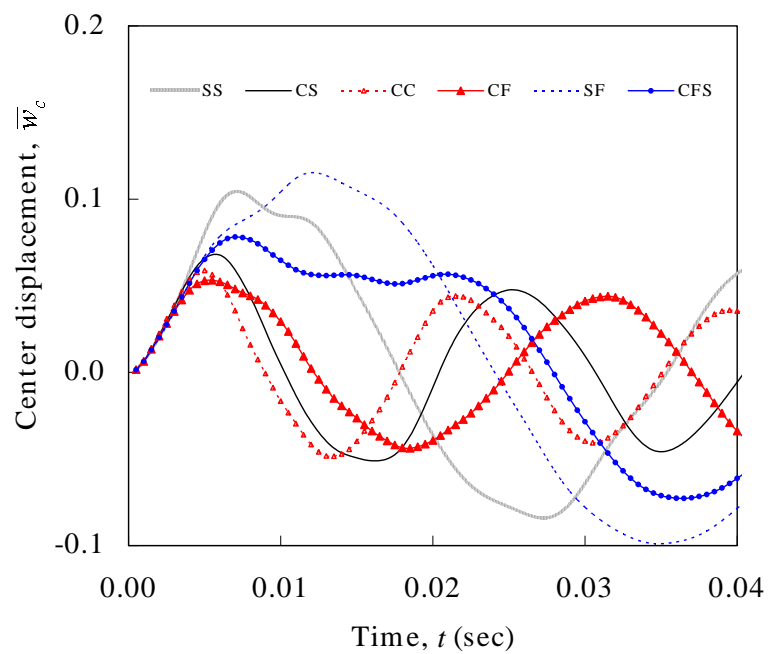
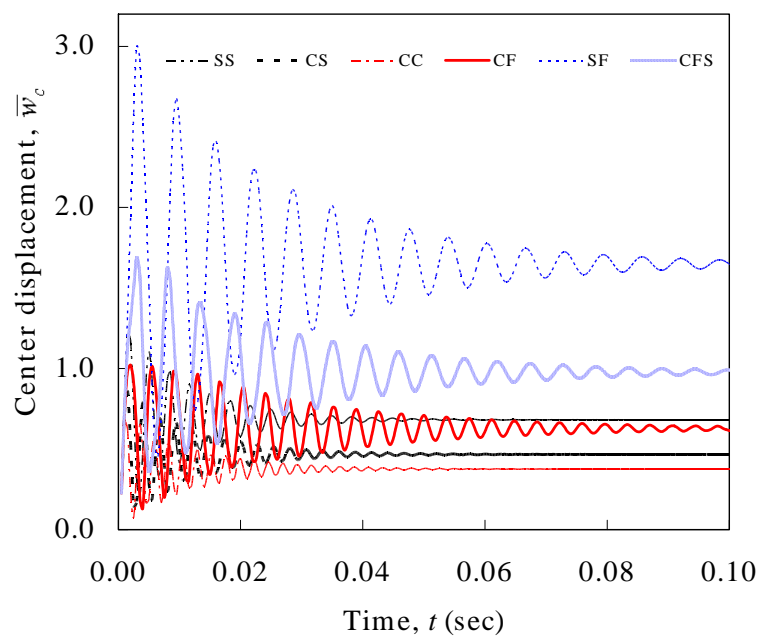


Figure 5.9 Effect of boundary conditions on the transient responses under uniformly distributed loading: (a) cross-ply laminates ($a/h=10$) with $q_0=10^7$, (b) cross-ply laminates ($a/h=100$) $q_0=10^4$, (c) angle-ply laminates ($a/h=10$) with $q_0=10^7$, (d) angle-ply laminates ($a/h=100$) $q_0=10^4$, (e) general angle-ply laminates ($a/h=10$) with $q_0=10^7$, (f) the asymmetric general angle-ply laminates ($a/h=100$) $q_0=10^4$

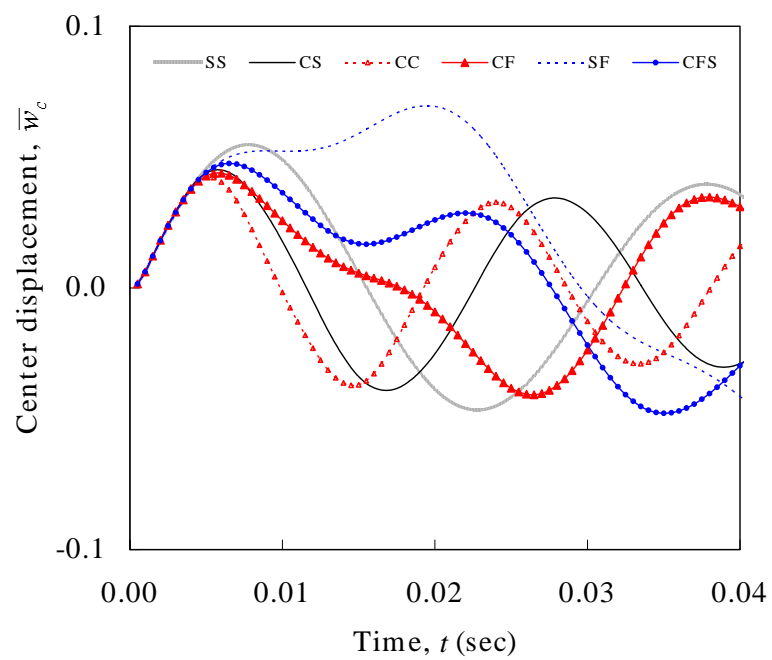


(b)

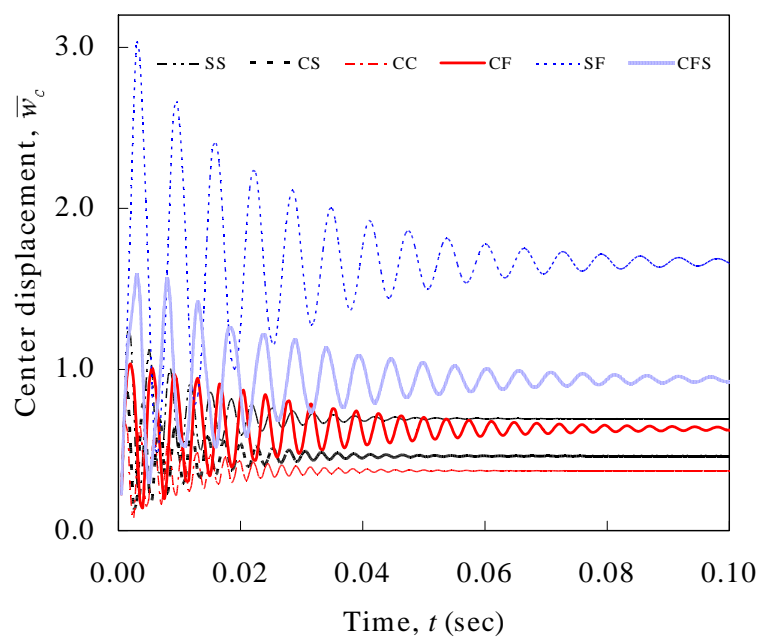


(c)

Figure 5.9 Continued

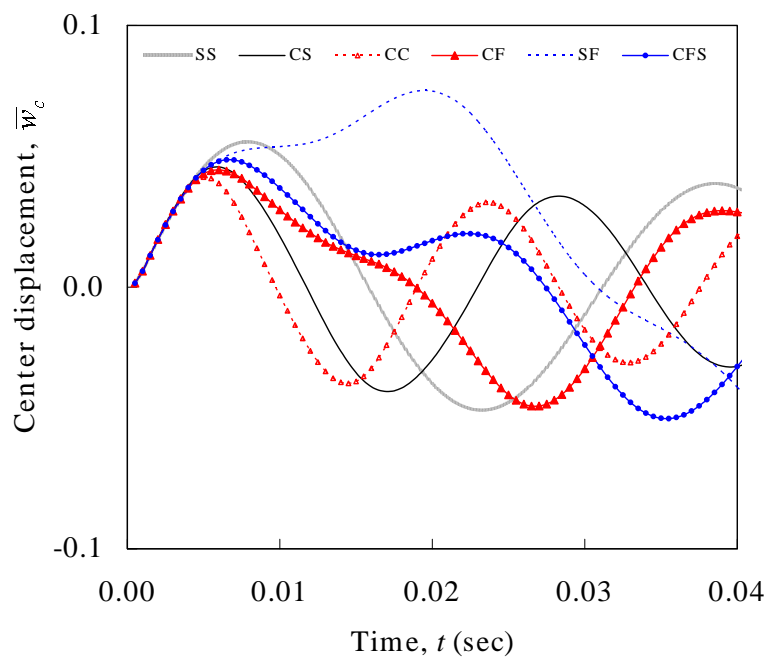


(d)



(e)

Figure 5.9 Continued



(f)

Figure 5.9 Continued

Table 5.8 Nondimensionalized maximum transverse deflections and deflection suppression time by nonlinear TSDT

Plate Thickness	Lamination Schemes	Loading Condition	Boundary Condition	\tilde{w}_{\max}	$t(\text{sec})$ at $\tilde{w}_{\max}/10$
$\frac{a}{h} = 10$	Symmetric cross-ply	Uniformly distributed load, $q = 10^7 q_0$	SSSS	1.1433	0.0245
			CCSS	0.5183	0.0290
			CCCC	0.4472	0.0280
			CCFF	0.5983	0.0745
			SSFF	1.8126	0.0475
			CFSS	1.5007	0.0475
	Symmetric angle-ply	Uniformly distributed Sinusoidal load, $q = 10^7 q_0$	SSSS	0.5320	0.0265
			CCSS	0.3962	0.0270
			CCCC	0.2997	0.0280
			CCFF	0.4947	0.0615
			SSFF	1.3937	0.0575
			CFSS	0.7511	0.0570
	Symmetric general angle-ply	Uniformly distributed Sinusoidal load, $q = 10^7 q_0$	SSSS	0.5349	0.0285
			CCSS	0.3914	0.0280
			CCCC	0.2926	0.0605
			CCFF	0.4907	0.0575
			SSFF	1.4437	0.0540
			CFSS	0.7149	0.0555
$\frac{a}{h} = 100$	Symmetric cross-ply	Uniformly distributed Impact load, $q = 10^4 q_0$	SSSS	0.1044	0.2020
			CCSS	0.0679	0.1870
			CCCC	0.0588	0.1820
			CCFF	0.0532	0.4840
			SSFF	0.1153	0.3890
			CFSS	0.0782	0.4380
	Symmetric angle-ply	Uniformly distributed Sinusoidal Impact load, $q = 10^4 q_0$	SSSS	0.0547	0.2210
			CCSS	0.0451	0.1950
			CCCC	0.0425	0.1850
			CCFF	0.0438	0.4410
			SSFF	0.0696	0.5320
			CFSS	0.0479	0.4630
	Asymmetric general angle-ply	Uniformly distributed Sinusoidal Impact load, $q = 10^4 q_0$	SSSS	0.0555	0.2240
			CCSS	0.0459	0.2070
			CCCC	0.0421	0.1910
			CCFF	0.0448	0.4270
			SSFF	0.0752	0.4910
			CFSS	0.0502	0.4350

5.3. Nonlinear Transient Results for Laminated Composite Shells

5.3.1. Effect of Shell Theories

The effect of shell theories on the deflection control is studied using the nonlinear finite element analysis. Figure 5.10 shows the deference between Donnell and Sanders shell theories on the nonlinear transient analysis. For thin ($a/h=100$) and thick ($a/h=10$) symmetric cross-ply laminated shells, transient behavior from the selected R_2/a values are shown. Tables 5.9 and 5.10 show the numerical values of nondimensionalized center displacements for thick and thin cross-ply shells, respectively. These tabular values contain the Donnell and Sanders shell theory results for the cylindrical, spherical and doubly-curved shell types. It is observed that as a/h and R_2/a value is decreasing, the numerical differences in deflection control become larger. However, as mentioned in Section 3 for linear case, it is hard to see the big differences in the deflection control effect even in nonlinear analysis. Thus, Sanders shell theory is selected in this study to show the numerical results for shallow shell case unless otherwise stated.

As mentioned in the previous section 5.2.1, the time derivatives are approximated by using the Newmark's direction integration method. Since no estimate on the time step for the stable nonlinear analysis is available, a convergence study has been conducted to select the appropriate time step that yields a stable and accurate solution while keeping the computational time to a minimum. $\Delta t = 0.0001$ sec for the thick ($a/h = 10$) and $\Delta t = 0.0005$ sec for the thin ($a/h = 100$) shells are selected the end of the convergence study. Figure 5.11 shows the effect of time increments on the nonlinear transient results of thick and thin cross-ply cylindrical shell with $R_2/a = 200$ under uniform loading.

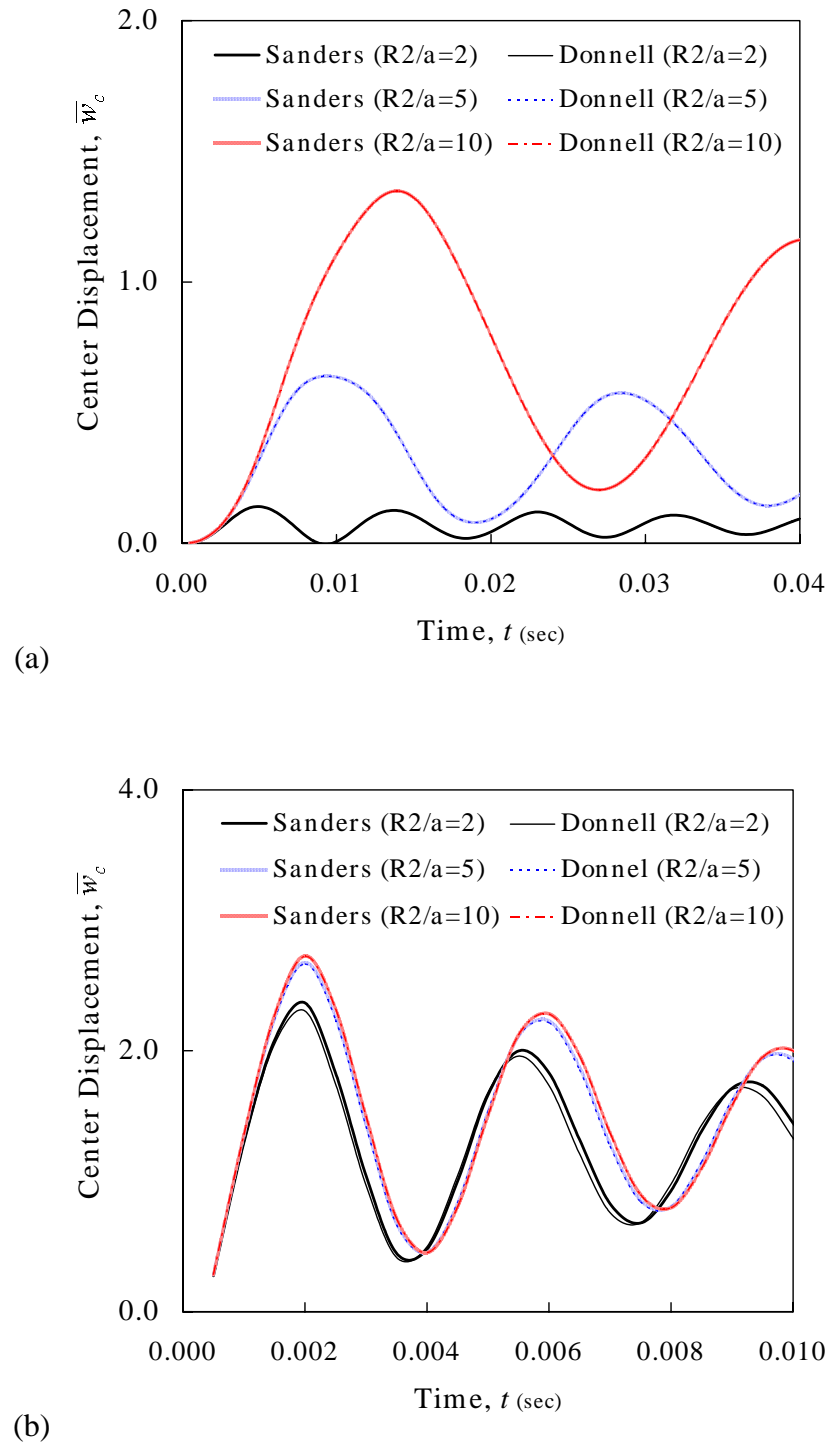


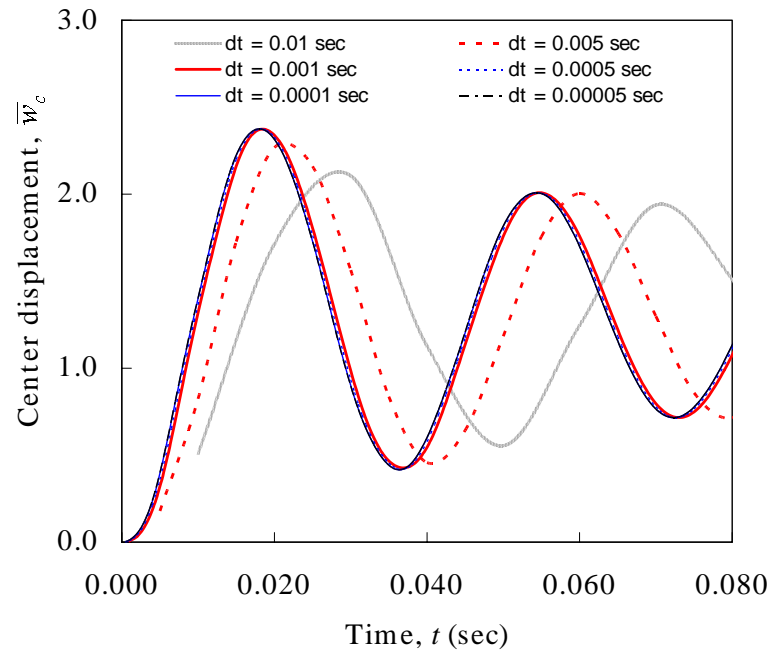
Figure 5.10 Effect of shell theory on the nonlinear transient analysis for the symmetric cross-ply cylindrical shell: (a) thin shell ($a/h=100$), (b) thick shell ($a/h=10$)

Table 5.9 Selected center displacement of the symmetric cross-ply thick ($a/h = 10$) shell with $R_2/a = 2$ by Donnell and Sanders shell theories

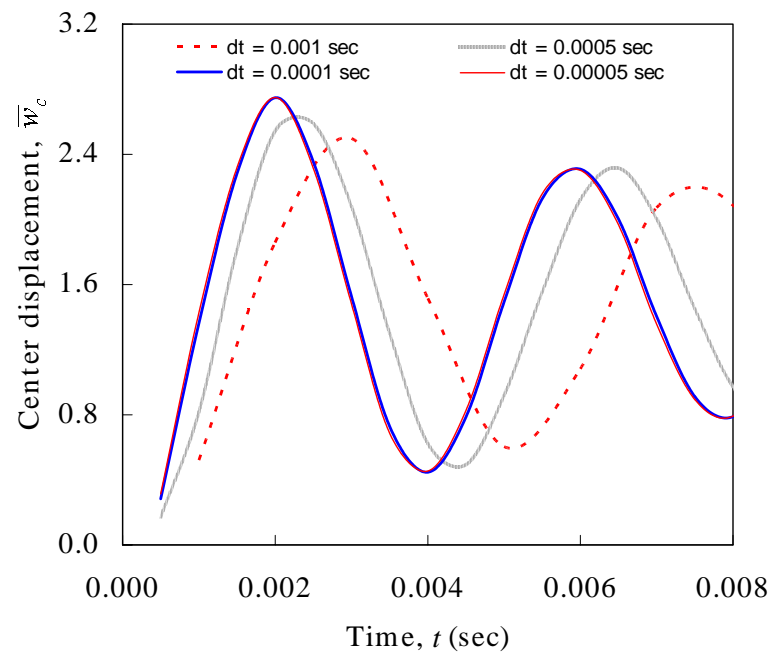
$t (\times 10^3 \text{ sec})$	Center Displacement (\bar{w}_c)					
	Donnell			Sanders		
	Cylindrical shell	Spherical shell	Doubly curved shell	Cylindrical shell	Spherical shell	Doubly curved shell
1	1.29520	1.16180	1.24010	1.28720	1.15010	1.23140
2	2.36660	1.48640	1.95170	2.30500	1.42130	1.89360
3	1.04570	0.29116	0.59766	0.97178	0.26968	0.55154
4	0.47827	0.90837	0.65336	0.49720	0.94202	0.68648
5	1.66100	1.37280	1.69060	1.68060	1.29920	1.66800
6	1.83100	0.52019	1.14260	1.73420	0.47227	1.05110
7	0.82918	0.78598	0.56680	0.76024	0.83772	0.57554
8	0.92622	1.26090	1.27600	0.97759	1.19950	1.30600
9	1.71240	0.69047	1.39810	1.70300	0.62236	1.31220
10	1.44620	0.74337	0.77151	1.33000	0.79441	0.72574
15	1.01510	0.87520	1.22950	1.02650	0.79435	1.23580
20	1.40130	0.95693	1.02040	1.38980	0.95405	0.96610
25	1.27050	0.83950	1.10450	1.20140	0.82265	1.10640
30	1.23210	0.92218	1.07920	1.22930	0.88134	1.03530
40	1.26530	0.89282	1.08750	1.22780	0.86167	1.05380
50	1.28010	0.88995	1.08600	1.24660	0.86765	1.05810
60	1.27390	0.89237	1.08420	1.24630	0.86994	1.05890
70	1.27300	0.89318	1.08340	1.24400	0.86948	1.05900
80	1.27370	0.89310	1.08300	1.24390	0.86922	1.05900
90	1.27390	0.89300	1.08290	1.24440	0.86925	1.05890
100	1.27390	0.89300	1.08280	1.24450	0.86928	1.05890
110	1.27370	0.89301	1.08280	1.24420	0.86928	1.05890
120	1.27360	0.89301	1.08290	1.24420	0.86929	1.05890
150	1.27360	0.89298	1.08280	1.24410	0.86926	1.05880
200	1.26760	0.88692	1.07670	1.23820	0.86320	1.05270

Table 5.10 Selected center displacement of the symmetric cross-ply thin ($a/h = 100$) shell with $R_2/a = 2$ by Donnell and Sanders shell theories

$t (\times 10^3 \text{ sec})$	Center Displacement (\bar{w}_c)					
	Donnell			Sanders		
	Cylindrical shell	Spherical shell	Doubly curved shell	Cylindrical shell	Spherical shell	Doubly curved shell
2	0.03714	0.02650	0.03186	0.03713	0.02649	0.03185
3	0.08376	0.03788	0.05981	0.08372	0.03785	0.05978
4	0.12634	0.02106	0.06521	0.12624	0.02101	0.06513
5	0.14099	-0.00204	0.03840	0.14077	-0.00203	0.03831
6	0.12226	0.00678	0.00560	0.12192	0.00683	0.00556
7	0.07968	0.03217	-0.00051	0.07928	0.03216	-0.00046
8	0.02954	0.03372	0.02274	0.02928	0.03364	0.02285
9	-0.00167	0.01511	0.05272	-0.00165	0.01506	0.05274
10	0.00676	0.00412	0.06352	0.00705	0.00414	0.06339
15	0.10740	0.00355	0.04161	0.10689	0.00357	0.04166
20	0.04428	0.00668	0.01046	0.04463	0.00672	0.01055
25	0.07721	0.00765	0.01919	0.07643	0.00768	0.01907
30	0.07849	0.00921	0.04312	0.07893	0.00927	0.04288
40	0.09343	0.01137	0.02776	0.09370	0.01143	0.02797
50	0.09606	0.01317	0.03168	0.09578	0.01323	0.03148
60	0.08870	0.01455	0.03577	0.08806	0.01462	0.03588
70	0.07596	0.01560	0.02762	0.07526	0.01566	0.02753
80	0.06530	0.01637	0.03681	0.06471	0.01642	0.03678
100	0.05989	0.01735	0.03496	0.05995	0.01739	0.03485
150	0.07261	0.01820	0.03277	0.07241	0.01820	0.03277
200	0.06823	0.01831	0.03212	0.06819	0.01830	0.03211
250	0.06972	0.01830	0.03217	0.06959	0.01829	0.03214
300	0.06922	0.01830	0.03223	0.06914	0.01828	0.03220
400	0.06933	0.01829	0.03223	0.06924	0.01828	0.03221
500	0.06783	0.01690	0.03077	0.06774	0.01689	0.03075



(a)



(b)

Figure 5.11 Effect of time increments on the nonlinear transient analysis for the symmetric cross-ply cylindrical shell ($R_2/a=200$): (a) thin shell ($a/h=100$), (b) thick shell ($a/h=10$)

5.3.2. Effect of R_2/a

In this section, the effect of R_2/a on the deflection suppression is studied. Figure 5.12 shows the effect of R_2/a for cylindrical cross-ply shell. The uniform loads $q_0 = 10^4$ for thick shell $a/h=10$, and $q_0 = 10^3$ for thin shell $a/h=100$ are applied with simply supported boundary condition. The maximum transverse deflection and the deflection suppression time is tabulated in Table 5.11 for each R_2/a value. Here the maximum deflection \tilde{w}_{\max} is defined as $\tilde{w}_{\max} = \bar{w}_{\max} - \bar{w}_{\text{converged}}$, where \bar{w}_{\max} is the maximum nondimensionalized center displacement and $\bar{w}_{\text{converged}}$ is the converged displacement value.

It is observed that it takes more deflection suppression time with increasing R_2/a value in both thin and thick shells. For the thin shell, the maximum deflection suppression time is 5 times faster than the others depending on R_2/a value. In the thick shell, R_2/a values bigger than $R_2/a = 50$ cases have the little differences between the transient behaviors.

5.3.3. Effect of Shell Types

Next, the effect of shell types on the deflection suppression characteristics is studied for spherical, cylindrical, and doubly curved CFRP shells. In this study doubly curved shell is chosen as $R_1 = 2R_2$ for specific example. The center displacements versus time for spherical, cylindrical, and doubly curved shells are shown in Figures 5.13 to 5.16. Figures 5.13 and 5.14 show the comparison of transient behavior of three shell types for thin and thick cases. For the thick shell with bigger R_2/a values, the difference between the shell types is hard to recognize. Selected maximum deflection and deflection suppression time for spherical and doubly curved shells are shown in Table 5.12. It is observed that it takes less deflection suppression time with decreasing R_2/a value for spherical and doubly curved shells. Thus the shell with the smallest R_2/a shows the maximum deflection suppression. It is also observed that the spherical shell has the biggest deflection

suppression and smallest maximum deflection and the cylindrical shell has the smallest deflection suppression and largest maximum deflection. It is because of the fact that spherical shell has the smallest R_1 and doubly curved shell (in this study $R_1 = 2R_2$), and cylindrical shell has the largest R_1 ($R_1 = \infty$) with the same R_2 value.

Table 5.11 Maximum transverse deflection and deflection suppression time for the symmetric cross-ply cylindrical shells

Thickness	R_2/a	\tilde{w}_{\max}	$t(\text{sec})$ at $\tilde{w}_{\max}/10$
Thin Shell $a/h = 100$	2	0.071646	0.114000
	5	0.293180	0.161500
	10	0.611730	0.176000
	20	0.845500	0.206500
	50	0.983200	0.225500
	100	1.033500	0.228000
	200	1.056300	0.232000
	500	1.066600	0.234000
	1000	1.069600	0.234000
	10^{99}	1.072400	0.235500
Thick Shell $a/h = 10$	2	1.093000	0.024000
	5	1.238800	0.025000
	10	1.262900	0.025500
	20	1.270300	0.025500
	50	1.273200	0.025500
	100	1.274000	0.025500
	200	1.274300	0.025500
	500	1.274500	0.025500
	1000	1.274600	0.025500
	10^{99}	1.274600	0.025500

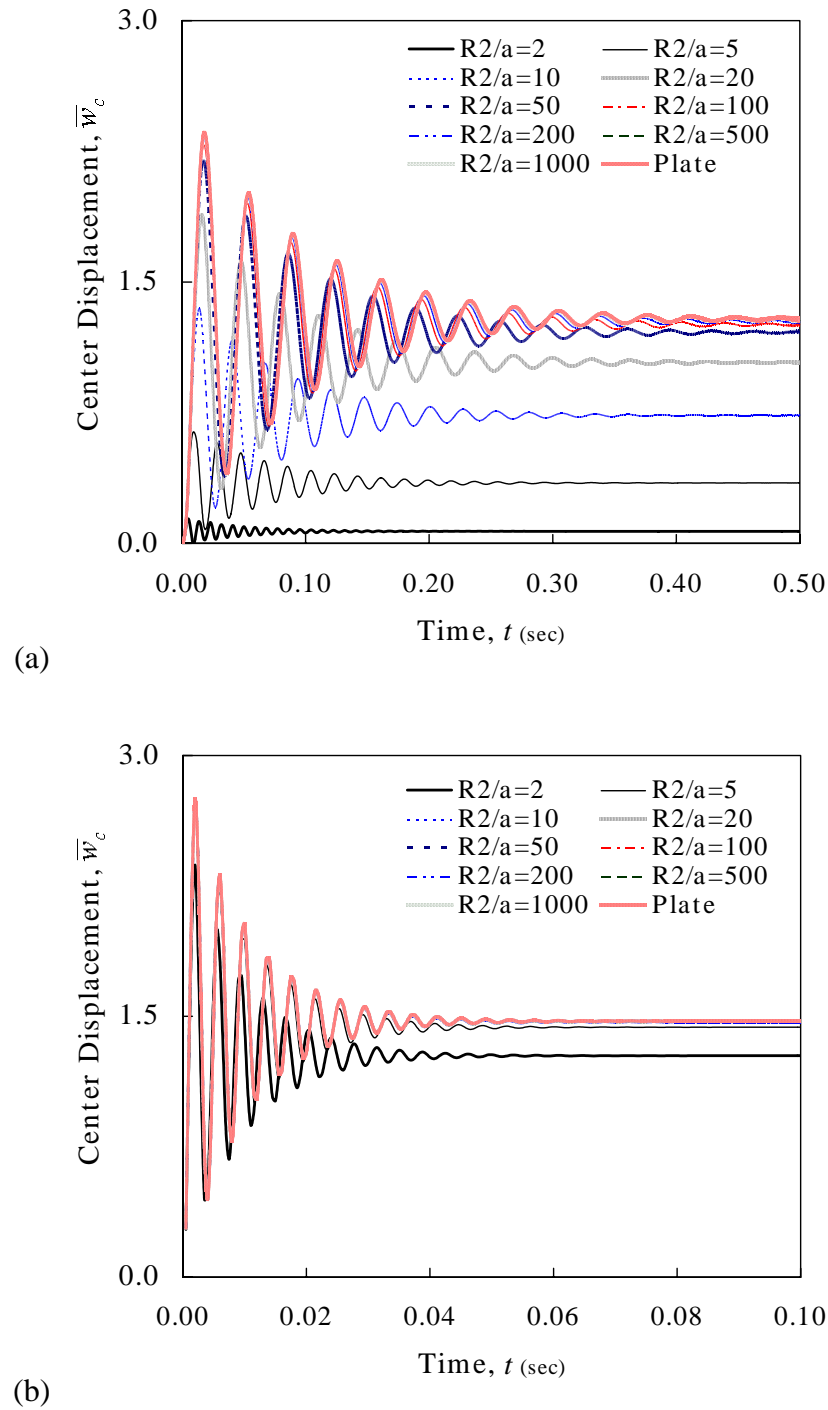
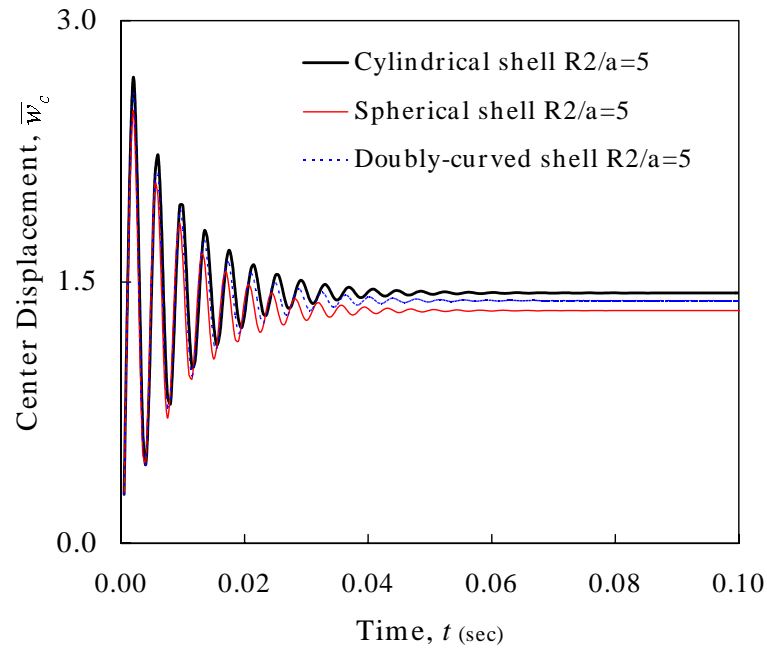
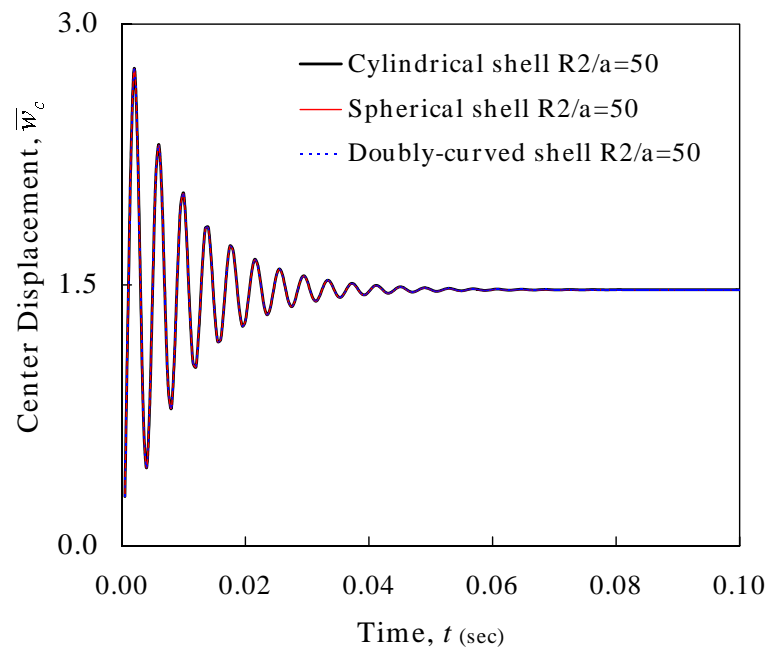


Figure 5.12 Effect of R_2/a for cylindrical cross-ply shell under uniform load in SSSS boundary condition; (a) thin shell ($a/h=100$), (b) thick shell ($a/h=10$)

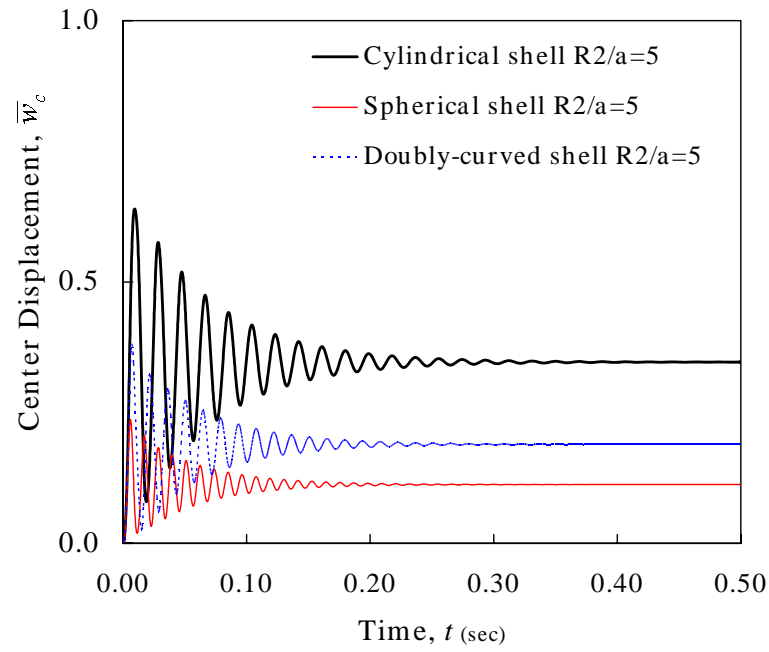


(a)

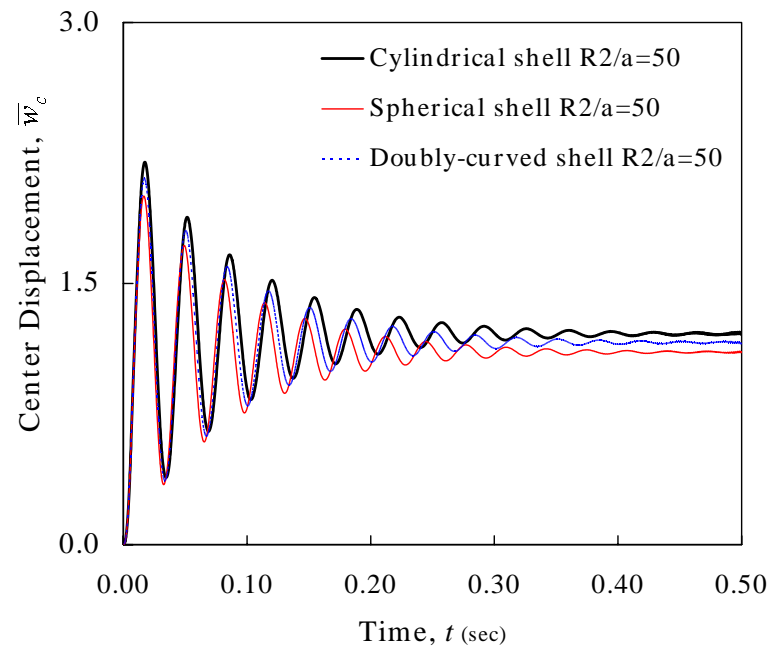


(b)

Figure 5.13 Effect of shell type for the cross-ply thick ($a/h=10$) shell under uniform load in SSSS boundary condition; (a) $R_2/a=5$, (b) $R_2/a=50$



(a)



(b)

Figure 5.14 Effect of shell type for the cross-ply thin ($a/h=100$) shell under uniform load in SSSS boundary condition; (a) $R_2/a=5$, (b) $R_2/a=50$

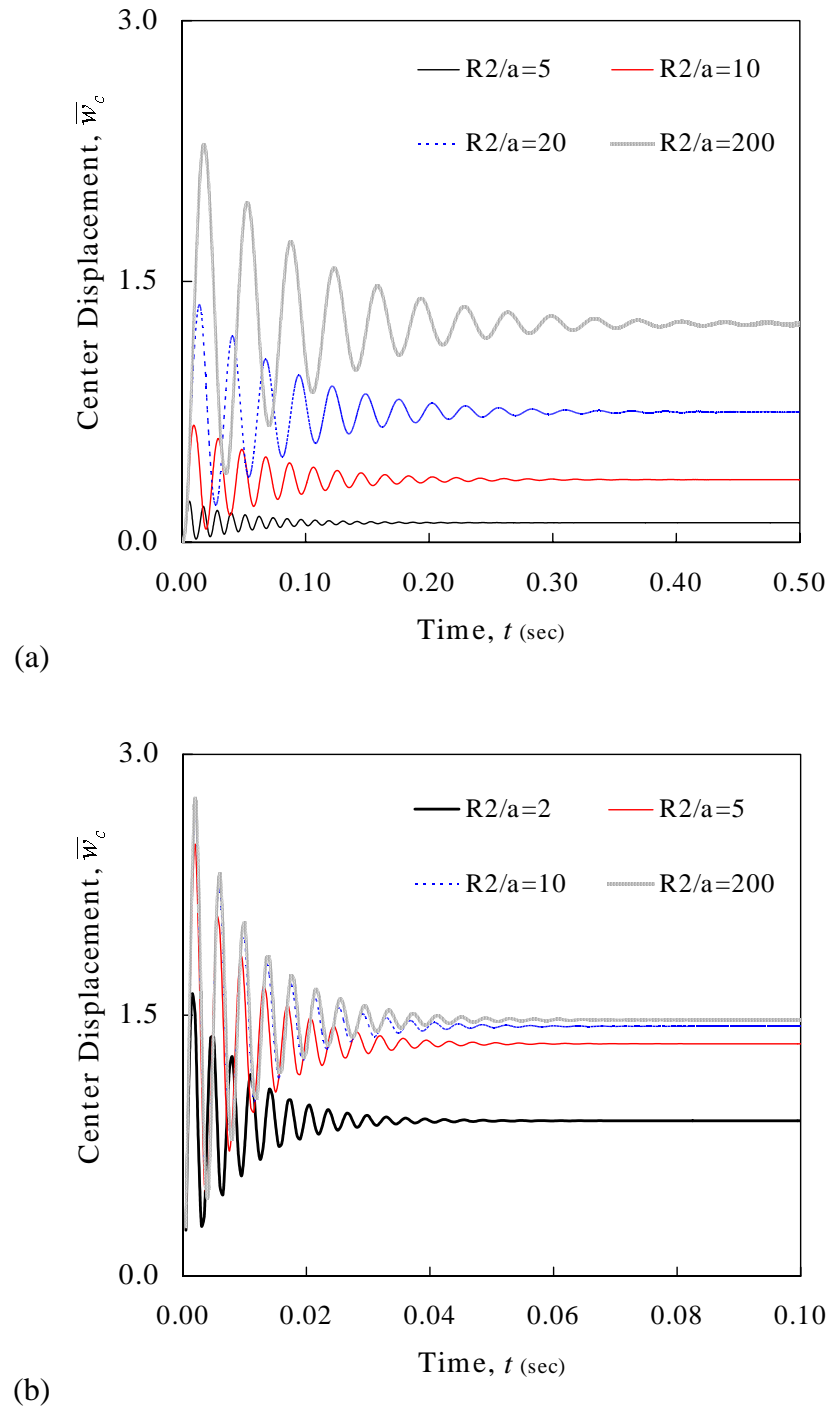


Figure 5.15 Effect of R_2/a for spherical cross-ply shell under uniform load in SSSS boundary condition; (a) thin shell ($a/h=100$), (b) thick shell ($a/h=10$)

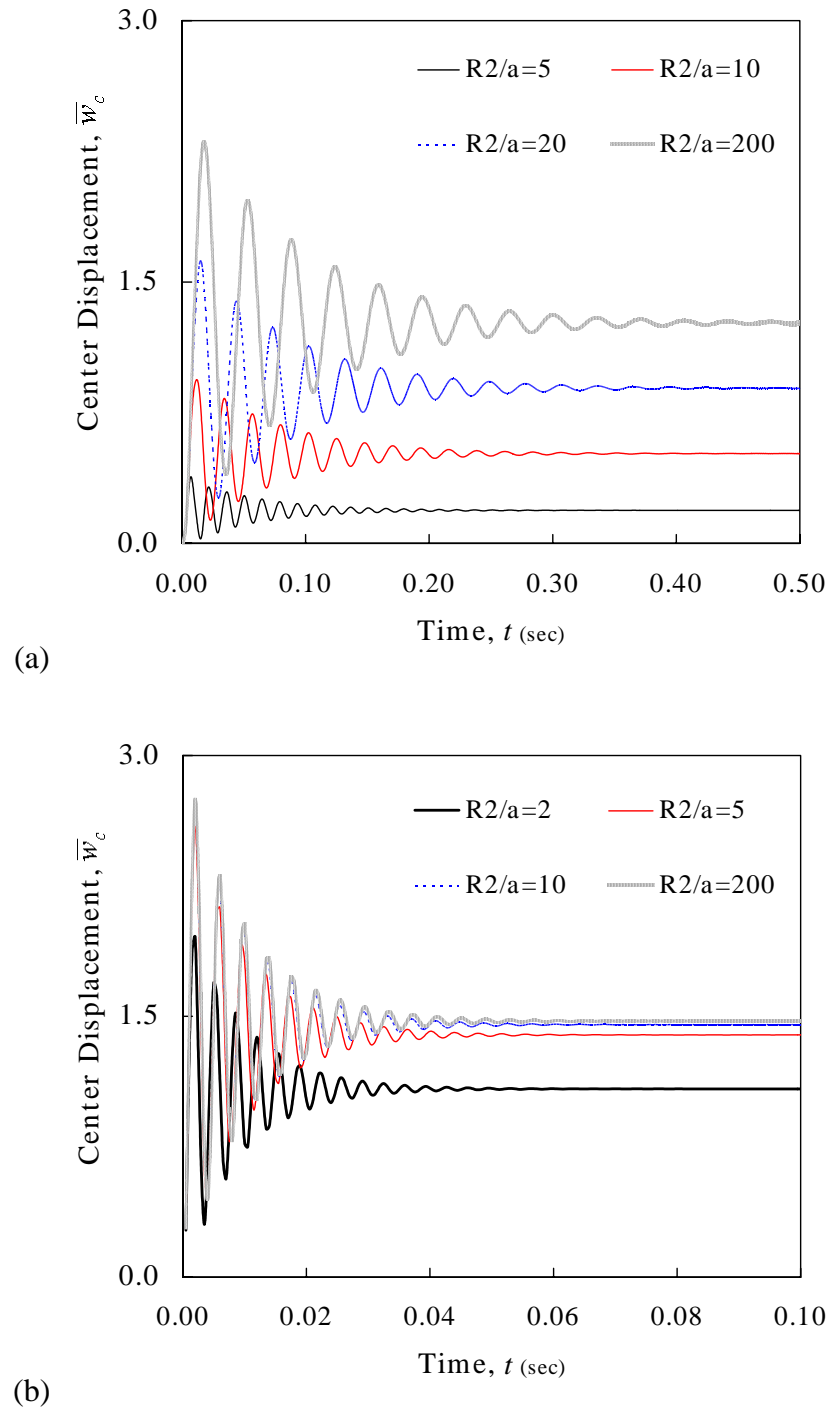


Figure 5.16 Effect of R_2/a for doubly-curved cross-ply shell under uniform load in SSSS boundary condition; (a) thin shell ($a/h=100$), (b) thick shell ($a/h=10$)

Table 5.12 Maximum transverse deflection and deflection suppression time for the symmetric cross-ply shells by Sanders shell theory

Thickness	R_2/a	Spherical Shell		Doubly Curved Shell	
		\tilde{w}_{\max}	$t(\text{sec})$ at $\tilde{w}_{\max}/10$	\tilde{w}_{\max}	$t(\text{sec})$ at $\tilde{w}_{\max}/10$
Thin Shell $a/h = 100$	2	0.019592	0.077000	0.034506	0.093500
	5	0.123990	0.119000	0.191890	0.137000
	10	0.312520	0.164000	0.424780	0.172000
	50	0.892100	0.212000	0.946900	0.218500
	100	0.978200	0.225000	1.011100	0.227000
	1000	1.059900	0.234000	1.073100	0.234500
Thick Shell $a/h = 10$	2	0.726790	0.023500	0.868800	0.022500
	5	1.146000	0.024500	1.199200	0.025000
	10	1.237100	0.025000	1.251600	0.025500
	50	1.271300	0.025500	1.272300	0.025500
	100	1.273200	0.025500	1.273500	0.025500
	1000	1.274500	0.025500	1.274400	0.025500

5.3.4. Effect of Lamination Schemes

The effect of lamination schemes on the deflection suppression characteristics is studied. Symmetric cross-ply (m,90,0,90,0)s, symmetric angle-ply (m,45,-45,45,-45)s and symmetric general angle-ply (m,45,-45,0,90)s laminations are considered for spherical, cylindrical, and doubly curved shells. Figures 5.17 – 5.19 show the effect of lamination schemes for cylindrical ($R_2/a=2$), spherical ($R_2/a=5$) and doubly-curved ($R_2/a=200$) shells respectively. All the examples are under uniformly distributed load and SSSS boundary condition. The effect of lamination on the deflection suppression time and maximum deflection can be seen in Table 5.13 as numerical values. It is reported that symmetric cross-ply shell has the biggest maximum deflection for all shell types and angle-ply shell shows the smaller deflection values than other lamination schemes.

5.3.5. *Effect of Boundary Conditions*

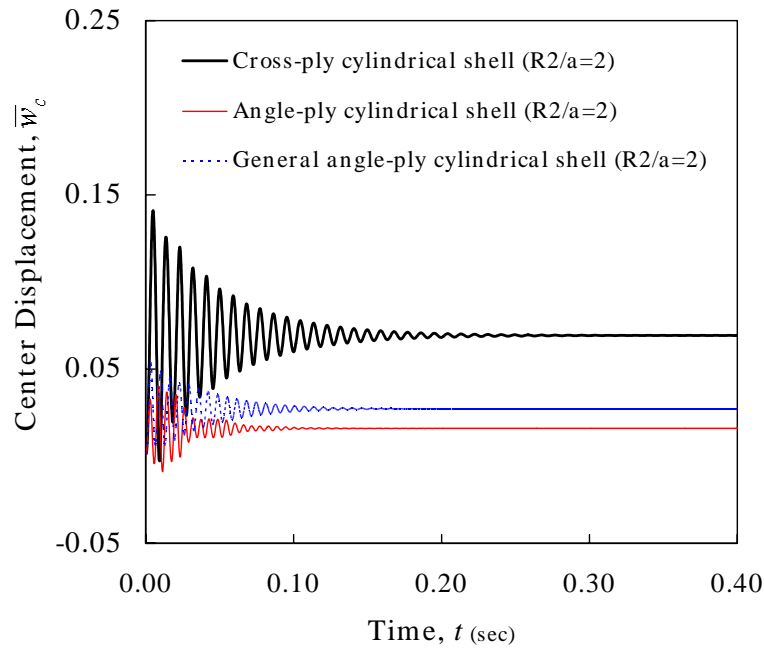
The effect of boundary condition of laminated composite shells on the deflection suppression is shown in Figures 5.20 – 5.22. Table 5.14 has the maximum deflection and deflection suppression time for each boundary condition. Each shell type, cylindrical, spherical, doubly-curved shell has the different R_1 and R_2 values, the maximum deflection can be found in SSFF boundary condition and the maximum deflection suppression occurs in CCCC boundary condition.

5.3.6. *Effect of Loading Conditions*

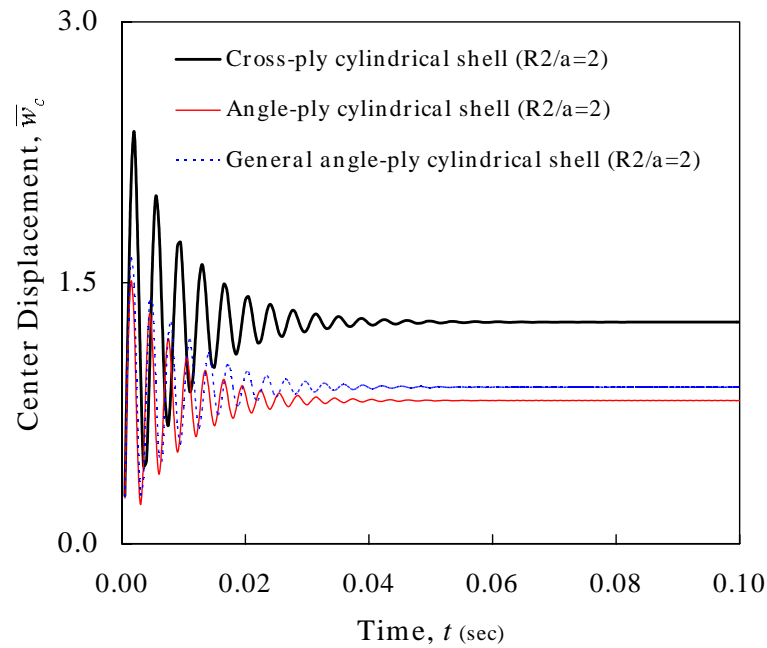
The effect of applied loading conditions on the deflection suppression is shown in Figure 5.23. Uniformly distributed load, uniformly distributed sinusoidal load, uniformly distributed impact load and uniformly distributed sinusoidal impact load are considered to study the loading effect. The deflection under the uniformly distributed load has the largest value regardless of shell type or thickness.

5.4. **Nonlinear Results under Thermomechanical Loads**

In this section, parametric studies for laminated composite plate and shell structures that are subjected to a temperature field in addition to the mechanical loading are conducted. Temperature changes often represented a significant factor, and sometimes the predominant cause of failure of composite structures subject to severe environmental loads. In fiber reinforced laminated composites such as CFRP, the thermal expansion coefficients in the direction of fibers are usually much smaller than those in the transverse direction.

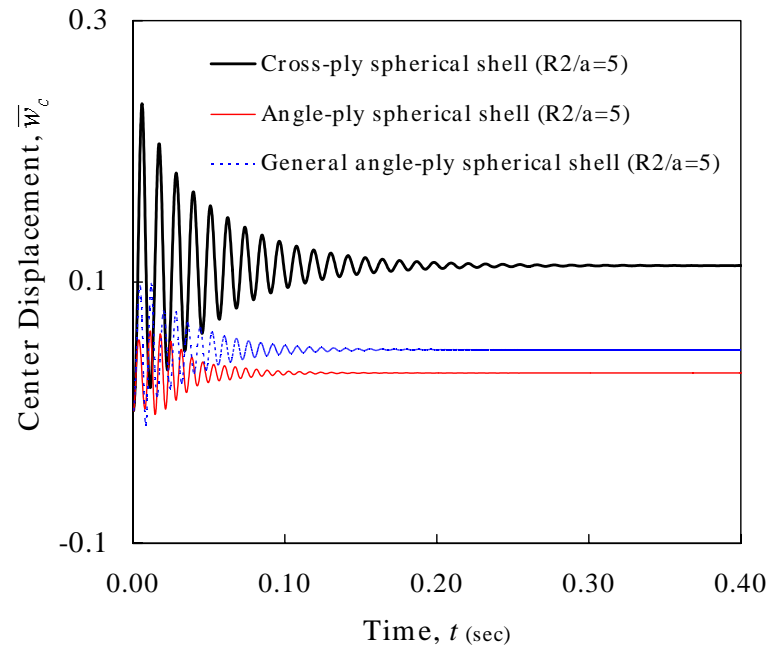


(a)

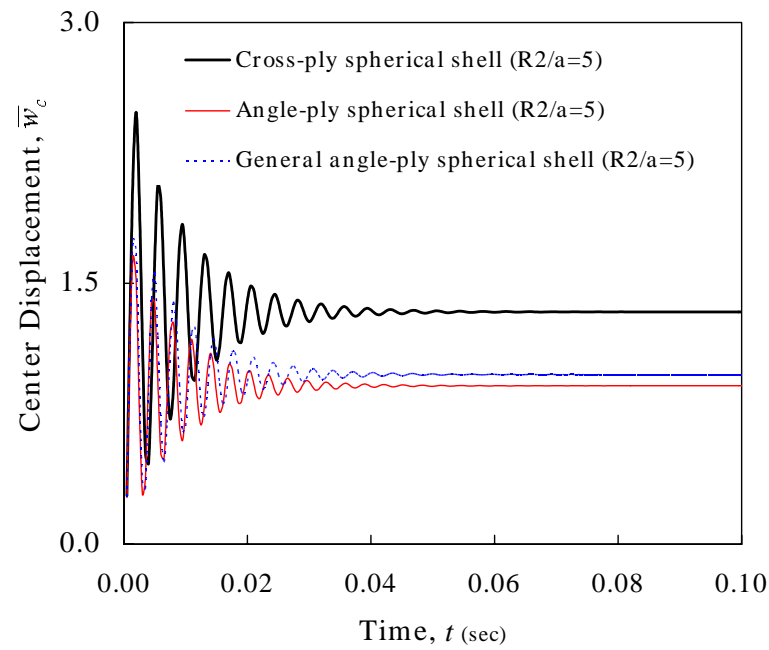


(b)

Figure 5.17 Effect of lamination schemes for cylindrical shell under uniform load in SSSS boundary condition; (a) thin shell ($a/h=100$), (b) thick shell ($a/h=10$)



(a)



(b)

Figure 5.18 Effect of lamination schemes for spherical shell under uniform load in SSSS boundary condition; (a) thin shell ($a/h=100$), (b) thick shell ($a/h=10$)

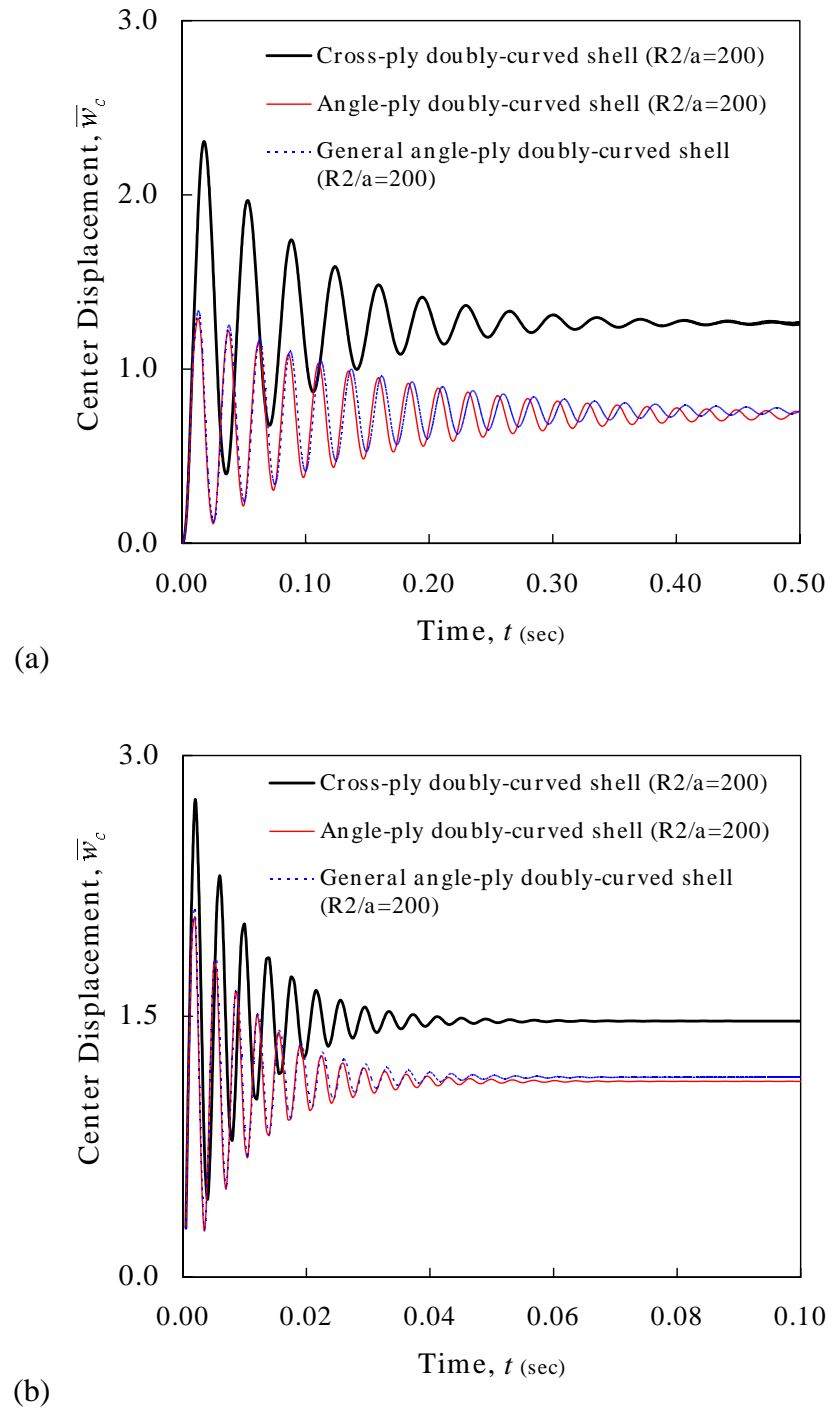


Figure 5.19 Effect of lamination schemes for doubly-curved shell under uniform load in SSSS boundary condition; (a) thin shell ($a/h=100$), (b) thick shell ($a/h=10$)

Table 5.13 Vibration suppression characteristics for the symmetric cross-ply laminated shells with the different lamination

Thickness	Shell Type	R_2/a	Lamination	\tilde{w}_{\max}	$t(\text{sec})$ at $\tilde{w}_{\max}/10$
Thin Shell $a/h = 100$	Cylindrical	2	Cross-ply	0.071648	0.114000
			Angle-ply	0.020724	0.066500
			General Angle-ply	0.026657	0.081500
	Spherical	5	Cross-ply	0.123960	0.119000
			Angle-ply	0.032041	0.074500
			General Angle-ply	0.050940	0.084000
	Doubly Curved	200	Cross-ply	1.048900	0.231000
			Angle-ply	0.534070	0.305500
			General Angle-ply	0.584150	0.335500
Thick Shell $a/h = 10$	Cylindrical	2	Cross-ply	1.092700	0.024000
			Angle-ply	0.687550	0.019500
			General Angle-ply	0.738630	0.020500
	Spherical	5	Cross-ply	1.146000	0.024500
			Angle-ply	0.744220	0.023500
			General Angle-ply	0.778160	0.024000
	Doubly Curved	200	Cross-ply	1.274100	0.025500
			Angle-ply	0.937800	0.026000
			General Angle-ply	0.965800	0.026000

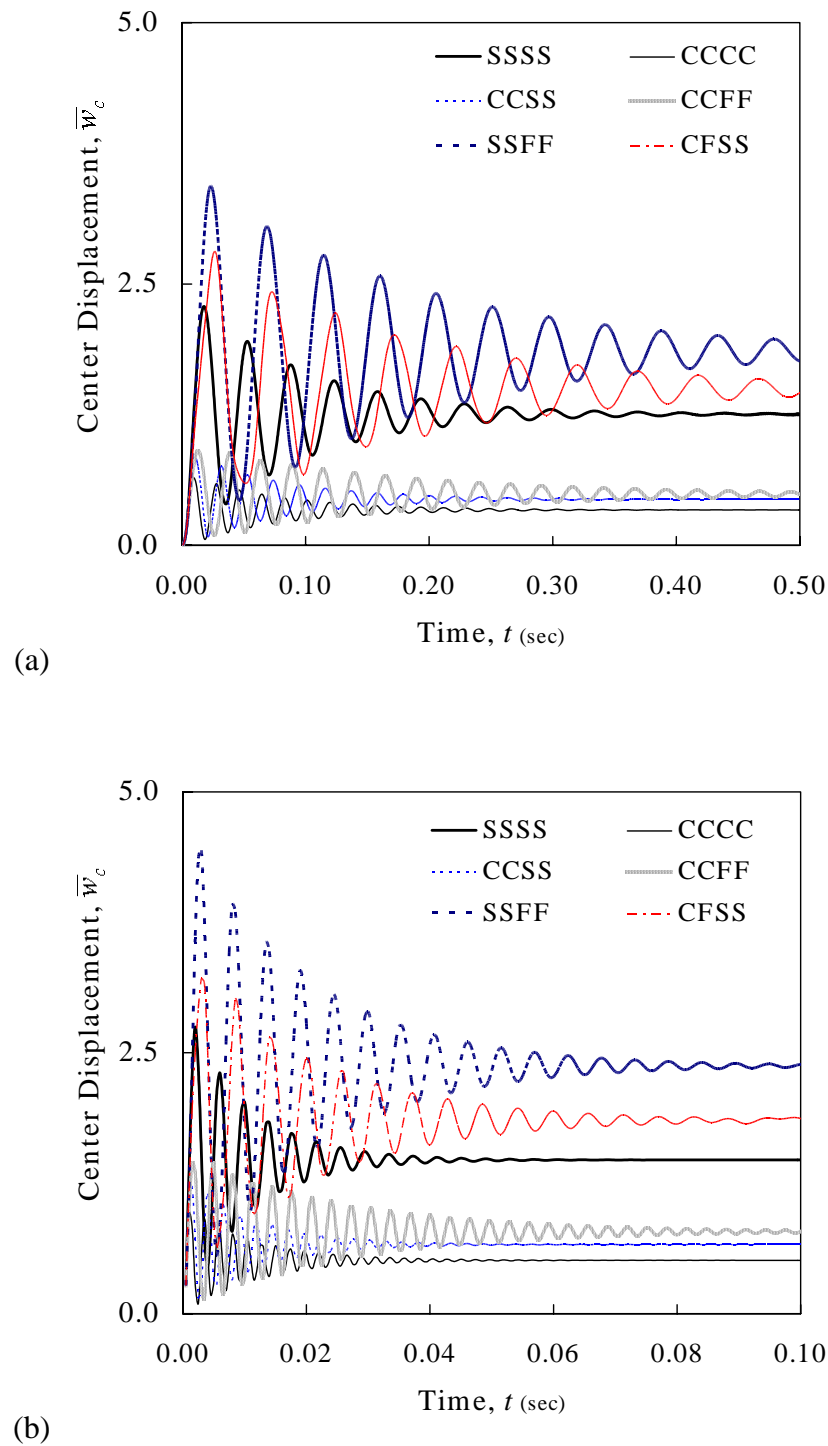
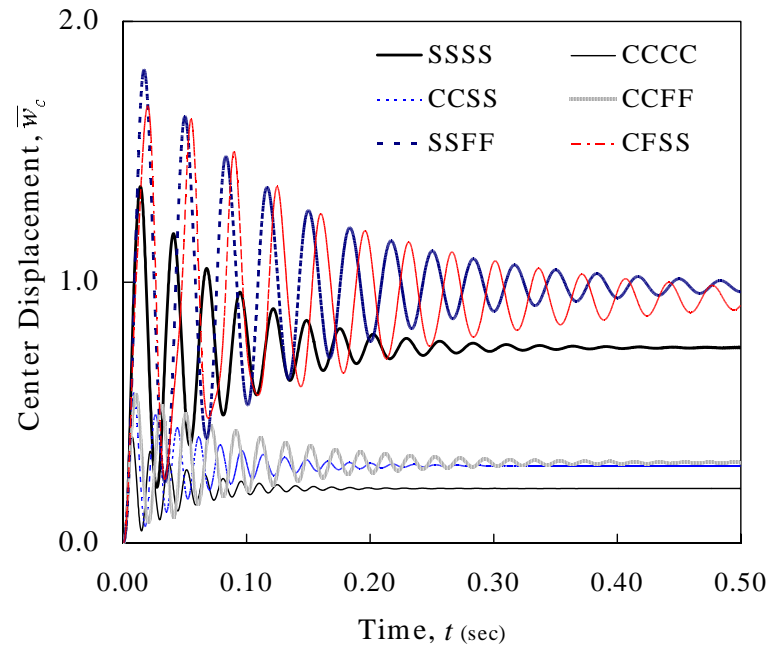
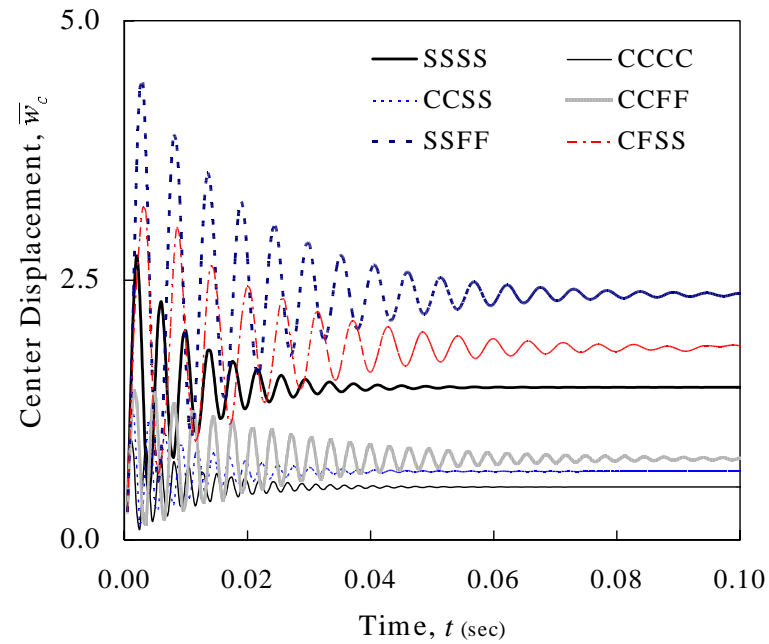


Figure 5.20 Effect of boundary conditions for cross-ply cylindrical shell under uniform load; (a) thin shell ($a/h=100$, $R_2/a=100$), (b) thick shell ($a/h=10$, $R_2/a=50$)

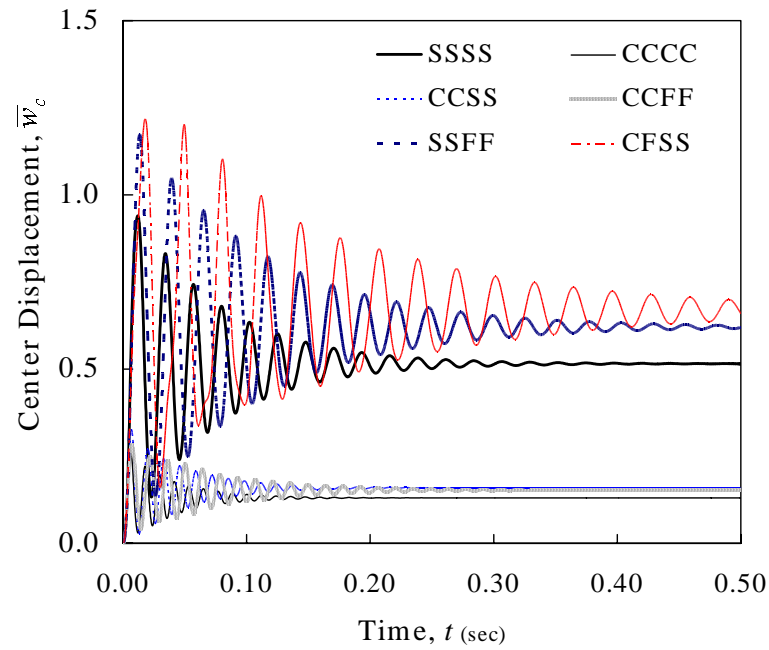


(a)

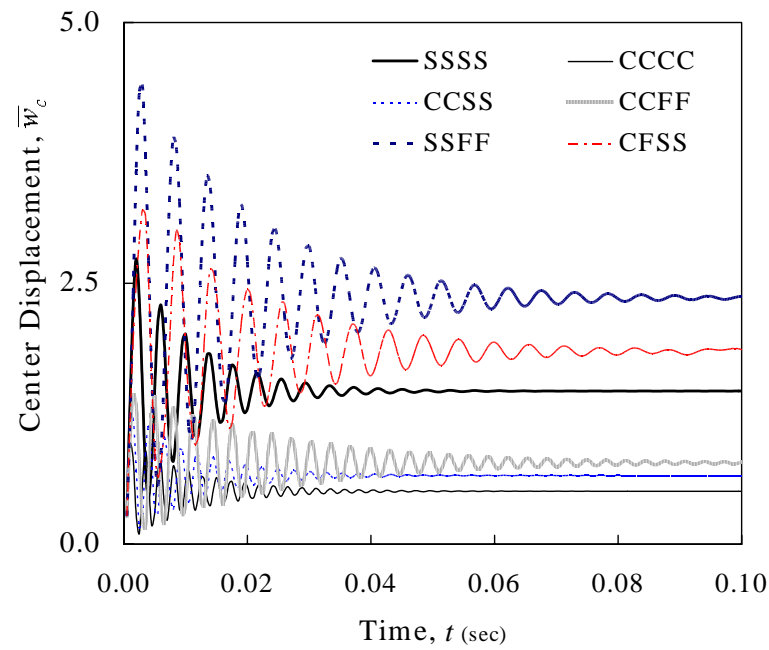


(b)

Figure 5.21 Effect of boundary conditions for cross-ply spherical shell under uniform load; (a) thin shell ($a/h=100$, $R_2/a=20$), (b) thick shell ($a/h=10$, $R_2/a=10$)



(a)

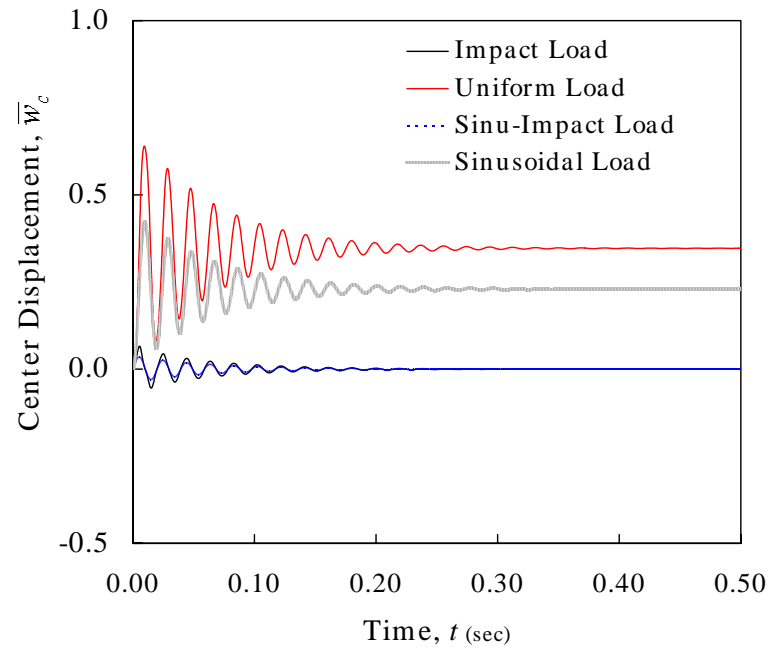


(b)

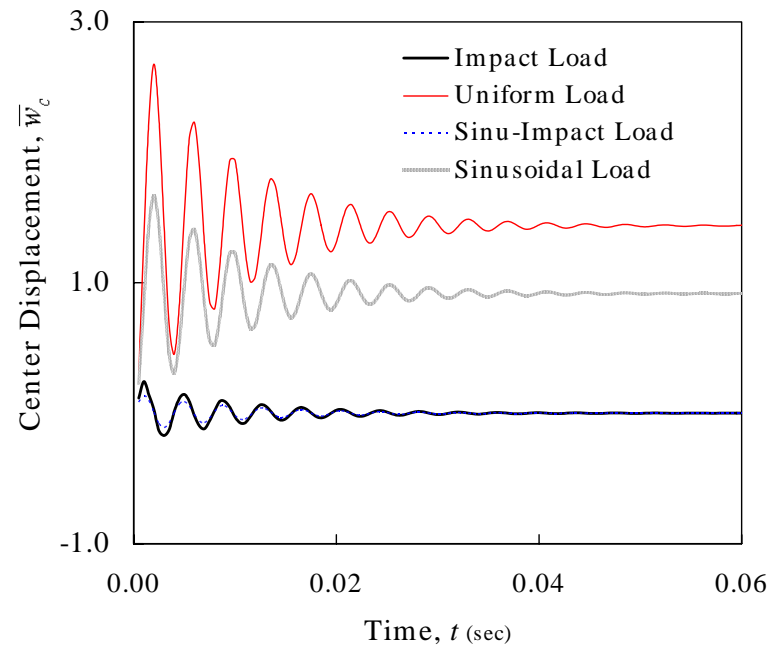
Figure 5.22 Effect of boundary conditions for cross-ply doubly-curved shell under uniform load; (a) thin shell ($a/h=100$, $R_2/a=10$), (b) thick shell ($a/h=10$, $R_2/a=20$)

Table 5.14 Nondimensionalized maximum transverse deflections and deflection suppression time by nonlinear TSDT

Thickness	Shell Type	R_2/a	Boundary Condition	\tilde{w}_{\max}	$t(\text{sec})$ at $\tilde{w}_{\max}/10$
$\frac{a}{h} = 100$	Cylindrical	100	SSSS	1.024900	0.229500
			CCCC	0.307740	0.176000
			CCSS	0.402020	0.179500
			CCFF	0.410440	0.392500
			SSFF	1.594400	0.436500
			CFSS	1.355100	0.468500
	Spherical	20	SSSS	0.618830	0.202500
			CCCC	0.197590	0.111000
			CCSS	0.278060	0.132000
			CCFF	0.260770	0.234500
			SSFF	0.836260	0.317000
			CFSS	0.744180	0.444000
	Doubly curved	10	SSSS	0.425350	0.171000
			CCCC	0.133960	0.089000
			CCSS	0.166440	0.112000
			CCFF	0.129180	0.150500
			SSFF	0.550670	0.248500
			CFSS	0.556810	0.398500
$\frac{a}{h} = 10$	Cylindrical	50	SSSS	1.273200	0.025500
			CCCC	0.449170	0.026500
			CCSS	0.561410	0.027500
			CCFF	0.651010	0.059000
			SSFF	2.050600	0.046000
			CFSS	1.341900	0.048500
	Spherical	10	SSSS	1.237100	0.025500
			CCCC	0.438030	0.024000
			CCSS	0.530840	0.024500
			CCFF	0.632780	0.052000
			SSFF	1.942700	0.045000
			CFSS	1.337900	0.048500
	Doubly curved	20	SSSS	1.266800	0.025500
			CCCC	0.389790	0.026500
			CCSS	0.554230	0.027500
			CCFF	0.638720	0.056000
			SSFF	2.029700	0.046000
			CFSS	1.339900	0.048500



(a)



(b)

Figure 5.23 Effect of loading conditions for cross-ply cylindrical shell in SSSS boundary condition; (a) thin shell ($a/h=100$, $R_2/a=5$), (b) thick shell ($a/h=10$, $R_2/a=5$)

As mentioned in the previous section, since thermal effects are taken into consideration with the understanding that the material properties are independent of temperature, temperature enters the formulation only through constitutive equations. The temperature field considered is assumed to be a constant distribution over the plate/shell structure surface and thickness. Laminated composite plate and shell models ($a/b = 1$) used in this section are the same as the previous ones. All numerical results are presented in terms of nondimensionalized. The nondimensionalized parameters used in this study are

$$\text{Load parameter} \quad p' = \frac{q_0 a^4}{E_2 h^4} \quad (5.1)$$

$$\text{Center deflection} \quad w' = \frac{w}{h}, \quad \bar{w}_c = 100 \times \frac{w_0 E_2 h^3}{a^4 q_0} \quad (5.2)$$

The following thermal expansion coefficients are used for this study,

$$\alpha_1 = 12.0 \cdot 10^{-6} / ^\circ c \text{ and } \alpha_2 = 12.0 \cdot 10^{-6} / ^\circ c \quad \text{for Terfenol-D}$$

$$\alpha_1 = 0.1 \cdot 10^{-6} / ^\circ c \text{ and } \alpha_2 = 22.0 \cdot 10^{-6} / ^\circ c \quad \text{for CFRP}$$

$$\alpha_1 = 1.8 \cdot 10^{-6} / ^\circ c \text{ and } \alpha_2 = 54.0 \cdot 10^{-6} / ^\circ c \quad \text{for Gr-Ep (AS)}$$

$$\alpha_1 = 6.3 \cdot 10^{-6} / ^\circ c \text{ and } \alpha_2 = 20.5 \cdot 10^{-6} / ^\circ c \quad \text{for Gl-Ep}$$

$$\alpha_1 = 4.5 \cdot 10^{-6} / ^\circ c \text{ and } \alpha_2 = 14.4 \cdot 10^{-6} / ^\circ c \quad \text{for Br-Ep}$$

5.4.1. Static Results under Thermomechanical Loads

The static analysis is performed for different mechanical and thermal loads. First, the behavior of the cross-ply laminate with simply supported boundary condition is studied under uniformly distributed mechanical load and thermal load. To see the effect of shear deformation on the response of thick laminated plates, CLPT, FSDT, and TSDT solutions are obtained for side-to-thickness ratio $a/h = 10$. Figure 5.24 shows the nondimensionalized center displacements of thick laminates by three different plate theories. It is observed that CLPT theory renders the plate stiffer compared to the other two theories. For selected mechanical and thermal loads, the center displacements for each theory are tabulated in Table 5.15. Next, the behavior of thin laminated plates under

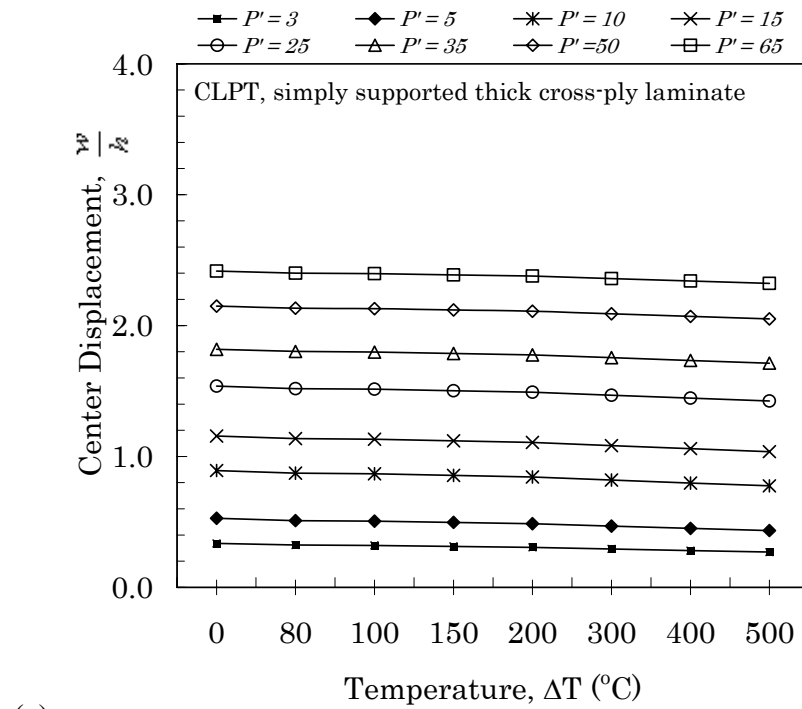
thermomechanical loading is considered. Using TSDT, the nonlinearities of center deflection due to the temperature effect are clearly shown in Figure 5.25 and Table 5.16.

Table 5.15 Nondimensionalized center displacements of the simply supported thick cross-ply laminate under thermomechanical loading by CLPT, FSDT, and TSD

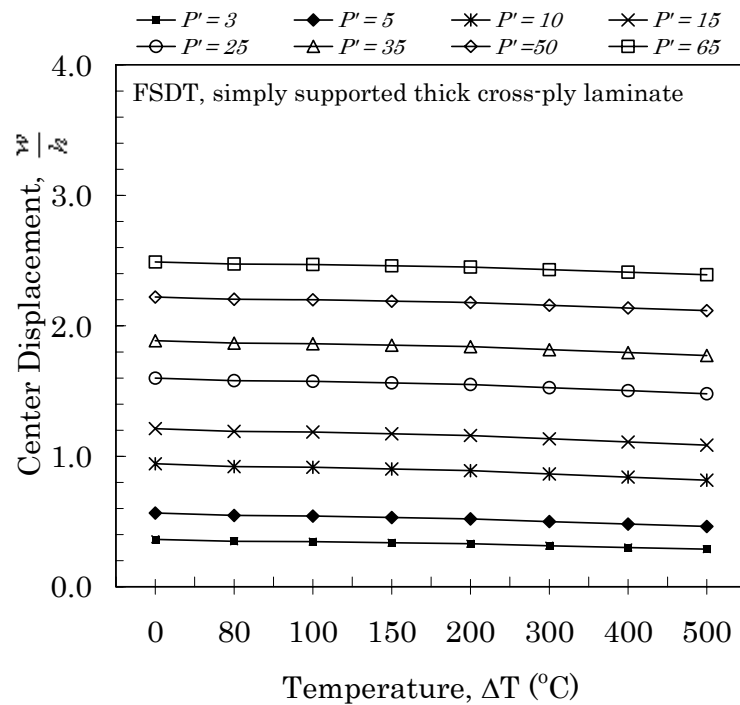
Temperature Rise, ΔT	60 $^{\circ}C$			100 $^{\circ}C$			300 $^{\circ}C$		
Plate Theory	CLPT	FSDT	TSDT	CLPT	FSDT	TSDT	CLPT	FSDT	TSDT
$p' = 0.5$	0.0565	0.0615	0.0658	0.0554	0.0601	0.0644	0.0502	0.0542	0.0585
$p' = 1$	0.1127	0.1225	0.1310	0.1104	0.1198	0.1283	0.1002	0.1081	0.1167
$p' = 3$	0.3265	0.3526	0.3780	0.3205	0.3457	0.3713	0.2931	0.3149	0.3409
$p' = 5$	0.5146	0.5513	0.5944	0.5063	0.5422	0.5854	0.4680	0.4999	0.5442
$p' = 10$	0.8777	0.9269	1.0228	0.8678	0.9162	1.0123	0.8201	0.8651	0.9622
$p' = 15$	1.1417	1.1964	1.3564	1.1318	1.1859	1.3459	1.0835	1.1347	1.2946
$p' = 25$	1.5234	1.5847	1.8924	1.5142	1.5749	1.8821	1.4687	1.5267	1.8312
$p' = 35$	1.8063	1.8722	2.3406	1.7977	1.8630	2.3304	1.7550	1.8177	2.2802
$p' = 50$	2.1374	2.2081	2.9286	2.1295	2.1997	2.9186	2.0901	2.1577	2.8693
$p' = 65$	2.4043	2.4779	3.4551	2.3969	2.4700	3.4454	2.3599	2.4306	3.3971

Table 5.16 Nonlinear nondimensionalized center displacements of the simply supported thin cross-ply laminate under thermomechanical loading by TSDT

Load Parameter, p'	Temperature rise ΔT ($^{\circ}C$)							
	0	10	20	30	40	50	60	70
10 (Linear)	0.11933	0.09656	0.08200	0.07188	0.06446	0.05876	0.05426	0.05062
10	0.11888	0.08339	0.06606	0.05581	0.04903	0.04421	0.04061	0.03784
20	0.23513	0.16626	0.13194	0.11154	0.09803	0.08839	0.08124	0.07567
30	0.34668	0.24817	0.19754	0.16712	0.14696	0.13260	0.12182	0.11349
40	0.45242	0.32869	0.26267	0.22254	0.19580	0.17670	0.16233	0.15121
50	0.55200	0.40751	0.32723	0.27772	0.24447	0.22075	0.20284	0.18897
60	0.64560	0.48441	0.39109	0.33260	0.29304	0.26471	0.24331	0.22671
70	0.73368	0.55925	0.45416	0.38713	0.34144	0.30849	0.28382	0.26452
80	0.81676	0.63198	0.51636	0.44127	0.38964	0.35224	0.32415	0.30206
90	0.89541	0.70258	0.57763	0.49497	0.43763	0.39588	0.36429	0.33965
100	0.97013	0.77110	0.63793	0.54821	0.48537	0.43938	0.40464	0.37721

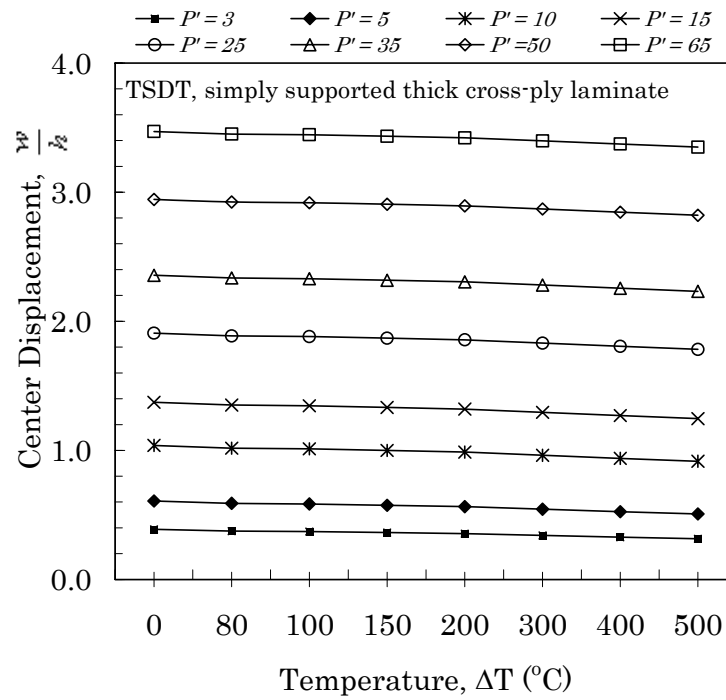


(a)



(b)

Figure 5.24 Effect of the plate theories on static behaviors of simply supported thick cross-ply laminates under mechanical and thermal load; (a) CLPT, (b) FSDT, (c) TSDT



(c)

Figure 5.24 Continued

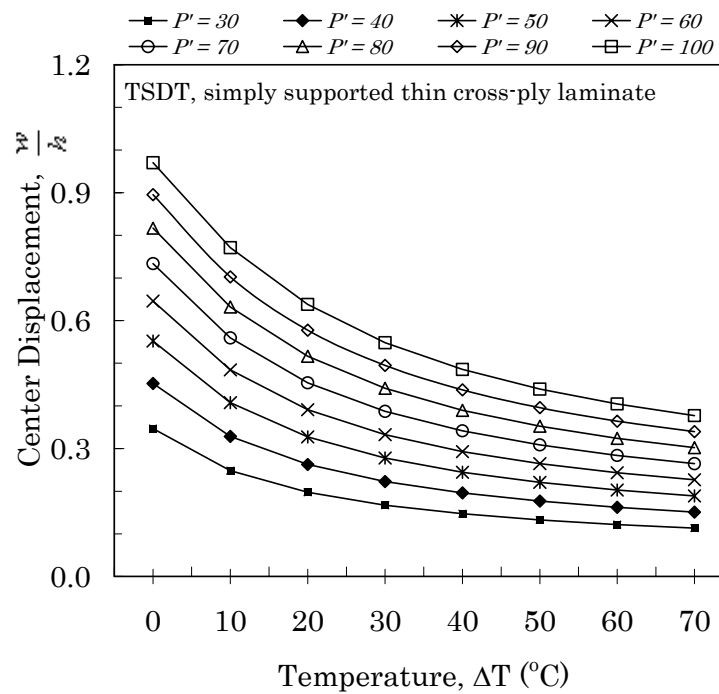


Figure 5.25 Thermomechanical behavior of simply supported thin cross-ply laminates

The typical nonlinear results of center deflection of thick and thin cross-ply and angle-ply plates are given in Figure 5.26. The effect of temperature rise $\Delta T = 200^\circ C$ for thick laminate and $\Delta T = 20^\circ C$ for thin laminate is considered, respectively. The effect of the thermal loading is apparent in the thin laminate with small temperature rise. The magnitude of center deflections of cross-ply laminate is bigger than that of angle-ply laminate.

The effects of R_2/a on the nonlinear deflection under thermomechanical loads are shown in Figure 5.27. The nondimensionalized center displacements of thick ($a/h=10$, $\Delta T=100^\circ C$) and thin ($a/h=100$, $\Delta T=10^\circ C$) cross-ply cylindrical shells are plotted. Figures 5.28 – 5.30 show the temperature effects of cross-ply cylindrical, doubly-curved and spherical shells, respectively. As thermal loads increase, the center deflections increase for any shell type or R_2/a value.

5.4.2. Laminated Composite Plates under Thermomechanical Loads

Nonlinear transient results of laminated composites under thermomechanical loadings are presented in this section. The critical time step for Newmark's scheme in nonlinear problem is selected to satisfy the stable and accurate solution condition. Time interval 0.1 and 0.5 milliseconds are chosen for the thick ($a/h=10$) and the thin ($a/h=100$) laminates.

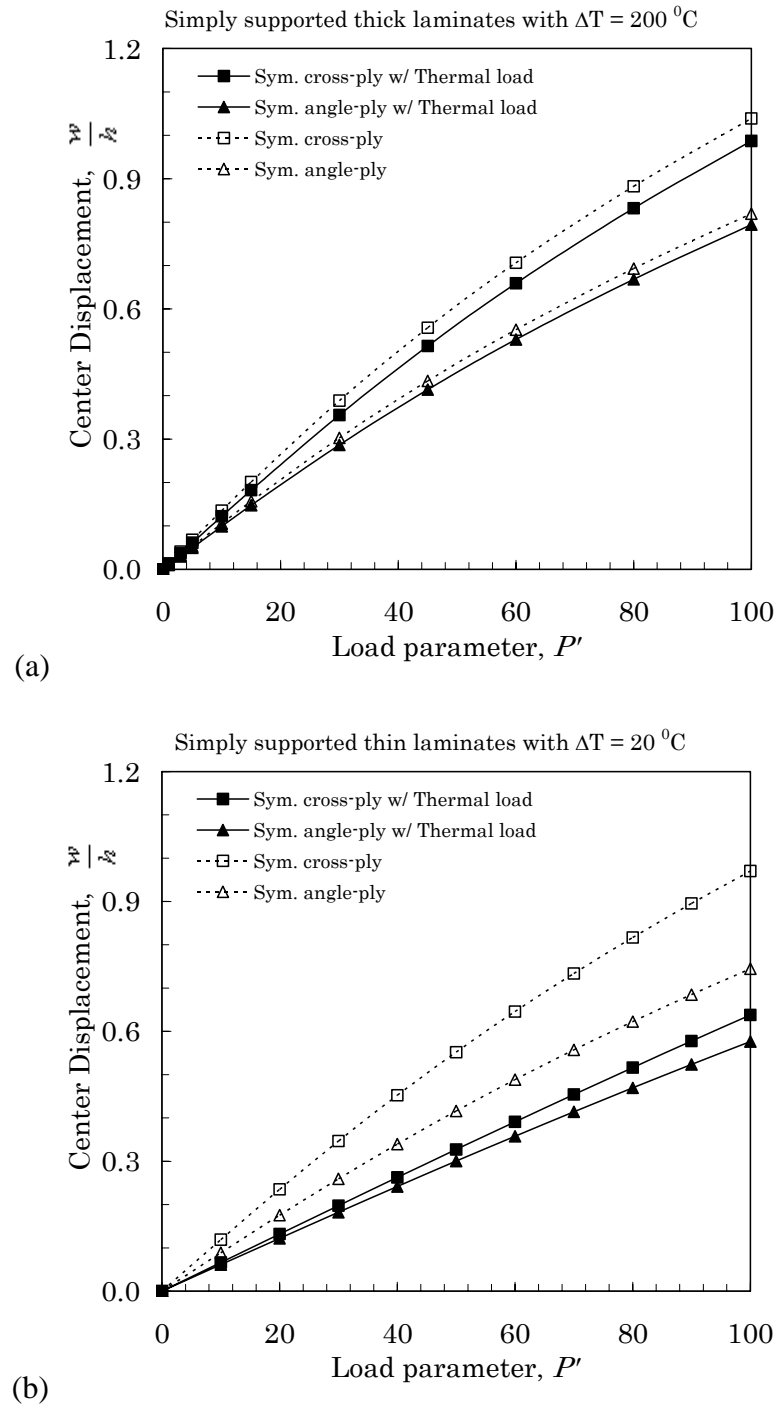
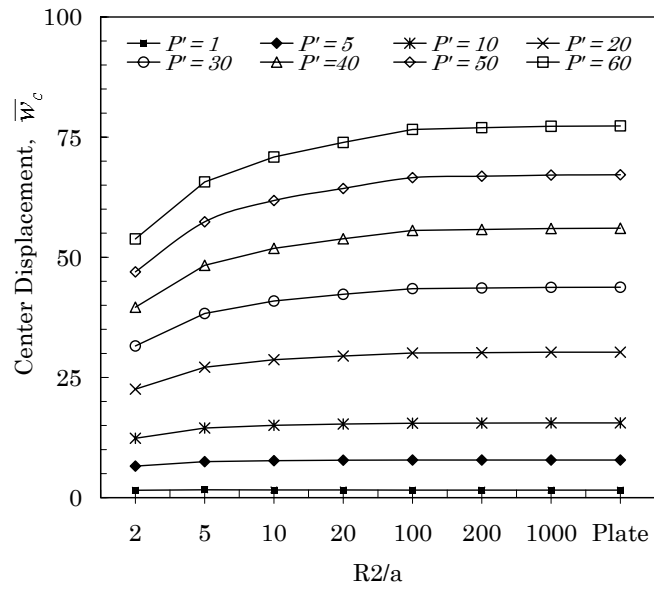
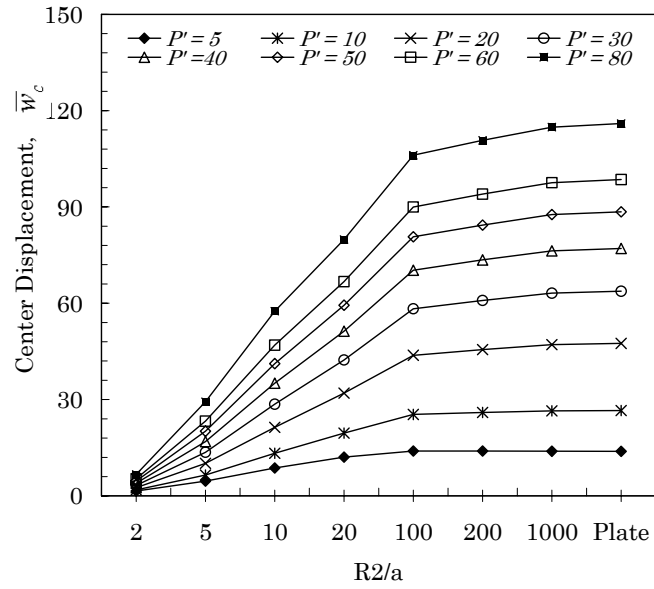


Figure 5.26 Effect of the laminations on static behaviors of simply supported laminated plates under mechanical and thermal load; (a) Thick laminate, (b) Thin laminate

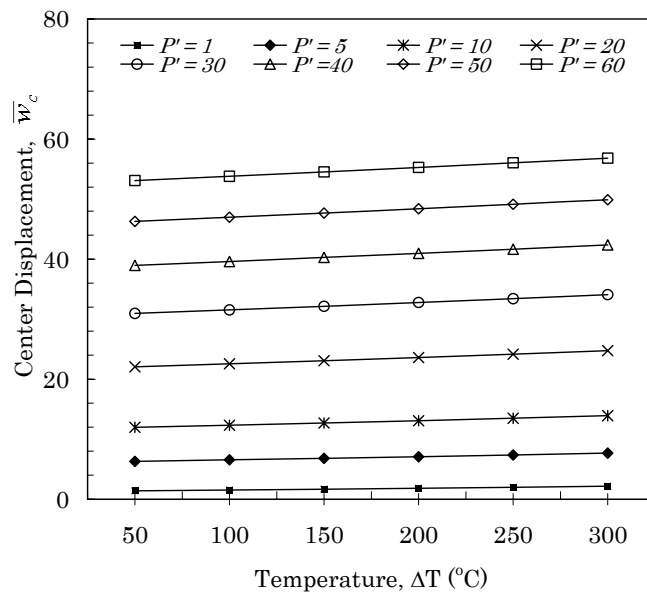


(a)

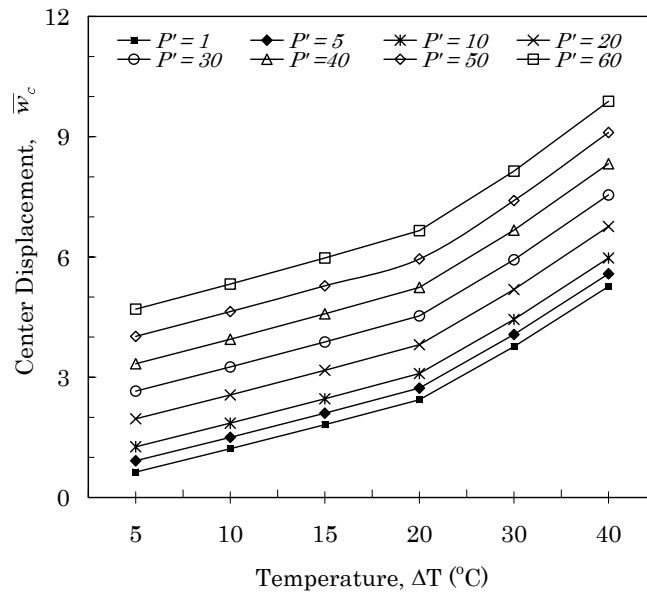


(b)

Figure 5.27 Effect of R_2/a on static behavior of cross-ply cylindrical shell under thermomechanical load: (a) Thick shell ($a/h=10$, $\Delta T=100^\circ C$), (b) Thin shell ($a/h=100$, $\Delta T=10^\circ C$)

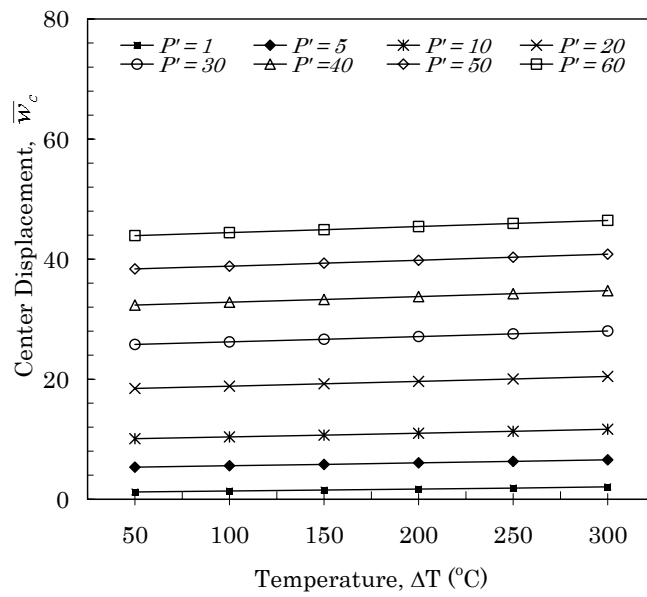


(a)

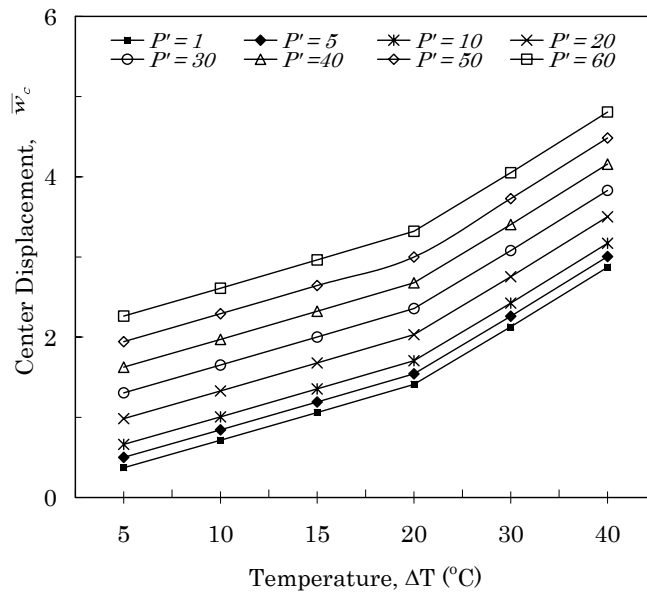


(b)

Figure 5.28 Temperature effect on static behavior of cross-ply cylindrical shell under thermomechanical load: (a) Thick shell ($a/h=10$, $R_2/a=2$), (b) Thin shell ($a/h=100$, $R_2/a=2$)

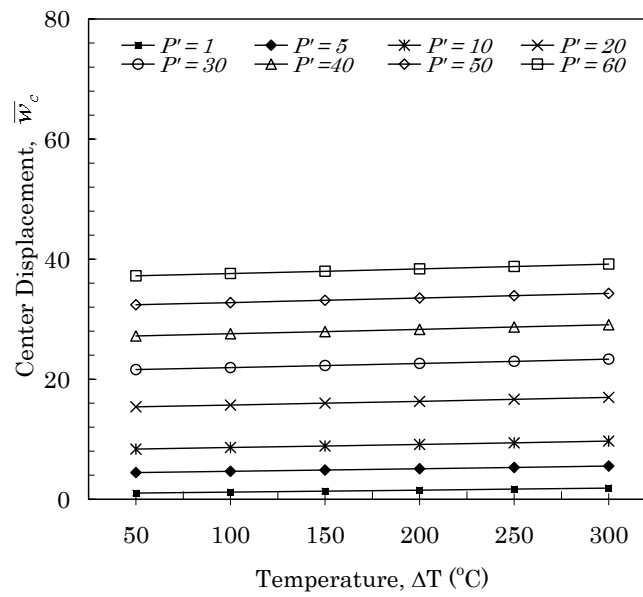


(a)

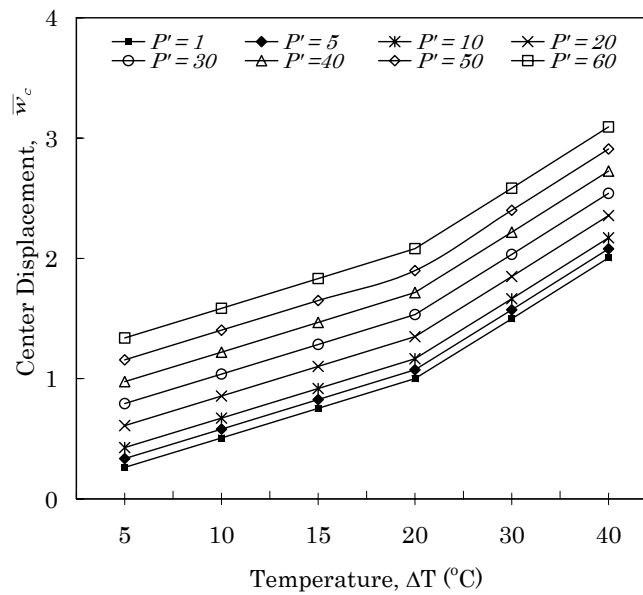


(b)

Figure 5.29 Temperature effect on static behavior of cross-ply doubly-curved shell under thermomechanical load: (a) Thick shell ($a/h=10$, $R_2/a=10$), (b) Thin shell ($a/h=100$, $R_2/a=10$)



(a)



(b)

Figure 5.30 Temperature effect on static behavior of cross-ply spherical shell under thermomechanical load: (a) Thick shell ($a/h=10$, $R_2/a=2$), (b) Thin shell ($a/h=100$, $R_2/a=2$)

First, the thermomechanical effect with different laminations is studied. The transient behavior of the laminated composites under thermomechanical loadings is shown in Figures 5.31, 5.32 and 5.33. The applied mechanical load parameters are 10^7 for thick laminates and 5×10^3 for thin laminates, respectively. Each mechanical load is selected to show the nonlinear behavior of laminates and that selected load makes the nonlinear problem can be solved without considering the load loop. The thermal load is applied to the opposite direction of the mechanical load in the thermomechanical simulations of laminated composite plates.

Uniformly distributed load and suddenly applied uniform load are considered with simply supported boundary condition in this study. The Figure includes the behaviors of uncontrolled case, the case without thermal load, and the case with thermal load. The considered thermal rise values are $\Delta T = 100, 200^\circ C$ for all thick laminates, $\Delta T = 20, 50^\circ C$ for thin cross-ply and angle-ply laminates, and $\Delta T = 20, 40^\circ C$ for thin general laminates. The effect of the thermal load is to reduce the amplitude and vibration suppression time. Here vibration suppression time is the time required to reduce the center deflections to 10% of its uncontrolled magnitude. The amplitude and period of the center deflections decrease with increasing thermal loading. The results of cross-ply, angle-ply and general laminates under thermomechanical loads can be seen in Figures 5.31, 5.32 and 5.33, respectively.

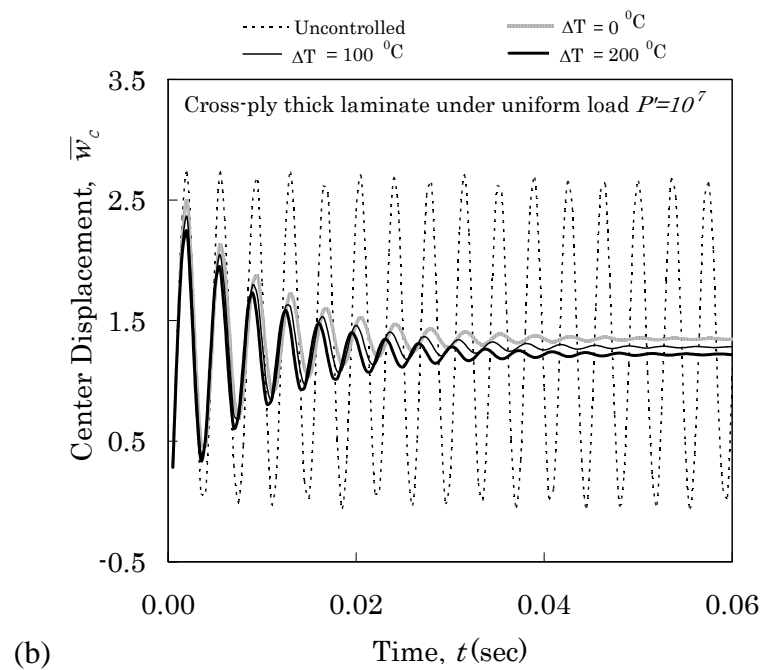
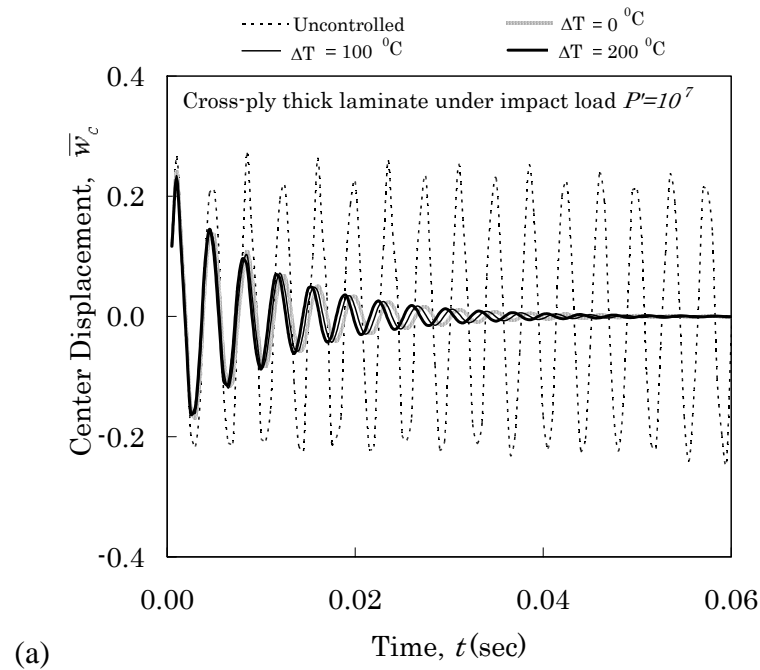


Figure 5.31 Transient behavior of the cross-ply laminates with simply supported boundary condition; (a) Thick laminate under impact load, (b) Thick laminate under uniform load, (c) Thin laminate under impact load, (d) Thin laminate under uniform load

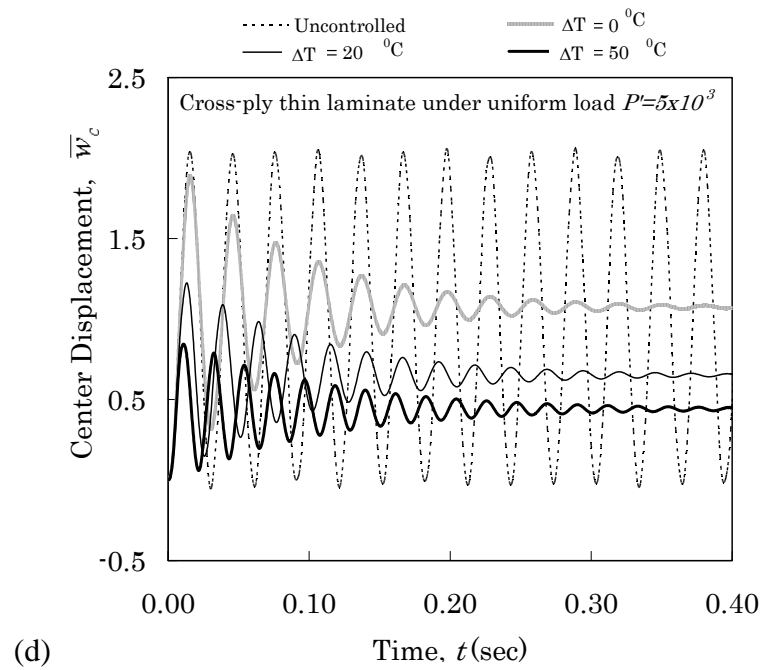
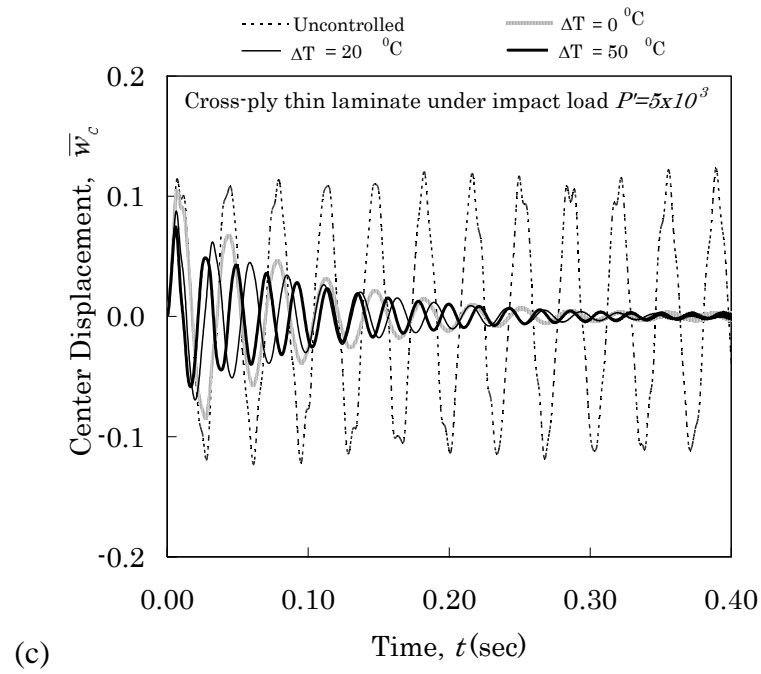


Figure 5.31 Continued

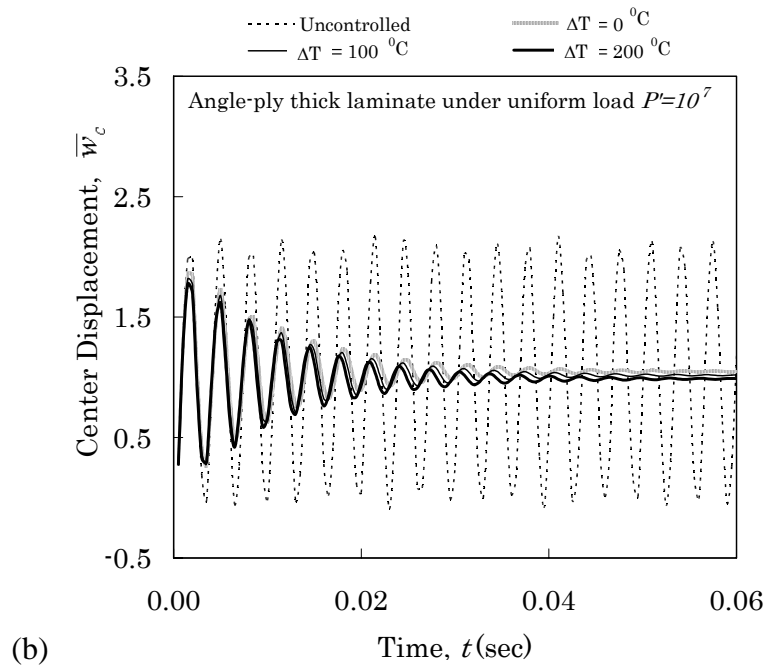
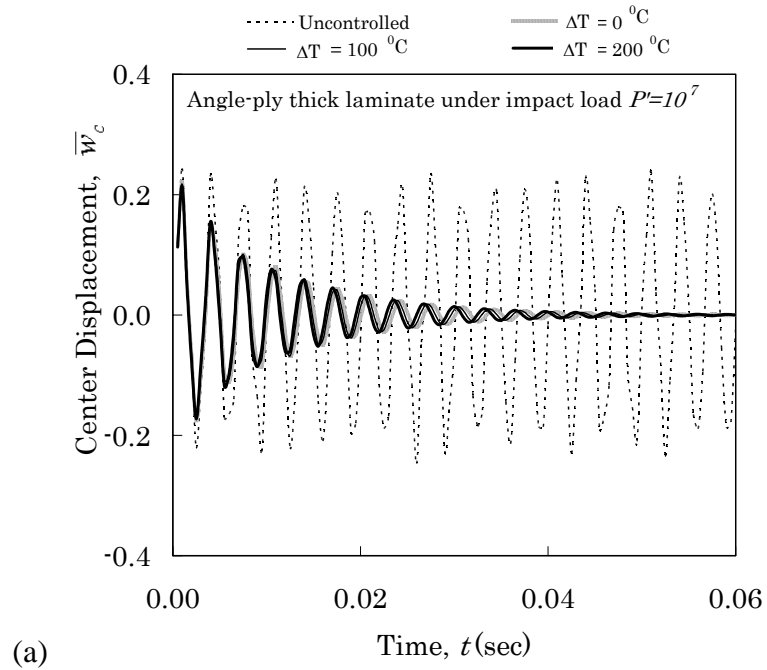


Figure 5.32 Transient behavior of the angle-ply laminates with simply supported boundary condition; (a) Thick laminate under impact load, (b) Thick laminate under uniform load, (c) Thin laminate under impact load, (d) Thin laminate under uniform load

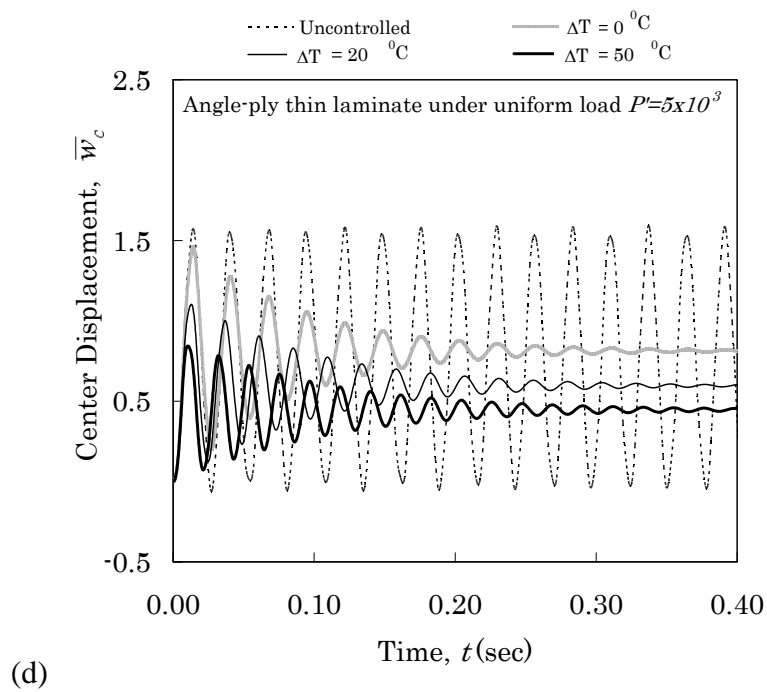
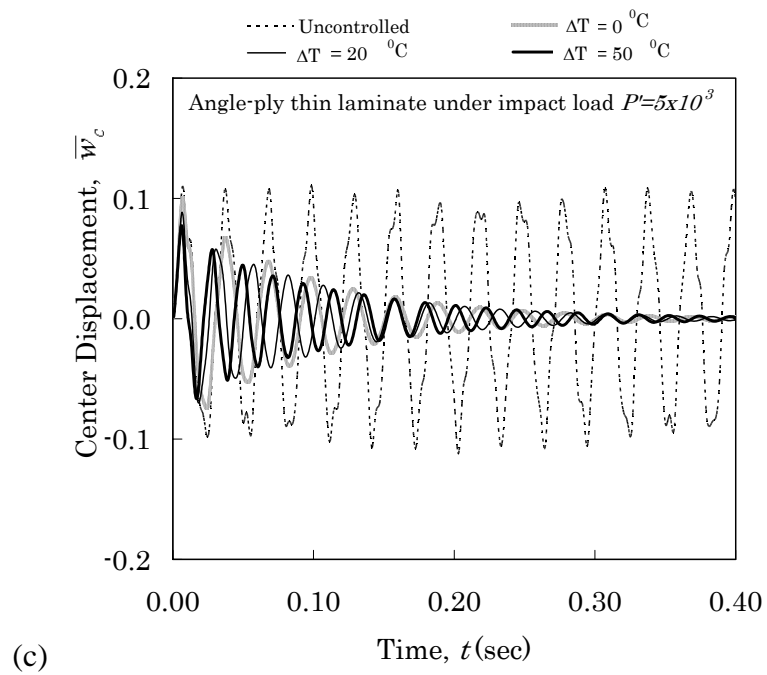
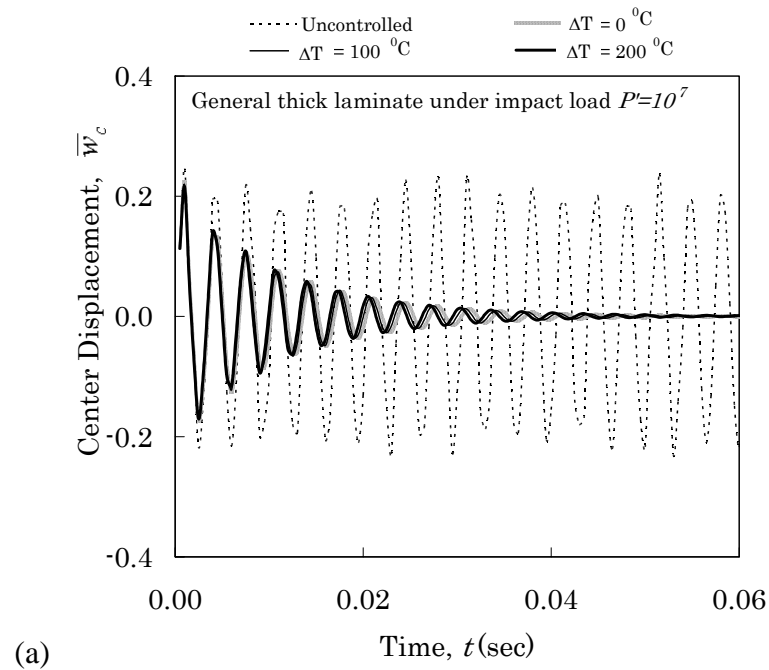
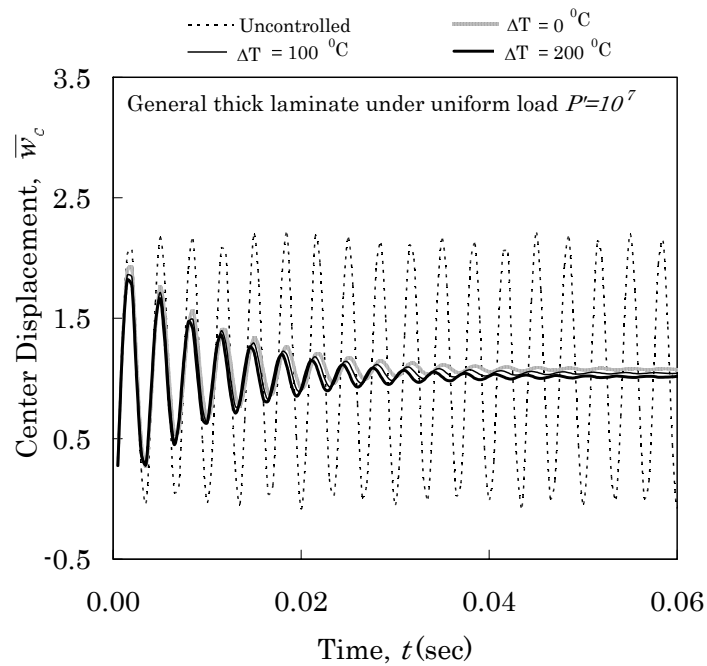


Figure 5.32 Continued



(a)



(b)

Figure 5.33 Transient behavior of the general laminates with simply supported boundary condition; (a) Thick laminate under impact load, (b) Thick laminate under uniform load, (c) Thin laminate under impact load, (d) Thin laminate under uniform load

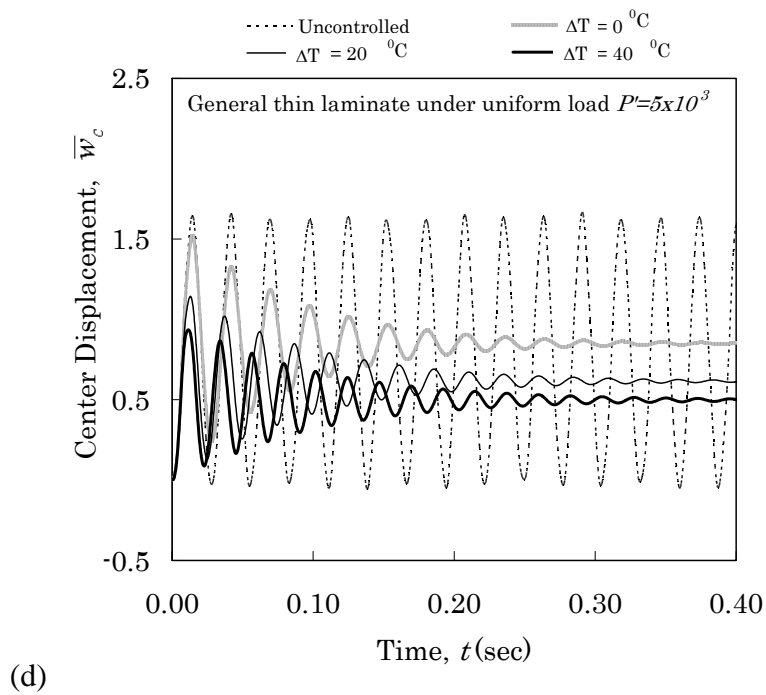
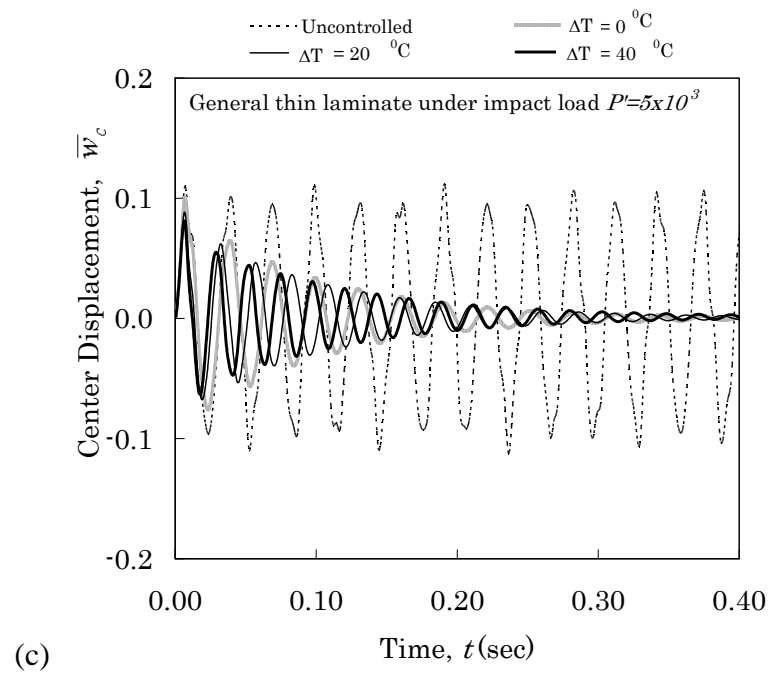


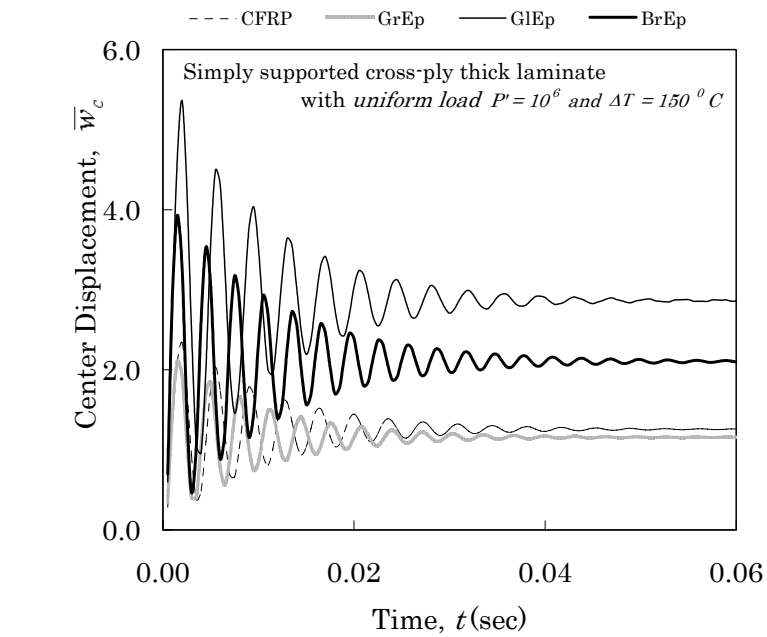
Figure 5.33 Continued

The effect of elastic material property on the vibration suppression response is studied under thermomechanical loading. Gr-Ep(AS), Gl-Ep, and Br-Ep are considered in addition to CFRP material, where the thermal expansion coefficients are shown in the beginning of this section. Figures 5.34 and 5.35 show the transient responses of thick and thin laminates, respectively. The mechanical load parameter 10^6 and thermal rise $\Delta T = 150^\circ C$ are used for thick laminates and $p' = 10^3$ and $\Delta T = 20^\circ C$ for thin laminates.

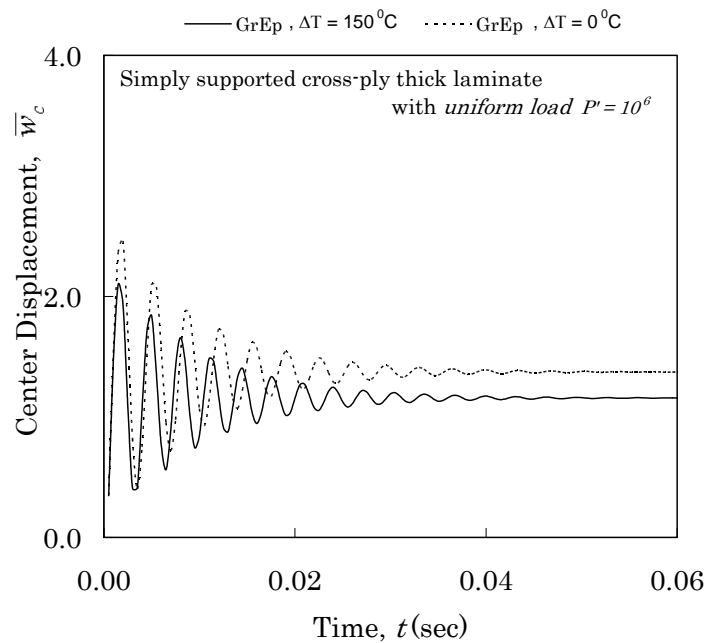
The maximum deflections and vibration suppression times of cross-ply laminates with different elastic materials under uniformly distributed mechanical loadings have been tabulated with and without thermal load in Table 5.17. Since the converged transient solutions for each material are different, the maximum deflection \tilde{w}_{\max} are defined as $\tilde{w}_{\max} = \bar{w}_{\max} - \bar{w}_{\text{converged}}$. It is observed that Gl-Ep shows the largest maximum deflection and the minimum vibration suppression time for thick laminates regardless of thermal effect.

Table 5.17 Nondimensionalized maximum center displacements and vibration suppression time of cross-ply laminates for different elastic materials

Plate Thickness	Elastic Material	Temperature Rise	\tilde{w}_{\max}	$t(\text{sec})$ at $\tilde{w}_{\max}/10$
$\frac{a}{h} = 10$	Gr-Ep (AS)	0	1.0874	0.0265
		150	0.9423	0.0240
	Gl-Ep	0	2.9160	0.0230
		150	2.5015	0.0245
	Br-Ep	0	2.0213	0.0285
		150	1.8231	0.0255
$\frac{a}{h} = 100$	Gr-Ep (AS)	0	1.0366	0.2110
		20	0.3231	0.2630
	Gl-Ep	0	2.5370	0.2130
		20	0.9914	0.2480
	Br-Ep	0	1.9293	0.2280
		20	0.7680	0.2730

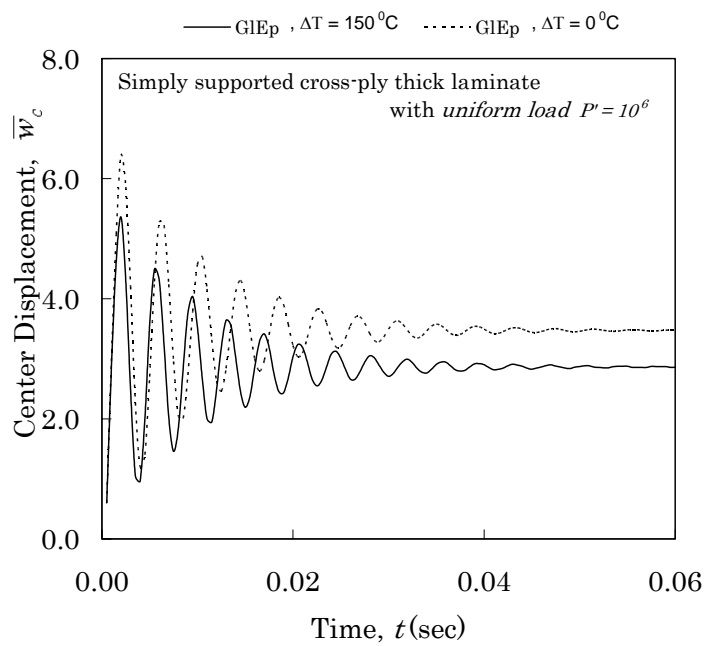


(a)

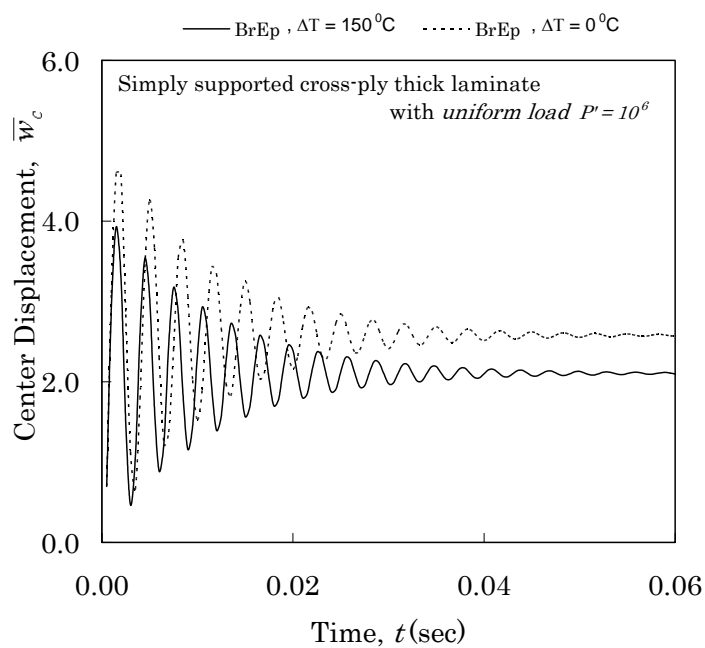


(b)

Figure 5.34 Effect of the elastic materials on the transient behavior of the thick cross-ply laminates with simply supported boundary condition; (a) Thick laminate under uniform load, (b) GrEp case, (c) GlEp case, (d) BrEp case

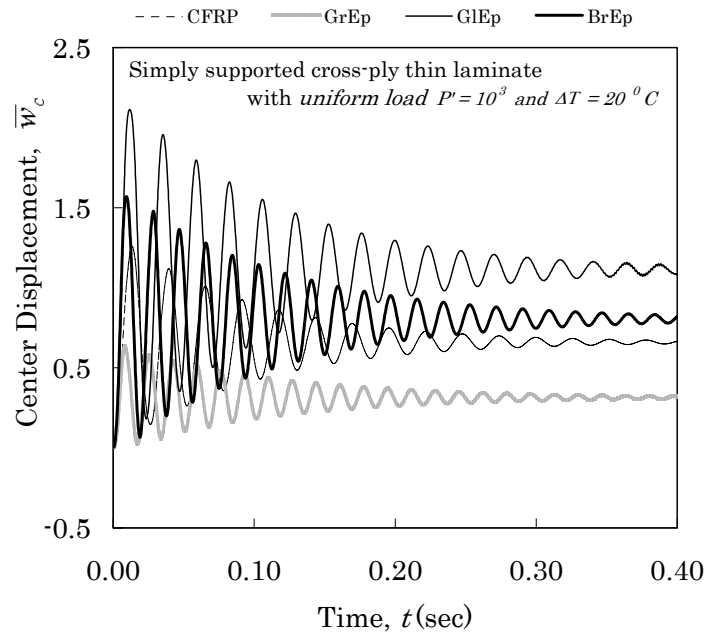


(c)

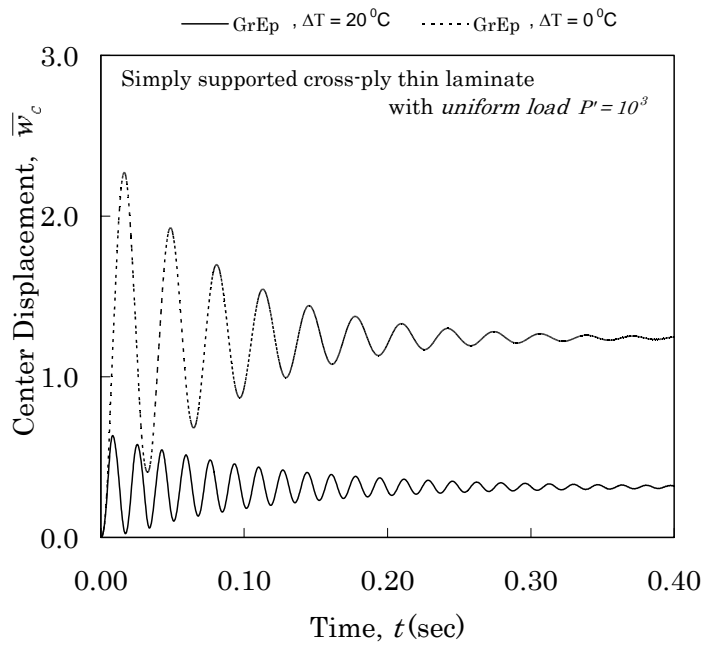


(d)

Figure 5.34 Continued

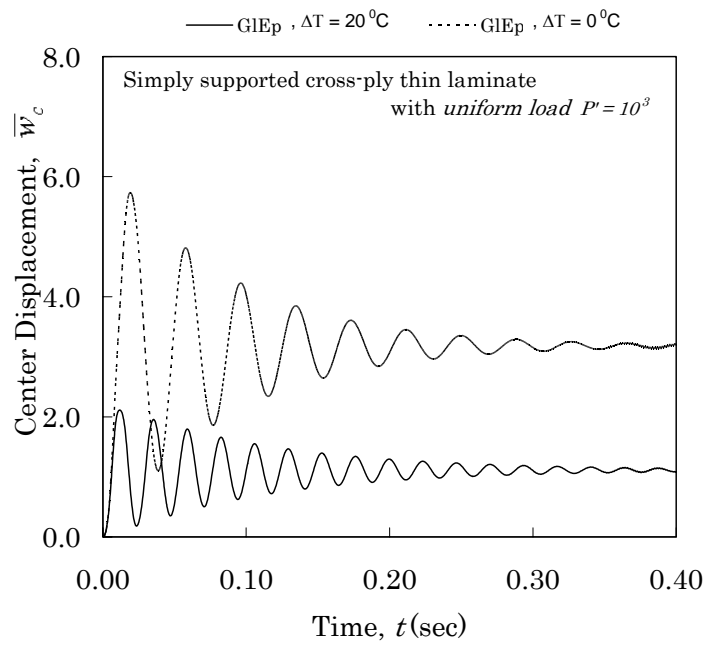


(a)

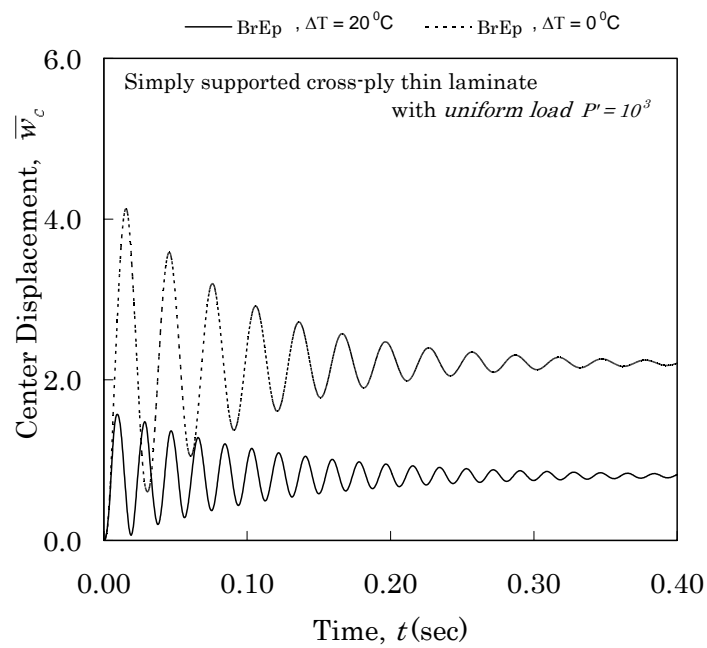


(b)

Figure 5.35 Effect of the elastic materials on the transient behavior of the thin cross-ply laminates with simply supported boundary condition; (a) Thin laminate under uniform load, (b) GrEp case, (c) GlEp case, (d) BrEp case



(c)



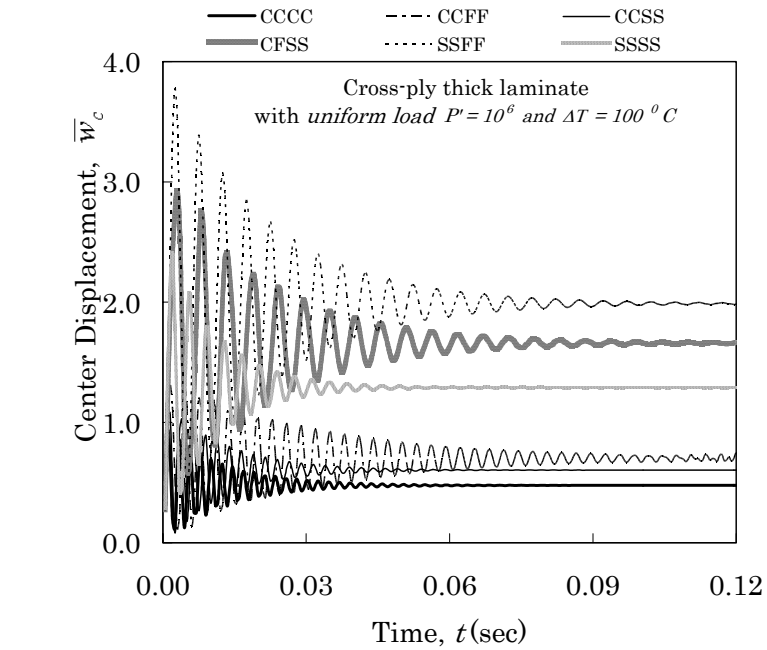
(d)

Figure 5.35 Continued

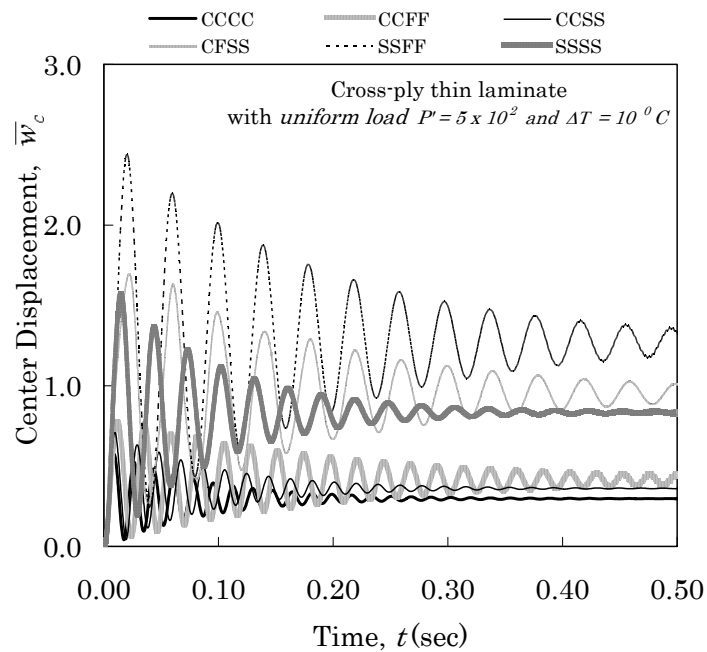
The following six boundary conditions are considered to see the differences in transient responses; SSSS, CCCC, CCSS, CCFF, SSFF, and CFSS. Where 'S' represents simply supported, 'C' clamped, and 'F' free edge conditions. Figure 5.36 contains the center displacements of cross-ply laminate for different boundary conditions under thermomechanical loading. The maximum deflections and vibration suppression times for each boundary condition have been tabulated in Table 5.18. It is observed that SSFF boundary condition shows the maximum deflection and CCCC shows the minimum deflection for thin and thick laminate under the thermal load in addition to the uniformly distributed mechanical load. The order of the boundary conditions with respect to the maximum center deflection value under thermomechanical loads is SSFF, CFSS, SSSS, CCFF, CCSS, and CCCC boundary conditions for all thin and thick laminated composite plates.

Table 5.18 Nondimensionalized maximum center displacements and vibration suppression time of CFRP cross-ply laminates under thermomechanical loading

Plate Thickness	Boundary Condition	\tilde{w}_{\max}	$t(\text{sec})$ at $\tilde{w}_{\max}/10$
$\frac{a}{h} = 10$	CCCC	0.4489	0.0300
	CCFF	0.6493	0.0990
	CCSS	0.4788	0.0315
	CFSS	1.2685	0.0565
	SSFF	1.7966	0.0525
	SSSS	1.1163	0.0240
$\frac{a}{h} = 100$	CCCC	0.2774	0.2000
	CCFF	0.3980	0.6920
	CCSS	0.3473	0.2210
	CFSS	0.7736	0.5000
	SSFF	1.2023	0.4970
	SSSS	0.7318	0.2200



(a)



(b)

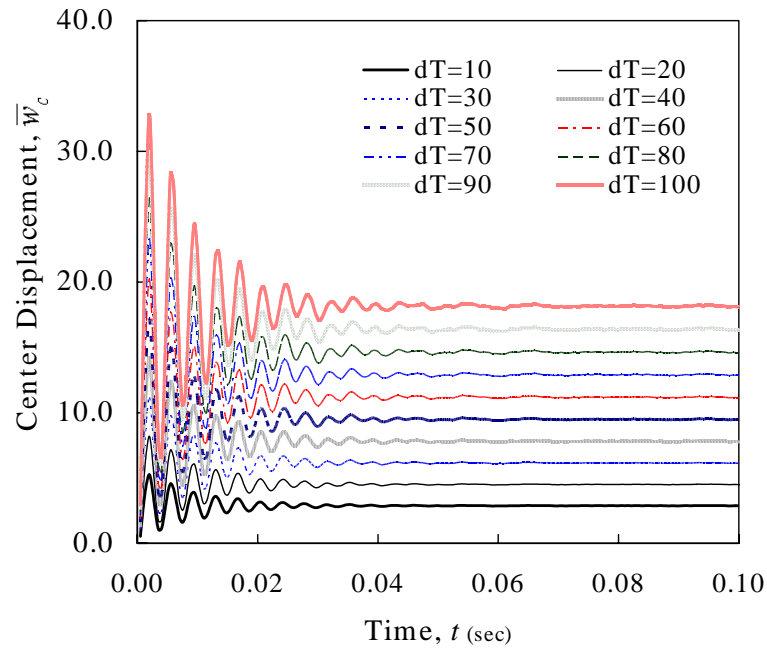
Figure 5.36 Effect of the boundary conditions on the transient behavior of the cross-ply laminates; (a) Thick laminate under thermomechanical load, (b) Thin laminate under thermomechanical load

5.4.3. Laminated Composite Shells under Thermomechanical Loads

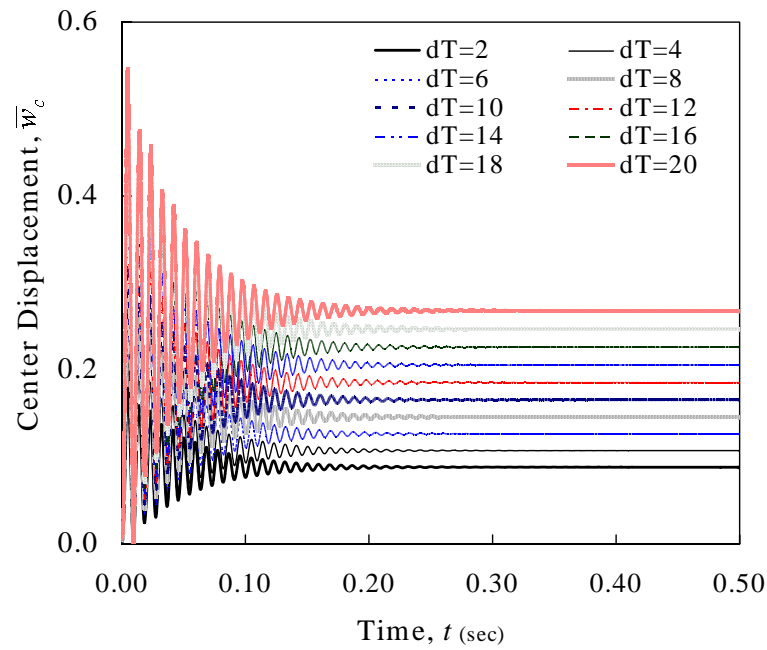
First, thermomechanical effect with different R_2/a value is studied. Nonlinear transient analysis of laminated composite shells under thermomechanical loadings is presented. The critical time 0.1 and 0.5 milliseconds are chosen for the thick ($a/h = 10$) and the thin ($a/h = 100$) shell laminates. The applied mechanical loadings are 10^4 for thick laminates and 10^3 for thin laminates. The thermal loading is applied in the same direction as the mechanical loading in laminated composite shell simulation. Figures 5.37 and 5.38 show the temperature effects on the deflection control of cross-ply cylindrical shell with different R_2/a value, 2, 200, respectively. The maximum deflection and the deflection suppression time are tabulated in Table 5.19 for different thermal increase. The deflection suppression characteristics of R_2/a effects are shown in Figure 5.39 for cylindrical and spherical thin shells. It is observed that the maximum deflection value increase with increasing thermal loading ΔT and takes more deflection suppression time with increasing R_2/a value in both thin and thick shells.

Figure 5.40 shows the effect of the shell types on the deflection suppression characteristics under thermomechanical load. Selected maximum deflection and deflection suppression time for each shell theory are tabulated in Table 5.20. Regardless of shell types, the effect of thermal load in the deflection suppression characteristics leads the increased maximum deflection and deflection suppression time.

The effect of boundary condition on the deflection suppression under thermomechanical loadings is shown in Figure 5.41. SSSS, CCCC, CCSS, CCFF and SSFF boundary conditions are considered with the selected ΔT and R_2/a . It is observed that the SSFF boundary condition gives the maximum deflection.

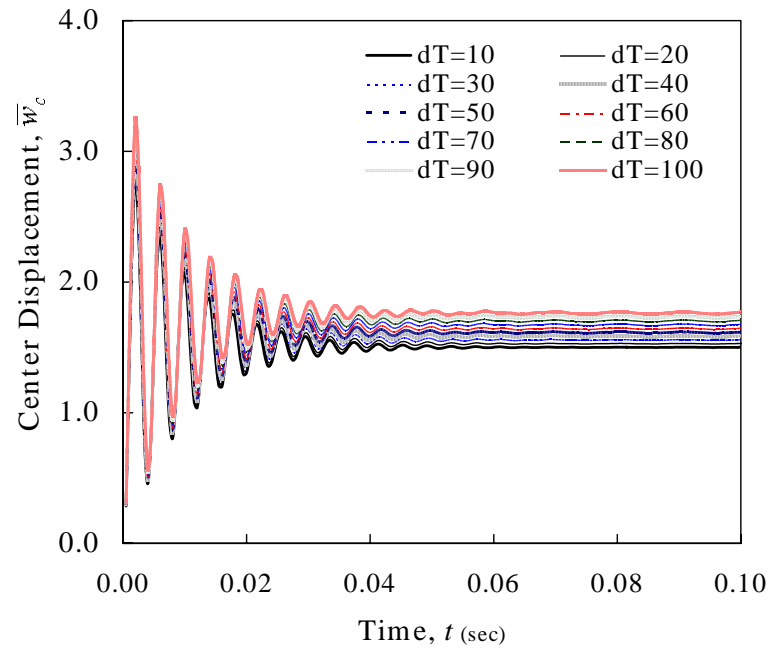


(a)

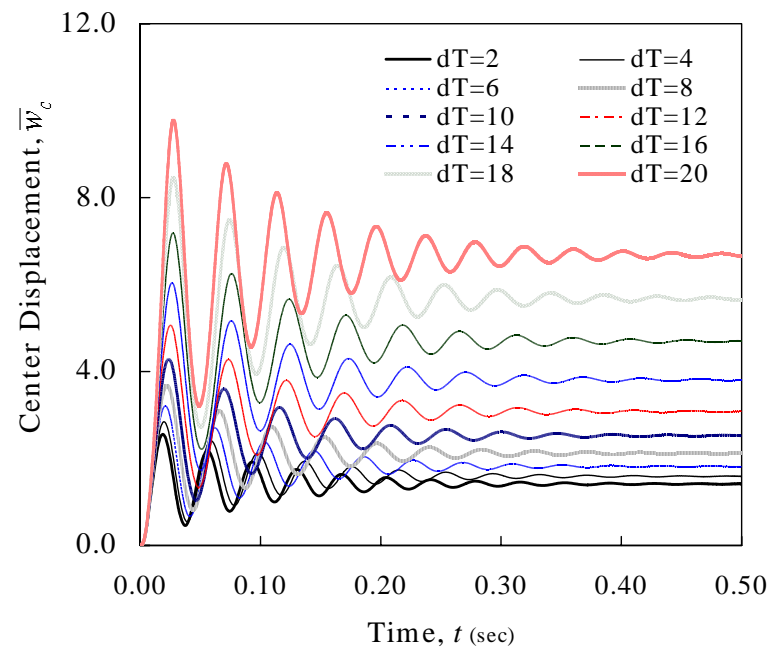


(b)

Figure 5.37 Temperature effect on nonlinear transient behavior of cross-ply cylindrical shell ($R_2/a=2$) under thermomechanical load: (a) Thick shell ($a/h=10$), (b) Thin shell ($a/h=100$)



(a)

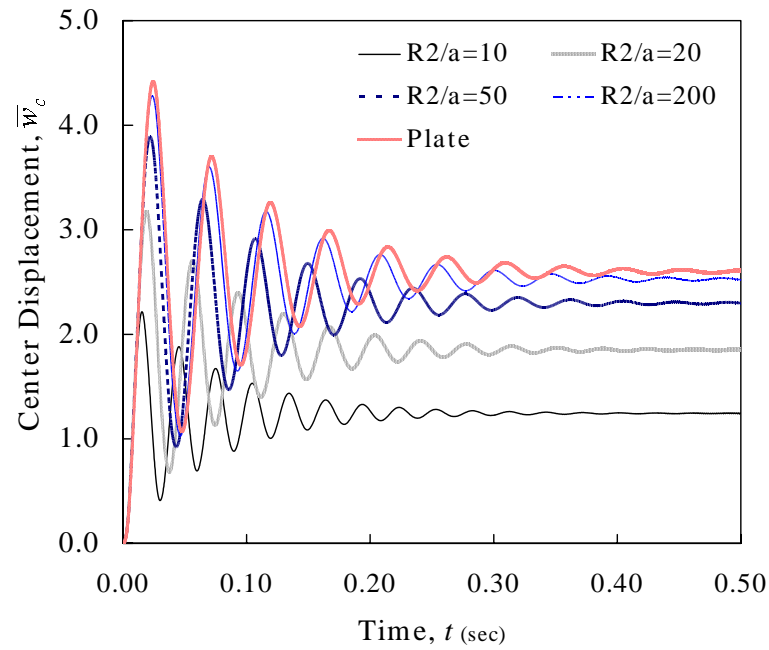


(b)

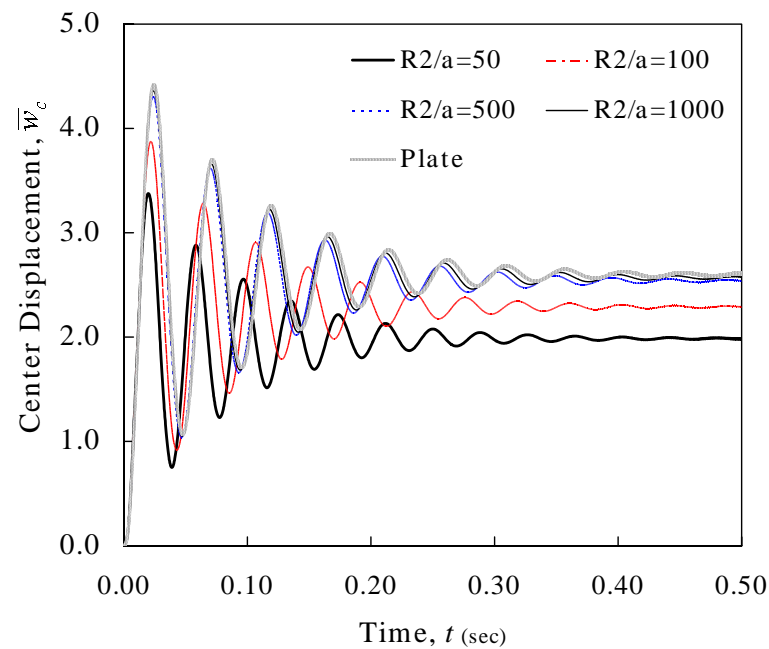
Figure 5.38 Temperature effect on nonlinear transient behavior of cross-ply cylindrical shell ($R_2/a=200$) under thermomechanical load: (a) Thick shell ($a/h=10$), (b) Thin shell ($a/h=100$)

Table 5.19 Maximum transverse deflection and vibration suppression time for the symmetric cross-ply cylindrical shells

Thickness	ΔT	$R_2/a = 2$		$R_2/a = 200$	
		\tilde{w}_{\max}	$t(\text{sec})$ at $\tilde{w}_{\max}/10$	\tilde{w}_{\max}	$t(\text{sec})$ at $\tilde{w}_{\max}/10$
Thin Shell $a/h = 100$	2	0.090926	0.105500	1.130600	0.207000
	4	0.110380	0.114500	1.246300	0.216500
	6	0.130000	0.114500	1.389800	0.229000
	8	0.151150	0.115000	1.543600	0.242500
	10	0.171970	0.115000	1.751000	0.255500
	12	0.192860	0.115500	1.975500	0.268000
	14	0.213850	0.115500	2.242000	0.272500
	16	0.234930	0.107000	2.475200	0.266500
	18	0.256120	0.107000	2.804500	0.297500
	20	0.277430	0.116500	3.125300	0.28100
Thick Shell $a/h = 10$	10	2.388200	0.024000	1.294900	0.025500
	20	3.698700	0.024500	1.316600	0.026000
	30	5.024100	0.028000	1.338300	0.026000
	40	6.364100	0.028000	1.360100	0.026000
	50	7.719700	0.028000	1.382000	0.026000
	60	9.089000	0.024500	1.403800	0.026000
	70	10.474000	0.024500	1.425700	0.026000
	80	11.873000	0.024500	1.447400	0.026000
	90	13.288000	0.028000	1.469200	0.026000
	100	14.717000	0.024500	1.490900	0.026000



(a)

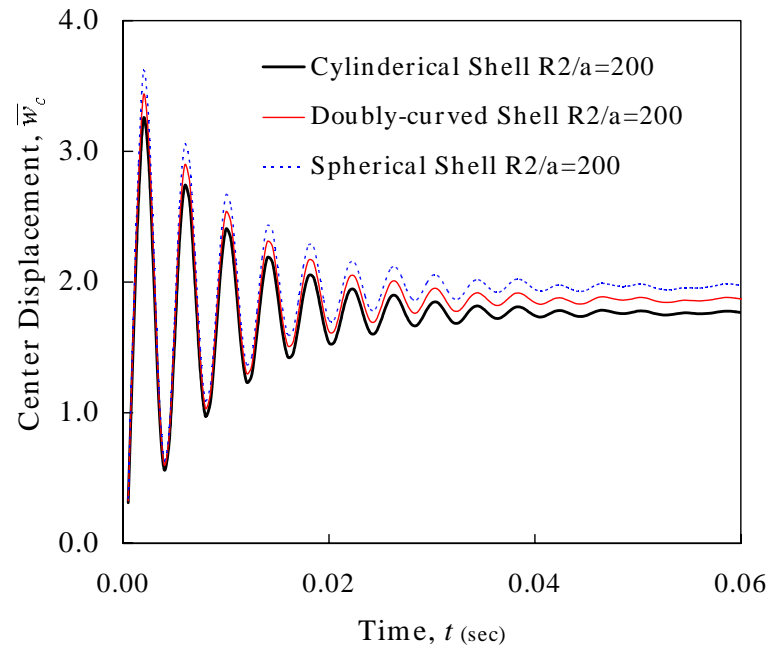


(b)

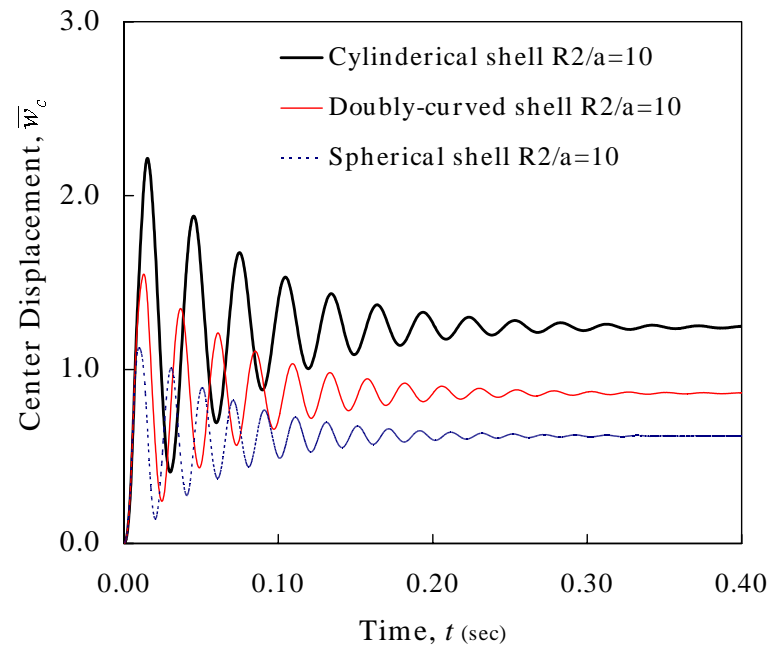
Figure 5.39 Effect of R_2/a on nonlinear transient behavior of cross-ply shell under thermomechanical load: (a) Cylindrical shell ($a/h=100$, $\Delta T=10^\circ C$), (b) Spherical shell ($a/h=100$, $\Delta T=10^\circ C$)

Table 5.20 Nondimensionalized maximum center displacements and vibration suppression time of cross-ply laminates for different shell types

Thickness	Shell Type	R_2/a	ΔT	\tilde{w}_{\max}	$t(\text{sec})$ at $\tilde{w}_{\max}/10$
$\frac{a}{h}=10$	Cylindrical	10	0	1.262900	0.025500
			100	4.381400	0.026000
	Spherical		0	1.237100	0.025000
			100	7.373700	0.026000
	Doubly curved		0	1.251600	0.025500
			100	5.876900	0.026000
$\frac{a}{h}=100$	Cylindrical	100	0	0.611730	0.176000
			10	1.709800	0.248500
	Spherical		0	0.312520	0.164000
			10	1.586700	0.235500
	Doubly curved		0	0.424780	0.172000
			10	1.643300	0.240500

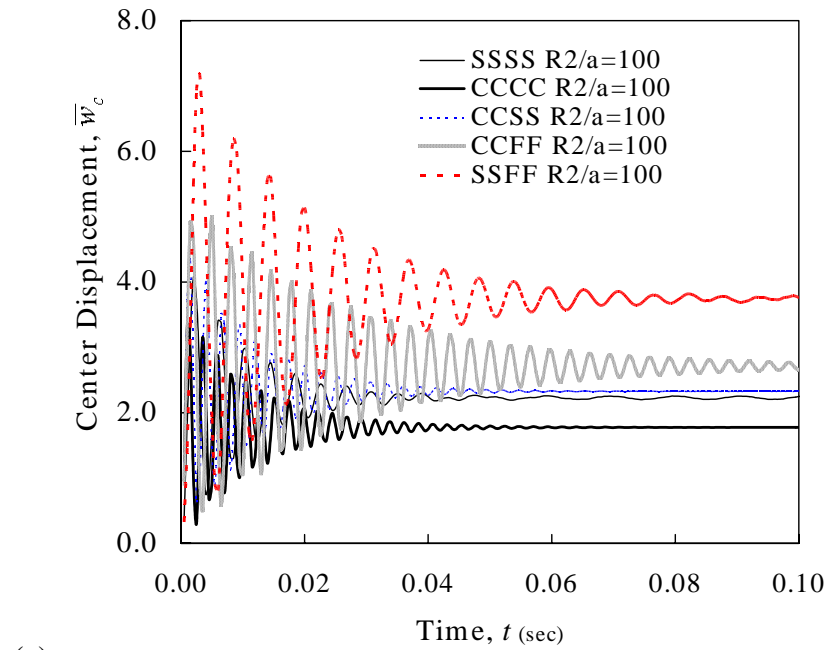


(a)

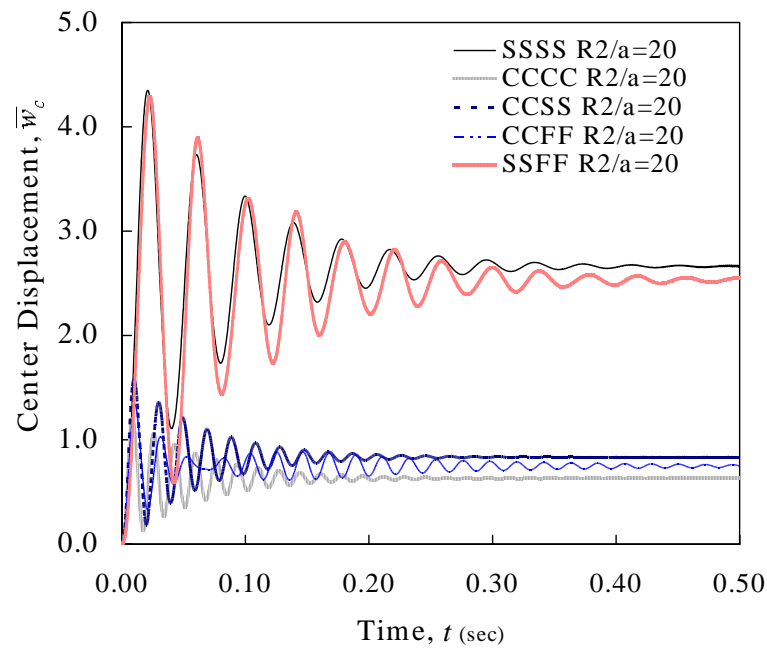


(b)

Figure 5.40 Effect of shell types on nonlinear transient behavior of cross-ply shell under thermomechanical load: (a) Thick shell ($a/h=10$, $\Delta T=100^\circ C$), (b) Thin shell ($a/h=100$, $\Delta T=10^\circ C$)



(a)



(b)

Figure 5.41 Effect of boundary conditions on nonlinear transient behavior of cross-ply shell under thermomechanical load: (a) Thick shell ($a/h=10$, $\Delta T=150^\circ C$, $R_2/a=100$), (b) Thin shell ($a/h=100$, $\Delta T=10^\circ C$, $R_2/a=20$)

6. CONCLUSIONS

6.1. Concluding Remarks

Theoretical formulations, analytical solutions for the linear case and finite element analysis results for laminated composite plate and shell structures with smart material laminae are presented in the study. A unified third-order shear deformation formulation that includes the classical plate theory and the first-order shear deformation theory as special cases is used to study vibration/deflection suppression characteristics. The *von Kármán* type geometric nonlinearity is accounted for in formulations of laminated composite plates. Third-order shear deformation theory based on Donnell and Sanders nonlinear shell kinematics is chosen for the laminated composite shell formulations.

The smart material used in this study to achieve damping of transverse deflection is the Terfenol-D magnetostrictive material, although in principle any other actuating material can be used. The simple control algorithm, a negative velocity feedback control, where the feedback amplitude varies by the negative velocity is used to control the structural system. The constant control gain is assumed in this study.

The exact solution of the linear equations of motion is based on the Navier solution procedure for the simply supported boundary condition. Displacement finite element formulation that considers the geometric nonlinearity and thermal loading through the third-order shear deformation theory is presented. The conforming element which has eight degrees of freedom, $(u_0, v_0, w_0, w_{0,x}, w_{0,y}, w_{0,xy}, \phi_x, \phi_y)$, per node is used to develop the finite element model.

Newton-Raphson iteration method which has the symmetric tangent stiffness matrix for all structural problems is used to solve the nonlinear problem. Newmark's time integration method, the constant average acceleration scheme, is selected to determine the transient response.

A number of parametric studies are carried out to understand the damping characteristics of laminated composites with embedded smart material layers. The effect of the different thickness, loading condition, material properties, boundary conditions, R_2/a and so on are presented. The observations are summarized below.

From the analytical result, it can be seen that the vibration suppression time decreases very rapidly as mode number increases. This is because the amplitude of vibration that has to be suppressed decreases as the mode number increases.

It is observed that the damping coefficient $-\alpha_d$ increases with the distance between the smart layer and mid-plane of the structures. This is because as the effect of the moment applied by the actuation of the smart material on the structure is more as the smart material is moved away from the mid-plane section. Thus, the vibration suppression time decreases as the smart material layers are moved from the mid-plane.

The effect of using different values of the feedback coefficient has also been studied. It is observed that for a lower value of the feedback coefficient the time taken to suppress the vibration is longer. This is because as the amount of actuation done by the smart material layer onto the laminated composites becomes less as the feedback value is less.

Use of quarter or full finite element models is validated first. It is found that for antisymmetric cross-ply, angle-ply, and general angle-ply laminates and symmetric cross-ply laminates with simply supported boundary conditions, a quadrant model of the plate and shell structures with proper symmetry boundary conditions may be used to reduce the computational effort.

It is observed that the CLPT theory gives higher frequencies of vibration than shear deformation theories. This is expected, as the CLPT theory renders the plate stiffer compared to the other two theories, FSDT and TSDT.

It is observed that Donnell shell theory gives higher frequency and damping coefficients than Sanders shell theory. As total thickness of shell structures is increasing

and R_2/a value is decreasing, the numerical differences in eigenvalue and deflection become larger. However, when one considers the vibration control behavior it is hard to see the differences.

The effect of R_2/a value in the laminated composite shell structure on the deflection suppression characteristics is studied. It is found that it takes more deflection suppression time with increasing R_2/a value in both thin and thick shells. It is observed that the spherical shell has the largest damping coefficient and frequency and the cylindrical shell has the smallest damping coefficient and frequency from the eigenvalue analysis. It is also observed that the spherical shell has the biggest deflection suppression and smallest maximum deflection and the cylindrical shell has the smallest deflection suppression and largest maximum deflection. It is because of the fact that spherical shell has the smallest R_1 and doubly curved shell (in this study $R_1 = 2R_2$), and cylindrical shell has the largest R_1 ($R_1 = \infty$).

The behavior of laminated composites with embedded magnetostrictive layers for different kinds of structural material has been studied. CFRP, Gr-Ep (AS), Gl-Ep and Br-Ep are the elastic materials used in this study. It is found that the suppression characteristics are similar for elastic materials having similar E_1/E_2 ratios. It is also observed that Gl-Ep shows the minimum vibration suppression time.

The nonlinear thermal effects are also investigated for various simulation conditions. The amplitude and period of the center deflections decrease with increasing thermal loading for all cases.

6.2. Recommendations for Future Work

The result of this study is a general nonlinear formulation and analytical and finite element solutions for the laminated composite plate and shell structures with linear constitutive relations of smart material.

As a possible continuation of this work is development of nonlinear constitutive relations for the magnetostrictive material followed by computer implementation of nonlinear finite element analysis of laminated composite plate/shell structures including the nonlinear constitutive relations of smart materials. Also, studies relating to the placement of smart material patches, instead of full layers, thereby achieving discrete actuation could be performed.

REFERENCES

- Ambartsumyan, S.A. (1964), *Theory of Anisotropic Shells*, WA Benjamin, Inc., New York.
- Anders, W.S., Rogers, C.A., and Fuller, C.R. (1991), "Control of sound radiation from shape memory alloy hybrid composite panels by adaptive alternate resonance tuning," *American Institute of Aeronautics and Astronautics Journal*, 29, 365-376.
- Ang, K.K., Reddy, J.N., and Wang, C.M. (2000), "Displacement control of timoshenko beams via induced strain actuators," *Smart Materials and Structures*, 9, 981-984.
- Anjanappa, M., and Bi, J. (1993), "Modelling, design and control of embedded Terfenol-D actuator," *Proceedings of SPIE, Smart Structures and Intelligent Systems*, Albuquerque, NM., 1917, 908-918.
- Anjanappa, M., and Bi, J. (1994a), "A theoretical and experimental study of magnetostrictive mini actuators," *Smart Materials and Structures*, 1, 83-91.
- Anjanappa, M., and Bi, J. (1994b), "Magnetostrictive mini actuators for smart structural application," *Smart Materials and Structures*, 3, 383-390.
- Anjanappa, M., and Wu, Y. (1996), "Modeling of embedded magnetostrictive particulate actuators," *Proceedings of SPIE, Smart Structures and Materials*, San Diego, CA., 2717, 517-527.
- Armstrong, W.D. (2000), "Nonlinear behavior of magnetostrictive particle actuated composite materials," *Journal of Applied Physics*, 87, 3027-3031.
- Bailey, T., and Hubbard, J.E. (1985), "Distributed piezoelectric polymer active vibration control of a cantilever beam," *American Institute of Aeronautics and Astronautics Journal*, 23, 605-611.
- Balas, M.J. (1979), "Direct output feedback control of large space structures," *Journal of the Astronautical Sciences*, 27, 157-180.
- Baumhauer, J.C., and Tiersten, H.F. (1973), "Nonlinear electroelastic equations for small fields superposed on a bias," *Journal of Acoustical Society of America*, 54, 1017-1034.
- Baz, A., Imam, K., and McCoy, J. (1990), "The dynamics of helical shape memory actuators," *Journal of Intelligent Material Systems and Structures*, 1, 105-133.
- Bert, C.W. (1980), "Analysis of shells." *Analysis & Performance of Composites* (edited by Broutman, L.J.), Wiley, New York.

- Bhattacharya, B., Vidyashankar, B.R. , Patsias, S., and Tomlinson, G.R. (2000), "Active and passive vibration control of flexible structures using a combination of magnetostrictive and ferro-magnetic alloys," *Proceedings of SPIE, Smart Structures and Materials*, Glasgow, U.K., 4037, 204-214.
- Bishop, R.B., and Dorf, R.C. (2001), *Modern Control System*, 9th Edition, Prentice Hall, Upper Saddle River, NJ.
- Bryant, M.D., Fernandez, B., and Wang, N. (1993), "Active vibration control in structures using magnetostrictive Terfenol with feedback and/or neural network controllers," *Journal of Intelligent Material Systems and Structures*, 4, 484-489.
- Carman, G. P., and Mitrovic, M. (1995), "Nonlinear constitutive relations for magnetostrictive materials with applications to 1-D problems," *Journal of Intelligent Material System and Structures*, 6, 673-683.
- Choi, Y., Sprecher, A.F., and Conrad, H. (1990), "Vibration characteristics of a composite beam containing electrorheological fluid," *Journal of Intelligent Material Systems and Structures*, 1, 91-104.
- Chung L.I., Lin C.C., and Chu S.Y. (1993), "Optimal direct output feedback of structural control," *Journal of Engineering Mechanics, ASME*, 119, 2157-2173.
- Clark, A.E. (1980), *Ferromagnetic Material*, 1, North-Holland Publishing Company, New York.
- Crawley, E.F., and Luis, J.D. (1987), "Use of piezoelectric actuators and elements of intelligent structure," *American Institute of Aeronautics and Astronautics Journal*, 25, 1373-1385.
- Cross, L.E., and Jang, S.J. (1988), "Electrostrictive materials." *Electronic Ceramics: Properties, Devices, and Applications* (edited by Levinson, L.M.), Marcel Dekker, Inc., New York.
- Dapino, M.J., Flatau, A.B., and Calkins, F.T. (1997) "Statistical analysis of Terfenol-D materials properties", *Proceedings of SPIE, Smart Structures and Materials*, San Diego, CA., 3041, 256-267.
- Dong, S.B., Pister, K.S., and Taylor, R.L. (1962), "On the theory of laminated anisotropic shells and plates," *Journal of Aerospace Science*, 29, 969-975.
- Dong, S.B., and Tso, K.W. (1972), "On a laminated orthotropic shell theory including transverse shear deformation," *Journal of Applied Mechanics*, 39, 1091-1096.

Donnell, L.N. (1935), "Stability of thin-walled tubes under torsion," *NACA Report 479*, NACA Langley Memorial Aeronautical Laboratory, Langley Field, VA.

Duenas, T.A., and Carman, G.P. (2000), "Large magnetostrictive response of Terfenol-D resin composite," *Journal of Applied Physics*, 87(9), 4696-4701.

Eda, H., Kobayashi, T., Nakamura, H., and Akiyama, T. (1995), "Giant magnetostriction compounds with structure textured by resin bound on giant magnetostriction fine powder in magnetic field and its actuator," *Transactions of Japanese Society for Mechanical Engineering, Series C*, 61, 168-217.

Flatau, A.B., Dapino, M.J., and Calkins, F.T. (1998), "High bandwidth tunability in smart absorber," *Proceedings of SPIE, Smart Structures and Materials*, San Diego, CA., 3327, 463-473.

Franklin G.F., Powell J.D., and Emami-Naeini, A. (2000), *Feedback Control of Dynamic Systems*, Prentice Hall, Upper Saddle River, NJ.

Gandhi, M.V., and Thompson, B.S. (1992), *Smart Materials and Structures*, Chapman & Hall, London.

Goodfriend, M.J., and Shoop, K.M. (1992), "Adaptive characteristics of the magnetostrictive alloy, Terfenol-D, for active vibration control," *Journal of Intelligent Material Systems and Structures*, 3, 245-254.

Gulati, S.T., and Essenberg, F. (1967), "Effects of anisotropy in axisymmetric cylindrical shells," *Journal of Applied Mechanics*, 34, 659-666.

Hudson, J., Busbridge, S.C., and Piercy, A.R. (1999), "Magnetomechanical properties of epoxy-bonded Terfenol-D composites," *Ferroelectrics*, 228, 283-295.

Hudson, J., Busbridge, S.C., and Piercy, A.R. (2000), "Dynamic magnetomechanical properties of epoxy-bonded composites," *Sensors and Actuators A-Physical*, 81, 294-296.

Institute of Electrical and Electronics Engineers (IEEE), Standard 319 (1976), *IEEE Standard on Magnetostrictive Materials; Piezo-magnetic Nomenclature*, New York.

Institute of Electrical and Electronics Engineers (IEEE), Standard 319 (1990), *IEEE Standard on Magnetostrictive Materials; Piezo-magnetic Nomenclature (Revision of IEEE Std 319-1971)*, New York.

Jones, L., and Garcia, E. (1996), "Self-sensing magnetostrictive actuator for vibration suppression," *Journal of Guidance Control and Dynamics*, 19(3), 713-715.

Joshi, S.P. (1991), "Nonlinear constitutive relations for piezoceramic materials." *Proceedings of the ADPA/AIAA/ASME/SPIE Conference on Active Materials and Adaptive Structures* (edited by Knowles, G.J.), Alexandria, VA., 217-222.

Kannan, K.S., and Dasgupta, A. (1997), "A nonlinear galerkin finite element theory for modeling magnetostrictive smart structures," *Smart Materials and Structures*, 6, 341-350.

Khdeir, A.A., and Reddy, J.N. (1999), "Free vibration of laminated composite plates using second-order shear deformation theory," *Computers & Structures*, 71, 617-626.

Kleinke, D.K., and Unas, H.M. (1994a), "Magnetostrictive force sensor," *Review of Scientific Instruments, American Institute of Physics*, 64, 1699-1710.

Kleinke, D.K., and Unas, H.M. (1994b), "Magnetostrictive strain sensor," *Review of Scientific Instruments, American Institute of Physics*, 64, 2361-2367.

Knops, R.J. (1963), "Two-dimensional electrostriction," *Quarterly Journal of Mechanics Applied Mathematics*, 16, 377-388.

Koiter, W.T. (1960), *The Theory of Thin Elastic Shells*, North-Holland, Amsterdam.

Koiter, W.T. (1966), "On the nonlinear theory of thin elastic shells," *Proceedings Koninklijke Nederlandse Akademie van Wetenschappen*, B69, Amsterdam, 1-54.

Kraus, H. (1967), *Thin Elastic Shells*, John Wiley, New York.

Krishna Murty, A.V., Anjanappa, M., and Wu, Y-F. (1997), "The use of magnetostrictive particle actuators for vibration attenuation of flexible beams," *Journal of Sound and Vibration*, 206, 133-149.

Krishna Murty, A.V., Anjanappa, M., Wu, Y-F., Bhattacharya, B., and Bhat, M.S. (1998), "Vibration suppression of laminated composite beams using embedded magnetostrictive layers," *Journal of the Institution of Engineers (India)*, 78, 38-44.

Lee, S.J., Reddy, J.N., and Rostam-Abadi, F. (2004), "Transient analysis of laminated composite plates with embedded smart-material layers," *Finite Elements in Analysis and Design*, 40, 463-483.

Librescu, L., Khdeir, A.A., and Frederick, D. (1989), "A shear deformation theory of laminated composite shallow shell-type panels and their response analysis I: free vibration and buckling," *Acta Mechanica*, 76, 1-33.

Lim, S.H., Kim, S.R., Kang, S.Y., Park, J.K., Nam, J.T., and Son, D. (1999), "Magnetostrictive properties of polymer-bonded Terfenol-D composites," *Journal of Magnetism and Magnetic Materials*, 191, 113-121.

Lowy, R. G. (1997), "Recent developments in smart structures with aeronautical applications," *Smart Materials and Structures*, 6, R11-R42.

Maugin, G.A. (1988), *Continuum Mechanics of Electromagnetic Solids*, North-Holland Series in Applied Mathematics and Mechanics, North-Holland, Amsterdam.

Naghdi, P.M. (1956), "A survey of recent progress in the theory of elastic shells," *Applied Mechanics Reviews*, 91(9), 365-368.

Nelson, D.F. (1978), "Theory of nonlinear electroacoustics of dielectric, piezoelectric, and pyroelectric crystals," *Journal of Acoustical Society of America*, 63, 1738-1748.

Newnham, R.E. (1993), "Ferroelectric sensors and actuators: smart ceramics." *Ferroelectric Ceramics* (edited by Setter, N. and Colla, E. L.), Springer Verlag, New York.

Pradhan, S.C., Ng, T.Y., Lam, K.Y., and Reddy, J.N. (2001), "Control of composite laminated plates using magnetostrictive layers," *Smart Materials and Structures*, 10(4), 657-667.

Pratt, J.R., and Flatau, A.B. (1995), "Development and analysis of self-sensing magnetostrictive actuator design," *Journal of Intelligent Material Systems and Structures*, 6, 639-648.

Pulliam, W., McKnight, G., and Carman, G. (2002), "Recent advances in magnetostrictive particulate composite technology," *Proceedings of SPIE, Smart Structures and Materials*, San Diego, CA., 4698, 271-281.

Reddy, J.N. (1983), "Geometrically nonlinear transient analysis of laminated composite plates," *American Institute of Aeronautics and Astronautics Journal*, 21(4), 621-629.

Reddy, J.N. (1984a), "A refined nonlinear theory of plates with transverse shear deformation," *International Journal of Solids and Structures*, 20, 881-896.

Reddy, J.N. (1984b), "A simple higher-order theory for laminated composite plates," *Journal of Applied Mechanics*, 51, 745-752.

Reddy, J.N. (1984c), "Exact solutions of moderately thick laminated shells," *Journal of Engineering Mechanics*, ASCE, 110, 794-809.

Reddy, J.N. (1993), *An Introduction to the Finite Element Method*, Second Edition, McGraw-Hill, New York.

Reddy, J.N. (1997), *Mechanics of Laminated Composite Plates: Theory and Analysis*, CRC Press, Boca Raton, FL.

Reddy, J.N. (1999a), *Theory and Analysis of Elastic Plates*, Taylor & Francis, Philadelphia, PA.

Reddy, J.N. (1999b), "On laminated composite plates with integrated sensors and actuators," *Engineering Structures*, 21, 568-593.

Reddy, J.N. (2002), *Energy Principles and Variational Methods in Applied Mechanics*, Second Edition, John Wiley & Sons, New York.

Reddy, J.N. (2004a), *An Introduction to Nonlinear Finite Element Analysis*, Oxford University Press, Oxford, U.K.

Reddy, J.N. (2004b), *Mechanics of Laminated Composite Plates and Shells: Theory and Analysis*, Second Edition, CRC Press, Boca Raton, FL.

Reddy, J.N., and Barbosa, J.A. (2000), "Vibration suppression of laminated composite beams," *Smart Materials and Structures*, 9, 49-58.

Reddy, J.N., and Chao, W.C. (1981), "A comparison of closed-form and finite element solutions of thick laminated anisotropic rectangular plates," *Nuclear Engineering and Design*, 64, 291-301.

Reddy, J.N., and Liu, C.F. (1985), "A higher-order shear deformation theory for laminated elastic shells," *International Journal of Engineering Science*, 23, 319-330.

Sanders Jr., J.L. (1959), "An Improved First Approximation Theory of Thin Shells," *NASA Technical Report R24*, NASA Langley Research Center, Hampton, VA.

Sanders Jr., J.L. (1963), "Nonlinear theories for thin shells," *Quarterly of Applied Mathematics*, 21, 21-36.

Smith, R.C. (1998), "A nonlinear optimal control method for magnetostrictive actuators," *Journal of Intelligent Material Systems and Structures*, 9, 468-486.

Srinivasan, A.V., and McFarland, D.M. (2001), *Smart Structures*, Cambridge University Press, Cambridge, U.K.

Tiersten, H.F. (1971), "On the nonlinear equations of thermoelectroelasticity," *International Journal of Engineering Science*, 9, 587-604.

Tiersten, H.F. (1993), "Electroelastic equations for electroded thin plates subject to large driving voltages," *Journal of Applied Physics*, 74, 3389-3393.

Toupin, R.A. (1956), "The elastic dielectric," *Archives of Rational Mechanics and Analysis*, 5, 849-915.

Tzou, H.S., Bao, Y., and Ye, R. (1994), "Theory on nonlinear piezothermoelastic shell laminates," *Proceedings of SPIE, Smart Structures and Materials*, Orlando, FL., 2190, 206-216.

Uchino, K. (1986), "Electrostrictive actuators: materials and applications," *Ceramic Bulletin*, 65, 647-652.

Whitney, J.M. (1970), "The effect of boundary condition on the response of laminated composites," *Journal of Composite Materials*, 4, 192-203.

Whitney, J.M., and Leissa, A.W. (1969), "Analysis of heterogeneous anisotropic plates," *Journal of Applied Mechanics*, 36, 969-975.

Whitney, J.M., and Pagano, N.J. (1970), "Shear deformation in heterogeneous anisotropic plates," *Journal of Applied Mechanics*, 37, 1031-1036.

Whitney, J.M., and Sun, C.T. (1974), "A refined theory for laminated anisotropic cylindrical shells," *Journal of Applied Mechanics*, 41, 471-476.

Yellin, J.M., and Shen, I.Y. (1996), "Integration and design of piezoelectric elements in intelligent structures," *Journal of Intelligent Material Systems and Structures*, 6, 733-743.

Zukas, J.A., and Vinson, J.R. (1971), "Laminated transversely isotropic cylindrical shells," *Journal of Applied Mechanics*, 38, 400-407.

APPENDIX A

EULER-LAGRANGE EQUATIONS OF TSDT SANDERS SHELL THEORY IN TERMS OF DISPLACEMENTS

A.1 Equation of motion by TSDT sanders shell theory for δu

$$\begin{aligned}
& A_{11} \left(\frac{\partial^2 u_0}{\partial X_1^2} + \frac{1}{R_1} \frac{\partial w_0}{\partial X_1} + \frac{\partial w_0}{\partial X_1} \frac{\partial^2 w_0}{\partial X_1^2} \right) + A_{12} \left(\frac{\partial^2 v_0}{\partial X_1 \partial X_2} + \frac{1}{R_2} \frac{\partial w_0}{\partial X_1} + \frac{\partial w_0}{\partial X_2} \frac{\partial^2 w_0}{\partial X_1 \partial X_2} \right) + A_{16} \left(\frac{\partial^2 v_0}{\partial X_1^2} + \frac{\partial^2 u_0}{\partial X_1 \partial X_2} + \right. \\
& \left. \frac{\partial^2 w_0}{\partial X_1^2} \frac{\partial w_0}{\partial X_2} + \frac{\partial w_0}{\partial X_1} \frac{\partial^2 w_0}{\partial X_1 \partial X_2} \right) + B_{11} \frac{\partial^2 \phi_1}{\partial X_1^2} + B_{12} \frac{\partial^2 \phi_2}{\partial X_1 \partial X_2} + B_{16} \left(\frac{\partial^2 \phi_2}{\partial X_1^2} + \frac{\partial^2 \phi_1}{\partial X_1 \partial X_2} \right) - c_1 E_{11} \left(\frac{\partial^2 \phi_1}{\partial X_1^2} + \frac{\partial^3 w_0}{\partial X_1^3} - \right. \\
& \left. \frac{1}{R_1} \frac{\partial^2 u_0}{\partial X_1^2} \right) - c_1 E_{12} \left(\frac{\partial^2 \phi_2}{\partial X_1 \partial X_2} + \frac{\partial^3 w_0}{\partial X_1 \partial X_2^2} - \frac{1}{R_2} \frac{\partial^2 v_0}{\partial X_1 \partial X_2} \right) - c_1 E_{16} \left(\frac{\partial^2 \phi_2}{\partial X_1^2} + \frac{\partial^2 \phi_1}{\partial X_1 \partial X_2} + 2 \frac{\partial^3 w_0}{\partial X_1^2 \partial X_2} - \frac{1}{R_2} \frac{\partial^2 v_0}{\partial X_1^2} \right. \\
& \left. - \frac{1}{R_1} \frac{\partial^2 u_0}{\partial X_1 \partial X_2} \right) + A_{16} \left(\frac{\partial^2 u_0}{\partial X_2 \partial X_1} + \frac{1}{R_1} \frac{\partial w_0}{\partial X_2} + \frac{\partial w_0}{\partial X_1} \frac{\partial^2 w_0}{\partial X_2 \partial X_1} \right) + A_{26} \left(\frac{\partial^2 v_0}{\partial X_2^2} + \frac{1}{R_2} \frac{\partial w_0}{\partial X_2} + \frac{\partial w_0}{\partial X_2} \frac{\partial^2 w_0}{\partial X_2^2} \right) + \\
& A_{66} \left(\frac{\partial^2 v_0}{\partial X_1 \partial X_2} + \frac{\partial^2 u_0}{\partial X_2^2} + \frac{\partial^2 w_0}{\partial X_2 \partial X_1} \frac{\partial w_0}{\partial X_2} + \frac{\partial w_0}{\partial X_1} \frac{\partial^2 w_0}{\partial X_2^2} \right) + B_{16} \frac{\partial^2 \phi_1}{\partial X_2 \partial X_1} + B_{26} \frac{\partial^2 \phi_2}{\partial X_2^2} + B_{66} \left(\frac{\partial^2 \phi_2}{\partial X_2 \partial X_1} + \frac{\partial^2 \phi_1}{\partial X_2^2} \right) - \\
& c_1 E_{16} \left(\frac{\partial^2 \phi_1}{\partial X_2 \partial X_1} + \frac{\partial^3 w_0}{\partial X_2 \partial X_1^2} - \frac{1}{R_1} \frac{\partial^2 u_0}{\partial X_1 \partial X_2} \right) - c_1 E_{26} \left(\frac{\partial^2 \phi_2}{\partial X_2^2} + \frac{\partial^3 w_0}{\partial X_2^3} - \frac{1}{R_2} \frac{\partial^2 v_0}{\partial X_2^2} \right) - c_1 E_{66} \left(\frac{\partial^2 \phi_2}{\partial X_2 \partial X_1} + \frac{\partial^2 \phi_1}{\partial X_2^2} + \right. \\
& \left. 2 \frac{\partial^3 w_0}{\partial X_1 \partial X_2^2} - \frac{1}{R_2} \frac{\partial^2 v_0}{\partial X_1 \partial X_2} - \frac{1}{R_1} \frac{\partial^2 u_0}{\partial X_2^2} \right) + \frac{1}{R_1} \left[\hat{A}_{45} \left(\phi_2 + \frac{\partial w_0}{\partial X_2} - \frac{v_0}{R_2} \right) + \hat{A}_{55} \left(\phi_1 + \frac{\partial w_0}{\partial X_1} - \frac{u_0}{R_1} \right) \right] + \frac{c_1}{R_1} [E_{11} \\
& \left(\frac{\partial^2 u_0}{\partial X_1^2} + \frac{1}{R_1} \frac{\partial w_0}{\partial X_1} + \frac{\partial w_0}{\partial X_1} \frac{\partial^2 w_0}{\partial X_1^2} \right) + E_{12} \left(\frac{\partial^2 v_0}{\partial X_1 \partial X_1} + \frac{1}{R_2} \frac{\partial w_0}{\partial X_1} + \frac{\partial w_0}{\partial X_2} \frac{\partial^2 w_0}{\partial X_1 \partial X_2} \right) + E_{16} \left(\frac{\partial^2 v_0}{\partial X_1^2} + \frac{\partial^2 u_0}{\partial X_1 \partial X_2} + \right. \\
& \left. \frac{\partial^2 w_0}{\partial X_1^2} \frac{\partial w_0}{\partial X_2} + \frac{\partial w_0}{\partial X_1} \frac{\partial^2 w_0}{\partial X_1 \partial X_2} \right) + F_{11} \frac{\partial^2 \phi_1}{\partial X_1^2} + F_{12} \frac{\partial^2 \phi_2}{\partial X_1 \partial X_2} + F_{16} \left(\frac{\partial^2 \phi_2}{\partial X_1^2} + \frac{\partial^2 \phi_1}{\partial X_1 \partial X_2} \right) - c_1 H_{11} \left(\frac{\partial^2 \phi_1}{\partial X_1^2} + \frac{\partial^3 w_0}{\partial X_1^3} - \right. \\
& \left. \frac{1}{R_1} \frac{\partial^2 u_0}{\partial X_1^2} \right) - c_1 H_{12} \left(\frac{\partial^2 \phi_2}{\partial X_1 \partial X_2} + \frac{\partial^3 w_0}{\partial X_1 \partial X_2^2} - \frac{1}{R_2} \frac{\partial^2 v_0}{\partial X_1 \partial X_2} \right) - c_1 H_{16} \left(\frac{\partial^2 \phi_2}{\partial X_1^2} + \frac{\partial^2 \phi_1}{\partial X_1 \partial X_2} + 2 \frac{\partial^3 w_0}{\partial X_1^2 \partial X_2} - \frac{1}{R_2} \frac{\partial^2 v_0}{\partial X_1^2} \right. \\
& \left. - \frac{1}{R_1} \frac{\partial^2 u_0}{\partial X_1 \partial X_2} \right) + E_{16} \left(\frac{\partial^2 u_0}{\partial X_2 \partial X_1} + \frac{1}{R_1} \frac{\partial w_0}{\partial X_2} + \frac{\partial w_0}{\partial X_1} \frac{\partial^2 w_0}{\partial X_2 \partial X_1} \right) + E_{26} \left(\frac{\partial^2 v_0}{\partial X_2^2} + \frac{1}{R_2} \frac{\partial w_0}{\partial X_2} + \frac{\partial w_0}{\partial X_2} \frac{\partial^2 w_0}{\partial X_2^2} \right) + E_{66} \\
& \left(\frac{\partial^2 v_0}{\partial X_1 \partial X_2} + \frac{\partial^2 u_0}{\partial X_2^2} + \frac{\partial^2 w_0}{\partial X_2 \partial X_1} \frac{\partial w_0}{\partial X_2} + \frac{\partial w_0}{\partial X_1} \frac{\partial^2 w_0}{\partial X_2^2} \right) + F_{16} \frac{\partial^2 \phi_1}{\partial X_2 \partial X_1} + F_{26} \frac{\partial^2 \phi_2}{\partial X_2^2} + F_{66} \left(\frac{\partial^2 \phi_2}{\partial X_2 \partial X_1} + \frac{\partial^2 \phi_1}{\partial X_2^2} \right) - c_1 H_{16} \\
& \left(\frac{\partial^2 \phi_1}{\partial X_2 \partial X_1} + \frac{\partial^3 w_0}{\partial X_2 \partial X_1^2} - \frac{1}{R_1} \frac{\partial^2 u_0}{\partial X_1 \partial X_2} \right) - c_1 H_{26} \left(\frac{\partial^2 \phi_2}{\partial X_2^2} + \frac{\partial^3 w_0}{\partial X_2^3} - \frac{1}{R_2} \frac{\partial^2 v_0}{\partial X_2^2} \right) - c_1 H_{66} \left(\frac{\partial^2 \phi_2}{\partial X_2 \partial X_1} + \frac{\partial^2 \phi_1}{\partial X_2^2} + 2 \right. \\
& \left. \frac{\partial^3 w_0}{\partial X_1 \partial X_2^2} - \frac{1}{R_2} \frac{\partial^2 v_0}{\partial X_1 \partial X_2} - \frac{1}{R_1} \frac{\partial^2 u_0}{\partial X_2^2} \right) \left] - \left(\tilde{A}_{31}^M + \frac{c_1}{R_1} \tilde{E}_{31}^M \right) \frac{\partial^2 w_0}{\partial X_1 \partial t} - \bar{I}_0 \frac{\partial^2 u_0}{\partial t^2} - \bar{J}_1 \frac{\partial^2 \phi_1}{\partial t^2} + c_1 \bar{I}_3 \frac{\partial^2}{\partial t^2} \left(\frac{\partial w_0}{\partial X_1} \right) = 0
\end{aligned}$$

A.2 Equation of motion by TSDT sanders shell theory for δv

$$\begin{aligned}
& A_{16} \left(\frac{\partial^2 u_0}{\partial X_1^2} + \frac{1}{R_1} \frac{\partial w_0}{\partial X_1} + \frac{\partial w_0}{\partial X_1} \frac{\partial^2 w_0}{\partial X_1^2} \right) + A_{26} \left(\frac{\partial^2 v_0}{\partial X_1 \partial X_2} + \frac{1}{R_2} \frac{\partial w_0}{\partial X_1} + \frac{\partial w_0}{\partial X_2} \frac{\partial^2 w_0}{\partial X_1 \partial X_2} \right) + A_{66} \left(\frac{\partial^2 v_0}{\partial X_1^2} + \frac{\partial^2 u_0}{\partial X_1 \partial X_2} + \right. \\
& \left. \frac{\partial^2 w_0}{\partial X_1^2} \frac{\partial w_0}{\partial X_2} + \frac{\partial w_0}{\partial X_1} \frac{\partial^2 w_0}{\partial X_1 \partial X_2} \right) + B_{16} \frac{\partial^2 \phi_1}{\partial X_1^2} + B_{26} \frac{\partial^2 \phi_2}{\partial X_1 \partial X_2} + B_{66} \left(\frac{\partial^2 \phi_2}{\partial X_1^2} + \frac{\partial^2 \phi_1}{\partial X_1 \partial X_2} \right) - c_1 E_{16} \left(\frac{\partial^2 \phi_1}{\partial X_1^2} + \frac{\partial^3 w_0}{\partial X_1^3} - \right. \\
& \left. \frac{1}{R_1} \frac{\partial^2 u_0}{\partial X_1^2} \right) - c_1 E_{26} \left(\frac{\partial^2 \phi_2}{\partial X_1 \partial X_2} + \frac{\partial^3 w_0}{\partial X_1 \partial X_2^2} - \frac{1}{R_2} \frac{\partial^2 v_0}{\partial X_1 \partial X_2} \right) - c_1 E_{66} \left(\frac{\partial^2 \phi_2}{\partial X_1^2} + \frac{\partial^2 \phi_1}{\partial X_1 \partial X_2} + 2 \frac{\partial^3 w_0}{\partial X_1^2 \partial X_2} - \frac{1}{R_2} \frac{\partial^2 v_0}{\partial X_1^2} \right. \\
& \left. - \frac{1}{R_1} \frac{\partial^2 u_0}{\partial X_1 \partial X_2} \right) + A_{12} \left(\frac{\partial^2 u_0}{\partial X_2 \partial X_1} + \frac{1}{R_1} \frac{\partial w_0}{\partial X_2} + \frac{\partial w_0}{\partial X_1} \frac{\partial^2 w_0}{\partial X_2 \partial X_1} \right) + A_{22} \left(\frac{\partial^2 v_0}{\partial X_2^2} + \frac{1}{R_2} \frac{\partial w_0}{\partial X_2} + \frac{\partial w_0}{\partial X_2} \frac{\partial^2 w_0}{\partial X_2^2} \right) + \\
& A_{26} \left(\frac{\partial^2 v_0}{\partial X_1 \partial X_2} + \frac{\partial^2 u_0}{\partial X_2^2} + \frac{\partial^2 w_0}{\partial X_2 \partial X_1} \frac{\partial w_0}{\partial X_2} + \frac{\partial w_0}{\partial X_1} \frac{\partial^2 w_0}{\partial X_2^2} \right) + B_{12} \frac{\partial^2 \phi_1}{\partial X_2 \partial X_1} + B_{22} \frac{\partial^2 \phi_2}{\partial X_2^2} + B_{26} \left(\frac{\partial^2 \phi_2}{\partial X_2 \partial X_1} + \frac{\partial^2 \phi_1}{\partial X_2^2} \right) - \\
& c_1 E_{12} \left(\frac{\partial^2 \phi_1}{\partial X_2 \partial X_1} + \frac{\partial^3 w_0}{\partial X_2 \partial X_1^2} - \frac{1}{R_1} \frac{\partial^2 u_0}{\partial X_1 \partial X_2} \right) - c_1 E_{22} \left(\frac{\partial^2 \phi_2}{\partial X_2^2} + \frac{\partial^3 w_0}{\partial X_2^3} - \frac{1}{R_2} \frac{\partial^2 v_0}{\partial X_2^2} \right) - c_1 E_{26} \left(\frac{\partial^2 \phi_2}{\partial X_2 \partial X_1} + \frac{\partial^2 \phi_1}{\partial X_2^2} + \right. \\
& \left. 2 \frac{\partial^3 w_0}{\partial X_1 \partial X_2^2} - \frac{1}{R_2} \frac{\partial^2 v_0}{\partial X_1 \partial X_2} - \frac{1}{R_1} \frac{\partial^2 u_0}{\partial X_2^2} \right) + \frac{1}{R_2} \left[\hat{A}_{44} \left(\phi_2 + \frac{\partial w_0}{\partial X_2} - \frac{v_0}{R_2} \right) + \hat{A}_{45} \left(\phi_1 + \frac{\partial w_0}{\partial X_1} - \frac{u_0}{R_1} \right) \right] + \frac{c_1}{R_2} [E_{12} \\
& \left(\frac{\partial^2 u_0}{\partial X_2 \partial X_1} + \frac{1}{R_1} \frac{\partial w_0}{\partial X_2} + \frac{\partial w_0}{\partial X_1} \frac{\partial^2 w_0}{\partial X_2 \partial X_1} \right) + E_{22} \left(\frac{\partial^2 v_0}{\partial X_2^2} + \frac{1}{R_2} \frac{\partial w_0}{\partial X_2} + \frac{\partial w_0}{\partial X_2} \frac{\partial^2 w_0}{\partial X_2^2} \right) + E_{26} \left(\frac{\partial^2 v_0}{\partial X_1 \partial X_2} + \frac{\partial^2 u_0}{\partial X_2^2} \right. \\
& \left. + \frac{\partial^2 w_0}{\partial X_2 \partial X_1} \frac{\partial w_0}{\partial X_2} + \frac{\partial w_0}{\partial X_1} \frac{\partial^2 w_0}{\partial X_2^2} \right) + F_{12} \frac{\partial^2 \phi_1}{\partial X_2 \partial X_1} + F_{22} \frac{\partial^2 \phi_2}{\partial X_2^2} + F_{26} \left(\frac{\partial^2 \phi_2}{\partial X_2 \partial X_1} + \frac{\partial^2 \phi_1}{\partial X_2^2} \right) - c_1 H_{12} \left(\frac{\partial^2 \phi_1}{\partial X_2 \partial X_1} + \right. \\
& \left. \frac{\partial^3 w_0}{\partial X_2 \partial X_1^2} - \frac{1}{R_1} \frac{\partial^2 u_0}{\partial X_1 \partial X_2} \right) - c_1 H_{22} \left(\frac{\partial^2 \phi_2}{\partial X_2^2} + \frac{\partial^3 w_0}{\partial X_2^3} - \frac{1}{R_2} \frac{\partial^2 v_0}{\partial X_2^2} \right) - c_1 H_{26} \left(\frac{\partial^2 \phi_2}{\partial X_2 \partial X_1} + \frac{\partial^2 \phi_1}{\partial X_2^2} + 2 \frac{\partial^3 w_0}{\partial X_1 \partial X_2^2} - \right. \\
& \left. \frac{1}{R_2} \frac{\partial^2 v_0}{\partial X_1 \partial X_2} - \frac{1}{R_1} \frac{\partial^2 u_0}{\partial X_2^2} \right) + E_{16} \left(\frac{\partial^2 u_0}{\partial X_1^2} + \frac{1}{R_1} \frac{\partial w_0}{\partial X_1} + \frac{\partial w_0}{\partial X_1} \frac{\partial^2 w_0}{\partial X_1^2} \right) + E_{26} \left(\frac{\partial^2 v_0}{\partial X_1 \partial X_2} + \frac{1}{R_2} \frac{\partial w_0}{\partial X_1} + \frac{\partial w_0}{\partial X_2} \frac{\partial^2 w_0}{\partial X_1 \partial X_2} \right) \\
& + E_{66} \left(\frac{\partial^2 v_0}{\partial X_1^2} + \frac{\partial^2 u_0}{\partial X_1 \partial X_2} + \frac{\partial^2 w_0}{\partial X_1^2} \frac{\partial w_0}{\partial X_2} + \frac{\partial w_0}{\partial X_1} \frac{\partial^2 w_0}{\partial X_1 \partial X_2} \right) + F_{16} \frac{\partial^2 \phi_1}{\partial X_1^2} + F_{26} \frac{\partial^2 \phi_2}{\partial X_1 \partial X_2} + F_{66} \left(\frac{\partial^2 \phi_2}{\partial X_1^2} + \frac{\partial^2 \phi_1}{\partial X_1 \partial X_2} \right) - \\
& c_1 H_{16} \left(\frac{\partial^2 \phi_1}{\partial X_1^2} + \frac{\partial^3 w_0}{\partial X_1^3} - \frac{1}{R_1} \frac{\partial^2 u_0}{\partial X_1^2} \right) - c_1 H_{26} \left(\frac{\partial^2 \phi_2}{\partial X_1 \partial X_2} + \frac{\partial^3 w_0}{\partial X_1 \partial X_2^2} - \frac{1}{R_2} \frac{\partial^2 v_0}{\partial X_1 \partial X_2} \right) - c_1 H_{66} \left(\frac{\partial^2 \phi_2}{\partial X_1^2} + \frac{\partial^2 \phi_1}{\partial X_1 \partial X_2} + \right. \\
& \left. 2 \frac{\partial^3 w_0}{\partial X_1^2 \partial X_2} - \frac{1}{R_2} \frac{\partial^2 v_0}{\partial X_1 \partial X_2} - \frac{1}{R_1} \frac{\partial^2 u_0}{\partial X_1 \partial X_2} \right) \left. \right] - \left(\tilde{A}_{32}^M + \frac{c_1}{R_2} \tilde{E}_{32}^M \right) \frac{\partial^2 w_0}{\partial X_2 \partial t} - \bar{I}'_0 \frac{\partial^2 v_0}{\partial t^2} - \bar{J}'_1 \frac{\partial^2 \phi_2}{\partial t^2} + c_1 \bar{I}'_3 \frac{\partial^2}{\partial t^2} \left(\frac{\partial w_0}{\partial X_2} \right) = 0
\end{aligned}$$

A.3 Equation of motion by TSDT sanders shell theory for δw

$$\begin{aligned}
& \hat{A}_{45} \left(\frac{\partial \phi_2}{\partial X_1} + \frac{\partial^2 w_0}{\partial X_1 \partial X_2} - \frac{1}{R_2} \frac{\partial v_0}{\partial X_1} \right) + \hat{A}_{55} \left(\frac{\partial \phi_1}{\partial X_1} + \frac{\partial^2 w_0}{\partial X_1^2} - \frac{1}{R_1} \frac{\partial u_0}{\partial X_1} \right) + \hat{A}_{44} \left(\frac{\partial \phi_2}{\partial X_2} + \frac{\partial^2 w_0}{\partial X_2^2} - \frac{1}{R_2} \frac{\partial v_0}{\partial X_2} \right) + \\
& \hat{A}_{45} \left(\frac{\partial \phi_1}{\partial X_2} + \frac{\partial^2 w_0}{\partial X_2 \partial X_1} - \frac{1}{R_1} \frac{\partial u_0}{\partial X_2} \right) + c_1 \left[E_{11} \left(\frac{\partial^3 u_0}{\partial X_1^3} + \frac{1}{R_1} \frac{\partial^2 w_0}{\partial X_1^2} + \frac{\partial^2 w_0}{\partial X_1^2} \frac{\partial^2 w_0}{\partial X_1^2} + \frac{\partial w_0}{\partial X_1} \frac{\partial^3 w_0}{\partial X_1^3} \right) + E_{12} \left(\frac{\partial^3 v_0}{\partial X_1^2 \partial X_2} \right. \right. \\
& + \frac{1}{R_2} \frac{\partial^2 w_0}{\partial X_1^2} + \frac{\partial^2 w_0}{\partial X_1 \partial X_2} \frac{\partial^2 w_0}{\partial X_1 \partial X_2} + \frac{\partial w_0}{\partial X_2} \frac{\partial^3 w_0}{\partial X_1^2 \partial X_2} \left. \right) + E_{16} \left(\frac{\partial^3 v_0}{\partial X_1^3} + \frac{\partial^3 u_0}{\partial X_1^2 \partial X_2} + \frac{\partial^3 w_0}{\partial X_1^3} \frac{\partial w_0}{\partial X_2} + \frac{\partial^2 w_0}{\partial X_1^2} \frac{\partial^2 w_0}{\partial X_1 \partial X_2} + \right. \\
& \left. \frac{\partial^2 w_0}{\partial X_1^2} \frac{\partial^2 w_0}{\partial X_1 \partial X_2} + \frac{\partial w_0}{\partial X_1} \frac{\partial^3 w_0}{\partial X_1^2 \partial X_2} \right) + F_{11} \frac{\partial^3 \phi_1}{\partial X_1^3} + F_{12} \frac{\partial^3 \phi_2}{\partial X_1^2 \partial X_2} + F_{16} \left(\frac{\partial^3 \phi_2}{\partial X_1^3} + \frac{\partial^3 \phi_1}{\partial X_1^2 \partial X_2} \right) - c_1 H_{11} \left(\frac{\partial^3 \phi_1}{\partial X_1^3} + \frac{\partial^4 w_0}{\partial X_1^4} \right. \\
& \left. - \frac{1}{R_1} \frac{\partial^3 u_0}{\partial X_1^3} \right) - c_1 H_{12} \left(\frac{\partial^3 \phi_2}{\partial X_1^2 \partial X_2} + \frac{\partial^4 w_0}{\partial X_1^2 \partial X_2^2} - \frac{1}{R_2} \frac{\partial^3 v_0}{\partial X_1^2 \partial X_2} \right) - c_1 H_{16} \left(\frac{\partial^3 \phi_2}{\partial X_1^3} + \frac{\partial^3 \phi_1}{\partial X_1^2 \partial X_2} + 2 \frac{\partial^4 w_0}{\partial X_1^3 \partial X_2} - \frac{1}{R_2} \right. \\
& \left. \frac{\partial^3 v_0}{\partial X_1^3} - \frac{1}{R_1} \frac{\partial^3 u_0}{\partial X_1^2 \partial X_2} \right) + E_{12} \left(\frac{\partial^3 u_0}{\partial X_2^2 \partial X_1} + \frac{1}{R_1} \frac{\partial^2 w_0}{\partial X_2^2} + \frac{\partial^2 w_0}{\partial X_2 \partial X_1} \frac{\partial^2 w_0}{\partial X_2 \partial X_1} + \frac{\partial w_0}{\partial X_1} \frac{\partial^3 w_0}{\partial X_2^2 \partial X_1} \right) + E_{22} \left(\frac{\partial^3 v_0}{\partial X_2^3} + \frac{1}{R_2} \right. \\
& \left. \frac{\partial^2 w_0}{\partial X_2^2} + \frac{\partial^2 w_0}{\partial X_2^2} \frac{\partial^2 w_0}{\partial X_2^2} + \frac{\partial w_0}{\partial X_2} \frac{\partial^3 w_0}{\partial X_2^3} \right) + E_{26} \left(\frac{\partial^3 v_0}{\partial X_1 \partial X_2^2} + \frac{\partial^3 u_0}{\partial X_2^3} + \frac{\partial^3 w_0}{\partial X_2^2 \partial X_1} \frac{\partial w_0}{\partial X_2} + \frac{\partial^2 w_0}{\partial X_2 \partial X_1} \frac{\partial^2 w_0}{\partial X_2^2} + \frac{\partial^2 w_0}{\partial X_2 \partial X_1} \right. \\
& \left. \frac{\partial^2 w_0}{\partial X_2^2} + \frac{\partial w_0}{\partial X_1} \frac{\partial^3 w_0}{\partial X_2^3} \right) + F_{12} \frac{\partial^3 \phi_1}{\partial X_2^2 \partial X_1} + F_{22} \frac{\partial^3 \phi_2}{\partial X_2^3} + F_{26} \left(\frac{\partial^3 \phi_2}{\partial X_2^2 \partial X_1} + \frac{\partial^3 \phi_1}{\partial X_2^3} \right) - c_1 H_{12} \left(\frac{\partial^3 \phi_1}{\partial X_2^2 \partial X_1} + \frac{\partial^4 w_0}{\partial X_2^2 \partial X_1^2} - \right. \\
& \left. \frac{1}{R_1} \frac{\partial^3 u_0}{\partial X_1 \partial X_2^2} \right) - c_1 H_{22} \left(\frac{\partial^3 \phi_2}{\partial X_2^3} + \frac{\partial^4 w_0}{\partial X_2^4} - \frac{1}{R_2} \frac{\partial^3 v_0}{\partial X_2^3} \right) - c_1 H_{26} \left(\frac{\partial^3 \phi_2}{\partial X_2^2 \partial X_1} + \frac{\partial^3 \phi_1}{\partial X_2^3} + 2 \frac{\partial^4 w_0}{\partial X_1 \partial X_2^3} - \frac{1}{R_2} \frac{\partial^3 v_0}{\partial X_1 \partial X_2^2} - \right. \\
& \left. \frac{1}{R_1} \frac{\partial^3 u_0}{\partial X_1 \partial X_2^3} \right) + 2E_{16} \left(\frac{\partial^3 u_0}{\partial X_2 \partial X_1^2} + \frac{1}{R_1} \frac{\partial^2 w_0}{\partial X_2 \partial X_1} + \frac{\partial^2 w_0}{\partial X_2 \partial X_1} \frac{\partial^2 w_0}{\partial X_1^2} + \frac{\partial w_0}{\partial X_1} \frac{\partial^3 w_0}{\partial X_2 \partial X_1^2} \right) + 2E_{26} \left(\frac{\partial^3 v_0}{\partial X_1 \partial X_2^2} + \frac{1}{R_2} \right. \\
& \left. \frac{\partial^2 w_0}{\partial X_2 \partial X_1} + \frac{\partial^2 w_0}{\partial X_2^2} \frac{\partial^2 w_0}{\partial X_1 \partial X_2} + \frac{\partial w_0}{\partial X_2} \frac{\partial^3 w_0}{\partial X_1 \partial X_2^2} \right) + 2E_{66} \left(\frac{\partial^3 v_0}{\partial X_2 \partial X_1^2} + \frac{\partial^3 u_0}{\partial X_1 \partial X_2^2} + \frac{\partial^3 w_0}{\partial X_2 \partial X_1^2} \frac{\partial w_0}{\partial X_2} + \frac{\partial^2 w_0}{\partial X_1^2} \frac{\partial^2 w_0}{\partial X_2^2} + \right. \\
& \left. \frac{\partial^2 w_0}{\partial X_2 \partial X_1} \frac{\partial^2 w_0}{\partial X_1 \partial X_2} + \frac{\partial w_0}{\partial X_1} \frac{\partial^3 w_0}{\partial X_1 \partial X_2^2} \right) + 2F_{16} \frac{\partial^3 \phi_1}{\partial X_2 \partial X_1^2} + 2F_{26} \frac{\partial^3 \phi_2}{\partial X_1 \partial X_2^2} + 2F_{66} \left(\frac{\partial^3 \phi_2}{\partial X_2 \partial X_1^2} + \frac{\partial^3 \phi_1}{\partial X_1 \partial X_2^2} \right) \\
& - 2c_1 H_{16} \left(\frac{\partial^3 \phi_1}{\partial X_2 \partial X_1^2} + \frac{\partial^4 w_0}{\partial X_2 \partial X_1^3} - \frac{1}{R_1} \frac{\partial^3 u_0}{\partial X_1^2 \partial X_2} \right) - 2c_1 H_{26} \left(\frac{\partial^3 \phi_2}{\partial X_1 \partial X_2^2} + \frac{\partial^4 w_0}{\partial X_1 \partial X_2^3} - \frac{1}{R_2} \frac{\partial^3 v_0}{\partial X_1 \partial X_2^2} \right) - 2c_1 H_{66} \\
& \left(\frac{\partial^3 \phi_2}{\partial X_2 \partial X_1^2} + \frac{\partial^3 \phi_1}{\partial X_1 \partial X_2^2} + 2 \frac{\partial^4 w_0}{\partial X_1^2 \partial X_2^2} - \frac{1}{R_2} \frac{\partial^3 v_0}{\partial X_1^2 \partial X_2} - \frac{1}{R_1} \frac{\partial^3 u_0}{\partial X_1 \partial X_2^2} \right) + \frac{\partial}{\partial X_1} \left(\frac{\partial w_0}{\partial X_1} \left[A_{11} \left[\frac{\partial u_0}{\partial X_1} + \frac{w}{R_1} + \frac{1}{2} \right. \right. \right. \\
& \left. \left. \left(\frac{\partial w_0}{\partial X_1} \right)^2 \right] + A_{12} \left[\frac{\partial v_0}{\partial X_2} + \frac{w}{R_2} + \frac{1}{2} \left(\frac{\partial w_0}{\partial X_2} \right)^2 \right] + A_{16} \left(\frac{\partial v_0}{\partial X_1} + \frac{\partial u_0}{\partial X_2} + \frac{\partial w_0}{\partial X_1} \frac{\partial w_0}{\partial X_2} \right) + B_{11} \frac{\partial \phi_1}{\partial X_1} + B_{12} \frac{\partial \phi_2}{\partial X_2} + B_{16} \right.
\end{aligned}$$

$$I_0 \frac{\partial^2 w_0}{\partial t^2} + c_1^2 I_6 \frac{\partial^2}{\partial t^2} \left(\frac{\partial^2 w_0}{\partial X_1^2} + \frac{\partial^2 w_0}{\partial X_2^2} \right) - c_1 \left[\bar{I}_3 \frac{\partial^2}{\partial t^2} \left(\frac{\partial u_0}{\partial X_1} \right) + \bar{I}_3' \frac{\partial^2}{\partial t^2} \left(\frac{\partial v_0}{\partial X_2} \right) + J_4 \frac{\partial^2}{\partial t^2} \left(\frac{\partial \phi_1}{\partial X_1} + \frac{\partial \phi_2}{\partial X_2} \right) \right] = 0$$

A.4 Equation of motion by TSDT sanders shell theory for $\delta\phi_1$

$$\begin{aligned} & \hat{B}_{11} \left(\frac{\partial^2 u_0}{\partial X_1^2} + \frac{1}{R_1} \frac{\partial w_0}{\partial X_1} + \frac{\partial w_0}{\partial X_1} \frac{\partial^2 w_0}{\partial X_1^2} \right) + \hat{B}_{12} \left(\frac{\partial^2 v_0}{\partial X_1 \partial X_2} + \frac{1}{R_2} \frac{\partial w_0}{\partial X_1} + \frac{\partial w_0}{\partial X_2} \frac{\partial^2 w_0}{\partial X_1 \partial X_2} \right) + \hat{B}_{16} \left(\frac{\partial^2 v_0}{\partial X_1^2} + \frac{\partial^2 u_0}{\partial X_1 \partial X_2} + \right. \\ & \left. \frac{\partial^2 w_0}{\partial X_1^2} \frac{\partial w_0}{\partial X_2} + \frac{\partial w_0}{\partial X_1} \frac{\partial^2 w_0}{\partial X_1 \partial X_2} \right) + \hat{D}_{11} \frac{\partial^2 \phi_1}{\partial X_1^2} + \hat{D}_{12} \frac{\partial^2 \phi_2}{\partial X_1 \partial X_2} + \hat{D}_{16} \left(\frac{\partial^2 \phi_2}{\partial X_1^2} + \frac{\partial^2 \phi_1}{\partial X_1 \partial X_2} \right) - c_1 \hat{F}_{11} \left(\frac{\partial^2 \phi_1}{\partial X_1^2} + \frac{\partial^3 w_0}{\partial X_1^3} - \right. \\ & \left. \frac{1}{R_1} \frac{\partial^2 u_0}{\partial X_1^2} \right) - c_1 \hat{F}_{12} \left(\frac{\partial^2 \phi_2}{\partial X_1 \partial X_2} + \frac{\partial^3 w_0}{\partial X_1 \partial X_2^2} - \frac{1}{R_2} \frac{\partial^2 v_0}{\partial X_1 \partial X_2} \right) - c_1 \hat{F}_{16} \left(\frac{\partial^2 \phi_2}{\partial X_1^2} + \frac{\partial^2 \phi_1}{\partial X_1 \partial X_2} + 2 \frac{\partial^3 w_0}{\partial X_1^2 \partial X_2} - \frac{1}{R_2} \frac{\partial^2 v_0}{\partial X_1^2} \right. \\ & \left. - \frac{1}{R_1} \frac{\partial^2 u_0}{\partial X_1 \partial X_2} \right) + \hat{B}_{16} \left(\frac{\partial^2 u_0}{\partial X_2 \partial X_1} + \frac{1}{R_1} \frac{\partial w_0}{\partial X_2} + \frac{\partial w_0}{\partial X_1} \frac{\partial^2 w_0}{\partial X_2 \partial X_1} \right) + \hat{B}_{26} \left(\frac{\partial^2 v_0}{\partial X_2^2} + \frac{1}{R_2} \frac{\partial w_0}{\partial X_2} + \frac{\partial w_0}{\partial X_2} \frac{\partial^2 w_0}{\partial X_2^2} \right) + \hat{B}_{66} \\ & \left(\frac{\partial^2 v_0}{\partial X_1 \partial X_2} + \frac{\partial^2 u_0}{\partial X_2^2} + \frac{\partial^2 w_0}{\partial X_2 \partial X_1} \frac{\partial w_0}{\partial X_2} + \frac{\partial w_0}{\partial X_1} \frac{\partial^2 w_0}{\partial X_2^2} \right) + \hat{D}_{16} \frac{\partial^2 \phi_1}{\partial X_2 \partial X_1} + \hat{D}_{26} \frac{\partial^2 \phi_2}{\partial X_2^2} + \hat{D}_{66} \left(\frac{\partial^2 \phi_2}{\partial X_2 \partial X_1} + \frac{\partial^2 \phi_1}{\partial X_2^2} \right) - \\ & c_1 \hat{F}_{16} \left(\frac{\partial^2 \phi_1}{\partial X_2 \partial X_1} + \frac{\partial^3 w_0}{\partial X_2 \partial X_1^2} - \frac{1}{R_1} \frac{\partial^2 u_0}{\partial X_1 \partial X_2} \right) - c_1 \hat{F}_{26} \left(\frac{\partial^2 \phi_2}{\partial X_2^2} + \frac{\partial^3 w_0}{\partial X_2^3} - \frac{1}{R_2} \frac{\partial^2 v_0}{\partial X_2^2} \right) - c_1 \hat{F}_{66} \left(\frac{\partial^2 \phi_2}{\partial X_2 \partial X_1} + \frac{\partial^2 \phi_1}{\partial X_2^2} + \right. \\ & \left. 2 \frac{\partial^3 w_0}{\partial X_1 \partial X_2^2} - \frac{1}{R_2} \frac{\partial^2 v_0}{\partial X_1 \partial X_2} - \frac{1}{R_1} \frac{\partial^2 u_0}{\partial X_2^2} \right) - \hat{A}_{45} \left(\phi_2 + \frac{\partial w_0}{\partial X_2} - \frac{v_0}{R_2} \right) - \hat{A}_{55} \left(\phi_1 + \frac{\partial w_0}{\partial X_1} - \frac{u_0}{R_1} \right) + (\tilde{B}_{31}^M - c_1 \tilde{E}_{31}^M) \\ & \frac{\partial^2 w_0}{\partial X_1 \partial t} - \bar{J}_1 \frac{\partial^2 u_0}{\partial t^2} - \bar{K}_2 \frac{\partial^2 \phi_1}{\partial t^2} + c_1 J_4 \frac{\partial^2}{\partial t^2} \left(\frac{\partial w_0}{\partial X_1} \right) = 0 \end{aligned}$$

A.5 Equation of motion by TSDT sanders shell theory for $\delta\phi_2$

$$\begin{aligned} & \hat{B}_{16} \left(\frac{\partial^2 u_0}{\partial X_1^2} + \frac{1}{R_1} \frac{\partial w_0}{\partial X_1} + \frac{\partial w_0}{\partial X_1} \frac{\partial^2 w_0}{\partial X_1^2} \right) + \hat{B}_{26} \left(\frac{\partial^2 v_0}{\partial X_1 \partial X_2} + \frac{1}{R_2} \frac{\partial w_0}{\partial X_1} + \frac{\partial w_0}{\partial X_2} \frac{\partial^2 w_0}{\partial X_1 \partial X_2} \right) + \hat{B}_{66} \left(\frac{\partial^2 v_0}{\partial X_1^2} + \frac{\partial^2 u_0}{\partial X_1 \partial X_2} + \right. \\ & \left. \frac{\partial^2 w_0}{\partial X_1^2} \frac{\partial w_0}{\partial X_2} + \frac{\partial w_0}{\partial X_1} \frac{\partial^2 w_0}{\partial X_1 \partial X_2} \right) + \hat{D}_{16} \frac{\partial^2 \phi_1}{\partial X_1^2} + \hat{D}_{26} \frac{\partial^2 \phi_2}{\partial X_1 \partial X_2} + \hat{D}_{66} \left(\frac{\partial^2 \phi_2}{\partial X_1^2} + \frac{\partial^2 \phi_1}{\partial X_1 \partial X_2} \right) - c_1 \hat{F}_{16} \left(\frac{\partial^2 \phi_1}{\partial X_1^2} + \frac{\partial^3 w_0}{\partial X_1^3} - \right. \\ & \left. \frac{1}{R_1} \frac{\partial^2 u_0}{\partial X_1^2} \right) - c_1 \hat{F}_{26} \left(\frac{\partial^2 \phi_2}{\partial X_1 \partial X_2} + \frac{\partial^3 w_0}{\partial X_1 \partial X_2^2} - \frac{1}{R_2} \frac{\partial^2 v_0}{\partial X_1 \partial X_2} \right) - c_1 \hat{F}_{66} \left(\frac{\partial^2 \phi_2}{\partial X_1^2} + \frac{\partial^2 \phi_1}{\partial X_1 \partial X_2} + 2 \frac{\partial^3 w_0}{\partial X_1^2 \partial X_2} - \frac{1}{R_2} \frac{\partial^2 v_0}{\partial X_1^2} \right. \\ & \left. - \frac{1}{R_1} \frac{\partial^2 u_0}{\partial X_1 \partial X_2} \right) + \hat{B}_{12} \left(\frac{\partial^2 u_0}{\partial X_2 \partial X_1} + \frac{1}{R_1} \frac{\partial w_0}{\partial X_2} + \frac{\partial w_0}{\partial X_1} \frac{\partial^2 w_0}{\partial X_2 \partial X_1} \right) + \hat{B}_{22} \left(\frac{\partial^2 v_0}{\partial X_2^2} + \frac{1}{R_2} \frac{\partial w_0}{\partial X_2} + \frac{\partial w_0}{\partial X_2} \frac{\partial^2 w_0}{\partial X_2^2} \right) + \hat{B}_{26} \end{aligned}$$

$$\begin{aligned}
& \left(\frac{\partial^2 v_0}{\partial X_1 \partial X_2} + \frac{\partial^2 u_0}{\partial X_2^2} + \frac{\partial^2 w_0}{\partial X_2 \partial X_1} \frac{\partial w_0}{\partial X_2} + \frac{\partial w_0}{\partial X_1} \frac{\partial^2 w_0}{\partial X_2^2} \right) + \hat{D}_{12} \frac{\partial^2 \phi_1}{\partial X_2 \partial X_1} + \hat{D}_{22} \frac{\partial^2 \phi_2}{\partial X_2^2} + \hat{D}_{26} \left(\frac{\partial^2 \phi_2}{\partial X_2 \partial X_1} + \frac{\partial^2 \phi_1}{\partial X_2^2} \right) - c_1 \\
& \hat{F}_{12} \left(\frac{\partial^2 \phi_1}{\partial X_2 \partial X_1} + \frac{\partial^3 w_0}{\partial X_2 \partial X_1^2} - \frac{1}{R_1} \frac{\partial^2 u_0}{\partial X_1 \partial X_2} \right) - c_1 \hat{F}_{22} \left(\frac{\partial^2 \phi_2}{\partial X_2^2} + \frac{\partial^3 w_0}{\partial X_2^3} - \frac{1}{R_2} \frac{\partial^2 v_0}{\partial X_2^2} \right) - c_1 \hat{F}_{26} \left(\frac{\partial^2 \phi_2}{\partial X_2 \partial X_1} + \frac{\partial^2 \phi_1}{\partial X_2^2} + \right. \\
& \left. 2 \frac{\partial^3 w_0}{\partial X_1 \partial X_2^2} - \frac{1}{R_2} \frac{\partial^2 v_0}{\partial X_1 \partial X_2} - \frac{1}{R_1} \frac{\partial^2 u_0}{\partial X_2^2} \right) - \hat{A}_{44} \left(\phi_2 + \frac{\partial w_0}{\partial X_2} - \frac{v_0}{R_2} \right) - \hat{A}_{45} \left(\phi_1 + \frac{\partial w_0}{\partial X_1} - \frac{u_0}{R_1} \right) + (\tilde{B}_{32}^M - c_1 \tilde{E}_{32}^M) \\
& \frac{\partial^2 w_0}{\partial X_2 \partial t} - \bar{J}'_1 \frac{\partial^2 v_0}{\partial t^2} - \bar{K}_2 \frac{\partial^2 \phi_2}{\partial t^2} + c_1 J_4 \frac{\partial^2}{\partial t^2} \left(\frac{\partial w_0}{\partial X_2} \right) = 0
\end{aligned}$$

APPENDIX B

FINITE ELEMENT COEFFICIENTS BY TSDT DONNELL (DMV) SHELL THEORY

B.1 Linear coefficients of laminated composite shells by Donnell shell theory

$$\begin{aligned}
K_{ij}^{11} &= \int_{\Omega^e} \left[A_{11} \frac{\partial \psi_i}{\partial X_1} \frac{\partial \psi_j}{\partial X_1} + A_{66} \frac{\partial \psi_i}{\partial X_2} \frac{\partial \psi_j}{\partial X_2} + A_{16} \left(\frac{\partial \psi_i}{\partial X_1} \frac{\partial \psi_j}{\partial X_2} + \frac{\partial \psi_i}{\partial X_2} \frac{\partial \psi_j}{\partial X_1} \right) \right] dX_1 dX_2 \\
K_{ij}^{12} &= \int_{\Omega^e} \left(A_{12} \frac{\partial \psi_i}{\partial X_1} \frac{\partial \psi_j}{\partial X_2} + A_{16} \frac{\partial \psi_i}{\partial X_1} \frac{\partial \psi_j}{\partial X_1} + A_{26} \frac{\partial \psi_i}{\partial X_2} \frac{\partial \psi_j}{\partial X_2} + A_{66} \frac{\partial \psi_i}{\partial X_2} \frac{\partial \psi_j}{\partial X_1} \right) dX_1 dX_2 \\
K_{ij}^{13} &= \int_{\Omega^e} \left\{ \left(\frac{A_{11}}{R_1} + \frac{A_{12}}{R_2} \right) \frac{\partial \psi_i}{\partial X_1} \varphi_j + \left(\frac{A_{16}}{R_1} + \frac{A_{26}}{R_2} \right) \frac{\partial \psi_i}{\partial X_2} \varphi_j + (-c_1) \left[\left(E_{11} \frac{\partial \psi_i}{\partial X_1} \frac{\partial^2 \varphi_j}{\partial X_1^2} + E_{12} \frac{\partial \psi_i}{\partial X_1} \frac{\partial^2 \varphi_j}{\partial X_2^2} \right. \right. \right. \\
&\quad \left. \left. + 2E_{16} \frac{\partial \psi_i}{\partial X_1} \frac{\partial^2 \varphi_j}{\partial X_1 \partial X_2} \right) + \left(E_{16} \frac{\partial \psi_i}{\partial X_2} \frac{\partial^2 \varphi_j}{\partial X_1^2} + E_{26} \frac{\partial \psi_i}{\partial X_2} \frac{\partial^2 \varphi_j}{\partial X_2^2} + 2E_{66} \frac{\partial \psi_i}{\partial X_2} \frac{\partial^2 \varphi_j}{\partial X_1 \partial X_2} \right) \right] \Big\} dX_1 dX_2 \\
K_{ij}^{14} &= \int_{\Omega^e} \left[\hat{B}_{11} \frac{\partial \psi_i}{\partial X_1} \frac{\partial \psi_j}{\partial X_1} + \hat{B}_{66} \frac{\partial \psi_i}{\partial X_2} \frac{\partial \psi_j}{\partial X_2} + \hat{B}_{16} \left(\frac{\partial \psi_i}{\partial X_1} \frac{\partial \psi_j}{\partial X_2} + \frac{\partial \psi_i}{\partial X_2} \frac{\partial \psi_j}{\partial X_1} \right) \right] dX_1 dX_2 \\
K_{ij}^{15} &= \int_{\Omega^e} \left(\hat{B}_{12} \frac{\partial \psi_i}{\partial X_1} \frac{\partial \psi_j}{\partial X_2} + \hat{B}_{16} \frac{\partial \psi_i}{\partial X_1} \frac{\partial \psi_j}{\partial X_1} + \hat{B}_{26} \frac{\partial \psi_i}{\partial X_2} \frac{\partial \psi_j}{\partial X_2} + \hat{B}_{66} \frac{\partial \psi_i}{\partial X_2} \frac{\partial \psi_j}{\partial X_1} \right) dX_1 dX_2 \\
K_{ij}^{21} &= \int_{\Omega^e} \left(A_{16} \frac{\partial \psi_i}{\partial X_1} \frac{\partial \psi_j}{\partial X_1} + A_{66} \frac{\partial \psi_i}{\partial X_1} \frac{\partial \psi_j}{\partial X_2} + A_{12} \frac{\partial \psi_i}{\partial X_2} \frac{\partial \psi_j}{\partial X_1} + A_{26} \frac{\partial \psi_i}{\partial X_2} \frac{\partial \psi_j}{\partial X_2} \right) dX_1 dX_2 \\
K_{ij}^{22} &= \int_{\Omega^e} \left[A_{22} \frac{\partial \psi_i}{\partial X_2} \frac{\partial \psi_j}{\partial X_2} + A_{66} \frac{\partial \psi_i}{\partial X_1} \frac{\partial \psi_j}{\partial X_1} + A_{26} \left(\frac{\partial \psi_i}{\partial X_1} \frac{\partial \psi_j}{\partial X_2} + \frac{\partial \psi_i}{\partial X_2} \frac{\partial \psi_j}{\partial X_1} \right) \right] dX_1 dX_2 \\
K_{ij}^{23} &= \int_{\Omega^e} \left\{ \left(\frac{A_{12}}{R_1} + \frac{A_{22}}{R_2} \right) \frac{\partial \psi_i}{\partial X_2} \varphi_j + \left(\frac{A_{16}}{R_1} + \frac{A_{26}}{R_2} \right) \frac{\partial \psi_i}{\partial X_1} \varphi_j + (-c_1) \left[\left(E_{12} \frac{\partial \psi_i}{\partial X_2} \frac{\partial^2 \varphi_j}{\partial X_1^2} + E_{22} \frac{\partial \psi_i}{\partial X_2} \frac{\partial^2 \varphi_j}{\partial X_2^2} \right. \right. \right. \\
&\quad \left. \left. + 2E_{26} \frac{\partial \psi_i}{\partial X_2} \frac{\partial^2 \varphi_j}{\partial X_1 \partial X_2} \right) + \left(E_{16} \frac{\partial \psi_i}{\partial X_1} \frac{\partial^2 \varphi_j}{\partial X_1^2} + E_{26} \frac{\partial \psi_i}{\partial X_1} \frac{\partial^2 \varphi_j}{\partial X_2^2} + 2E_{66} \frac{\partial \psi_i}{\partial X_1} \frac{\partial^2 \varphi_j}{\partial X_1 \partial X_2} \right) \right] \Big\} dX_1 dX_2 \\
K_{ij}^{24} &= \int_{\Omega^e} \left(\hat{B}_{16} \frac{\partial \psi_i}{\partial X_1} \frac{\partial \psi_j}{\partial X_1} + \hat{B}_{66} \frac{\partial \psi_i}{\partial X_1} \frac{\partial \psi_j}{\partial X_2} + \hat{B}_{12} \frac{\partial \psi_i}{\partial X_2} \frac{\partial \psi_j}{\partial X_1} + \hat{B}_{26} \frac{\partial \psi_i}{\partial X_2} \frac{\partial \psi_j}{\partial X_2} \right) dX_1 dX_2 \\
K_{ij}^{25} &= \int_{\Omega^e} \left[\hat{B}_{22} \frac{\partial \psi_i}{\partial X_2} \frac{\partial \psi_j}{\partial X_2} + \hat{B}_{66} \frac{\partial \psi_i}{\partial X_1} \frac{\partial \psi_j}{\partial X_1} + \hat{B}_{26} \left(\frac{\partial \psi_i}{\partial X_1} \frac{\partial \psi_j}{\partial X_2} + \frac{\partial \psi_i}{\partial X_2} \frac{\partial \psi_j}{\partial X_1} \right) \right] dX_1 dX_2 \\
K_{ij}^{31} &= \int_{\Omega^e} \left\{ \left(\frac{A_{11}}{R_1} + \frac{A_{12}}{R_2} \right) \varphi_i \frac{\partial \psi_j}{\partial X_1} + \left(\frac{A_{16}}{R_1} + \frac{A_{26}}{R_2} \right) \varphi_i \frac{\partial \psi_j}{\partial X_2} + (-c_1) \left[\frac{\partial^2 \varphi_i}{\partial X_1^2} \left(E_{11} \frac{\partial \psi_j}{\partial X_1} + E_{16} \frac{\partial \psi_j}{\partial X_2} \right) \right. \right. \\
&\quad \left. \left. + \frac{\partial^2 \varphi_i}{\partial X_1 \partial X_2} (E_{12} + E_{26}) + \frac{\partial^2 \varphi_i}{\partial X_2^2} (E_{16} + E_{22}) \right] \right\} dX_1 dX_2
\end{aligned}$$

$$\begin{aligned}
& +2 \frac{\partial^2 \varphi_i}{\partial X_1 \partial X_2} \left(E_{16} \frac{\partial \psi_j}{\partial X_1} + E_{66} \frac{\partial \psi_j}{\partial X_2} \right) + \frac{\partial^2 \varphi_i}{\partial X_2^2} \left(E_{12} \frac{\partial \psi_j}{\partial X_1} + E_{26} \frac{\partial \psi_j}{\partial X_2} \right) \Bigg\} dX_1 dX_2 \\
K_{ij}^{32} = & \int_{\Omega^e} \left\{ \left(\frac{A_{12}}{R_1} + \frac{A_{22}}{R_2} \right) \varphi_i \frac{\partial \psi_j}{\partial X_2} + \left(\frac{A_{16}}{R_1} + \frac{A_{26}}{R_2} \right) \varphi_i \frac{\partial \psi_j}{\partial X_1} + (-c_1) \left[\frac{\partial^2 \varphi_i}{\partial X_1^2} \left(E_{12} \frac{\partial \psi_j}{\partial X_2} + E_{16} \frac{\partial \psi_j}{\partial X_1} \right) \right. \right. \\
& \left. \left. + 2 \frac{\partial^2 \varphi_i}{\partial X_1 \partial X_2} \left(E_{26} \frac{\partial \psi_j}{\partial X_2} + E_{66} \frac{\partial \psi_j}{\partial X_1} \right) + \frac{\partial^2 \varphi_i}{\partial X_2^2} \left(E_{22} \frac{\partial \psi_j}{\partial X_2} + E_{26} \frac{\partial \psi_j}{\partial X_1} \right) \right] \right\} dX_1 dX_2 \\
K_{ij}^{33} = & \int_{\Omega^e} \left\{ \left[A_{11} \left(\frac{1}{R_1} \right)^2 + A_{12} \left(\frac{2}{R_1 R_2} \right) + A_{22} \left(\frac{1}{R_2} \right)^2 \right] \varphi_i \varphi_j + (-c_1) \left[\left(\frac{E_{11}}{R_1} + \frac{E_{12}}{R_2} \right) \left(\varphi_i \frac{\partial^2 \varphi_j}{\partial X_1^2} + \frac{\partial^2 \varphi_i}{\partial X_1^2} \varphi_j \right) \right. \right. \\
& \left. \left. + 2 \left(\frac{E_{16}}{R_1} + \frac{E_{26}}{R_2} \right) \left(\varphi_i \frac{\partial^2 \varphi_j}{\partial X_1 \partial X_2} + \frac{\partial^2 \varphi_i}{\partial X_1 \partial X_2} \varphi_j \right) + \left(\frac{E_{12}}{R_1} + \frac{E_{22}}{R_2} \right) \left(\varphi_i \frac{\partial^2 \varphi_j}{\partial X_2^2} + \frac{\partial^2 \varphi_i}{\partial X_2^2} \varphi_j \right) \right] + \right. \\
& \frac{\partial \varphi_i}{\partial X_1} \left(\hat{A}_{45} \frac{\partial \varphi_j}{\partial X_2} + \hat{A}_{55} \frac{\partial \varphi_j}{\partial X_1} \right) + \frac{\partial \varphi_i}{\partial X_2} \left(\hat{A}_{44} \frac{\partial \varphi_j}{\partial X_2} + \hat{A}_{45} \frac{\partial \varphi_j}{\partial X_1} \right) + (c_1)^2 \left[\frac{\partial^2 \varphi_i}{\partial X_1^2} \left(H_{11} \frac{\partial^2 \varphi_j}{\partial X_1^2} + H_{12} \frac{\partial^2 \varphi_j}{\partial X_2^2} \right. \right. \\
& \left. \left. + 2 H_{16} \frac{\partial^2 \varphi_j}{\partial X_1 \partial X_2} \right) + 2 \frac{\partial^2 \varphi_i}{\partial X_1 \partial X_2} \left(H_{16} \frac{\partial^2 \varphi_j}{\partial X_1^2} + H_{26} \frac{\partial^2 \varphi_j}{\partial X_2^2} + 2 H_{66} \frac{\partial^2 \varphi_j}{\partial X_1 \partial X_2} \right) + \frac{\partial^2 \varphi_i}{\partial X_2^2} \left(H_{12} \frac{\partial^2 \varphi_j}{\partial X_1^2} + \right. \right. \\
& \left. \left. H_{22} \frac{\partial^2 \varphi_j}{\partial X_2^2} + 2 H_{26} \frac{\partial^2 \varphi_j}{\partial X_1 \partial X_2} \right) \right] \Bigg\} dX_1 dX_2 \\
K_{ij}^{34} = & \int_{\Omega^e} \left\{ \left(\frac{\hat{B}_{11}}{R_1} + \frac{\hat{B}_{12}}{R_2} \right) \varphi_i \frac{\partial \psi_j}{\partial X_1} + \left(\frac{\hat{B}_{16}}{R_1} + \frac{\hat{B}_{26}}{R_2} \right) \varphi_i \frac{\partial \psi_j}{\partial X_2} + \hat{A}_{55} \frac{\partial \varphi_i}{\partial X_1} \psi_j + \hat{A}_{45} \frac{\partial \varphi_i}{\partial X_2} \psi_j - c_1 \left[\frac{\partial^2 \varphi_i}{\partial X_1^2} \left(\hat{F}_{11} \frac{\partial \psi_j}{\partial X_1} \right. \right. \right. \\
& \left. \left. + \hat{F}_{16} \frac{\partial \psi_j}{\partial X_2} \right) + 2 \frac{\partial^2 \varphi_i}{\partial X_1 \partial X_2} \left(\hat{F}_{16} \frac{\partial \psi_j}{\partial X_1} + \hat{F}_{66} \frac{\partial \psi_j}{\partial X_2} \right) + \frac{\partial^2 \varphi_i}{\partial X_2^2} \left(\hat{F}_{12} \frac{\partial \psi_j}{\partial X_1} + \hat{F}_{26} \frac{\partial \psi_j}{\partial X_2} \right) \right] \Bigg\} dX_1 dX_2 \\
K_{ij}^{35} = & \int_{\Omega^e} \left\{ \left(\frac{\hat{B}_{12}}{R_1} + \frac{\hat{B}_{22}}{R_2} \right) \varphi_i \frac{\partial \psi_j}{\partial X_2} + \left(\frac{\hat{B}_{16}}{R_1} + \frac{\hat{B}_{26}}{R_2} \right) \varphi_i \frac{\partial \psi_j}{\partial X_1} + \hat{A}_{45} \frac{\partial \varphi_i}{\partial X_1} \psi_j + \hat{A}_{44} \frac{\partial \varphi_i}{\partial X_2} \psi_j - c_1 \left[\frac{\partial^2 \varphi_i}{\partial X_1^2} \left(\hat{F}_{12} \frac{\partial \psi_j}{\partial X_2} \right. \right. \right. \\
& \left. \left. + \hat{F}_{16} \frac{\partial \psi_j}{\partial X_1} \right) + 2 \frac{\partial^2 \varphi_i}{\partial X_1 \partial X_2} \left(\hat{F}_{26} \frac{\partial \psi_j}{\partial X_2} + \hat{F}_{66} \frac{\partial \psi_j}{\partial X_1} \right) + \frac{\partial^2 \varphi_i}{\partial X_2^2} \left(\hat{F}_{22} \frac{\partial \psi_j}{\partial X_2} + \hat{F}_{26} \frac{\partial \psi_j}{\partial X_1} \right) \right] \Bigg\} dX_1 dX_2 \\
K_{ij}^{41} = & \int_{\Omega^e} \left[\hat{B}_{11} \frac{\partial \psi_i}{\partial X_1} \frac{\partial \psi_j}{\partial X_1} + \hat{B}_{66} \frac{\partial \psi_i}{\partial X_2} \frac{\partial \psi_j}{\partial X_2} + \hat{B}_{16} \left(\frac{\partial \psi_i}{\partial X_1} \frac{\partial \psi_j}{\partial X_2} + \frac{\partial \psi_i}{\partial X_2} \frac{\partial \psi_j}{\partial X_1} \right) \right] dX_1 dX_2 \\
K_{ij}^{42} = & \int_{\Omega^e} \left(\hat{B}_{12} \frac{\partial \psi_i}{\partial X_1} \frac{\partial \psi_j}{\partial X_2} + \hat{B}_{16} \frac{\partial \psi_i}{\partial X_1} \frac{\partial \psi_j}{\partial X_1} + \hat{B}_{26} \frac{\partial \psi_i}{\partial X_2} \frac{\partial \psi_j}{\partial X_2} + \hat{B}_{66} \frac{\partial \psi_i}{\partial X_2} \frac{\partial \psi_j}{\partial X_1} \right) dX_1 dX_2 \\
K_{ij}^{43} = & \int_{\Omega^e} \left\{ \left(\frac{\hat{B}_{11}}{R_1} + \frac{\hat{B}_{12}}{R_2} \right) \frac{\partial \psi_i}{\partial X_1} \varphi_j + \left(\frac{\hat{B}_{16}}{R_1} + \frac{\hat{B}_{26}}{R_2} \right) \frac{\partial \psi_i}{\partial X_2} \varphi_j + \hat{A}_{45} \psi_i \frac{\partial \varphi_j}{\partial X_2} + \hat{A}_{55} \psi_i \frac{\partial \varphi_j}{\partial X_1} - c_1 \left[\frac{\partial \psi_i}{\partial X_1} \left(\hat{F}_{11} \frac{\partial^2 \varphi_j}{\partial X_1^2} \right. \right. \right.
\end{aligned}$$

$$\begin{aligned}
& + \hat{F}_{12} \frac{\partial^2 \varphi_j}{\partial X_2^2} + 2\hat{F}_{16} \frac{\partial^2 \varphi_j}{\partial X_1 \partial X_2} \Big) + \frac{\partial \psi_i}{\partial X_2} \Big(\hat{F}_{16} \frac{\partial^2 \varphi_j}{\partial X_1^2} + \hat{F}_{26} \frac{\partial^2 \varphi_j}{\partial X_2^2} + 2\hat{F}_{66} \frac{\partial^2 \varphi_j}{\partial X_1 \partial X_2} \Big) \Big] \Big\} dX_1 dX_2 \\
K_{ij}^{44} = & \int_{\Omega^e} \Big[\hat{A}_{55} \psi_i \psi_j + \Big(\hat{D}_{11} - c_1 \hat{F}_{11} \Big) \frac{\partial \psi_i}{\partial X_1} \frac{\partial \psi_j}{\partial X_1} + \Big(\hat{D}_{66} - c_1 \hat{F}_{66} \Big) \frac{\partial \psi_i}{\partial X_2} \frac{\partial \psi_j}{\partial X_2} + \Big(\hat{D}_{16} - c_1 \hat{F}_{16} \Big) \Big(\frac{\partial \psi_i}{\partial X_1} \frac{\partial \psi_j}{\partial X_2} + \\
& \frac{\partial \psi_i}{\partial X_2} \frac{\partial \psi_j}{\partial X_1} \Big) \Big] dX_1 dX_2 \\
K_{ij}^{45} = & \int_{\Omega^e} \Big[\hat{A}_{45} \psi_i \psi_j + \Big(\hat{D}_{12} - c_1 \hat{F}_{12} \Big) \frac{\partial \psi_i}{\partial X_1} \frac{\partial \psi_j}{\partial X_2} + \Big(\hat{D}_{16} - c_1 \hat{F}_{16} \Big) \frac{\partial \psi_i}{\partial X_1} \frac{\partial \psi_j}{\partial X_1} + \Big(\hat{D}_{26} - c_1 \hat{F}_{26} \Big) \frac{\partial \psi_i}{\partial X_2} \frac{\partial \psi_j}{\partial X_2} + \\
& \Big(\hat{D}_{66} - c_1 \hat{F}_{66} \Big) \frac{\partial \psi_i}{\partial X_2} \frac{\partial \psi_j}{\partial X_1} \Big] dX_1 dX_2 \\
K_{ij}^{51} = & \int_{\Omega^e} \Big(\hat{B}_{16} \frac{\partial \psi_i}{\partial X_1} \frac{\partial \psi_j}{\partial X_1} + \hat{B}_{66} \frac{\partial \psi_i}{\partial X_1} \frac{\partial \psi_j}{\partial X_2} + \hat{B}_{12} \frac{\partial \psi_i}{\partial X_2} \frac{\partial \psi_j}{\partial X_1} + \hat{B}_{26} \frac{\partial \psi_i}{\partial X_2} \frac{\partial \psi_j}{\partial X_2} \Big) dX_1 dX_2 \\
K_{ij}^{52} = & \int_{\Omega^e} \Big[\hat{B}_{22} \frac{\partial \psi_i}{\partial X_2} \frac{\partial \psi_j}{\partial X_2} + \hat{B}_{66} \frac{\partial \psi_i}{\partial X_1} \frac{\partial \psi_j}{\partial X_1} + \hat{B}_{26} \Big(\frac{\partial \psi_i}{\partial X_1} \frac{\partial \psi_j}{\partial X_2} + \frac{\partial \psi_i}{\partial X_2} \frac{\partial \psi_j}{\partial X_1} \Big) \Big] dX_1 dX_2 \\
K_{ij}^{53} = & \int_{\Omega^e} \Big\{ \Big(\frac{\hat{B}_{12}}{R_1} + \frac{\hat{B}_{22}}{R_2} \Big) \frac{\partial \psi_i}{\partial X_2} \varphi_j + \Big(\frac{\hat{B}_{16}}{R_1} + \frac{\hat{B}_{26}}{R_2} \Big) \frac{\partial \psi_i}{\partial X_1} \varphi_j + \hat{A}_{44} \psi_i \frac{\partial \varphi_j}{\partial X_2} + \hat{A}_{45} \psi_i \frac{\partial \varphi_j}{\partial X_1} - c_1 \Big[\frac{\partial \psi_i}{\partial X_2} \Big(\hat{F}_{12} \frac{\partial^2 \varphi_j}{\partial X_1^2} \\
& + \hat{F}_{22} \frac{\partial^2 \varphi_j}{\partial X_2^2} + 2\hat{F}_{26} \frac{\partial^2 \varphi_j}{\partial X_1 \partial X_2} \Big) + \frac{\partial \psi_i}{\partial X_1} \Big(\hat{F}_{16} \frac{\partial^2 \varphi_j}{\partial X_1^2} + \hat{F}_{26} \frac{\partial^2 \varphi_j}{\partial X_2^2} + 2\hat{F}_{66} \frac{\partial^2 \varphi_j}{\partial X_1 \partial X_2} \Big) \Big] \Big\} dX_1 dX_2 \\
K_{ij}^{54} = & \int_{\Omega^e} \Big[\hat{A}_{45} \psi_i \psi_j + \Big(\hat{D}_{16} - c_1 \hat{F}_{16} \Big) \frac{\partial \psi_i}{\partial X_1} \frac{\partial \psi_j}{\partial X_1} + \Big(\hat{D}_{66} - c_1 \hat{F}_{66} \Big) \frac{\partial \psi_i}{\partial X_1} \frac{\partial \psi_j}{\partial X_2} + \Big(\hat{D}_{12} - c_1 \hat{F}_{12} \Big) \frac{\partial \psi_i}{\partial X_2} \frac{\partial \psi_j}{\partial X_1} + \\
& \Big(\hat{D}_{26} - c_1 \hat{F}_{26} \Big) \frac{\partial \psi_i}{\partial X_2} \frac{\partial \psi_j}{\partial X_2} \Big] dX_1 dX_2 \\
K_{ij}^{55} = & \int_{\Omega^e} \Big[\hat{A}_{44} \psi_i \psi_j + \Big(\hat{D}_{66} - c_1 \hat{F}_{66} \Big) \frac{\partial \psi_i}{\partial X_1} \frac{\partial \psi_j}{\partial X_1} + \Big(\hat{D}_{22} - c_1 \hat{F}_{22} \Big) \frac{\partial \psi_i}{\partial X_2} \frac{\partial \psi_j}{\partial X_2} + \Big(\hat{D}_{26} - c_1 \hat{F}_{26} \Big) \Big(\frac{\partial \psi_i}{\partial X_1} \frac{\partial \psi_j}{\partial X_2} + \\
& \frac{\partial \psi_i}{\partial X_2} \frac{\partial \psi_j}{\partial X_1} \Big) \Big] dX_1 dX_2 \\
M_{ij}^{11} = & \int_{\Omega^e} I_0 \psi_i \psi_j dX_1 dX_2 \\
M_{ij}^{22} = & \int_{\Omega^e} I_0 \psi_i \psi_j dX_1 dX_2 \\
M_{ij}^{31} = M_{ji}^{13} = & -c_1 \int_{\Omega^e} I_3 \frac{\partial \varphi_i}{\partial X_1} \psi_j dX_1 dX_2
\end{aligned}$$

$$\begin{aligned}
M_{ij}^{32} &= M_{ji}^{23} = -c_1 \int_{\Omega^e} I_3 \frac{\partial \varphi_i}{\partial X_2} \psi_j dX_1 dX_2 \\
M_{ij}^{33} &= \int_{\Omega^e} \left[I_0 \varphi_i \varphi_j + c_1^2 I_6 \left(\frac{\partial \varphi_i}{\partial X_1} \frac{\partial \varphi_j}{\partial X_1} + \frac{\partial \varphi_i}{\partial X_2} \frac{\partial \varphi_j}{\partial X_2} \right) \right] dX_1 dX_2 \\
M_{ij}^{41} &= M_{ji}^{14} = \int_{\Omega^e} J_1 \psi_i \psi_j dX_1 dX_2 \\
M_{ij}^{43} &= M_{ji}^{34} = -c_1 J_4 \int_{\Omega^e} \psi_i \frac{\partial \varphi_j}{\partial X_1} dX_1 dX_2 \\
M_{ij}^{52} &= M_{ji}^{25} = \int_{\Omega^e} J_1 \psi_i \psi_j dX_1 dX_2 \\
M_{ij}^{53} &= M_{ji}^{35} = -c_1 J_4 \int_{\Omega^e} \psi_i \frac{\partial \varphi_j}{\partial X_2} dX_1 dX_2 \\
M_{ij}^{44} &= \int_{\Omega^e} K_2 \psi_i \psi_j dX_1 dX_2 \\
M_{ij}^{55} &= \int_{\Omega^e} K_2 \psi_i \psi_j dX_1 dX_2 \\
M_{ij}^{12} &= M_{ij}^{15} = M_{ij}^{21} = M_{ij}^{24} = M_{ij}^{42} = M_{ij}^{45} = M_{ij}^{51} = M_{ij}^{54} = 0 \\
C_{ij}^{13} &= \int_{\Omega^e} \tilde{A}_{31}^M \frac{\partial \psi_i}{\partial X_1} \varphi_j dX_1 dX_2 \\
C_{ij}^{23} &= \int_{\Omega^e} \tilde{A}_{32}^M \frac{\partial \psi_i}{\partial X_2} \varphi_j dX_1 dX_2 \\
C_{ij}^{33} &= -c_1 \int_{\Omega^e} \left(\tilde{E}_{31}^M \frac{\partial^2 \varphi_i}{\partial X_1^2} + \tilde{E}_{32}^M \frac{\partial^2 \varphi_i}{\partial X_2^2} \right) \varphi_j dX_1 dX_2 + \int_{\Omega^e} \left(\frac{\tilde{A}_{31}^M}{R_1} + \frac{\tilde{A}_{32}^M}{R_2} \right) \varphi_i \varphi_j dX_1 dX_2 \\
C_{ij}^{43} &= \int_{\Omega^e} (\tilde{B}_{31}^M - c_1 \tilde{E}_{31}^M) \frac{\partial \psi_i}{\partial X_1} \varphi_j dX_1 dX_2 \\
C_{ij}^{53} &= \int_{\Omega^e} (\tilde{B}_{32}^M - c_1 \tilde{E}_{32}^M) \frac{\partial \psi_i}{\partial X_2} \varphi_j dX_1 dX_2 \\
C_{ij}^{11} &= C_{ij}^{12} = C_{ij}^{14} = C_{ij}^{15} = C_{ij}^{21} = C_{ij}^{22} = C_{ij}^{24} = C_{ij}^{25} = C_{ij}^{31} = C_{ij}^{32} = C_{ij}^{34} = C_{ij}^{35} = 0 \\
C_{ij}^{41} &= C_{ij}^{42} = C_{ij}^{44} = C_{ij}^{45} = C_{ij}^{51} = C_{ij}^{52} = C_{ij}^{54} = C_{ij}^{55} = 0 \\
F_i^1 &= \oint_{\Gamma^e} (N_1 n_1 + N_6 n_2) \psi_i ds \\
F_i^2 &= \oint_{\Gamma^e} (N_6 n_1 + N_2 n_2) \psi_i ds \\
F_i^3 &= \int_{\Omega^e} q \varphi_i dX_1 dX_2 + \oint_{\Gamma^e} \left(\bar{V}_n \varphi_i + p_m \frac{\partial \varphi_i}{\partial n} \right) ds \\
F_i^4 &= \oint_{\Gamma^e} (\bar{M}_1 n_1 + \bar{M}_6 n_2) \psi_i ds \\
F_i^5 &= \oint_{\Gamma^e} (\bar{M}_6 n_1 + \bar{M}_2 n_2) \psi_i ds
\end{aligned}$$

$$\begin{aligned}
F_i^{T1} &= \int_{\Omega^e} \left(\frac{\partial \psi_i}{\partial X_1} N_1^T + \frac{\partial \psi_i}{\partial X_2} N_6^T \right) dX_1 dX_2 \\
F_i^{T2} &= \int_{\Omega^e} \left(\frac{\partial \psi_i}{\partial X_1} N_6^T + \frac{\partial \psi_i}{\partial X_2} N_2^T \right) dX_1 dX_2 \\
F_i^{T3} &= -c_1 \int_{\Omega^e} \left(\frac{\partial^2 \varphi_i}{\partial X_1^2} P_1^T + 2 \frac{\partial^2 \varphi_i}{\partial X_1 \partial X_2} P_6^T + \frac{\partial^2 \varphi_i}{\partial X_2^2} P_2^T \right) dX_1 dX_2 + \int_{\Omega^e} \left(\frac{N_1^T}{R_1} + \frac{N_2^T}{R_2} \right) \varphi_i dX_1 dX_2 \\
F_i^{T4} &= \int_{\Omega^e} \left[\frac{\partial \psi_i}{\partial X_1} (M_1^T - c_1 P_1^T) + \frac{\partial \psi_i}{\partial X_2} (M_6^T - c_1 P_6^T) \right] dX_1 dX_2 \\
F_i^{T5} &= \int_{\Omega^e} \left[\frac{\partial \psi_i}{\partial X_1} (M_6^T - c_1 P_6^T) + \frac{\partial \psi_i}{\partial X_2} (M_2^T - c_1 P_2^T) \right] dX_1 dX_2
\end{aligned}$$

B.2 Additional nonlinear coefficients of laminated composite shells by Donnell shell theory

$$\begin{aligned}
(K_{ij}^{13})_{NL} &= \left(\frac{1}{2} \right) \int_{\Omega^e} \left\{ \left[\frac{\partial \psi_i}{\partial X_1} \left(A_{11} \frac{\partial w_0}{\partial X_1} \frac{\partial \varphi_j}{\partial X_1} + A_{12} \frac{\partial w_0}{\partial X_2} \frac{\partial \varphi_j}{\partial X_2} + A_{16} \left(\frac{\partial w_0}{\partial X_1} \frac{\partial \varphi_j}{\partial X_2} + \frac{\partial w_0}{\partial X_2} \frac{\partial \varphi_j}{\partial X_1} \right) \right) \right. \right. \\
&\quad \left. \left. + \frac{\partial \psi_i}{\partial X_2} \left(A_{16} \frac{\partial w_0}{\partial X_1} \frac{\partial \varphi_j}{\partial X_1} + A_{26} \frac{\partial w_0}{\partial X_2} \frac{\partial \varphi_j}{\partial X_2} + A_{66} \left(\frac{\partial w_0}{\partial X_1} \frac{\partial \varphi_j}{\partial X_2} + \frac{\partial w_0}{\partial X_2} \frac{\partial \varphi_j}{\partial X_1} \right) \right) \right] \right\} dX_1 dX_2 \\
(K_{ij}^{23})_{NL} &= \left(\frac{1}{2} \right) \int_{\Omega^e} \left\{ \left[\frac{\partial \psi_i}{\partial X_2} \left(A_{12} \frac{\partial w_0}{\partial X_1} \frac{\partial \varphi_j}{\partial X_1} + A_{22} \frac{\partial w_0}{\partial X_2} \frac{\partial \varphi_j}{\partial X_2} + A_{26} \left(\frac{\partial w_0}{\partial X_1} \frac{\partial \varphi_j}{\partial X_2} + \frac{\partial w_0}{\partial X_2} \frac{\partial \varphi_j}{\partial X_1} \right) \right) \right. \right. \\
&\quad \left. \left. + \frac{\partial \psi_i}{\partial X_1} \left(A_{16} \frac{\partial w_0}{\partial X_1} \frac{\partial \varphi_j}{\partial X_1} + A_{26} \frac{\partial w_0}{\partial X_2} \frac{\partial \varphi_j}{\partial X_2} + A_{66} \left(\frac{\partial w_0}{\partial X_1} \frac{\partial \varphi_j}{\partial X_2} + \frac{\partial w_0}{\partial X_2} \frac{\partial \varphi_j}{\partial X_1} \right) \right) \right] \right\} dX_1 dX_2 \\
(K_{ij}^{31})_{NL} &= \int_{\Omega^e} \left\{ \frac{\partial \varphi_i}{\partial X_1} \left[\frac{\partial w_0}{\partial X_1} \left(A_{11} \frac{\partial \psi_j}{\partial X_1} + A_{16} \frac{\partial \psi_j}{\partial X_2} \right) + \frac{\partial w_0}{\partial X_2} \left(A_{16} \frac{\partial \psi_j}{\partial X_1} + A_{66} \frac{\partial \psi_j}{\partial X_2} \right) \right] \right. \\
&\quad \left. + \frac{\partial \varphi_i}{\partial X_2} \left[\frac{\partial w_0}{\partial X_1} \left(A_{16} \frac{\partial \psi_j}{\partial X_1} + A_{66} \frac{\partial \psi_j}{\partial X_2} \right) + \frac{\partial w_0}{\partial X_2} \left(A_{12} \frac{\partial \psi_j}{\partial X_1} + A_{26} \frac{\partial \psi_j}{\partial X_2} \right) \right] \right\} dX_1 dX_2 \\
(K_{ij}^{32})_{NL} &= \int_{\Omega^e} \left\{ \frac{\partial \varphi_i}{\partial X_1} \left[\frac{\partial w_0}{\partial X_1} \left(A_{12} \frac{\partial \psi_j}{\partial X_2} + A_{16} \frac{\partial \psi_j}{\partial X_1} \right) + \frac{\partial w_0}{\partial X_2} \left(A_{26} \frac{\partial \psi_j}{\partial X_2} + A_{66} \frac{\partial \psi_j}{\partial X_1} \right) \right] \right. \\
&\quad \left. + \frac{\partial \varphi_i}{\partial X_2} \left[\frac{\partial w_0}{\partial X_1} \left(A_{26} \frac{\partial \psi_j}{\partial X_2} + A_{66} \frac{\partial \psi_j}{\partial X_1} \right) + \frac{\partial w_0}{\partial X_2} \left(A_{22} \frac{\partial \psi_j}{\partial X_2} + A_{26} \frac{\partial \psi_j}{\partial X_1} \right) \right] \right\} dX_1 dX_2
\end{aligned}$$

$$\begin{aligned}
(K_{ij}^{43})_{NL} &= \left(\frac{1}{2}\right) \int_{\Omega^e} \left\{ \frac{\partial \psi_i}{\partial X_1} \left[\hat{B}_{11} \frac{\partial w_0}{\partial X_1} \frac{\partial \varphi_j}{\partial X_1} + \hat{B}_{12} \frac{\partial w_0}{\partial X_2} \frac{\partial \varphi_j}{\partial X_2} + \hat{B}_{16} \left(\frac{\partial w_0}{\partial X_1} \frac{\partial \varphi_j}{\partial X_2} + \frac{\partial w_0}{\partial X_2} \frac{\partial \varphi_j}{\partial X_1} \right) \right] \right. \\
&\quad \left. + \frac{\partial \psi_i}{\partial X_2} \left[\hat{B}_{16} \frac{\partial w_0}{\partial X_1} \frac{\partial \varphi_j}{\partial X_1} + \hat{B}_{26} \frac{\partial w_0}{\partial X_2} \frac{\partial \varphi_j}{\partial X_2} + \hat{B}_{66} \left(\frac{\partial w_0}{\partial X_1} \frac{\partial \varphi_j}{\partial X_2} + \frac{\partial w_0}{\partial X_2} \frac{\partial \varphi_j}{\partial X_1} \right) \right] \right\} dX_1 dX_2 \\
(K_{ij}^{53})_{NL} &= \left(\frac{1}{2}\right) \int_{\Omega^e} \left\{ \frac{\partial \psi_i}{\partial X_2} \left[\hat{B}_{12} \frac{\partial w_0}{\partial X_1} \frac{\partial \varphi_j}{\partial X_1} + \hat{B}_{22} \frac{\partial w_0}{\partial X_2} \frac{\partial \varphi_j}{\partial X_2} + \hat{B}_{26} \left(\frac{\partial w_0}{\partial X_1} \frac{\partial \varphi_j}{\partial X_2} + \frac{\partial w_0}{\partial X_2} \frac{\partial \varphi_j}{\partial X_1} \right) \right] \right. \\
&\quad \left. + \frac{\partial \psi_i}{\partial X_1} \left[\hat{B}_{16} \frac{\partial w_0}{\partial X_1} \frac{\partial \varphi_j}{\partial X_1} + \hat{B}_{26} \frac{\partial w_0}{\partial X_2} \frac{\partial \varphi_j}{\partial X_2} + \hat{B}_{66} \left(\frac{\partial w_0}{\partial X_1} \frac{\partial \varphi_j}{\partial X_2} + \frac{\partial w_0}{\partial X_2} \frac{\partial \varphi_j}{\partial X_1} \right) \right] \right\} dX_1 dX_2 \\
(C_{ij}^{33})_{NL} &= \int_{\Omega^e} \left(\tilde{A}_{31}^M \frac{\partial w_0}{\partial X_1} \frac{\partial \varphi_i}{\partial X_1} + \tilde{A}_{32}^M \frac{\partial w_0}{\partial X_2} \frac{\partial \varphi_i}{\partial X_2} \right) \varphi_j dX_1 dX_2
\end{aligned}$$

B.3 Tangent stiffness coefficients of laminated composite shells by Donnell shell theory

$$\begin{aligned}
T_{ij}^{11} &= \sum_{\gamma=1}^5 \sum_{k=1}^{n^*} \frac{\partial K_{ik}^{1\gamma}}{\partial u_j} \Delta_k^\gamma + K_{ij}^{11} = K_{ij}^{11} \\
T_{ij}^{12} &= \sum_{\gamma=1}^5 \sum_{k=1}^{n^*} \frac{\partial K_{ik}^{1\gamma}}{\partial v_j} \Delta_k^\gamma + K_{ij}^{12} = K_{ij}^{12} \\
T_{ij}^{13} &= \sum_{\gamma=1}^5 \sum_{k=1}^{n^*} \frac{\partial K_{ik}^{1\gamma}}{\partial \Delta_j^3} \Delta_k^\gamma + K_{ij}^{13} = \sum_{k=1}^{n^*} \frac{\partial K_{ik}^{13}}{\partial \Delta_j} \bar{\Delta}_k + K_{ij}^{13} \\
\sum_{k=1}^{n^*} \frac{\partial K_{ik}^{13}}{\partial \Delta_j} \bar{\Delta}_k &= \frac{1}{2} \int_{\Omega^e} \left\{ \left[\frac{\partial \psi_i}{\partial X_1} \left(A_{11} \frac{\partial w_0}{\partial X_1} \frac{\partial \varphi_j}{\partial X_1} + A_{12} \frac{\partial w_0}{\partial X_2} \frac{\partial \varphi_j}{\partial X_2} + A_{16} \left(\frac{\partial w_0}{\partial X_1} \frac{\partial \varphi_j}{\partial X_2} + \frac{\partial w_0}{\partial X_2} \frac{\partial \varphi_j}{\partial X_1} \right) \right) \right. \right. \\
&\quad \left. \left. + \frac{\partial \psi_i}{\partial X_2} \left(A_{16} \frac{\partial w_0}{\partial X_1} \frac{\partial \varphi_j}{\partial X_1} + A_{26} \frac{\partial w_0}{\partial X_2} \frac{\partial \varphi_j}{\partial X_2} + A_{66} \left(\frac{\partial w_0}{\partial X_1} \frac{\partial \varphi_j}{\partial X_2} + \frac{\partial w_0}{\partial X_2} \frac{\partial \varphi_j}{\partial X_1} \right) \right) \right] \right\} dX_1 dX_2 \\
T_{ij}^{14} &= \sum_{\gamma=1}^5 \sum_{k=1}^{n^*} \frac{\partial K_{ik}^{1\gamma}}{\partial X_j} \Delta_k^\gamma + K_{ij}^{14} = K_{ij}^{14} \\
T_{ij}^{15} &= \sum_{\gamma=1}^5 \sum_{k=1}^{n^*} \frac{\partial K_{ik}^{1\gamma}}{\partial Y_j} \Delta_k^\gamma + K_{ij}^{15} = K_{ij}^{15} \\
T_{ij}^{21} &= \sum_{\gamma=1}^5 \sum_{k=1}^{n^*} \frac{\partial K_{ik}^{2\gamma}}{\partial u_j} \Delta_k^\gamma + K_{ij}^{21} = K_{ij}^{21} \\
T_{ij}^{22} &= \sum_{\gamma=1}^5 \sum_{k=1}^{n^*} \frac{\partial K_{ik}^{2\gamma}}{\partial v_j} \Delta_k^\gamma + K_{ij}^{22} = K_{ij}^{22} \\
T_{ij}^{23} &= \sum_{\gamma=1}^5 \sum_{k=1}^{n^*} \frac{\partial K_{ik}^{2\gamma}}{\partial \Delta_j^3} \Delta_k^\gamma + K_{ij}^{23} = \sum_{k=1}^{n^*} \frac{\partial K_{ik}^{23}}{\partial \Delta_j} \bar{\Delta}_k + K_{ij}^{23}
\end{aligned}$$

$$\begin{aligned}
\sum_{k=1}^{n^*} \frac{\partial K_{ik}^{23}}{\partial \bar{\Delta}_j} \bar{\Delta}_k &= \frac{1}{2} \int_{\Omega^e} \left\{ \left[\frac{\partial \psi_i}{\partial X_2} \left(A_{12} \frac{\partial w_0}{\partial X_1} \frac{\partial \varphi_j}{\partial X_1} + A_{22} \frac{\partial w_0}{\partial X_2} \frac{\partial \varphi_j}{\partial X_2} + A_{26} \left(\frac{\partial w_0}{\partial X_1} \frac{\partial \varphi_j}{\partial X_2} + \frac{\partial w_0}{\partial X_2} \frac{\partial \varphi_j}{\partial X_1} \right) \right) \right. \right. \\
&\quad \left. \left. + \frac{\partial \psi_i}{\partial X_1} \left(A_{16} \frac{\partial w_0}{\partial X_1} \frac{\partial \varphi_j}{\partial X_1} + A_{26} \frac{\partial w_0}{\partial X_2} \frac{\partial \varphi_j}{\partial X_2} + A_{66} \left(\frac{\partial w_0}{\partial X_1} \frac{\partial \varphi_j}{\partial X_2} + \frac{\partial w_0}{\partial X_2} \frac{\partial \varphi_j}{\partial X_1} \right) \right) \right] \right\} dX_1 dX_2 \\
T_{ij}^{24} &= \sum_{\gamma=1}^5 \sum_{k=1}^{n^*} \frac{\partial K_{ik}^{2\gamma}}{\partial X_j} \Delta_k^\gamma + K_{ij}^{24} = K_{ij}^{24} \\
T_{ij}^{25} &= \sum_{\gamma=1}^5 \sum_{k=1}^{n^*} \frac{\partial K_{ik}^{2\gamma}}{\partial Y_j} \Delta_k^\gamma + K_{ij}^{25} = K_{ij}^{25} \\
T_{ij}^{31} &= \sum_{\gamma=1}^5 \sum_{k=1}^{n^*} \frac{\partial K_{ik}^{3\gamma}}{\partial u_j} \Delta_k^\gamma + K_{ij}^{31} = K_{ij}^{31} \\
T_{ij}^{32} &= \sum_{\gamma=1}^5 \sum_{k=1}^{n^*} \frac{\partial K_{ik}^{3\gamma}}{\partial v_j} \Delta_k^\gamma + K_{ij}^{32} = K_{ij}^{32} \\
T_{ij}^{33} &= \sum_{\gamma=1}^5 \sum_{k=1}^{n^*} \frac{\partial K_{ik}^{3\gamma}}{\partial \bar{\Delta}_j} \Delta_k^\gamma + K_{ij}^{33} \\
&= \sum_{k=1}^{n^*} \left(\frac{\partial K_{ik}^{31}}{\partial \bar{\Delta}_j} u_k + \frac{\partial K_{ik}^{32}}{\partial \bar{\Delta}_j} v_k + \frac{\partial K_{ik}^{33}}{\partial \bar{\Delta}_j} \bar{\Delta}_k + \frac{\partial K_{ik}^{34}}{\partial \bar{\Delta}_j} X_k + \frac{\partial K_{ik}^{35}}{\partial \bar{\Delta}_j} Y_k \right) + K_{ij}^{33} \\
\sum_{k=1}^{n^*} \frac{\partial K_{ik}^{31}}{\partial \bar{\Delta}_j} u_k &= \int_{\Omega^e} \left\{ \frac{\partial u}{\partial X_1} \left[A_{11} \frac{\partial \varphi_i}{\partial X_1} \frac{\partial \varphi_j}{\partial X_1} + A_{12} \frac{\partial \varphi_i}{\partial X_2} \frac{\partial \varphi_j}{\partial X_2} + A_{16} \left(\frac{\partial \varphi_i}{\partial X_1} \frac{\partial \varphi_j}{\partial X_2} + \frac{\partial \varphi_i}{\partial X_2} \frac{\partial \varphi_j}{\partial X_1} \right) \right] \right. \\
&\quad \left. + \frac{\partial u}{\partial X_2} \left[A_{26} \frac{\partial \varphi_i}{\partial X_2} \frac{\partial \varphi_j}{\partial X_2} + A_{16} \frac{\partial \varphi_i}{\partial X_1} \frac{\partial \varphi_j}{\partial X_1} + A_{66} \left(\frac{\partial \varphi_i}{\partial X_2} \frac{\partial \varphi_j}{\partial X_1} + \frac{\partial \varphi_i}{\partial X_1} \frac{\partial \varphi_j}{\partial X_2} \right) \right] \right\} dX_1 dX_2 \\
\sum_{k=1}^{n^*} \frac{\partial K_{ik}^{32}}{\partial \bar{\Delta}_j} v_k &= \int_{\Omega^e} \left\{ \frac{\partial v}{\partial X_1} \left[A_{16} \frac{\partial \varphi_i}{\partial X_1} \frac{\partial \varphi_j}{\partial X_1} + A_{26} \frac{\partial \varphi_i}{\partial X_2} \frac{\partial \varphi_j}{\partial X_2} + A_{66} \left(\frac{\partial \varphi_i}{\partial X_1} \frac{\partial \varphi_j}{\partial X_2} + \frac{\partial \varphi_i}{\partial X_2} \frac{\partial \varphi_j}{\partial X_1} \right) \right] \right. \\
&\quad \left. + \frac{\partial v}{\partial X_2} \left[A_{12} \frac{\partial \varphi_i}{\partial X_1} \frac{\partial \varphi_j}{\partial X_1} + A_{22} \frac{\partial \varphi_i}{\partial X_2} \frac{\partial \varphi_j}{\partial X_2} + A_{26} \left(\frac{\partial \varphi_i}{\partial X_2} \frac{\partial \varphi_j}{\partial X_1} + \frac{\partial \varphi_i}{\partial X_1} \frac{\partial \varphi_j}{\partial X_2} \right) \right] \right\} dX_1 dX_2 \\
\sum_{k=1}^{n^*} \frac{\partial K_{ik}^{33}}{\partial \bar{\Delta}_j} \bar{\Delta}_k &= \left(\frac{1}{2} \right) \int_{\Omega^e} \left(-c_1 \right) \left\{ \frac{\partial^2 \varphi_i}{\partial X_1^2} \left[\frac{\partial w_0}{\partial X_1} \left(E_{11} \frac{\partial \varphi_j}{\partial X_1} + E_{16} \frac{\partial \varphi_j}{\partial X_2} \right) + \frac{\partial w_0}{\partial X_2} \left(E_{12} \frac{\partial \varphi_j}{\partial X_2} + E_{16} \frac{\partial \varphi_j}{\partial X_1} \right) \right] + 2 \frac{\partial^2 \varphi_i}{\partial X_1 \partial X_2} \right. \\
&\quad \left[\frac{\partial w_0}{\partial X_1} \left(E_{16} \frac{\partial \varphi_j}{\partial X_1} + E_{66} \frac{\partial \varphi_j}{\partial X_2} \right) + \frac{\partial w_0}{\partial X_2} \left(E_{26} \frac{\partial \varphi_j}{\partial X_2} + E_{66} \frac{\partial \varphi_j}{\partial X_1} \right) \right] + \frac{\partial^2 \varphi_i}{\partial X_2^2} \left[\frac{\partial w_0}{\partial X_1} \left(E_{12} \frac{\partial \varphi_j}{\partial X_1} + E_{26} \frac{\partial \varphi_j}{\partial X_2} \right) \right. \\
&\quad \left. \left. + \frac{\partial w_0}{\partial X_2} \left(E_{22} \frac{\partial \varphi_j}{\partial X_2} + E_{26} \frac{\partial \varphi_j}{\partial X_1} \right) \right] \right\} + \varphi_i \left[\left(\frac{A_{11}}{R_1} + \frac{A_{12}}{R_2} \right) \frac{\partial w_0}{\partial X_1} \frac{\partial \varphi_j}{\partial X_1} + \left(\frac{A_{12}}{R_1} + \frac{A_{22}}{R_2} \right) \frac{\partial w_0}{\partial X_2} \frac{\partial \varphi_j}{\partial X_2} + \left(\frac{A_{16}}{R_1} + \right. \right. \\
&\quad \left. \left. \frac{A_{26}}{R_2} \right) \left(\frac{\partial w_0}{\partial X_1} \frac{\partial \varphi_j}{\partial X_2} + \frac{\partial \varphi_j}{\partial X_1} \frac{\partial w_0}{\partial X_2} \right) \right] + \frac{\partial \varphi_i}{\partial X_1} \left[2 A_{11} \left(\frac{\partial w_0}{\partial X_1} \right)^2 \frac{\partial \varphi_j}{\partial X_1} + A_{12} \left[\frac{\partial \varphi_j}{\partial X_1} \left(\frac{\partial w_0}{\partial X_2} \right)^2 + \frac{\partial w_0}{\partial X_1} \frac{\partial w_0}{\partial X_2} \frac{\partial \varphi_j}{\partial X_2} \right] \right]
\end{aligned}$$

$$\begin{aligned}
& + A_{16} \left[3 \frac{\partial w_0}{\partial X_1} \frac{\partial w_0}{\partial X_2} \frac{\partial \varphi_j}{\partial X_1} + \left(\frac{\partial w_0}{\partial X_1} \right)^2 \frac{\partial \varphi_j}{\partial X_2} \right] - 2c_1 \frac{\partial \varphi_j}{\partial X_1} \left(E_{11} \frac{\partial^2 w_0}{\partial X_1^2} + E_{12} \frac{\partial^2 w_0}{\partial X_2^2} + 2E_{16} \frac{\partial^2 w_0}{\partial X_1 \partial X_2} \right) + A_{16} \\
& \left[\frac{\partial \varphi_j}{\partial X_1} \frac{\partial w_0}{\partial X_2} \frac{\partial w_0}{\partial X_1} + \left(\frac{\partial w_0}{\partial X_1} \right)^2 \frac{\partial \varphi_j}{\partial X_2} \right] + 2A_{26} \left(\frac{\partial w_0}{\partial X_2} \right)^2 \frac{\partial \varphi_j}{\partial X_2} + A_{66} \left[\frac{\partial \varphi_j}{\partial X_1} \left(\frac{\partial w_0}{\partial X_2} \right)^2 + 3 \frac{\partial w_0}{\partial X_1} \frac{\partial w_0}{\partial X_2} \frac{\partial \varphi_j}{\partial X_2} \right] - \\
& 2c_1 \frac{\partial \varphi_j}{\partial X_2} \left(E_{16} \frac{\partial^2 w_0}{\partial X_1^2} + E_{26} \frac{\partial^2 w_0}{\partial X_2^2} + 2E_{66} \frac{\partial^2 w_0}{\partial X_1 \partial X_2} \right) \left\} + \frac{\partial \varphi_i}{\partial X_2} \left\{ 2A_{16} \left(\frac{\partial w_0}{\partial X_1} \right)^2 \frac{\partial \varphi_j}{\partial X_1} + A_{26} \left[\frac{\partial \varphi_j}{\partial X_1} \left(\frac{\partial w_0}{\partial X_2} \right)^2 \right. \right. \\
& \left. \left. + \frac{\partial w_0}{\partial X_1} \frac{\partial w_0}{\partial X_2} \frac{\partial \varphi_j}{\partial X_2} \right] + A_{66} \left[3 \frac{\partial w_0}{\partial X_1} \frac{\partial w_0}{\partial X_2} \frac{\partial \varphi_j}{\partial X_1} + \left(\frac{\partial w_0}{\partial X_1} \right)^2 \frac{\partial \varphi_j}{\partial X_2} \right] - 2c_1 \frac{\partial \varphi_j}{\partial X_1} \left(E_{16} \frac{\partial^2 w_0}{\partial X_1^2} + E_{26} \frac{\partial^2 w_0}{\partial X_2^2} + \right. \right. \\
& \left. \left. 2E_{66} \frac{\partial^2 w_0}{\partial X_1 \partial X_2} \right) + A_{12} \left[\frac{\partial \varphi_j}{\partial X_1} \frac{\partial w_0}{\partial X_2} \frac{\partial w_0}{\partial X_1} + \left(\frac{\partial w_0}{\partial X_1} \right)^2 \frac{\partial \varphi_j}{\partial X_2} \right] + 2A_{22} \left(\frac{\partial w_0}{\partial X_2} \right)^2 \frac{\partial \varphi_j}{\partial X_2} + A_{26} \left[\frac{\partial \varphi_j}{\partial X_1} \left(\frac{\partial w_0}{\partial X_2} \right)^2 \right. \right. \\
& \left. \left. + 3 \frac{\partial w_0}{\partial X_1} \frac{\partial w_0}{\partial X_2} \frac{\partial \varphi_j}{\partial X_2} \right] - 2c_1 \frac{\partial \varphi_j}{\partial X_2} \left(E_{12} \frac{\partial^2 w_0}{\partial X_1^2} + E_{22} \frac{\partial^2 w_0}{\partial X_2^2} + 2E_{26} \frac{\partial^2 w_0}{\partial X_1 \partial X_2} \right) \right\} + 2 \left(\frac{A_{11}}{R_1} + \frac{A_{12}}{R_2} \right) \left[\frac{\partial \varphi_i}{\partial X_1} \right. \\
& \left. \varphi_j \frac{\partial w_0}{\partial X_1} w_0 + (w_0)^2 \frac{\partial \varphi_i}{\partial X_1} \frac{\partial \varphi_j}{\partial X_1} \right] + 2 \left(\frac{A_{16}}{R_1} + \frac{A_{26}}{R_2} \right) \left[\frac{\partial \varphi_i}{\partial X_1} \varphi_j \frac{\partial w_0}{\partial X_2} w_0 + (w_0)^2 \frac{\partial \varphi_i}{\partial X_1} \frac{\partial \varphi_j}{\partial X_2} \right] + 2 \left(\frac{A_{16}}{R_1} + \right. \\
& \left. \frac{A_{26}}{R_2} \right) \left[\frac{\partial \varphi_i}{\partial X_2} \varphi_j \frac{\partial w_0}{\partial X_1} w_0 + (w_0)^2 \frac{\partial \varphi_i}{\partial X_2} \frac{\partial \varphi_j}{\partial X_1} \right] + 2 \left(\frac{A_{12}}{R_1} + \frac{A_{22}}{R_2} \right) \left[\frac{\partial \varphi_i}{\partial X_2} \varphi_j \frac{\partial w_0}{\partial X_2} w_0 + (w_0)^2 \frac{\partial \varphi_i}{\partial X_2} \frac{\partial \varphi_j}{\partial X_2} \right] \\
& dX_1 dX_2 \\
\sum_{k=1}^{n^*} \frac{\partial K_{ik}^{34}}{\partial \Delta_j} X_k &= \int_{\Omega^e} \left\{ \frac{\partial \phi_x}{\partial X_1} \left[\hat{B}_{11} \frac{\partial \varphi_i}{\partial X_1} \frac{\partial \varphi_j}{\partial X_1} + \hat{B}_{12} \frac{\partial \varphi_i}{\partial X_2} \frac{\partial \varphi_j}{\partial X_2} + \hat{B}_{16} \left(\frac{\partial \varphi_i}{\partial X_1} \frac{\partial \varphi_j}{\partial X_2} + \frac{\partial \varphi_i}{\partial X_2} \frac{\partial \varphi_j}{\partial X_1} \right) \right. \right. \\
& \left. \left. + \frac{\partial \phi_x}{\partial X_2} \left[\hat{B}_{16} \frac{\partial \varphi_i}{\partial X_1} \frac{\partial \varphi_j}{\partial X_1} + \hat{B}_{26} \frac{\partial \varphi_i}{\partial X_2} \frac{\partial \varphi_j}{\partial X_2} + \hat{B}_{66} \left(\frac{\partial \varphi_i}{\partial X_1} \frac{\partial \varphi_j}{\partial X_2} + \frac{\partial \varphi_i}{\partial X_2} \frac{\partial \varphi_j}{\partial X_1} \right) \right] \right\} dX_1 dX_2 \\
\sum_{k=1}^{n^*} \frac{\partial K_{ik}^{35}}{\partial \Delta_j} X_k &= \int_{\Omega^e} \left\{ \frac{\partial \phi_y}{\partial X_1} \left[\hat{B}_{16} \frac{\partial \varphi_i}{\partial X_1} \frac{\partial \varphi_j}{\partial X_1} + \hat{B}_{26} \frac{\partial \varphi_i}{\partial X_2} \frac{\partial \varphi_j}{\partial X_2} + \hat{B}_{66} \left(\frac{\partial \varphi_i}{\partial X_1} \frac{\partial \varphi_j}{\partial X_2} + \frac{\partial \varphi_i}{\partial X_2} \frac{\partial \varphi_j}{\partial X_1} \right) \right. \right. \\
& \left. \left. + \frac{\partial \phi_y}{\partial X_2} \left[\hat{B}_{12} \frac{\partial \varphi_i}{\partial X_1} \frac{\partial \varphi_j}{\partial X_1} + \hat{B}_{22} \frac{\partial \varphi_i}{\partial X_2} \frac{\partial \varphi_j}{\partial X_2} + \hat{B}_{26} \left(\frac{\partial \varphi_i}{\partial X_1} \frac{\partial \varphi_j}{\partial X_2} + \frac{\partial \varphi_i}{\partial X_2} \frac{\partial \varphi_j}{\partial X_1} \right) \right] \right\} dX_1 dX_2 \\
T_{ij}^{34} &= \sum_{\gamma=1}^5 \sum_{k=1}^{n^*} \frac{\partial K_{ik}^{3\gamma}}{\partial X_j} \Delta_k^\gamma + K_{ij}^{34} = K_{ij}^{34} \\
T_{ij}^{35} &= \sum_{\gamma=1}^5 \sum_{k=1}^{n^*} \frac{\partial K_{ik}^{3\gamma}}{\partial Y_j} \Delta_k^\gamma + K_{ij}^{35} = K_{ij}^{35} \\
T_{ij}^{41} &= \sum_{\gamma=1}^5 \sum_{k=1}^{n^*} \frac{\partial K_{ik}^{4\gamma}}{\partial u_j} \Delta_k^\gamma + K_{ij}^{41} = K_{ij}^{41}
\end{aligned}$$

$$\begin{aligned}
T_{ij}^{42} &= \sum_{\gamma=1}^5 \sum_{k=1}^{n^*} \frac{\partial K_{ik}^{4\gamma}}{\partial v_j} \Delta_k^\gamma + K_{ij}^{42} = K_{ij}^{42} \\
T_{ij}^{43} &= \sum_{\gamma=1}^5 \sum_{k=1}^{n^*} \frac{\partial K_{ik}^{4\gamma}}{\partial \Delta_j^3} \Delta_k^\gamma + K_{ij}^{43} = \sum_{k=1}^{n^*} \frac{\partial K_{ik}^{43}}{\partial \Delta_j} \bar{\Delta}_k + K_{ij}^{43} \\
\sum_{k=1}^{n^*} \frac{\partial K_{ik}^{43}}{\partial \Delta_j} \bar{\Delta}_k &= \frac{1}{2} \int_{\Omega^e} \left\{ \frac{\partial \psi_i}{\partial X_1} \left[\hat{B}_{11} \frac{\partial w_0}{\partial X_1} \frac{\partial \varphi_j}{\partial X_1} + \hat{B}_{12} \frac{\partial w_0}{\partial X_2} \frac{\partial \varphi_j}{\partial X_2} + \hat{B}_{16} \left(\frac{\partial w_0}{\partial X_1} \frac{\partial \varphi_j}{\partial X_2} + \frac{\partial w_0}{\partial X_2} \frac{\partial \varphi_j}{\partial X_1} \right) \right] \right. \\
&\quad \left. + \frac{\partial \psi_i}{\partial X_2} \left[\hat{B}_{16} \frac{\partial w_0}{\partial X_1} \frac{\partial \varphi_j}{\partial X_1} + \hat{B}_{26} \frac{\partial w_0}{\partial X_2} \frac{\partial \varphi_j}{\partial X_2} + \hat{B}_{66} \left(\frac{\partial w_0}{\partial X_1} \frac{\partial \varphi_j}{\partial X_2} + \frac{\partial w_0}{\partial X_2} \frac{\partial \varphi_j}{\partial X_1} \right) \right] \right\} dX_1 dX_2 \\
T_{ij}^{44} &= \sum_{\gamma=1}^5 \sum_{k=1}^{n^*} \frac{\partial K_{ik}^{4\gamma}}{\partial X_j} \Delta_k^\gamma + K_{ij}^{44} = K_{ij}^{44} \\
T_{ij}^{45} &= \sum_{\gamma=1}^5 \sum_{k=1}^{n^*} \frac{\partial K_{ik}^{4\gamma}}{\partial Y_j} \Delta_k^\gamma + K_{ij}^{45} = K_{ij}^{45} \\
T_{ij}^{51} &= \sum_{\gamma=1}^5 \sum_{k=1}^{n^*} \frac{\partial K_{ik}^{5\gamma}}{\partial u_j} \Delta_k^\gamma + K_{ij}^{51} = K_{ij}^{51} \\
T_{ij}^{52} &= \sum_{\gamma=1}^5 \sum_{k=1}^{n^*} \frac{\partial K_{ik}^{5\gamma}}{\partial v_j} \Delta_k^\gamma + K_{ij}^{52} = K_{ij}^{52} \\
T_{ij}^{53} &= \sum_{\gamma=1}^5 \sum_{k=1}^{n^*} \frac{\partial K_{ik}^{5\gamma}}{\partial \Delta_j^3} \Delta_k^\gamma + K_{ij}^{53} = \sum_{k=1}^{n^*} \frac{\partial K_{ik}^{53}}{\partial \Delta_j} \bar{\Delta}_k + K_{ij}^{53} \\
\sum_{k=1}^{n^*} \frac{\partial K_{ik}^{53}}{\partial \Delta_j} \bar{\Delta}_k &= \frac{1}{2} \int_{\Omega^e} \left\{ \frac{\partial \psi_i}{\partial X_2} \left[\hat{B}_{12} \frac{\partial w_0}{\partial X_1} \frac{\partial \varphi_j}{\partial X_1} + \hat{B}_{22} \frac{\partial w_0}{\partial X_2} \frac{\partial \varphi_j}{\partial X_2} + \hat{B}_{26} \left(\frac{\partial w_0}{\partial X_1} \frac{\partial \varphi_j}{\partial X_2} + \frac{\partial w_0}{\partial X_2} \frac{\partial \varphi_j}{\partial X_1} \right) \right] \right. \\
&\quad \left. + \frac{\partial \psi_i}{\partial X_1} \left[\hat{B}_{16} \frac{\partial w_0}{\partial X_1} \frac{\partial \varphi_j}{\partial X_1} + \hat{B}_{26} \frac{\partial w_0}{\partial X_2} \frac{\partial \varphi_j}{\partial X_2} + \hat{B}_{66} \left(\frac{\partial w_0}{\partial X_1} \frac{\partial \varphi_j}{\partial X_2} + \frac{\partial w_0}{\partial X_2} \frac{\partial \varphi_j}{\partial X_1} \right) \right] \right\} dX_1 dX_2 \\
T_{ij}^{54} &= \sum_{\gamma=1}^5 \sum_{k=1}^{n^*} \frac{\partial K_{ik}^{5\gamma}}{\partial X_j} \Delta_k^\gamma + K_{ij}^{54} = K_{ij}^{54} \\
T_{ij}^{55} &= \sum_{\gamma=1}^5 \sum_{k=1}^{n^*} \frac{\partial K_{ik}^{5\gamma}}{\partial Y_j} \Delta_k^\gamma + K_{ij}^{55} = K_{ij}^{55}
\end{aligned}$$

APPENDIX C

FINITE ELEMENT COEFFICIENTS BY TSDT SANDERS (SANDERS-KOITER)

SHELL THEORY

C.1 Linear coefficients of laminated composite shells by Sanders shell theory

$$\begin{aligned}
 K_{ij}^{11} &= \int_{\Omega^e} \left\{ \left[A_{11} + 2 \frac{c_1}{R_1} E_{11} + \left(\frac{c_1}{R_1} \right)^2 H_{11} \right] \frac{\partial \psi_i}{\partial X_1} \frac{\partial \psi_j}{\partial X_1} + \left[A_{66} + 2 \frac{c_1}{R_1} E_{66} + \left(\frac{c_1}{R_1} \right)^2 H_{66} \right] \frac{\partial \psi_i}{\partial X_2} \frac{\partial \psi_j}{\partial X_2} + \right. \\
 &\quad \left. \left[A_{16} + 2 \frac{c_1}{R_1} E_{16} + \left(\frac{c_1}{R_1} \right)^2 H_{16} \right] \left(\frac{\partial \psi_i}{\partial X_1} \frac{\partial \psi_j}{\partial X_2} + \frac{\partial \psi_i}{\partial X_2} \frac{\partial \psi_j}{\partial X_1} \right) + \left(\frac{1}{R_1} \right)^2 \hat{A}_{55} \psi_i \psi_j \right\} dX_1 dX_2 \\
 K_{ij}^{12} &= \int_{\Omega^e} \left\{ \left[A_{12} + \left(\frac{c_1}{R_1} + \frac{c_1}{R_2} \right) E_{12} + \left(\frac{c_1}{R_1} \right) \left(\frac{c_1}{R_2} \right) H_{12} \right] \frac{\partial \psi_i}{\partial X_1} \frac{\partial \psi_j}{\partial X_2} + \left[A_{16} + \left(\frac{c_1}{R_1} + \frac{c_1}{R_2} \right) E_{16} + \left(\frac{c_1}{R_1} \right) \right. \right. \\
 &\quad \left. \left(\frac{c_1}{R_2} \right) H_{16} \right] \frac{\partial \psi_i}{\partial X_1} \frac{\partial \psi_j}{\partial X_1} + \left[A_{26} + \left(\frac{c_1}{R_1} + \frac{c_1}{R_2} \right) E_{26} + \left(\frac{c_1}{R_1} \right) \left(\frac{c_1}{R_2} \right) H_{26} \right] \frac{\partial \psi_i}{\partial X_2} \frac{\partial \psi_j}{\partial X_2} + \\
 &\quad \left. \left[A_{66} + \left(\frac{c_1}{R_1} + \frac{c_1}{R_2} \right) E_{66} + \left(\frac{c_1}{R_1} \right) \left(\frac{c_1}{R_2} \right) H_{66} \right] \frac{\partial \psi_i}{\partial X_2} \frac{\partial \psi_j}{\partial X_1} \right\} dX_1 dX_2 \\
 K_{ij}^{13} &= \int_{\Omega^e} \left\{ \left[\left(\frac{A_{11}}{R_1} + \frac{A_{12}}{R_2} \right) + \frac{c_1}{R_1} \left(\frac{E_{11}}{R_1} + \frac{E_{12}}{R_2} \right) \right] \frac{\partial \psi_i}{\partial X_1} \varphi_j + \left[\left(\frac{A_{16}}{R_1} + \frac{A_{26}}{R_2} \right) + \frac{c_1}{R_1} \left(\frac{E_{16}}{R_1} + \frac{E_{26}}{R_2} \right) \right] \frac{\partial \psi_i}{\partial X_2} \varphi_j - \right. \\
 &\quad c_1 \left[\left(E_{11} + \frac{c_1}{R_1} H_{11} \right) \frac{\partial \psi_i}{\partial X_1} \frac{\partial^2 \varphi_j}{\partial X_1^2} + \left(E_{12} + \frac{c_1}{R_1} H_{12} \right) \frac{\partial \psi_i}{\partial X_1} \frac{\partial^2 \varphi_j}{\partial X_2^2} + 2 \left(E_{16} + \frac{c_1}{R_1} H_{16} \right) \frac{\partial \psi_i}{\partial X_1} \frac{\partial^2 \varphi_j}{\partial X_1 \partial X_2} \right. \\
 &\quad \left. + \left(E_{16} + \frac{c_1}{R_1} H_{16} \right) \frac{\partial \psi_i}{\partial X_2} \frac{\partial^2 \varphi_j}{\partial X_1^2} + \left(E_{26} + \frac{c_1}{R_1} H_{26} \right) \frac{\partial \psi_i}{\partial X_2} \frac{\partial^2 \varphi_j}{\partial X_2^2} + 2 \left(E_{66} + \frac{c_1}{R_1} H_{66} \right) \frac{\partial \psi_i}{\partial X_2} \frac{\partial^2 \varphi_j}{\partial X_2 \partial X_1} \right] \\
 &\quad \left. - \frac{1}{R_1} \left(\hat{A}_{45} \psi_i \frac{\partial \varphi_j}{\partial X_2} + \hat{A}_{55} \psi_i \frac{\partial \varphi_j}{\partial X_1} \right) \right\} dX_1 dX_2 \\
 K_{ij}^{14} &= \int_{\Omega^e} \left\{ \left(\hat{B}_{11} + \frac{c_1}{R_1} \hat{F}_{11} \right) \frac{\partial \psi_i}{\partial X_1} \frac{\partial \psi_j}{\partial X_1} + \left(\hat{B}_{66} + \frac{c_1}{R_1} \hat{F}_{66} \right) \frac{\partial \psi_i}{\partial X_2} \frac{\partial \psi_j}{\partial X_2} + \left(\hat{B}_{16} + \frac{c_1}{R_1} \hat{F}_{16} \right) \left(\frac{\partial \psi_i}{\partial X_1} \frac{\partial \psi_j}{\partial X_2} + \right. \right. \\
 &\quad \left. \left. \frac{\partial \psi_i}{\partial X_2} \frac{\partial \psi_j}{\partial X_1} \right) - \frac{1}{R_1} \hat{A}_{55} \psi_i \psi_j \right\} dX_1 dX_2 \\
 K_{ij}^{15} &= \int_{\Omega^e} \left\{ \left(\hat{B}_{12} + \frac{c_1}{R_1} \hat{F}_{12} \right) \frac{\partial \psi_i}{\partial X_1} \frac{\partial \psi_j}{\partial X_2} + \left(\hat{B}_{16} + \frac{c_1}{R_1} \hat{F}_{16} \right) \frac{\partial \psi_i}{\partial X_1} \frac{\partial \psi_j}{\partial X_1} + \left(\hat{B}_{26} + \frac{c_1}{R_1} \hat{F}_{26} \right) \frac{\partial \psi_i}{\partial X_2} \frac{\partial \psi_j}{\partial X_2} + \right. \\
 &\quad \left. \left(\hat{B}_{66} + \frac{c_1}{R_1} \hat{F}_{66} \right) \frac{\partial \psi_i}{\partial X_2} \frac{\partial \psi_j}{\partial X_1} - \frac{1}{R_1} \hat{A}_{45} \psi_i \psi_j \right\} dX_1 dX_2
 \end{aligned}$$

$$\begin{aligned}
K_{ij}^{21} &= \int_{\Omega^e} \left\{ \left[A_{12} + \left(\frac{c_1}{R_1} + \frac{c_1}{R_2} \right) E_{12} + \left(\frac{c_1}{R_1} \right) \left(\frac{c_1}{R_2} \right) H_{12} \right] \frac{\partial \psi_i}{\partial X_2} \frac{\partial \psi_j}{\partial X_1} + \left[A_{16} + \left(\frac{c_1}{R_1} + \frac{c_1}{R_2} \right) E_{16} + \left(\frac{c_1}{R_1} \right) \right. \right. \\
&\quad \left. \left(\frac{c_1}{R_2} \right) H_{16} \right] \frac{\partial \psi_i}{\partial X_1} \frac{\partial \psi_j}{\partial X_1} + \left[A_{26} + \left(\frac{c_1}{R_1} + \frac{c_1}{R_2} \right) E_{26} + \left(\frac{c_1}{R_1} \right) \left(\frac{c_1}{R_2} \right) H_{26} \right] \frac{\partial \psi_i}{\partial X_2} \frac{\partial \psi_j}{\partial X_2} + \\
&\quad \left. \left[A_{66} + \left(\frac{c_1}{R_1} + \frac{c_1}{R_2} \right) E_{66} + \left(\frac{c_1}{R_1} \right) \left(\frac{c_1}{R_2} \right) H_{66} \right] \frac{\partial \psi_i}{\partial X_1} \frac{\partial \psi_j}{\partial X_2} \right\} dX_1 dX_2 \\
K_{ij}^{22} &= \int_{\Omega^e} \left\{ \left[A_{66} + 2 \frac{c_1}{R_2} E_{66} + \left(\frac{c_1}{R_2} \right)^2 H_{66} \right] \frac{\partial \psi_i}{\partial X_1} \frac{\partial \psi_j}{\partial X_1} + \left[A_{22} + 2 \frac{c_1}{R_2} E_{22} + \left(\frac{c_1}{R_2} \right)^2 H_{22} \right] \frac{\partial \psi_i}{\partial X_2} \frac{\partial \psi_j}{\partial X_2} + \right. \\
&\quad \left. \left[A_{26} + 2 \frac{c_1}{R_2} E_{26} + \left(\frac{c_1}{R_2} \right)^2 H_{26} \right] \left(\frac{\partial \psi_i}{\partial X_1} \frac{\partial \psi_j}{\partial X_2} + \frac{\partial \psi_i}{\partial X_2} \frac{\partial \psi_j}{\partial X_1} \right) + \left(\frac{1}{R_2} \right)^2 \hat{A}_{44} \psi_i \psi_j \right\} dX_1 dX_2 \\
K_{ij}^{23} &= \int_{\Omega^e} \left\{ \left[\left(\frac{A_{12}}{R_1} + \frac{A_{22}}{R_2} \right) + \frac{c_1}{R_2} \left(\frac{E_{12}}{R_1} + \frac{E_{22}}{R_2} \right) \right] \frac{\partial \psi_i}{\partial X_2} \varphi_j + \left[\left(\frac{A_{16}}{R_1} + \frac{A_{26}}{R_2} \right) + \frac{c_1}{R_2} \left(\frac{E_{16}}{R_1} + \frac{E_{26}}{R_2} \right) \right] \frac{\partial \psi_i}{\partial X_1} \varphi_j - \right. \\
&\quad c_1 \left[\left(E_{12} + \frac{c_1}{R_2} H_{12} \right) \frac{\partial \psi_i}{\partial X_2} \frac{\partial^2 \varphi_j}{\partial X_1^2} + \left(E_{22} + \frac{c_1}{R_2} H_{22} \right) \frac{\partial \psi_i}{\partial X_2} \frac{\partial^2 \varphi_j}{\partial X_2^2} + 2 \left(E_{26} + \frac{c_1}{R_2} H_{26} \right) \frac{\partial \psi_i}{\partial X_2} \frac{\partial^2 \varphi_j}{\partial X_1 \partial X_2} \right. \\
&\quad \left. + \left(E_{16} + \frac{c_1}{R_2} H_{16} \right) \frac{\partial \psi_i}{\partial X_1} \frac{\partial^2 \varphi_j}{\partial X_1^2} + \left(E_{26} + \frac{c_1}{R_2} H_{26} \right) \frac{\partial \psi_i}{\partial X_1} \frac{\partial^2 \varphi_j}{\partial X_2^2} + 2 \left(E_{66} + \frac{c_1}{R_2} H_{66} \right) \frac{\partial \psi_i}{\partial X_1} \frac{\partial^2 \varphi_j}{\partial X_1 \partial X_2} \right] \\
&\quad \left. - \frac{1}{R_2} \left(\hat{A}_{44} \psi_i \frac{\partial \varphi_j}{\partial X_2} + \hat{A}_{45} \psi_i \frac{\partial \varphi_j}{\partial X_1} \right) \right\} dX_1 dX_2 \\
K_{ij}^{24} &= \int_{\Omega^e} \left[\left(\hat{B}_{16} + \frac{c_1}{R_2} \hat{F}_{16} \right) \frac{\partial \psi_i}{\partial X_1} \frac{\partial \psi_j}{\partial X_1} + \left(\hat{B}_{66} + \frac{c_1}{R_2} \hat{F}_{66} \right) \frac{\partial \psi_i}{\partial X_1} \frac{\partial \psi_j}{\partial X_2} + \left(\hat{B}_{12} + \frac{c_1}{R_2} \hat{F}_{12} \right) \frac{\partial \psi_i}{\partial X_2} \frac{\partial \psi_j}{\partial X_1} + \right. \\
&\quad \left. \left(\hat{B}_{26} + \frac{c_1}{R_1} \hat{F}_{26} \right) \frac{\partial \psi_i}{\partial X_2} \frac{\partial \psi_j}{\partial X_2} - \frac{1}{R_2} \hat{A}_{45} \psi_i \psi_j \right] dX_1 dX_2 \\
K_{ij}^{25} &= \int_{\Omega^e} \left[\left(\hat{B}_{22} + \frac{c_1}{R_2} \hat{F}_{22} \right) \frac{\partial \psi_i}{\partial X_2} \frac{\partial \psi_j}{\partial X_2} + \left(\hat{B}_{66} + \frac{c_1}{R_2} \hat{F}_{66} \right) \frac{\partial \psi_i}{\partial X_1} \frac{\partial \psi_j}{\partial X_1} + \left(\hat{B}_{26} + \frac{c_1}{R_2} \hat{F}_{26} \right) \left(\frac{\partial \psi_i}{\partial X_1} \frac{\partial \psi_j}{\partial X_2} + \right. \right. \\
&\quad \left. \left. \frac{\partial \psi_i}{\partial X_2} \frac{\partial \psi_j}{\partial X_1} \right) - \frac{1}{R_2} \hat{A}_{44} \psi_i \psi_j \right] dX_1 dX_2 \\
K_{ij}^{31} &= \int_{\Omega^e} \left\{ \left[\left(\frac{A_{11}}{R_1} + \frac{A_{12}}{R_2} \right) + \frac{c_1}{R_1} \left(\frac{E_{11}}{R_1} + \frac{E_{12}}{R_2} \right) \right] \varphi_i \frac{\partial \psi_j}{\partial X_1} + \left[\left(\frac{A_{16}}{R_1} + \frac{A_{26}}{R_2} \right) + \frac{c_1}{R_1} \left(\frac{E_{16}}{R_1} + \frac{E_{26}}{R_2} \right) \right] \varphi_i \frac{\partial \psi_j}{\partial X_2} - c_1 \right. \\
&\quad \left[\left(E_{11} + \frac{c_1}{R_1} H_{11} \right) \frac{\partial^2 \varphi_i}{\partial X_1^2} \frac{\partial \psi_j}{\partial X_1} + \left(E_{12} + \frac{c_1}{R_1} H_{12} \right) \frac{\partial^2 \varphi_i}{\partial X_2^2} \frac{\partial \psi_j}{\partial X_1} + 2 \left(E_{16} + \frac{c_1}{R_1} H_{16} \right) \frac{\partial^2 \varphi_i}{\partial X_1 \partial X_2} \frac{\partial \psi_j}{\partial X_1} \right] + \\
&\quad \left. \left[\left(E_{16} + \frac{c_1}{R_1} H_{16} \right) \frac{\partial^2 \varphi_i}{\partial X_1^2} \frac{\partial \psi_j}{\partial X_2} + \left(E_{26} + \frac{c_1}{R_1} H_{26} \right) \frac{\partial^2 \varphi_i}{\partial X_2^2} \frac{\partial \psi_j}{\partial X_2} + 2 \left(E_{66} + \frac{c_1}{R_1} H_{66} \right) \frac{\partial^2 \varphi_i}{\partial X_1 \partial X_2} \frac{\partial \psi_j}{\partial X_2} \right] \right\}
\end{aligned}$$

$$\begin{aligned}
& -\frac{1}{R_1} \left(\hat{A}_{45} \frac{\partial \varphi_i}{\partial X_2} \psi_j + \hat{A}_{55} \frac{\partial \varphi_i}{\partial X_1} \psi_j \right) \Bigg\} dX_1 dX_2 \\
K_{ij}^{32} = & \int_{\Omega^e} \left\{ \left[\left(\frac{A_{12}}{R_1} + \frac{A_{22}}{R_2} \right) + \frac{c_1}{R_2} \left(\frac{E_{12}}{R_1} + \frac{E_{22}}{R_2} \right) \right] \varphi_i \frac{\partial \psi_j}{\partial X_2} + \left[\left(\frac{A_{16}}{R_1} + \frac{A_{26}}{R_2} \right) + \frac{c_1}{R_2} \left(\frac{E_{16}}{R_1} + \frac{E_{26}}{R_2} \right) \right] \varphi_i \frac{\partial \psi_j}{\partial X_1} - c_1 \right. \\
& \left[\left(E_{12} + \frac{c_1}{R_2} H_{12} \right) \frac{\partial^2 \varphi_i}{\partial X_1^2} \frac{\partial \psi_j}{\partial X_2} + \left(E_{22} + \frac{c_1}{R_2} H_{22} \right) \frac{\partial^2 \varphi_i}{\partial X_2^2} \frac{\partial \psi_j}{\partial X_2} + 2 \left(E_{26} + \frac{c_1}{R_2} H_{26} \right) \frac{\partial^2 \varphi_i}{\partial X_1 \partial X_2} \frac{\partial \psi_j}{\partial X_2} \right] + \\
& \left[\left(E_{16} + \frac{c_1}{R_2} H_{16} \right) \frac{\partial^2 \varphi_i}{\partial X_1^2} \frac{\partial \psi_j}{\partial X_1} + \left(E_{26} + \frac{c_1}{R_2} H_{26} \right) \frac{\partial^2 \varphi_i}{\partial X_2^2} \frac{\partial \psi_j}{\partial X_1} + 2 \left(E_{66} + \frac{c_1}{R_2} H_{66} \right) \frac{\partial^2 \varphi_i}{\partial X_1 \partial X_2} \frac{\partial \psi_j}{\partial X_1} \right] \\
& \left. - \frac{1}{R_2} \left(\hat{A}_{44} \frac{\partial \varphi_i}{\partial X_2} \psi_j + \hat{A}_{45} \frac{\partial \varphi_i}{\partial X_1} \psi_j \right) \right\} dX_1 dX_2 \\
K_{ij}^{33} = & \int_{\Omega^e} \left\{ \left[A_{11} \left(\frac{1}{R_1} \right)^2 + A_{12} \left(\frac{2}{R_1 R_2} \right) + A_{22} \left(\frac{1}{R_2} \right)^2 \right] \varphi_i \varphi_j + (-c_1) \left[\left(\frac{E_{11}}{R_1} + \frac{E_{12}}{R_2} \right) \left(\varphi_i \frac{\partial^2 \varphi_j}{\partial X_1^2} + \frac{\partial^2 \varphi_i}{\partial X_1^2} \varphi_j \right) \right. \right. \\
& + 2 \left(\frac{E_{16}}{R_1} + \frac{E_{26}}{R_2} \right) \left(\varphi_i \frac{\partial^2 \varphi_j}{\partial X_1 \partial X_2} + \frac{\partial^2 \varphi_i}{\partial X_1 \partial X_2} \varphi_j \right) + \left. \left(\frac{E_{12}}{R_1} + \frac{E_{22}}{R_2} \right) \left(\varphi_i \frac{\partial^2 \varphi_j}{\partial X_2^2} + \frac{\partial^2 \varphi_i}{\partial X_2^2} \varphi_j \right) \right] + \\
& \frac{\partial \varphi_i}{\partial X_1} \left(\hat{A}_{45} \frac{\partial \varphi_j}{\partial X_2} + \hat{A}_{55} \frac{\partial \varphi_j}{\partial X_1} \right) + \frac{\partial \varphi_i}{\partial X_2} \left(\hat{A}_{44} \frac{\partial \varphi_j}{\partial X_2} + \hat{A}_{45} \frac{\partial \varphi_j}{\partial X_1} \right) + (c_1)^2 \left[\frac{\partial^2 \varphi_i}{\partial X_1^2} \left(H_{11} \frac{\partial^2 \varphi_j}{\partial X_1^2} + H_{12} \frac{\partial^2 \varphi_j}{\partial X_2^2} \right. \right. \\
& + 2 H_{16} \frac{\partial^2 \varphi_j}{\partial X_1 \partial X_2} \left. \right) + 2 \frac{\partial^2 \varphi_i}{\partial X_1 \partial X_2} \left(H_{16} \frac{\partial^2 \varphi_j}{\partial X_1^2} + H_{26} \frac{\partial^2 \varphi_j}{\partial X_2^2} + 2 H_{66} \frac{\partial^2 \varphi_j}{\partial X_1 \partial X_2} \right) + \frac{\partial^2 \varphi_i}{\partial X_2^2} \left(H_{12} \frac{\partial^2 \varphi_j}{\partial X_1^2} + \right. \\
& \left. \left. H_{22} \frac{\partial^2 \varphi_j}{\partial X_2^2} + 2 H_{26} \frac{\partial^2 \varphi_j}{\partial X_1 \partial X_2} \right) \right] \Bigg\} dX_1 dX_2 \\
K_{ij}^{34} = & \int_{\Omega^e} \left\{ \left(\frac{\hat{B}_{11}}{R_1} + \frac{\hat{B}_{12}}{R_2} \right) \varphi_i \frac{\partial \psi_j}{\partial X_1} + \left(\frac{\hat{B}_{16}}{R_1} + \frac{\hat{B}_{26}}{R_2} \right) \varphi_i \frac{\partial \psi_j}{\partial X_2} + \hat{A}_{55} \frac{\partial \varphi_i}{\partial X_1} \psi_j + \hat{A}_{45} \frac{\partial \varphi_i}{\partial X_2} \psi_j - c_1 \left[\frac{\partial^2 \varphi_i}{\partial X_1^2} \left(\hat{F}_{11} \frac{\partial \psi_j}{\partial X_1} \right. \right. \right. \\
& \left. \left. + \hat{F}_{16} \frac{\partial \psi_j}{\partial X_2} \right) + 2 \frac{\partial^2 \varphi_i}{\partial X_1 \partial X_2} \left(\hat{F}_{16} \frac{\partial \psi_j}{\partial X_1} + \hat{F}_{66} \frac{\partial \psi_j}{\partial X_2} \right) + \frac{\partial^2 \varphi_i}{\partial X_2^2} \left(\hat{F}_{12} \frac{\partial \psi_j}{\partial X_1} + \hat{F}_{26} \frac{\partial \psi_j}{\partial X_2} \right) \right] \Bigg\} dX_1 dX_2 \\
K_{ij}^{35} = & \int_{\Omega^e} \left\{ \left(\frac{\hat{B}_{12}}{R_1} + \frac{\hat{B}_{22}}{R_2} \right) \varphi_i \frac{\partial \psi_j}{\partial X_2} + \left(\frac{\hat{B}_{16}}{R_1} + \frac{\hat{B}_{26}}{R_2} \right) \varphi_i \frac{\partial \psi_j}{\partial X_1} + \hat{A}_{45} \frac{\partial \varphi_i}{\partial X_1} \psi_j + \hat{A}_{44} \frac{\partial \varphi_i}{\partial X_2} \psi_j - c_1 \left[\frac{\partial^2 \varphi_i}{\partial X_1^2} \left(\hat{F}_{12} \frac{\partial \psi_j}{\partial X_2} \right. \right. \right. \\
& \left. \left. + \hat{F}_{16} \frac{\partial \psi_j}{\partial X_1} \right) + 2 \frac{\partial^2 \varphi_i}{\partial X_1 \partial X_2} \left(\hat{F}_{26} \frac{\partial \psi_j}{\partial X_2} + \hat{F}_{66} \frac{\partial \psi_j}{\partial X_1} \right) + \frac{\partial^2 \varphi_i}{\partial X_2^2} \left(\hat{F}_{22} \frac{\partial \psi_j}{\partial X_2} + \hat{F}_{26} \frac{\partial \psi_j}{\partial X_1} \right) \right] \Bigg\} dX_1 dX_2 \\
K_{ij}^{41} = & \int_{\Omega^e} \left\{ \left(\hat{B}_{11} + \frac{c_1}{R_1} \hat{F}_{11} \right) \frac{\partial \psi_i}{\partial X_1} \frac{\partial \psi_j}{\partial X_1} + \left(\hat{B}_{66} + \frac{c_1}{R_1} \hat{F}_{66} \right) \frac{\partial \psi_i}{\partial X_2} \frac{\partial \psi_j}{\partial X_2} + \left(\hat{B}_{16} + \frac{c_1}{R_1} \hat{F}_{16} \right) \left(\frac{\partial \psi_i}{\partial X_1} \frac{\partial \psi_j}{\partial X_2} + \right. \right. \\
& \left. \left. \frac{\partial \psi_i}{\partial X_2} \frac{\partial \psi_j}{\partial X_1} \right) - \frac{1}{R_1} \left(\hat{A}_{55} \psi_i \psi_j \right) \right\} dX_1 dX_2
\end{aligned}$$

$$\begin{aligned}
K_{ij}^{42} &= \int_{\Omega^e} \left[\left(\hat{B}_{12} + \frac{c_1}{R_2} \hat{F}_{12} \right) \frac{\partial \psi_i}{\partial X_1} \frac{\partial \psi_j}{\partial X_2} + \left(\hat{B}_{16} + \frac{c_1}{R_2} \hat{F}_{16} \right) \frac{\partial \psi_i}{\partial X_1} \frac{\partial \psi_j}{\partial X_1} + \left(\hat{B}_{26} + \frac{c_1}{R_2} \hat{F}_{26} \right) \frac{\partial \psi_i}{\partial X_2} \frac{\partial \psi_j}{\partial X_2} + \right. \\
&\quad \left. \left(\hat{B}_{66} + \frac{c_1}{R_2} \hat{F}_{66} \right) \frac{\partial \psi_i}{\partial X_2} \frac{\partial \psi_j}{\partial X_1} - \frac{1}{R_2} \left(\hat{A}_{45} \psi_i \psi_j \right) \right] dX_1 dX_2 \\
K_{ij}^{43} &= \int_{\Omega^e} \left\{ \left(\frac{\hat{B}_{11}}{R_1} + \frac{\hat{B}_{12}}{R_2} \right) \frac{\partial \psi_i}{\partial X_1} \varphi_j + \left(\frac{\hat{B}_{16}}{R_1} + \frac{\hat{B}_{26}}{R_2} \right) \frac{\partial \psi_i}{\partial X_2} \varphi_j + \hat{A}_{45} \psi_i \frac{\partial \varphi_j}{\partial X_2} + \hat{A}_{55} \psi_i \frac{\partial \varphi_j}{\partial X_1} - c_1 \left[\frac{\partial \psi_i}{\partial X_1} \left(\hat{F}_{11} \frac{\partial^2 \varphi_j}{\partial X_1^2} \right. \right. \right. \\
&\quad \left. \left. + \hat{F}_{12} \frac{\partial^2 \varphi_j}{\partial X_2^2} + 2 \hat{F}_{16} \frac{\partial^2 \varphi_j}{\partial X_1 \partial X_2} \right) + \frac{\partial \psi_i}{\partial X_2} \left(\hat{F}_{16} \frac{\partial^2 \varphi_j}{\partial X_1^2} + \hat{F}_{26} \frac{\partial^2 \varphi_j}{\partial X_2^2} + 2 \hat{F}_{66} \frac{\partial^2 \varphi_j}{\partial X_1 \partial X_2} \right) \right] \right\} dX_1 dX_2 \\
K_{ij}^{44} &= \int_{\Omega^e} \left[\hat{A}_{55} \psi_i \psi_j + \left(\hat{D}_{11} - c_1 \hat{F}_{11} \right) \frac{\partial \psi_i}{\partial X_1} \frac{\partial \psi_j}{\partial X_1} + \left(\hat{D}_{66} - c_1 \hat{F}_{66} \right) \frac{\partial \psi_i}{\partial X_2} \frac{\partial \psi_j}{\partial X_2} + \left(\hat{D}_{16} - c_1 \hat{F}_{16} \right) \left(\frac{\partial \psi_i}{\partial X_1} \frac{\partial \psi_j}{\partial X_2} + \right. \right. \\
&\quad \left. \left. \frac{\partial \psi_i}{\partial X_2} \frac{\partial \psi_j}{\partial X_1} \right) \right] dX_1 dX_2 \\
K_{ij}^{45} &= \int_{\Omega^e} \left[\hat{A}_{45} \psi_i \psi_j + \left(\hat{D}_{12} - c_1 \hat{F}_{12} \right) \frac{\partial \psi_i}{\partial X_1} \frac{\partial \psi_j}{\partial X_2} + \left(\hat{D}_{16} - c_1 \hat{F}_{16} \right) \frac{\partial \psi_i}{\partial X_1} \frac{\partial \psi_j}{\partial X_1} + \left(\hat{D}_{26} - c_1 \hat{F}_{26} \right) \frac{\partial \psi_i}{\partial X_2} \frac{\partial \psi_j}{\partial X_2} + \right. \\
&\quad \left. \left(\hat{D}_{66} - c_1 \hat{F}_{66} \right) \frac{\partial \psi_i}{\partial X_2} \frac{\partial \psi_j}{\partial X_1} \right] dX_1 dX_2 \\
K_{ij}^{51} &= \int_{\Omega^e} \left[\left(\hat{B}_{16} + \frac{c_1}{R_1} \hat{F}_{16} \right) \frac{\partial \psi_i}{\partial X_1} \frac{\partial \psi_j}{\partial X_1} + \left(\hat{B}_{66} + \frac{c_1}{R_1} \hat{F}_{66} \right) \frac{\partial \psi_i}{\partial X_1} \frac{\partial \psi_j}{\partial X_2} + \left(\hat{B}_{12} + \frac{c_1}{R_1} \hat{F}_{12} \right) \frac{\partial \psi_i}{\partial X_2} \frac{\partial \psi_j}{\partial X_1} + \right. \\
&\quad \left. \left(\hat{B}_{26} + \frac{c_1}{R_1} \hat{F}_{26} \right) \frac{\partial \psi_i}{\partial X_2} \frac{\partial \psi_j}{\partial X_2} - \frac{1}{R_1} \left(\hat{A}_{45} \psi_i \psi_j \right) \right] dX_1 dX_2 \\
K_{ij}^{52} &= \int_{\Omega^e} \left[\left(\hat{B}_{22} + \frac{c_1}{R_2} \hat{F}_{22} \right) \frac{\partial \psi_i}{\partial X_2} \frac{\partial \psi_j}{\partial X_2} + \left(\hat{B}_{66} + \frac{c_1}{R_2} \hat{F}_{66} \right) \frac{\partial \psi_i}{\partial X_1} \frac{\partial \psi_j}{\partial X_1} + \left(\hat{B}_{26} + \frac{c_1}{R_2} \hat{F}_{26} \right) \left(\frac{\partial \psi_i}{\partial X_1} \frac{\partial \psi_j}{\partial X_2} \right. \right. \\
&\quad \left. \left. + \frac{\partial \psi_i}{\partial X_2} \frac{\partial \psi_j}{\partial X_1} \right) - \frac{1}{R_2} \left(\hat{A}_{44} \psi_i \psi_j \right) \right] dX_1 dX_2 \\
K_{ij}^{53} &= \int_{\Omega^e} \left\{ \left(\frac{\hat{B}_{12}}{R_1} + \frac{\hat{B}_{22}}{R_2} \right) \frac{\partial \psi_i}{\partial X_2} \varphi_j + \left(\frac{\hat{B}_{16}}{R_1} + \frac{\hat{B}_{26}}{R_2} \right) \frac{\partial \psi_i}{\partial X_1} \varphi_j + \hat{A}_{44} \psi_i \frac{\partial \varphi_j}{\partial X_2} + \hat{A}_{45} \psi_i \frac{\partial \varphi_j}{\partial X_1} - c_1 \left[\frac{\partial \psi_i}{\partial X_2} \left(\hat{F}_{12} \frac{\partial^2 \varphi_j}{\partial X_1^2} \right. \right. \right. \\
&\quad \left. \left. + \hat{F}_{22} \frac{\partial^2 \varphi_j}{\partial X_2^2} + 2 \hat{F}_{26} \frac{\partial^2 \varphi_j}{\partial X_1 \partial X_2} \right) + \frac{\partial \psi_i}{\partial X_1} \left(\hat{F}_{16} \frac{\partial^2 \varphi_j}{\partial X_1^2} + \hat{F}_{26} \frac{\partial^2 \varphi_j}{\partial X_2^2} + 2 \hat{F}_{66} \frac{\partial^2 \varphi_j}{\partial X_1 \partial X_2} \right) \right] \right\} dX_1 dX_2 \\
K_{ij}^{54} &= \int_{\Omega^e} \left[\hat{A}_{45} \psi_i \psi_j + \left(\hat{D}_{16} - c_1 \hat{F}_{16} \right) \frac{\partial \psi_i}{\partial X_1} \frac{\partial \psi_j}{\partial X_1} + \left(\hat{D}_{66} - c_1 \hat{F}_{66} \right) \frac{\partial \psi_i}{\partial X_1} \frac{\partial \psi_j}{\partial X_2} + \left(\hat{D}_{12} - c_1 \hat{F}_{12} \right) \frac{\partial \psi_i}{\partial X_2} \frac{\partial \psi_j}{\partial X_1} + \right. \\
&\quad \left. \left(\hat{D}_{26} - c_1 \hat{F}_{26} \right) \frac{\partial \psi_i}{\partial X_2} \frac{\partial \psi_j}{\partial X_2} \right] dX_1 dX_2
\end{aligned}$$

$$K_{ij}^{55} = \int_{\Omega^e} \left[\hat{A}_{44} \psi_i \psi_j + \left(\hat{D}_{66} - c_1 \hat{F}_{66} \right) \frac{\partial \psi_i}{\partial X_1} \frac{\partial \psi_j}{\partial X_1} + \left(\hat{D}_{22} - c_1 \hat{F}_{22} \right) \frac{\partial \psi_i}{\partial X_2} \frac{\partial \psi_j}{\partial X_2} + \left(\hat{D}_{26} - c_1 \hat{F}_{26} \right) \left(\frac{\partial \psi_i}{\partial X_1} \frac{\partial \psi_j}{\partial X_2} + \frac{\partial \psi_i}{\partial X_2} \frac{\partial \psi_j}{\partial X_1} \right) \right] dX_1 dX_2$$

$$M_{ij}^{11} = \int_{\Omega^e} \bar{I}_0 \psi_i \psi_j dX_1 dX_2$$

$$M_{ij}^{22} = \int_{\Omega^e} \bar{I}'_0 \psi_i \psi_j dX_1 dX_2$$

$$M_{ij}^{31} = M_{ji}^{13} = -c_1 \int_{\Omega^e} \bar{I}_3 \frac{\partial \varphi_i}{\partial X_1} \psi_j dX_1 dX_2$$

$$M_{ij}^{32} = M_{ji}^{23} = -c_1 \int_{\Omega^e} \bar{I}'_3 \frac{\partial \varphi_i}{\partial X_2} \psi_j dX_1 dX_2$$

$$M_{ij}^{33} = \int_{\Omega^e} \left[I_0 \varphi_i \varphi_j + c_1^2 I_6 \left(\frac{\partial \varphi_i}{\partial X_1} \frac{\partial \varphi_j}{\partial X_1} + \frac{\partial \varphi_i}{\partial X_2} \frac{\partial \varphi_j}{\partial X_2} \right) \right] dX_1 dX_2$$

$$M_{ij}^{41} = M_{ji}^{14} = \int_{\Omega^e} \bar{J}_1 \psi_i \psi_j dX_1 dX_2$$

$$M_{ij}^{43} = M_{ji}^{34} = -c_1 J_4 \int_{\Omega^e} \psi_i \frac{\partial \varphi_j}{\partial X_1} dX_1 dX_2$$

$$M_{ij}^{44} = \int_{\Omega^e} \bar{K}_2 \psi_i \psi_j dX_1 dX_2$$

$$M_{ij}^{52} = M_{ji}^{25} = \int_{\Omega^e} \bar{J}'_1 \psi_i \psi_j dX_1 dX_2$$

$$M_{ij}^{53} = M_{ji}^{35} = -c_1 J_4 \int_{\Omega^e} \psi_i \frac{\partial \varphi_j}{\partial X_2} dX_1 dX_2$$

$$M_{ij}^{55} = \int_{\Omega^e} \bar{K}_2 \psi_i \psi_j dX_1 dX_2$$

$$M_{ij}^{12} = M_{ij}^{15} = M_{ij}^{21} = M_{ij}^{24} = M_{ij}^{42} = M_{ij}^{45} = M_{ij}^{51} = M_{ij}^{54} = 0$$

$$C_{ij}^{13} = \int_{\Omega^e} \left(\tilde{A}_{31}^M + \frac{c_1}{R_1} \tilde{E}_{31}^M \right) \frac{\partial \psi_i}{\partial X_1} \varphi_j dX_1 dX_2$$

$$C_{ij}^{23} = \int_{\Omega^e} \left(\tilde{A}_{32}^M + \frac{c_1}{R_2} \tilde{E}_{32}^M \right) \frac{\partial \psi_i}{\partial X_2} \varphi_j dX_1 dX_2$$

$$C_{ij}^{33} = \int_{\Omega^e} \left[\left(\frac{\tilde{A}_{31}^M}{R_1} + \frac{\tilde{A}_{32}^M}{R_2} \right) \varphi_i \varphi_j - c_1 \left(\tilde{E}_{31}^M \frac{\partial^2 \varphi_i}{\partial X_1^2} + \tilde{E}_{32}^M \frac{\partial^2 \varphi_i}{\partial X_2^2} \right) \varphi_j \right] dX_1 dX_2$$

$$C_{ij}^{43} = \int_{\Omega^e} (\tilde{B}_{31}^M - c_1 \tilde{E}_{31}^M) \frac{\partial \psi_i}{\partial X_1} \varphi_j dX_1 dX_2$$

$$C_{ij}^{53} = \int_{\Omega^e} (\tilde{B}_{32}^M - c_1 \tilde{E}_{32}^M) \frac{\partial \psi_i}{\partial X_2} \varphi_j dX_1 dX_2$$

$$C_{ij}^{11} = C_{ij}^{12} = C_{ij}^{14} = C_{ij}^{15} = C_{ij}^{21} = C_{ij}^{22} = C_{ij}^{24} = C_{ij}^{25} = C_{ij}^{31} = C_{ij}^{32} = C_{ij}^{34} = C_{ij}^{35} = 0$$

$$C_{ij}^{41} = C_{ij}^{42} = C_{ij}^{44} = C_{ij}^{45} = C_{ij}^{51} = C_{ij}^{52} = C_{ij}^{54} = C_{ij}^{55} = 0$$

$$F_i^1 = \oint_{\Gamma^e} \left[\left(N_1 + \frac{c_1}{R_1} P_1 \right) n_1 + \left(N_6 + \frac{c_1}{R_1} P_6 \right) n_2 \right] \psi_i ds$$

$$F_i^2 = \oint_{\Gamma^e} \left[\left(N_6 + \frac{c_1}{R_2} P_6 \right) n_1 + \left(N_2 + \frac{c_1}{R_2} P_2 \right) n_2 \right] \psi_i ds$$

$$F_i^3 = \int_{\Omega^e} q \varphi_i dX_1 dX_2 + \oint_{\Gamma^e} \left(\bar{V}_n \varphi_i + p_{nn} \frac{\partial \varphi_i}{\partial n} \right) ds$$

$$F_i^4 = \oint_{\Gamma^e} (\bar{M}_1 n_1 + \bar{M}_6 n_2) \psi_i ds, \quad F_i^5 = \oint_{\Gamma^e} (\bar{M}_6 n_1 + \bar{M}_2 n_2) \psi_i ds$$

$$F_i^{T1} = \int_{\Omega^e} \left[\frac{\partial \psi_i}{\partial X_1} \left(N_1^T + \frac{c_1}{R_1} P_1^T \right) + \frac{\partial \psi_i}{\partial X_2} \left(N_6^T + \frac{c_1}{R_1} P_6^T \right) \right] dX_1 dX_2$$

$$F_i^{T2} = \int_{\Omega^e} \left[\frac{\partial \psi_i}{\partial X_1} \left(N_6^T + \frac{c_1}{R_2} P_6^T \right) + \frac{\partial \psi_i}{\partial X_2} \left(N_2^T + \frac{c_1}{R_2} P_2^T \right) \right] dX_1 dX_2$$

$$F_i^{T3} = \int_{\Omega^e} \left[\left(\frac{N_1^T}{R_1} + \frac{N_2^T}{R_2} \right) \varphi_i - c_1 \left(\frac{\partial^2 \varphi_i}{\partial X_1^2} P_1^T + 2 \frac{\partial^2 \varphi_i}{\partial X_1 \partial X_2} P_6^T + \frac{\partial^2 \varphi_i}{\partial X_2^2} P_2^T \right) \right] dX_1 dX_2$$

$$F_i^{T4} = \int_{\Omega^e} \left[\frac{\partial \psi_i}{\partial X_1} (M_1^T - c_1 P_1^T) + \frac{\partial \psi_i}{\partial X_2} (M_6^T - c_1 P_6^T) \right] dX_1 dX_2$$

$$F_i^{T5} = \int_{\Omega^e} \left[\frac{\partial \psi_i}{\partial X_1} (M_6^T - c_1 P_6^T) + \frac{\partial \psi_i}{\partial X_2} (M_2^T - c_1 P_2^T) \right] dX_1 dX_2$$

C.2 Additional nonlinear coefficients of laminated composite shells by Sanders shell theory

$$(K_{ij}^{13})_{NL} = \left(\frac{1}{2} \right) \int_{\Omega^e} \left\{ \frac{\partial \psi_i}{\partial X_1} \left[\left(A_{11} + \frac{c_1}{R_1} E_{11} \right) \frac{\partial w_0}{\partial X_1} \frac{\partial \varphi_j}{\partial X_1} + \left(A_{12} + \frac{c_1}{R_1} E_{12} \right) \frac{\partial w_0}{\partial X_2} \frac{\partial \varphi_j}{\partial X_2} + \left(A_{16} + \frac{c_1}{R_1} E_{16} \right) \left(\frac{\partial w_0}{\partial X_1} \frac{\partial \varphi_j}{\partial X_2} + \frac{\partial w_0}{\partial X_2} \frac{\partial \varphi_j}{\partial X_1} \right) \right] + \frac{\partial \psi_i}{\partial X_2} \left[\left(A_{16} + \frac{c_1}{R_1} E_{16} \right) \frac{\partial w_0}{\partial X_1} \frac{\partial \varphi_j}{\partial X_1} + \left(A_{26} + \frac{c_1}{R_1} E_{26} \right) \frac{\partial w_0}{\partial X_2} \frac{\partial \varphi_j}{\partial X_2} + \left(A_{66} + \frac{c_1}{R_1} E_{66} \right) \left(\frac{\partial w_0}{\partial X_1} \frac{\partial \varphi_j}{\partial X_2} + \frac{\partial w_0}{\partial X_2} \frac{\partial \varphi_j}{\partial X_1} \right) \right] \right\} dX_1 dX_2$$

$$(K_{ij}^{23})_{NL} = \left(\frac{1}{2} \right) \int_{\Omega^e} \left\{ \frac{\partial \psi_i}{\partial X_2} \left[\left(A_{12} + \frac{c_1}{R_2} E_{12} \right) \frac{\partial w_0}{\partial X_1} \frac{\partial \varphi_j}{\partial X_1} + \left(A_{22} + \frac{c_1}{R_2} E_{22} \right) \frac{\partial w_0}{\partial X_2} \frac{\partial \varphi_j}{\partial X_2} + \left(A_{26} + \frac{c_1}{R_2} E_{26} \right) \left(\frac{\partial w_0}{\partial X_1} \frac{\partial \varphi_j}{\partial X_2} + \frac{\partial w_0}{\partial X_2} \frac{\partial \varphi_j}{\partial X_1} \right) \right] + \frac{\partial \psi_i}{\partial X_1} \left[\left(A_{16} + \frac{c_1}{R_2} E_{16} \right) \frac{\partial w_0}{\partial X_1} \frac{\partial \varphi_j}{\partial X_1} + \left(A_{26} + \frac{c_1}{R_2} E_{26} \right) \left(\frac{\partial w_0}{\partial X_1} \frac{\partial \varphi_j}{\partial X_2} + \frac{\partial w_0}{\partial X_2} \frac{\partial \varphi_j}{\partial X_1} \right) \right] \right\} dX_1 dX_2$$

$$\begin{aligned}
& \frac{\partial w_0}{\partial X_2} \frac{\partial \varphi_j}{\partial X_2} + \left(A_{66} + \frac{c_1}{R_2} E_{66} \right) \left(\frac{\partial w_0}{\partial X_1} \frac{\partial \varphi_j}{\partial X_2} + \frac{\partial w_0}{\partial X_2} \frac{\partial \varphi_j}{\partial X_1} \right) \Bigg] \Bigg\} dX_1 dX_2 \\
(K_{ij}^{31})_{NL} = & \int_{\Omega^e} \left(\frac{\partial \varphi_i}{\partial X_1} \left\{ \frac{\partial w_0}{\partial X_1} \left[\left(A_{11} + \frac{c_1}{R_1} E_{11} \right) \frac{\partial \psi_j}{\partial X_1} + \left(A_{16} + \frac{c_1}{R_1} E_{16} \right) \frac{\partial \psi_j}{\partial X_2} \right] + \frac{\partial w_0}{\partial X_2} \left[\left(A_{16} + \frac{c_1}{R_1} E_{16} \right) \frac{\partial \psi_j}{\partial X_1} \right. \right. \right. \\
& + \left. \left. \left(A_{66} + \frac{c_1}{R_1} E_{66} \right) \frac{\partial \psi_j}{\partial X_2} \right] \right\} + \frac{\partial \varphi_i}{\partial X_2} \left\{ \frac{\partial w_0}{\partial X_1} \left[\left(A_{16} + \frac{c_1}{R_1} E_{16} \right) \frac{\partial \psi_j}{\partial X_1} + \left(A_{66} + \frac{c_1}{R_1} E_{66} \right) \frac{\partial \psi_j}{\partial X_2} \right] \right. \\
& + \left. \frac{\partial w_0}{\partial X_2} \left[\left(A_{12} + \frac{c_1}{R_1} E_{12} \right) \frac{\partial \psi_j}{\partial X_1} + \left(A_{26} + \frac{c_1}{R_1} E_{26} \right) \frac{\partial \psi_j}{\partial X_2} \right] \right\} \Bigg) dX_1 dX_2 \\
(K_{ij}^{32})_{NL} = & \int_{\Omega^e} \left(\frac{\partial \varphi_i}{\partial X_1} \left\{ \frac{\partial w_0}{\partial X_1} \left[\left(A_{12} + \frac{c_1}{R_2} E_{12} \right) \frac{\partial \psi_j}{\partial X_2} + \left(A_{16} + \frac{c_1}{R_2} E_{16} \right) \frac{\partial \psi_j}{\partial X_1} \right] + \frac{\partial w_0}{\partial X_2} \left[\left(A_{26} + \frac{c_1}{R_2} E_{26} \right) \frac{\partial \psi_j}{\partial X_2} \right. \right. \right. \\
& + \left. \left. \left(A_{66} + \frac{c_1}{R_2} E_{66} \right) \frac{\partial \psi_j}{\partial X_1} \right] \right\} + \frac{\partial \varphi_i}{\partial X_2} \left\{ \frac{\partial w_0}{\partial X_1} \left[\left(A_{26} + \frac{c_1}{R_2} E_{26} \right) \frac{\partial \psi_j}{\partial X_2} + \left(A_{66} + \frac{c_1}{R_2} E_{66} \right) \frac{\partial \psi_j}{\partial X_1} \right] \right. \\
& + \left. \frac{\partial w_0}{\partial X_2} \left[\left(A_{22} + \frac{c_1}{R_2} E_{22} \right) \frac{\partial \psi_j}{\partial X_2} + \left(A_{26} + \frac{c_1}{R_2} E_{26} \right) \frac{\partial \psi_j}{\partial X_1} \right] \right\} \Bigg) dX_1 dX_2 \\
(K_{ij}^{33})_{NL} = & \left(\frac{1}{2} \right) \int_{\Omega^e} \left((-c_1) \left\{ \frac{\partial^2 \varphi_i}{\partial X_1^2} \left[\frac{\partial w_0}{\partial X_1} \left(E_{11} \frac{\partial \varphi_j}{\partial X_1} + E_{16} \frac{\partial \varphi_j}{\partial X_2} \right) + \frac{\partial w_0}{\partial X_2} \left(E_{12} \frac{\partial \varphi_j}{\partial X_2} + E_{16} \frac{\partial \varphi_j}{\partial X_1} \right) \right] + 2 \frac{\partial^2 \varphi_i}{\partial X_1 \partial X_2} \right. \right. \\
& \left[\frac{\partial w_0}{\partial X_1} \left(E_{16} \frac{\partial \varphi_j}{\partial X_1} + E_{66} \frac{\partial \varphi_j}{\partial X_2} \right) + \frac{\partial w_0}{\partial X_2} \left(E_{26} \frac{\partial \varphi_j}{\partial X_2} + E_{66} \frac{\partial \varphi_j}{\partial X_1} \right) \right] + \frac{\partial^2 \varphi_i}{\partial X_2^2} \left[\frac{\partial w_0}{\partial X_1} \left(E_{12} \frac{\partial \varphi_j}{\partial X_1} + E_{26} \frac{\partial \varphi_j}{\partial X_2} \right) \right. \\
& + \left. \frac{\partial w_0}{\partial X_2} \left(E_{22} \frac{\partial \varphi_j}{\partial X_2} + E_{26} \frac{\partial \varphi_j}{\partial X_1} \right) \right] \Bigg\} + \varphi_i \left[\left(\frac{A_{11}}{R_1} + \frac{A_{12}}{R_2} \right) \frac{\partial w_0}{\partial X_1} \frac{\partial \varphi_j}{\partial X_1} + \left(\frac{A_{12}}{R_1} + \frac{A_{22}}{R_2} \right) \frac{\partial w_0}{\partial X_2} \frac{\partial \varphi_j}{\partial X_2} + \left(\frac{A_{16}}{R_1} + \right. \right. \\
& \left. \frac{A_{26}}{R_2} \right) \left(\frac{\partial w_0}{\partial X_1} \frac{\partial \varphi_j}{\partial X_2} + \frac{\partial \varphi_j}{\partial X_1} \frac{\partial w_0}{\partial X_2} \right) + \frac{\partial \varphi_i}{\partial X_1} \left\{ \frac{\partial w_0}{\partial X_1} \left[2 \left(\frac{A_{11}}{R_1} + \frac{A_{12}}{R_2} \right) w_0 \varphi_j + A_{11} \frac{\partial w_0}{\partial X_1} \frac{\partial \varphi_j}{\partial X_1} + A_{12} \frac{\partial w_0}{\partial X_2} \frac{\partial \varphi_j}{\partial X_2} \right. \right. \\
& + A_{16} \left(\frac{\partial w_0}{\partial X_1} \frac{\partial \varphi_j}{\partial X_2} + \frac{\partial \varphi_j}{\partial X_1} \frac{\partial w_0}{\partial X_2} \right) - 2c_1 \left(E_{11} \frac{\partial^2 \varphi_j}{\partial X_1^2} + E_{12} \frac{\partial^2 \varphi_j}{\partial X_2^2} + 2E_{16} \frac{\partial^2 \varphi_j}{\partial X_1 \partial X_2} \right) \Bigg] \Bigg\} + \frac{\partial w_0}{\partial X_2} \left[2 \left(\frac{A_{16}}{R_1} \right. \right. \\
& + \left. \frac{A_{26}}{R_2} \right) w_0 \varphi_j + A_{16} \frac{\partial w_0}{\partial X_1} \frac{\partial \varphi_j}{\partial X_1} + A_{26} \frac{\partial w_0}{\partial X_2} \frac{\partial \varphi_j}{\partial X_2} + A_{66} \left(\frac{\partial w_0}{\partial X_1} \frac{\partial \varphi_j}{\partial X_2} + \frac{\partial \varphi_j}{\partial X_1} \frac{\partial w_0}{\partial X_2} \right) - 2c_1 \left(E_{16} \frac{\partial^2 \varphi_j}{\partial X_1^2} + \right. \\
& \left. E_{26} \frac{\partial^2 \varphi_j}{\partial X_2^2} + 2E_{66} \frac{\partial^2 \varphi_j}{\partial X_1 \partial X_2} \right) \Bigg] \Bigg\} + \frac{\partial \varphi_i}{\partial X_2} \left\{ \frac{\partial w_0}{\partial X_1} \left[2 \left(\frac{A_{16}}{R_1} + \frac{A_{26}}{R_2} \right) w_0 \varphi_j + A_{16} \frac{\partial w_0}{\partial X_1} \frac{\partial \varphi_j}{\partial X_1} + A_{26} \frac{\partial w_0}{\partial X_2} \frac{\partial \varphi_j}{\partial X_2} \right. \right. \\
& + A_{66} \left(\frac{\partial w_0}{\partial X_1} \frac{\partial \varphi_j}{\partial X_2} + \frac{\partial \varphi_j}{\partial X_1} \frac{\partial w_0}{\partial X_2} \right) - 2c_1 \left(E_{16} \frac{\partial^2 \varphi_j}{\partial X_1^2} + E_{26} \frac{\partial^2 \varphi_j}{\partial X_2^2} + 2E_{66} \frac{\partial^2 \varphi_j}{\partial X_1 \partial X_2} \right) \Bigg] \Bigg\} + \frac{\partial w_0}{\partial X_2} \left[2 \left(\frac{A_{12}}{R_1} + \right. \right.
\end{aligned}$$

$$\begin{aligned}
& \left. \frac{A_{22}}{R_2} \right) w_0 \varphi_j + A_{12} \frac{\partial w_0}{\partial X_1} \frac{\partial \varphi_j}{\partial X_1} + A_{22} \frac{\partial w_0}{\partial X_2} \frac{\partial \varphi_j}{\partial X_2} + A_{26} \left(\frac{\partial w_0}{\partial X_1} \frac{\partial \varphi_j}{\partial X_2} + \frac{\partial \varphi_j}{\partial X_1} \frac{\partial w_0}{\partial X_2} \right) - 2c_1 \left(E_{12} \frac{\partial^2 \varphi_j}{\partial X_1^2} + \right. \\
& \left. E_{22} \frac{\partial^2 \varphi_j}{\partial X_2^2} + 2E_{26} \frac{\partial^2 \varphi_j}{\partial X_1 \partial X_2} \right) \Bigg] \Bigg] dX_1 dX_2 \\
(K_{ij}^{33})_{NL} &= \int_{\Omega^e} \left[N_1^T \frac{\partial \varphi_i}{\partial X_1} \frac{\partial \varphi_j}{\partial X_1} + N_2^T \frac{\partial \varphi_i}{\partial X_2} \frac{\partial \varphi_j}{\partial X_2} + N_6^T \left(\frac{\partial \varphi_i}{\partial X_1} \frac{\partial \varphi_j}{\partial X_2} + \frac{\partial \varphi_i}{\partial X_2} \frac{\partial \varphi_j}{\partial X_1} \right) \right] dX_1 dX_2 \\
(K_{ij}^{34})_{NL} &= \int_{\Omega^e} \left\{ \frac{\partial \varphi_i}{\partial X_1} \left[\frac{\partial w_0}{\partial X_1} \left(\hat{B}_{11} \frac{\partial \psi_j}{\partial X_1} + \hat{B}_{16} \frac{\partial \psi_j}{\partial X_2} \right) + \frac{\partial w_0}{\partial X_2} \left(\hat{B}_{16} \frac{\partial \psi_j}{\partial X_1} + \hat{B}_{66} \frac{\partial \psi_j}{\partial X_2} \right) \right] + \right. \\
& \left. \frac{\partial \varphi_i}{\partial X_2} \left[\frac{\partial w_0}{\partial X_1} \left(\hat{B}_{16} \frac{\partial \psi_j}{\partial X_1} + \hat{B}_{66} \frac{\partial \psi_j}{\partial X_2} \right) + \frac{\partial w_0}{\partial X_2} \left(\hat{B}_{12} \frac{\partial \psi_j}{\partial X_1} + \hat{B}_{26} \frac{\partial \psi_j}{\partial X_2} \right) \right] \right\} dX_1 dX_2 \\
(K_{ij}^{35})_{NL} &= \int_{\Omega^e} \left\{ \frac{\partial \varphi_i}{\partial X_1} \left[\frac{\partial w_0}{\partial X_1} \left(\hat{B}_{12} \frac{\partial \psi_j}{\partial X_2} + \hat{B}_{16} \frac{\partial \psi_j}{\partial X_1} \right) + \frac{\partial w_0}{\partial X_2} \left(\hat{B}_{26} \frac{\partial \psi_j}{\partial X_2} + \hat{B}_{66} \frac{\partial \psi_j}{\partial X_1} \right) \right] + \right. \\
& \left. \frac{\partial \varphi_i}{\partial X_2} \left[\frac{\partial w_0}{\partial X_1} \left(\hat{B}_{26} \frac{\partial \psi_j}{\partial X_2} + \hat{B}_{66} \frac{\partial \psi_j}{\partial X_1} \right) + \frac{\partial w_0}{\partial X_2} \left(\hat{B}_{22} \frac{\partial \psi_j}{\partial X_2} + \hat{B}_{26} \frac{\partial \psi_j}{\partial X_1} \right) \right] \right\} dX_1 dX_2 \\
(K_{ij}^{43})_{NL} &= \left(\frac{1}{2} \right) \int_{\Omega^e} \left\{ \frac{\partial \psi_i}{\partial X_1} \left[\hat{B}_{11} \frac{\partial w_0}{\partial X_1} \frac{\partial \varphi_j}{\partial X_1} + \hat{B}_{12} \frac{\partial w_0}{\partial X_2} \frac{\partial \varphi_j}{\partial X_2} + \hat{B}_{16} \left(\frac{\partial w_0}{\partial X_1} \frac{\partial \varphi_j}{\partial X_2} + \frac{\partial w_0}{\partial X_2} \frac{\partial \varphi_j}{\partial X_1} \right) \right] \right. \\
& \left. + \frac{\partial \psi_i}{\partial X_2} \left[\hat{B}_{16} \frac{\partial w_0}{\partial X_1} \frac{\partial \varphi_j}{\partial X_1} + \hat{B}_{26} \frac{\partial w_0}{\partial X_2} \frac{\partial \varphi_j}{\partial X_2} + \hat{B}_{66} \left(\frac{\partial w_0}{\partial X_1} \frac{\partial \varphi_j}{\partial X_2} + \frac{\partial w_0}{\partial X_2} \frac{\partial \varphi_j}{\partial X_1} \right) \right] \right\} dX_1 dX_2 \\
(K_{ij}^{53})_{NL} &= \left(\frac{1}{2} \right) \int_{\Omega^e} \left\{ \frac{\partial \psi_i}{\partial X_2} \left[\hat{B}_{12} \frac{\partial w_0}{\partial X_1} \frac{\partial \varphi_j}{\partial X_1} + \hat{B}_{22} \frac{\partial w_0}{\partial X_2} \frac{\partial \varphi_j}{\partial X_2} + \hat{B}_{26} \left(\frac{\partial w_0}{\partial X_1} \frac{\partial \varphi_j}{\partial X_2} + \frac{\partial w_0}{\partial X_2} \frac{\partial \varphi_j}{\partial X_1} \right) \right] \right. \\
& \left. + \frac{\partial \psi_i}{\partial X_1} \left[\hat{B}_{16} \frac{\partial w_0}{\partial X_1} \frac{\partial \varphi_j}{\partial X_1} + \hat{B}_{26} \frac{\partial w_0}{\partial X_2} \frac{\partial \varphi_j}{\partial X_2} + \hat{B}_{66} \left(\frac{\partial w_0}{\partial X_1} \frac{\partial \varphi_j}{\partial X_2} + \frac{\partial w_0}{\partial X_2} \frac{\partial \varphi_j}{\partial X_1} \right) \right] \right\} dX_1 dX_2 \\
(C_{ij}^{33})_{NL} &= \int_{\Omega^e} \left(\tilde{A}_{31}^M \frac{\partial w_0}{\partial X_1} \frac{\partial \varphi_i}{\partial X_1} + \tilde{A}_{32}^M \frac{\partial w_0}{\partial X_2} \frac{\partial \varphi_i}{\partial X_2} \right) \varphi_j dX_1 dX_2
\end{aligned}$$

C.3 Tangent stiffness coefficients of laminated composite shells by Sanders shell theory

$$\begin{aligned}
T_{ij}^{11} &= \sum_{\gamma=1}^5 \sum_{k=1}^{n^*} \frac{\partial K_{ik}^{1\gamma}}{\partial u_j} \Delta_k^\gamma + K_{ij}^{11} = K_{ij}^{11} \\
T_{ij}^{12} &= \sum_{\gamma=1}^5 \sum_{k=1}^{n^*} \frac{\partial K_{ik}^{1\gamma}}{\partial v_j} \Delta_k^\gamma + K_{ij}^{12} = K_{ij}^{12}
\end{aligned}$$

$$\begin{aligned}
T_{ij}^{13} &= \sum_{\gamma=1}^5 \sum_{k=1}^{n^*} \frac{\partial K_{ik}^{1\gamma}}{\partial \Delta_j^3} \Delta_k^\gamma + K_{ij}^{13} = \sum_{k=1}^{n^*} \frac{\partial K_{ik}^{13}}{\partial \bar{\Delta}_j} \bar{\Delta}_k + K_{ij}^{13} \\
\sum_{k=1}^{n^*} \frac{\partial K_{ik}^{13}}{\partial \bar{\Delta}_j} \bar{\Delta}_k &= \left(\frac{1}{2} \right) \int_{\Omega^e} \left\{ \frac{\partial \psi_i}{\partial X_1} \left[\left(A_{11} + \frac{c_1}{R_1} E_{11} \right) \frac{\partial w_0}{\partial X_1} \frac{\partial \varphi_j}{\partial X_1} + \left(A_{12} + \frac{c_1}{R_1} E_{12} \right) \frac{\partial w_0}{\partial X_2} \frac{\partial \varphi_j}{\partial X_2} + \left(A_{16} + \frac{c_1}{R_1} E_{16} \right) \right. \right. \\
&\quad \left. \left(\frac{\partial w_0}{\partial X_1} \frac{\partial \varphi_j}{\partial X_2} + \frac{\partial w_0}{\partial X_2} \frac{\partial \varphi_j}{\partial X_1} \right) \right] + \frac{\partial \psi_i}{\partial X_2} \left[\left(A_{16} + \frac{c_1}{R_1} E_{16} \right) \frac{\partial w_0}{\partial X_1} \frac{\partial \varphi_j}{\partial X_1} + \left(A_{26} + \frac{c_1}{R_1} E_{26} \right) \frac{\partial w_0}{\partial X_2} \right. \\
&\quad \left. \frac{\partial \varphi_j}{\partial X_2} + \left(A_{66} + \frac{c_1}{R_1} E_{66} \right) \left(\frac{\partial w_0}{\partial X_1} \frac{\partial \varphi_j}{\partial X_2} + \frac{\partial w_0}{\partial X_2} \frac{\partial \varphi_j}{\partial X_1} \right) \right] \right\} dX_1 dX_2
\end{aligned}$$

$$T_{ij}^{14} = \sum_{\gamma=1}^5 \sum_{k=1}^{n^*} \frac{\partial K_{ik}^{1\gamma}}{\partial X_j} \Delta_k^\gamma + K_{ij}^{14} = K_{ij}^{14}$$

$$T_{ij}^{15} = \sum_{\gamma=1}^5 \sum_{k=1}^{n^*} \frac{\partial K_{ik}^{1\gamma}}{\partial Y_j} \Delta_k^\gamma + K_{ij}^{15} = K_{ij}^{15}$$

$$T_{ij}^{21} = \sum_{\gamma=1}^5 \sum_{k=1}^{n^*} \frac{\partial K_{ik}^{2\gamma}}{\partial u_j} \Delta_k^\gamma + K_{ij}^{21} = K_{ij}^{21}$$

$$T_{ij}^{22} = \sum_{\gamma=1}^5 \sum_{k=1}^{n^*} \frac{\partial K_{ik}^{2\gamma}}{\partial v_j} \Delta_k^\gamma + K_{ij}^{22} = K_{ij}^{22}$$

$$T_{ij}^{23} = \sum_{\gamma=1}^5 \sum_{k=1}^{n^*} \frac{\partial K_{ik}^{2\gamma}}{\partial \Delta_j^3} \Delta_k^\gamma + K_{ij}^{23} = \sum_{k=1}^{n^*} \frac{\partial K_{ik}^{23}}{\partial \bar{\Delta}_j} \bar{\Delta}_k + K_{ij}^{23}$$

$$\begin{aligned}
\sum_{k=1}^{n^*} \frac{\partial K_{ik}^{23}}{\partial \bar{\Delta}_j} \bar{\Delta}_k &= \left(\frac{1}{2} \right) \int_{\Omega^e} \left\{ \frac{\partial \psi_i}{\partial X_2} \left[\left(A_{12} + \frac{c_1}{R_2} E_{12} \right) \frac{\partial w_0}{\partial X_1} \frac{\partial \varphi_j}{\partial X_1} + \left(A_{22} + \frac{c_1}{R_2} E_{22} \right) \frac{\partial w_0}{\partial X_2} \frac{\partial \varphi_j}{\partial X_2} + \left(A_{26} + \frac{c_1}{R_2} E_{26} \right) \right. \right. \\
&\quad \left. \left(\frac{\partial w_0}{\partial X_1} \frac{\partial \varphi_j}{\partial X_2} + \frac{\partial w_0}{\partial X_2} \frac{\partial \varphi_j}{\partial X_1} \right) \right] + \frac{\partial \psi_i}{\partial X_1} \left[\left(A_{16} + \frac{c_1}{R_2} E_{16} \right) \frac{\partial w_0}{\partial X_1} \frac{\partial \varphi_j}{\partial X_1} + \left(A_{26} + \frac{c_1}{R_2} E_{26} \right) \frac{\partial w_0}{\partial X_2} \right. \\
&\quad \left. \frac{\partial \varphi_j}{\partial X_2} + \left(A_{66} + \frac{c_1}{R_2} E_{66} \right) \left(\frac{\partial w_0}{\partial X_1} \frac{\partial \varphi_j}{\partial X_2} + \frac{\partial w_0}{\partial X_2} \frac{\partial \varphi_j}{\partial X_1} \right) \right] \right\} dX_1 dX_2
\end{aligned}$$

$$T_{ij}^{24} = \sum_{\gamma=1}^5 \sum_{k=1}^{n^*} \frac{\partial K_{ik}^{2\gamma}}{\partial X_j} \Delta_k^\gamma + K_{ij}^{24} = K_{ij}^{24}$$

$$T_{ij}^{25} = \sum_{\gamma=1}^5 \sum_{k=1}^{n^*} \frac{\partial K_{ik}^{2\gamma}}{\partial Y_j} \Delta_k^\gamma + K_{ij}^{25} = K_{ij}^{25}$$

$$T_{ij}^{31} = \sum_{\gamma=1}^5 \sum_{k=1}^{n^*} \frac{\partial K_{ik}^{3\gamma}}{\partial u_j} \Delta_k^\gamma + K_{ij}^{31} = K_{ij}^{31}$$

$$T_{ij}^{32} = \sum_{\gamma=1}^5 \sum_{k=1}^{n^*} \frac{\partial K_{ik}^{3\gamma}}{\partial v_j} \Delta_k^\gamma + K_{ij}^{32} = K_{ij}^{32}$$

$$T_{ij}^{33} = \sum_{\gamma=1}^5 \sum_{k=1}^{n^*} \frac{\partial K_{ik}^{3\gamma}}{\partial \Delta_j^3} \Delta_k^\gamma + K_{ij}^{33} = \sum_{k=1}^{n^*} \left(\frac{\partial K_{ik}^{31}}{\partial \bar{\Delta}_j} u_k + \frac{\partial K_{ik}^{32}}{\partial \bar{\Delta}_j} v_k + \frac{\partial K_{ik}^{33}}{\partial \bar{\Delta}_j} \bar{\Delta}_k + \frac{\partial K_{ik}^{34}}{\partial \bar{\Delta}_j} X_k + \frac{\partial K_{ik}^{35}}{\partial \bar{\Delta}_j} Y_k \right) + K_{ij}^{33}$$

$$\begin{aligned}
\sum_{k=1}^{n^*} \frac{\partial K_{ik}^{31}}{\partial \bar{\Delta}_j} u_k &= \int_{\Omega^*} \left\{ \frac{\partial u}{\partial X_1} \left[\left(A_{11} + \frac{c_1}{R_1} E_{11} \right) \frac{\partial \varphi_i}{\partial X_1} \frac{\partial \varphi_j}{\partial X_1} + \left(A_{12} + \frac{c_1}{R_1} E_{12} \right) \frac{\partial \varphi_i}{\partial X_2} \frac{\partial \varphi_j}{\partial X_2} + \left(A_{16} + \frac{c_1}{R_1} E_{16} \right) \right. \right. \\
&\quad \left. \left(\frac{\partial \varphi_i}{\partial X_1} \frac{\partial \varphi_j}{\partial X_2} + \frac{\partial \varphi_i}{\partial X_2} \frac{\partial \varphi_j}{\partial X_1} \right) \right] + \frac{\partial u}{\partial X_2} \left[\left(A_{26} + \frac{c_1}{R_1} E_{26} \right) \frac{\partial \varphi_i}{\partial X_2} \frac{\partial \varphi_j}{\partial X_2} + \left(A_{16} + \frac{c_1}{R_1} E_{16} \right) \right. \\
&\quad \left. \frac{\partial \varphi_i}{\partial X_1} \frac{\partial \varphi_j}{\partial X_1} + \left(A_{66} + \frac{c_1}{R_1} E_{66} \right) \left(\frac{\partial \varphi_i}{\partial X_2} \frac{\partial \varphi_j}{\partial X_1} + \frac{\partial \varphi_i}{\partial X_1} \frac{\partial \varphi_j}{\partial X_2} \right) \right] \right\} dX_1 dX_2 \\
\sum_{k=1}^{n^*} \frac{\partial K_{ik}^{32}}{\partial \bar{\Delta}_j} v_k &= \int_{\Omega^*} \left\{ \frac{\partial v}{\partial X_1} \left[\left(A_{16} + \frac{c_1}{R_2} E_{16} \right) \frac{\partial \varphi_i}{\partial X_1} \frac{\partial \varphi_j}{\partial X_1} + \left(A_{26} + \frac{c_1}{R_2} E_{26} \right) \frac{\partial \varphi_i}{\partial X_2} \frac{\partial \varphi_j}{\partial X_2} + \left(A_{66} + \frac{c_1}{R_2} E_{66} \right) \right. \right. \\
&\quad \left. \left(\frac{\partial \varphi_i}{\partial X_1} \frac{\partial \varphi_j}{\partial X_2} + \frac{\partial \varphi_i}{\partial X_2} \frac{\partial \varphi_j}{\partial X_1} \right) \right] + \frac{\partial v}{\partial X_2} \left[\left(A_{12} + \frac{c_1}{R_2} E_{12} \right) \frac{\partial \varphi_i}{\partial X_1} \frac{\partial \varphi_j}{\partial X_1} + \left(A_{22} + \frac{c_1}{R_2} E_{22} \right) \right. \\
&\quad \left. \frac{\partial \varphi_i}{\partial X_2} \frac{\partial \varphi_j}{\partial X_2} + \left(A_{26} + \frac{c_1}{R_2} E_{26} \right) \left(\frac{\partial \varphi_i}{\partial X_2} \frac{\partial \varphi_j}{\partial X_1} + \frac{\partial \varphi_i}{\partial X_1} \frac{\partial \varphi_j}{\partial X_2} \right) \right] \right\} dX_1 dX_2 \\
\sum_{k=1}^{n^*} \frac{\partial K_{ik}^{33}}{\partial \bar{\Delta}_j} \bar{\Delta}_k &= \left(\frac{1}{2} \right) \int_{\Omega^*} \left(-c_1 \right) \left\{ \frac{\partial^2 \varphi_i}{\partial X_1^2} \left[\frac{\partial w_0}{\partial X_1} \left(E_{11} \frac{\partial \varphi_j}{\partial X_1} + E_{16} \frac{\partial \varphi_j}{\partial X_2} \right) + \frac{\partial w_0}{\partial X_2} \left(E_{12} \frac{\partial \varphi_j}{\partial X_2} + E_{16} \frac{\partial \varphi_j}{\partial X_1} \right) \right] + 2 \frac{\partial^2 \varphi_i}{\partial X_1 \partial X_2} \right. \\
&\quad \left[\frac{\partial w_0}{\partial X_1} \left(E_{16} \frac{\partial \varphi_j}{\partial X_1} + E_{66} \frac{\partial \varphi_j}{\partial X_2} \right) + \frac{\partial w_0}{\partial X_2} \left(E_{26} \frac{\partial \varphi_j}{\partial X_2} + E_{66} \frac{\partial \varphi_j}{\partial X_1} \right) \right] + \frac{\partial^2 \varphi_i}{\partial X_2^2} \left[\frac{\partial w_0}{\partial X_1} \left(E_{12} \frac{\partial \varphi_j}{\partial X_1} + E_{26} \frac{\partial \varphi_j}{\partial X_2} \right) \right. \\
&\quad \left. \left. + \frac{\partial w_0}{\partial X_2} \left(E_{22} \frac{\partial \varphi_j}{\partial X_2} + E_{26} \frac{\partial \varphi_j}{\partial X_1} \right) \right] \right\} + \varphi_i \left[\left(\frac{A_{11}}{R_1} + \frac{A_{12}}{R_2} \right) \frac{\partial w_0}{\partial X_1} \frac{\partial \varphi_j}{\partial X_1} + \left(\frac{A_{12}}{R_1} + \frac{A_{22}}{R_2} \right) \frac{\partial w_0}{\partial X_2} \frac{\partial \varphi_j}{\partial X_2} + \left(\frac{A_{16}}{R_1} + \right. \right. \\
&\quad \left. \left. \frac{A_{26}}{R_2} \right) \left(\frac{\partial w_0}{\partial X_1} \frac{\partial \varphi_j}{\partial X_2} + \frac{\partial \varphi_j}{\partial X_1} \frac{\partial w_0}{\partial X_2} \right) \right] + \frac{\partial \varphi_i}{\partial X_1} \left\{ 2A_{11} \left(\frac{\partial w_0}{\partial X_1} \right)^2 \frac{\partial \varphi_j}{\partial X_1} + A_{12} \left[\frac{\partial \varphi_j}{\partial X_1} \left(\frac{\partial w_0}{\partial X_2} \right)^2 + \frac{\partial w_0}{\partial X_1} \frac{\partial w_0}{\partial X_2} \frac{\partial \varphi_j}{\partial X_2} \right] \right. \\
&\quad \left. + A_{16} \left[3 \frac{\partial w_0}{\partial X_1} \frac{\partial w_0}{\partial X_2} \frac{\partial \varphi_j}{\partial X_1} + \left(\frac{\partial w_0}{\partial X_1} \right)^2 \frac{\partial \varphi_j}{\partial X_2} \right] - 2c_1 \frac{\partial \varphi_j}{\partial X_1} \left(E_{11} \frac{\partial^2 w_0}{\partial X_1^2} + E_{12} \frac{\partial^2 w_0}{\partial X_2^2} + 2E_{16} \frac{\partial^2 w_0}{\partial X_1 \partial X_2} \right) + A_{16} \right. \\
&\quad \left[\frac{\partial \varphi_j}{\partial X_1} \frac{\partial w_0}{\partial X_2} \frac{\partial w_0}{\partial X_1} + \left(\frac{\partial w_0}{\partial X_1} \right)^2 \frac{\partial \varphi_j}{\partial X_2} \right] + 2A_{26} \left(\frac{\partial w_0}{\partial X_2} \right)^2 \frac{\partial \varphi_j}{\partial X_2} + A_{66} \left[\frac{\partial \varphi_j}{\partial X_1} \left(\frac{\partial w_0}{\partial X_2} \right)^2 + 3 \frac{\partial w_0}{\partial X_1} \frac{\partial w_0}{\partial X_2} \frac{\partial \varphi_j}{\partial X_2} \right] - \\
&\quad 2c_1 \frac{\partial \varphi_j}{\partial X_2} \left(E_{16} \frac{\partial^2 w_0}{\partial X_1^2} + E_{26} \frac{\partial^2 w_0}{\partial X_2^2} + 2E_{66} \frac{\partial^2 w_0}{\partial X_1 \partial X_2} \right) \left\} + \frac{\partial \varphi_i}{\partial X_2} \left\{ 2A_{16} \left(\frac{\partial w_0}{\partial X_1} \right)^2 \frac{\partial \varphi_j}{\partial X_1} + A_{26} \left[\frac{\partial \varphi_j}{\partial X_1} \left(\frac{\partial w_0}{\partial X_2} \right)^2 \right. \right. \\
&\quad \left. \left. + \frac{\partial w_0}{\partial X_1} \frac{\partial w_0}{\partial X_2} \frac{\partial \varphi_j}{\partial X_2} \right] + A_{66} \left[3 \frac{\partial w_0}{\partial X_1} \frac{\partial w_0}{\partial X_2} \frac{\partial \varphi_j}{\partial X_1} + \left(\frac{\partial w_0}{\partial X_1} \right)^2 \frac{\partial \varphi_j}{\partial X_2} \right] - 2c_1 \frac{\partial \varphi_j}{\partial X_1} \left(E_{16} \frac{\partial^2 w_0}{\partial X_1^2} + E_{26} \frac{\partial^2 w_0}{\partial X_2^2} + \right. \right. \\
&\quad \left. \left. 2E_{66} \frac{\partial^2 w_0}{\partial X_1 \partial X_2} \right) + A_{12} \left[\frac{\partial \varphi_j}{\partial X_1} \frac{\partial w_0}{\partial X_2} \frac{\partial w_0}{\partial X_1} + \left(\frac{\partial w_0}{\partial X_1} \right)^2 \frac{\partial \varphi_j}{\partial X_2} \right] + 2A_{22} \left(\frac{\partial w_0}{\partial X_2} \right)^2 \frac{\partial \varphi_j}{\partial X_2} + A_{26} \left[\frac{\partial \varphi_j}{\partial X_1} \left(\frac{\partial w_0}{\partial X_2} \right)^2 \right. \right.
\end{aligned}$$

$$\begin{aligned}
& + 3 \frac{\partial w_0}{\partial X_1} \frac{\partial w_0}{\partial X_2} \frac{\partial \varphi_j}{\partial X_2} \Big] - 2c_1 \frac{\partial \varphi_j}{\partial X_2} \left(E_{12} \frac{\partial^2 w_0}{\partial X_1^2} + E_{22} \frac{\partial^2 w_0}{\partial X_2^2} + 2E_{26} \frac{\partial^2 w_0}{\partial X_1 \partial X_2} \right) \Big\} + 2 \left(\frac{A_{11}}{R_1} + \frac{A_{12}}{R_2} \right) \left[\frac{\partial \varphi_i}{\partial X_1} \right. \\
& \left. \varphi_j \frac{\partial w_0}{\partial X_1} w_0 + (w_0)^2 \frac{\partial \varphi_i}{\partial X_1} \frac{\partial \varphi_j}{\partial X_1} \right] + 2 \left(\frac{A_{16}}{R_1} + \frac{A_{26}}{R_2} \right) \left[\frac{\partial \varphi_i}{\partial X_1} \varphi_j \frac{\partial w_0}{\partial X_2} w_0 + (w_0)^2 \frac{\partial \varphi_i}{\partial X_1} \frac{\partial \varphi_j}{\partial X_2} \right] + 2 \left(\frac{A_{16}}{R_1} + \right. \\
& \left. \frac{A_{26}}{R_2} \right) \left[\frac{\partial \varphi_i}{\partial X_2} \varphi_j \frac{\partial w_0}{\partial X_1} w_0 + (w_0)^2 \frac{\partial \varphi_i}{\partial X_2} \frac{\partial \varphi_j}{\partial X_1} \right] + 2 \left(\frac{A_{12}}{R_1} + \frac{A_{22}}{R_2} \right) \left[\frac{\partial \varphi_i}{\partial X_2} \varphi_j \frac{\partial w_0}{\partial X_2} w_0 + (w_0)^2 \frac{\partial \varphi_i}{\partial X_2} \frac{\partial \varphi_j}{\partial X_2} \right] \Big] \\
& dX_1 dX_2 \\
\sum_{k=1}^{n^*} \frac{\partial K_{ik}^{34}}{\partial \bar{\Delta}_j} X_k &= \int_{\Omega^e} \left\{ \frac{\partial \phi_x}{\partial X_1} \left[\hat{B}_{11} \frac{\partial \varphi_i}{\partial X_1} \frac{\partial \varphi_j}{\partial X_1} + \hat{B}_{12} \frac{\partial \varphi_i}{\partial X_2} \frac{\partial \varphi_j}{\partial X_2} + \hat{B}_{16} \left(\frac{\partial \varphi_i}{\partial X_1} \frac{\partial \varphi_j}{\partial X_2} + \frac{\partial \varphi_i}{\partial X_2} \frac{\partial \varphi_j}{\partial X_1} \right) \right. \right. \\
& \left. \left. + \frac{\partial \phi_x}{\partial X_2} \left[\hat{B}_{16} \frac{\partial \varphi_i}{\partial X_1} \frac{\partial \varphi_j}{\partial X_1} + \hat{B}_{26} \frac{\partial \varphi_i}{\partial X_2} \frac{\partial \varphi_j}{\partial X_2} + \hat{B}_{66} \left(\frac{\partial \varphi_i}{\partial X_1} \frac{\partial \varphi_j}{\partial X_2} + \frac{\partial \varphi_i}{\partial X_2} \frac{\partial \varphi_j}{\partial X_1} \right) \right] \right\} dX_1 dX_2 \\
\sum_{k=1}^{n^*} \frac{\partial K_{ik}^{35}}{\partial \bar{\Delta}_j} X_k &= \int_{\Omega^e} \left\{ \frac{\partial \phi_y}{\partial X_1} \left[\hat{B}_{16} \frac{\partial \varphi_i}{\partial X_1} \frac{\partial \varphi_j}{\partial X_1} + \hat{B}_{26} \frac{\partial \varphi_i}{\partial X_2} \frac{\partial \varphi_j}{\partial X_2} + \hat{B}_{66} \left(\frac{\partial \varphi_i}{\partial X_1} \frac{\partial \varphi_j}{\partial X_2} + \frac{\partial \varphi_i}{\partial X_2} \frac{\partial \varphi_j}{\partial X_1} \right) \right. \right. \\
& \left. \left. + \frac{\partial \phi_y}{\partial X_2} \left[\hat{B}_{12} \frac{\partial \varphi_i}{\partial X_1} \frac{\partial \varphi_j}{\partial X_1} + \hat{B}_{22} \frac{\partial \varphi_i}{\partial X_2} \frac{\partial \varphi_j}{\partial X_2} + \hat{B}_{26} \left(\frac{\partial \varphi_i}{\partial X_1} \frac{\partial \varphi_j}{\partial X_2} + \frac{\partial \varphi_i}{\partial X_2} \frac{\partial \varphi_j}{\partial X_1} \right) \right] \right\} dX_1 dX_2 \\
T_{ij}^{34} &= \sum_{\gamma=1}^5 \sum_{k=1}^{n^*} \frac{\partial K_{ik}^{3\gamma}}{\partial X_j} \Delta_k^\gamma + K_{ij}^{34} = K_{ij}^{34} \\
T_{ij}^{35} &= \sum_{\gamma=1}^5 \sum_{k=1}^{n^*} \frac{\partial K_{ik}^{3\gamma}}{\partial Y_j} \Delta_k^\gamma + K_{ij}^{35} = K_{ij}^{35} \\
T_{ij}^{41} &= \sum_{\gamma=1}^5 \sum_{k=1}^{n^*} \frac{\partial K_{ik}^{4\gamma}}{\partial u_j} \Delta_k^\gamma + K_{ij}^{41} = K_{ij}^{41} \\
T_{ij}^{42} &= \sum_{\gamma=1}^5 \sum_{k=1}^{n^*} \frac{\partial K_{ik}^{4\gamma}}{\partial v_j} \Delta_k^\gamma + K_{ij}^{42} = K_{ij}^{42} \\
T_{ij}^{43} &= \sum_{\gamma=1}^5 \sum_{k=1}^{n^*} \frac{\partial K_{ik}^{4\gamma}}{\partial \Delta_j^3} \Delta_k^\gamma + K_{ij}^{43} = \sum_{k=1}^{n^*} \frac{\partial K_{ik}^{43}}{\partial \bar{\Delta}_j} \bar{\Delta}_k + K_{ij}^{43} \\
\sum_{k=1}^{n^*} \frac{\partial K_{ik}^{43}}{\partial \bar{\Delta}_j} \bar{\Delta}_k &= \frac{1}{2} \int_{\Omega^e} \left\{ \frac{\partial \psi_i}{\partial X_1} \left[\hat{B}_{11} \frac{\partial w_0}{\partial X_1} \frac{\partial \varphi_j}{\partial X_1} + \hat{B}_{12} \frac{\partial w_0}{\partial X_2} \frac{\partial \varphi_j}{\partial X_2} + \hat{B}_{16} \left(\frac{\partial w_0}{\partial X_1} \frac{\partial \varphi_j}{\partial X_2} + \frac{\partial w_0}{\partial X_2} \frac{\partial \varphi_j}{\partial X_1} \right) \right] \right. \\
& \left. + \frac{\partial \psi_i}{\partial X_2} \left[\hat{B}_{16} \frac{\partial w_0}{\partial X_1} \frac{\partial \varphi_j}{\partial X_1} + \hat{B}_{26} \frac{\partial w_0}{\partial X_2} \frac{\partial \varphi_j}{\partial X_2} + \hat{B}_{66} \left(\frac{\partial w_0}{\partial X_1} \frac{\partial \varphi_j}{\partial X_2} + \frac{\partial w_0}{\partial X_2} \frac{\partial \varphi_j}{\partial X_1} \right) \right] \right\} dX_1 dX_2 \\
T_{ij}^{44} &= \sum_{\gamma=1}^5 \sum_{k=1}^{n^*} \frac{\partial K_{ik}^{4\gamma}}{\partial X_j} \Delta_k^\gamma + K_{ij}^{44} = K_{ij}^{44} \\
T_{ij}^{45} &= \sum_{\gamma=1}^5 \sum_{k=1}^{n^*} \frac{\partial K_{ik}^{4\gamma}}{\partial Y_j} \Delta_k^\gamma + K_{ij}^{45} = K_{ij}^{45}
\end{aligned}$$

$$T_{ij}^{51} = \sum_{\gamma=1}^5 \sum_{k=1}^{n^*} \frac{\partial K_{ik}^{5\gamma}}{\partial u_j} \Delta_k^\gamma + K_{ij}^{51} = K_{ij}^{51}$$

$$T_{ij}^{52} = \sum_{\gamma=1}^5 \sum_{k=1}^{n^*} \frac{\partial K_{ik}^{5\gamma}}{\partial v_j} \Delta_k^\gamma + K_{ij}^{52} = K_{ij}^{52}$$

$$T_{ij}^{53} = \sum_{\gamma=1}^5 \sum_{k=1}^{n^*} \frac{\partial K_{ik}^{5\gamma}}{\partial \Delta_j^3} \Delta_k^\gamma + K_{ij}^{53} = \sum_{k=1}^{n^*} \frac{\partial K_{ik}^{53}}{\partial \bar{\Delta}_j} \bar{\Delta}_k + K_{ij}^{53}$$

$$\begin{aligned} \sum_{k=1}^{n^*} \frac{\partial K_{ik}^{53}}{\partial \bar{\Delta}_j} \bar{\Delta}_k &= \frac{1}{2} \int_{\Omega^*} \left\{ \frac{\partial \psi_i}{\partial X_2} \left[\hat{B}_{12} \frac{\partial w_0}{\partial X_1} \frac{\partial \varphi_j}{\partial X_1} + \hat{B}_{22} \frac{\partial w_0}{\partial X_2} \frac{\partial \varphi_j}{\partial X_2} + \hat{B}_{26} \left(\frac{\partial w_0}{\partial X_1} \frac{\partial \varphi_j}{\partial X_2} + \frac{\partial w_0}{\partial X_2} \frac{\partial \varphi_j}{\partial X_1} \right) \right] \right. \\ &\quad \left. + \frac{\partial \psi_i}{\partial X_1} \left[\hat{B}_{16} \frac{\partial w_0}{\partial X_1} \frac{\partial \varphi_j}{\partial X_1} + \hat{B}_{26} \frac{\partial w_0}{\partial X_2} \frac{\partial \varphi_j}{\partial X_2} + \hat{B}_{66} \left(\frac{\partial w_0}{\partial X_1} \frac{\partial \varphi_j}{\partial X_2} + \frac{\partial w_0}{\partial X_2} \frac{\partial \varphi_j}{\partial X_1} \right) \right] \right\} dX_1 dX_2 \end{aligned}$$

$$T_{ij}^{54} = \sum_{\gamma=1}^5 \sum_{k=1}^{n^*} \frac{\partial K_{ik}^{5\gamma}}{\partial X_j} \Delta_k^\gamma + K_{ij}^{54} = K_{ij}^{54}$$

$$T_{ij}^{55} = \sum_{\gamma=1}^5 \sum_{k=1}^{n^*} \frac{\partial K_{ik}^{5\gamma}}{\partial Y_j} \Delta_k^\gamma + K_{ij}^{55} = K_{ij}^{55}$$

VITA

Mr. Seung Joon Lee received his Bachelor of Science degree in February 1995 and Master of Science degree in February 1997 in civil engineering from Yeungnam University, Korea. His master's thesis is "Evaluation of Occupant Risk by Flail Space Model for Roadside Guardrails". In Fall 1998, he pursued his studies in the Department of Civil Engineering at Texas A&M University. Mr. Lee strengthened his study in the field of Roadside Safety Structures through his working in Safety and Structural System Division of Texas Transportation Institute (TTI) as a Graduate Research Assistant for his first three years at Texas A&M University.

Mr. Lee worked as a Graduate Research Assistant from Fall 2001 while working toward his doctoral degree in the Department of Civil Engineering at Texas A&M University, College Station, TX. under Professor J. N. Reddy, University Distinguished Professor and holder of the Oscar S. Wyatt Endowed Chair. He received his Ph. D. degree in May 2004.

His areas of interest are Composite Materials and Structures, Smart Structures, Computational Mechanics, Roadside Safety Structure Design, and Computer Simulation of Vehicle Dynamics.

He can be reached at his permanent address: Seung Joon Lee

245-16 Naedang-Dong Seo-Gu

Taegu, KOREA (R.O.K.) 703-803